DEVELOPMENT OF MICROARRAY TECHNIQUES FOR THE STUDY OF GENE EXPRESSION IN THE EUROPEAN EEL (*ANGUILLA ANGUILLA*) DURING SILVERING AND MIGRATION TO SEAWATER

Iain Stuart McWilliam

A Thesis Submitted for the Degree of PhD
at the
University of St. Andrews

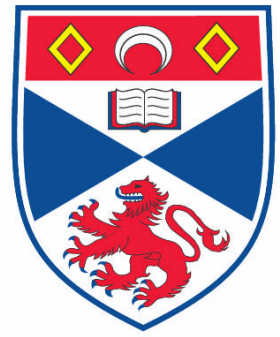

2008

Development of microarray techniques for the study of gene expression in the European eel (*Anguilla anguilla*) during silvering and migration to seawater

Iain Stuart M^{c}William

A thesis presented for the degree of Doctor of Philosophy at the University of St Andrews

February 2007

Acknowledgements

This study was carried out within the Biomolecular Osmoregulatory Research Group at the University of St Andrews and was funded by the Natural Environment Research Council; grant NER/T/S/2001/00282. The group is headed by Dr Gordon Cramb and thanks go to him for providing guidance and expertise where mine fell short. Thanks also to Dr Svetlana Kalujnaia who was directly involved in the study and to Dr Chris Cutler who was there at its inception. The other members of the group and technical staff, past and present have also helped me along the way; Dr Lara Meischke in particular was always a refuge of sanity. A special thank you to Dr Val Smith and the members of her Comparative Immunology Group who were always accommodating and helpful with my QPCR experiments.

To my friends who brightened up my periods of experimental darkness; Jamie, Paul, Vic, Rob, Timda, Stevie, Ally and the rest of the Crusties and surfing mates; Alice (who even after witnessing my entire PhD rollercoaster hasn't been dissuaded from taking the plunge); to my friends from undergrad days, Fearghal, Babs, Kirsty and Aki; to all the Friday night St Andrews pub crowd and finally to Mother Nature who sends me waves. I'm lucky to know you all and I promise there'll be no more eel chat for a while.

Huge thanks to all my family for their love and support, especially to my brothers and their clans, Peter *et al* and Grant *et al* (I really am getting a job now), to my granddad Neil, and of course to Mum and Dad who proofread the whole thing but more importantly gave me the opportunities and freedom that got me here in the first place.

À Susan, tu es toujours là pour moi, je pourrais ne jamais l'avoir fini sans toi, je serez toujours là pour toi, je t'aime.

Declarations

I, Iain Stuart M^{c}William, hereby certify that this thesis, which is approximately 65,000 words in length, has been written by me, that it is the record of work carried out by me and that it has not been submitted in any previous application for a higher degree.
Date
Signature of candidate

I was admitted as a research student in October 2001 and as a candidate for the degree of PhD in October 2002; the higher study for which this is a record was carried out in the University of St Andrews between October 2002 and January 2007.
Date
Signature of candidate

I hereby certify that the candidate has fulfilled the conditions of the Resolution and Regulations appropriate for the degree of PhD in the University of St Andrews and that the candidate is qualified to submit this thesis in application for that degree.
Date:
Signature of supervisor

In submitting this thesis to the University of St Andrews I understand that I am giving permission for it to be made available for use in accordance with the regulation of the University Library for the time being in force, subject to any copyright vested in the work not being affected thereby. I understand that the title and abstract will be published, and that a copy of the work may be made and supplied to any bona fide library or research worker, that my thesis will be electronically accessible for personal or research use, and that the library has the right to migrate my thesis into new electronic forms as required to ensure continued access to the thesis. I have obtained any third-party copyright permissions that may be required in order to allow such access and migration.
Date:
Signature of candidate

Appendices on the accompanying CD.

Appendix 1 CloneMiner cDNA Library Construction Kit

Appendix 2 PCR-Select cDNA Subtranction Kit User Manual

Appendix 3 Kalujnaia, S., McWilliam, I. S., Feilen, A. L., Nicholson, J., Zaguinaiko, V. A., Hazon, N., Cutler, C. P., Balment, R. J., Cossins, A. R., Hughes, M. et al. (2007). Salinity adaptation and gene profiling analysis in the European eel (*Anguilla anguilla*) using microarray technology. *General and Comparative Endocrinology.*

Appendix 4 Kalujnaia, S., McWilliam, I. S., Zaguinaiko, V. A., Feilen, A. L., Nicholson, J., Hazon, N., Cutler, C. P. and Cramb, G. (2007b). A transcriptomic approach to the study of osmoregulation in European eel *Anguilla anguilla*. *Physiol. Genomics*.

1.0 Abstract

The European eel, *Anguilla anguilla*, has a complex life-cycle involving migrations between the Sargasso Sea and the river systems of Europe and North Africa. The requirement to move across large salinity gradients presents a significant physiological challenge and the developmental stages of the eel are closely linked to these migrations. Microarrays were created to elucidate gene expression changes occurring during;

i. **The transition from juvenile yellow to the adult sexually maturing, migrating silver eel and;**
ii. **Salinity adaptation during the migration from freshwater to seawater.**

Groups (n = 6) of freshwater-acclimated yellow or silver eels were transferred to seawater for between 6 hours and 5 months and complementary control groups were transferred to freshwater. Brain, kidney, intestine and gill cDNA libraries were constructed using suppression subtractive hybridisation (SSH) techniques and a novel protocol based on Invitrogen's Gateway cloning system. The latter technique produced a low redundancy (~4 %) EST bank with a wide range of insert sizes (0.5 – 10 kb). Two microarray types were produced; one comprised 5760 clones from the two brain libraries whilst the other was a multi-tissue microarray incorporating 6144 clones from the SSH libraries. Pooled RNA samples were probed against the microarrays to highlight differentially expressed genes. Real-time quantitative PCR (QPCR) was used to validate the observed expression changes of selected genes in the tissues of individual fish. Following yellow to silver transformation of freshwater-adapted eels, the expression of tyrosine 3-mono-oxygenase/tryptophan 5-mono-oxygenase activation protein (14-3-3) and vaccinia related kinase 3 was shown to be consistently elevated. Prolactin expression increased in the brains of silver eels following two-day seawater-acclimation but QPCR analysis revealed high variation amongst freshwater-adapted eels. This is the first eel microarray study and the expression profiles highlighted herein will provide new avenues for research into the sexual development and salinity acclimation of *A. anguilla*

1.1 Table of abbreviations

14-3-3	Tyrosine 3-mono-oxygenase/tryptophan 5-mono-oxygenase activation protein
BCP	1bromo-2chloropropane
2G	Second generation
AANAT	Arylalkylamine *N*-acetyltransferase
AQP	Aquaporin
Blast	Basic local alignment search tool
Camp	Cyclic adenosine monophosphate
CDNA	Complimentary deoxyribo nucleic acid
CFTR	Cystic fibrosis transmembrane conductance regulator
Cm^R	Chloramphenicol resistance
CSA	Carbon spacer arm
Ct	Treshold cycle
CV	Column volumes
DART-PCR	Data analysis for real time PCR
DCTP	Deoxycytidine triphosphate
DEPC	Diethylpyrocarbonate
DNA	Deoxyribonucleic acid
DNTP	Deoxyribonucleotide triphosphate
DTT	Dithiothreitol
DUTP	Deoxyuridine triphosphate
E	Efficiency
EAE	Epithelial anion echanger
EDTA	Ethylenediaminetetraacetic acid
EEO	Electroendosmosistype
ERK	Extracellular signal regulated kinase
EST	Expressed sequence tag
FW	Fresh water
GAPDH	Glyceraldehyde-3-phosphate dehydrogenase
HPLC	High pressure liquid chromatography
HSP	Heat shock protein
IHF	Host integration factor
IQD	Interquartale distance
Kan^R	Kanamycin resistance gene
LB	Luria broth
LMF	Liverpool microarray facility
Lowess	Locally weighted estimated
MADSCAN	Microarray data suites of computed analysis
MAPK	Mitogen activated protein kinase
MDR	Multi drug resistance

MIAME	Minimum information about a microarray experiments
MOPS	3-(N-Morpholino)-propanesulfonic acid
MRNA	Messenger RNA
MW	Molecular weight
NABs	NeutrAvidin™ biotin-binding protein agarose beads
NEB	New England biolabs
NERC	Natural environment research council
NHE	Sodium/hydrogen exchanger
NKCC	Na^+,K^+,$2Cl^-$ cotransporter
P	Phosphate group
PCR	Polymerase chain reaction
PKC	Protein kinase C
PMCA	Plasma membrane Ca^{2+}-ATPase
PMT	Photomultiplier tube
QPCR	Real time quantitative polymerase chain reaction
REST	Relative Expression Software Tool
RNA	RiboNucleic acid
RPL-P0	Acidic ribosomal phosphoprotein P0
Rpm	Revolutions per minute
RRNA	Ribosomal RiboNucleic acid
RT	Reverse transcriptase
SA-PMPs	Streptavidin Magnesphere® Paramagnetic Particles
SDS	Sodium dodecyl sulfate
SERCA	Sarco/endoplasmic reticulum Ca^{2+} ATPase
SMART	Switching mechanism at the 5' end of RNA
SSH	Suppressive subtraction hybridisation
SSH	Suppression subtractive hybridisation
SW	Salt water
TAE	Tris-Acetate-EDTA
TIFF	Tag image file format
Tm	Annealing temperature
UV	Ultra Violet
VRK	Vaccinia related kinase

2.0 Introduction

‘‘Eels are derived from the so-called 'earth's guts' that grow spontaneously in mud and in humid ground; in fact, eels have at times been seen to emerge out of such earthworms, and on other occasions have been rendered visible when the earthworms were laid open by either scraping or cutting” (Aristotle, 350 B.C.). The reproductive habits of the eel have perplexed researchers since ancient times and still to this day eel spawning in the wild has yet to be observed.

The European eel (*Anguilla anguilla*) is a euryhaline, facultative catadromous teleost (Tsukamoto and Arai, 2001; Tsukamoto, 1998), which spends the majority of its adult life in fresh or brackish water (Tzeng, 2000). It returns to the sea in order to spawn (Moriarty, 1978) and once hatched, the eel larvae drift back to European coastal waters whereupon the young eels migrate into river systems and develop into adults. This life-cycle necessitates the ability to adapt physiologically to fresh, brackish and marine environments at distinct life stages. As an osmoregulator, *A. anguilla* maintains a relatively stable blood plasma osmolality whether in brackish water, freshwater or seawater. Each aquatic habitat poses a different osmoregulatory challenge to the eel due to the markedly different salinities of the water; subsequently, different strategies have evolved to maintain osmotic homeostasis. The transitions between environments of different salinities are associated with the developmental and morphological stages of the eel. The elopomorphs, which encompass *A. anguilla*, are some of the most ancient teleosts, having diverged ~350 million years ago (Lauder and Liem, 1983). As such, they may exhibit conserved characteristics which are less evolutionarily derived than other teleosts (Weltzien et al., 2006). The eel therefore provides an excellent study organism to examine both development and osmoregulation.

In addition to their scientific interest, eels are increasingly under threat as a species due to massive reductions in their populations over the last half-

century (Stone, 2003). The decline in eel numbers has been estimated at 99% since 1980 (Dekker, 2003) and in 2005 the Swedish Species Information Centre was the first organisation to classify the eel as critically endangered.

Eels are also of worldwide economic interest, with the global market approaching an estimated £1.5 billion (Heinsbroek, 1991). Global aquaculture production of eels increased exponentially in the latter half of the 20th century but now appears to have reached a plateau (Figure 2.0.a). Due to the complexity of the eel life-cycle, captive breeding of the eel has remained elusive. Fertilised eggs from the Japanese eel, A. japonica, were obtained following hormone treatments as far back as 1974 (Yamamoto and Yamauchi, 1974) but similar experiments with A. anguilla have had limited success (Palstra et al., 2005). In 2005, the one remaining segment of the Japanese eel life-cycle in captivity was achieved; development of glass eels from larvae (Kagawa et al., 2005), however, this has still to be replicated in the European eel. Eel aquaculture, without a viable alternative, has therefore always relied solely on wild caught, post-larval eels as seed stock. Since 1950, however, eel capture rates have plummeted which is reflected in the worldwide crash in eel populations (Figure 2.0.b), leading to unsustainable aquaculture practices (EU-Communication:IP/03/1332, 2005). The exact reasons for the population decline are not understood but it has been associated with over fishing (Castonguay et al., 1994; Dekker, 2003), impaired reproduction due to dioxin contamination (Castonguay et al., 1994; Palstra et al., 2006), viral disease (van Ginneken et al., 2004) and diminished fat stores due to insufficient food stores in inland waters (Svedäng and Wickstrom, 1997). The current eel crisis has had direct implications for the direction of current eel research, with calls for specific research into the reproduction and development coming from the European Parliament (Dossier reference: INI/2005/2032, 2005,). The present study will add to the body of knowledge regarding the sexual development and physiology of the eel.

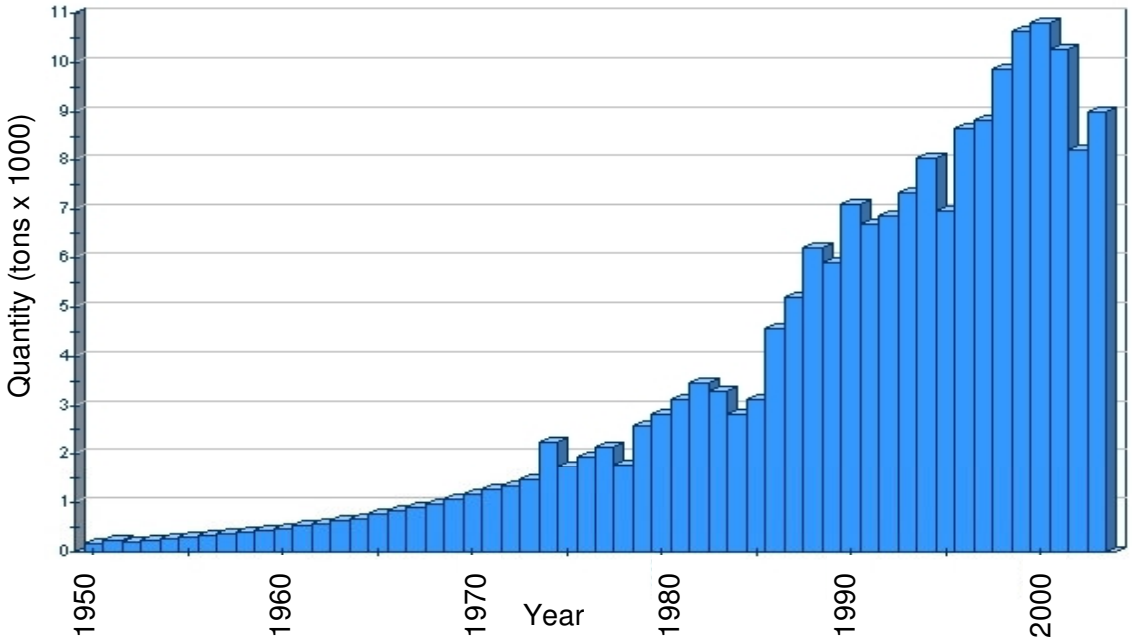

Figure 2.0.a. Global aquaculture production of *A. anguilla* over the last 60 years. Source: Food and Agriculture Organisation of the United Nations.

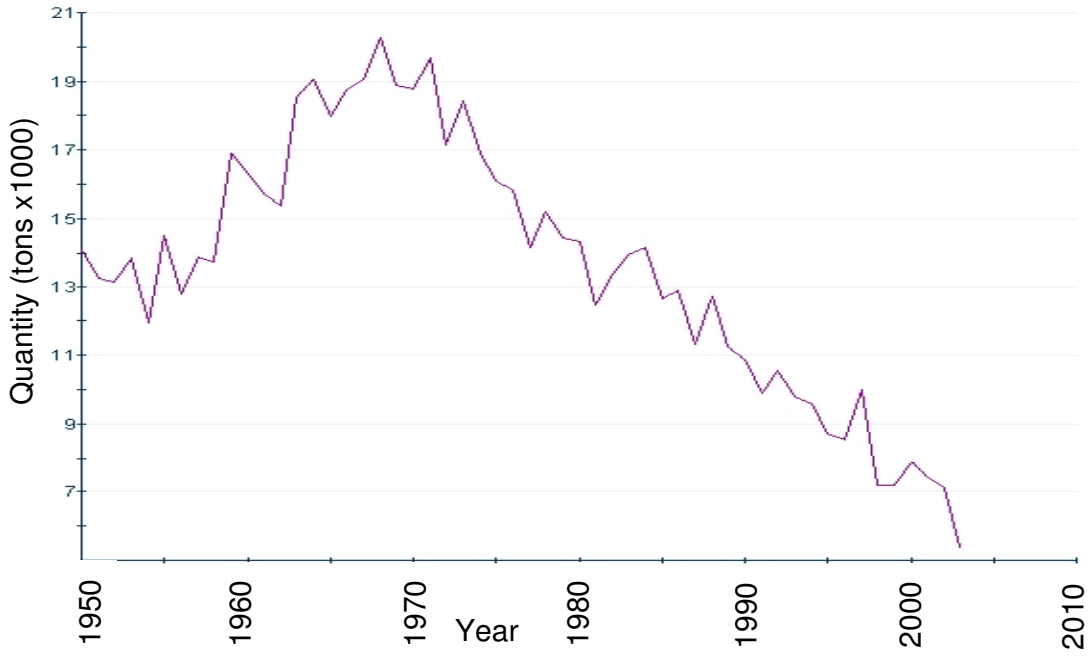

Figure 2.0.b. Global wild *A. anguilla* capture over the last 60 years. Source: Food and Agriculture Organisation of the United Nations.

2.1 The eel life-cycle

From egg to elver: Spawning of *A. anguilla* is believed to occur between November and July (Wang and Tzeng, 2000) in the Sargasso Sea, which is a floating lens of warm water in the south east Atlantic (Schmidt, 1922). The location of European eel spawning has never been observed first hand but it is implied from the results of a study carried out by Johannes Schmidt using tow nets to study the spatial distribution of eels of varying sizes in the Atlantic (Schmidt, 1922). He showed that there is an increase in eel length which directly correlates to increasing distance from the Sargasso Sea (Figure 2.1.a).

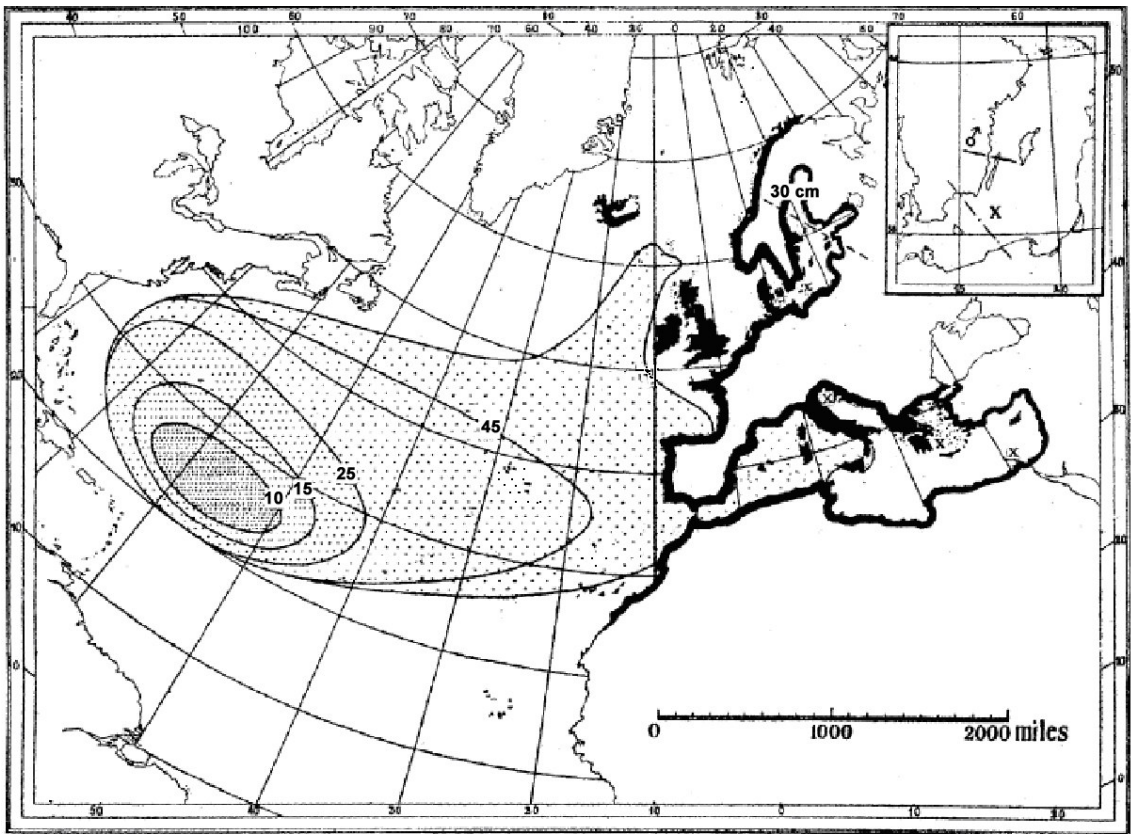

Figure 2.1.a. Distribution of eel larvae. Length increases from ~10 mm in the vicinity of The Sargasso Sea, (20-35 N Latitude and 30-70 W Longitude) to >45 mm in European waters. Reproduced from Schmidt, 1922.

When eel larvae hatch they are known as leptocephali, the name being derived from the Greek; lepto- (thin) and -kephalos (headed). They have a transparent, leaf-like body shape which is suitable for drifting in ocean currents (Figure 2.1.a). The Gulf Stream and North Atlantic Current carry them towards North African and European estuaries. Estimates of the time taken for migration to European coastal waters vary from an average of 350 days (Wang and Tzeng, 2000) up to 2-7 years (Van Utrecht, 1985). The large variation in estimates owes, impart, to the difficulty in determinig the age of eels (Deelder, 1981), debate as to whether the leptocephali actively swim towards their destination (Lecomte-Finiger, 1992; Wang and Tzeng, 2000) and to the inherent variability in the accuracy of otolith analysis between researchers (Svedäng 1998).

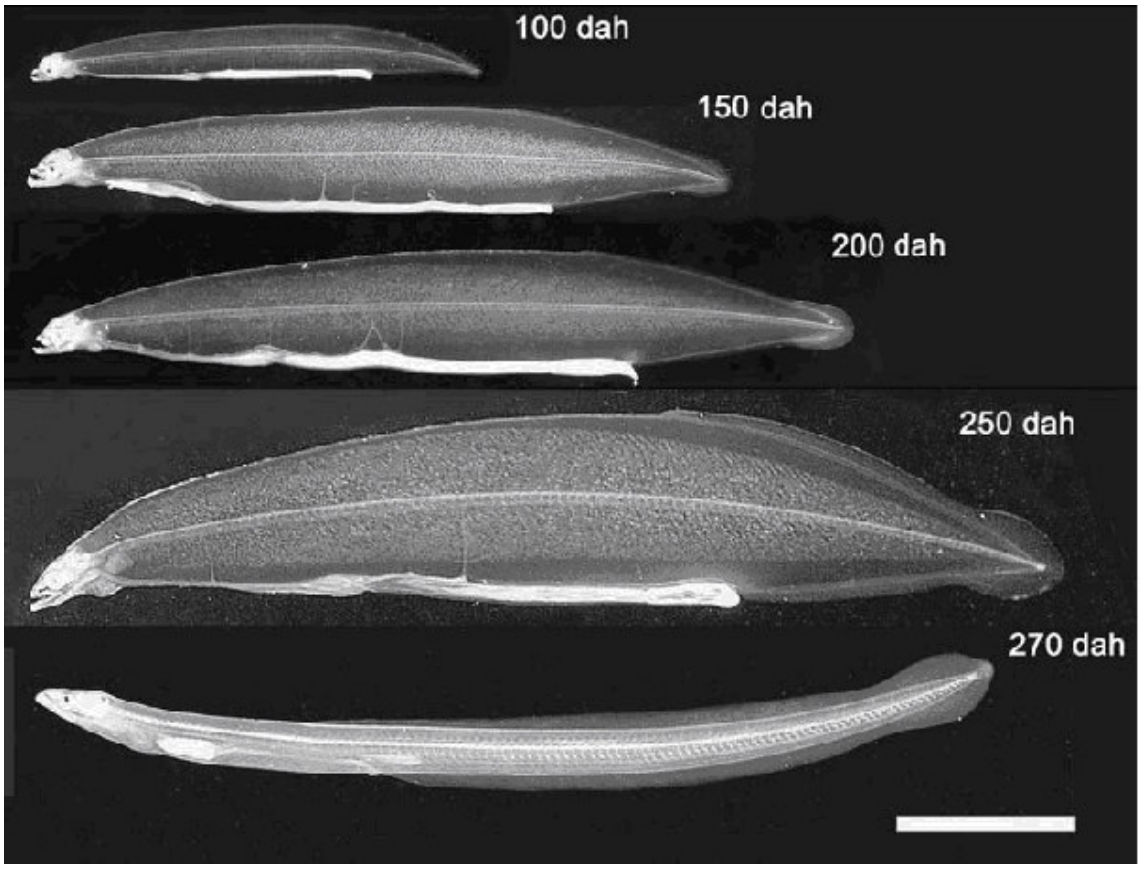

Figure 2.1.b. Growth of captive-bred *A. japonica* larvae. Scale bar = 10 mm, dah = days after hatching. Reproduced from Tanaka (2003).

Upon reaching the continental shelf the leptocephali undergo a metamorphosis into glass eels. During this development the eels become more cylindrical in shape and both buoyancy and drifting ability diminish. Subsequently they swim proactively to estuaries where they become pigmented elvers. This journey from the continental shelf to the estuaries takes an average of 98 days (Wang and Tzeng, 2000). The majority of elvers migrate up into river systems where they become fresh water-adapted yellow eels (Moriarty, 1978). Some eels, however, remain in marine environments for the entirety of their life-cycle or move down rivers as immature adult yellow eels to inhabit the brackish waters of estuaries (Tsukamoto and Arai, 2001).

Yellow eels are sexually immature and may reside in rivers for up to 50 years (Poole and Reynolds, 1998) with the average age at maturity being 12-20 years in northern Europe but only 6-8 in southern Europe and North Africa (Tesch and Greenwood, 1977). Some eels remain in marine or brackish water around estuaries throughout their lives, as shown by Tsukamoto (2001). He examined the strontium:calcium ratio in the layers of otoliths (the calcium carbonate deposits found in the inner ear of all fish, which can be used to show temporal use of freshwater or seawater habitats) and concluded that some eels never enter freshwater.

The development from yellow to the final silver life stage (silvering) occurs prior to migration but the cue for its onset is not well characterised. It is not directly linked to age or size (Svedäng 1996; Vøllestad, 1992) but it has been postulated to be associated with the accumulation of mesenteric fat (Larsson, 1990). This corresponds with the link shown between mesenteric fat levels and hormone regulation during the sexual maturation of Atlantic salmon (Rowe, 1991). Energy reserves are required for the return migration (~6000 km) to the Sargasso Sea, as it is reported that eels do not eat during their trans-oceanic crossing (Tucker, 1959).

Traditionally, eels undergoing sexually development have been classified into two groups; yellow and silver (Feunteun et al., 2000). Recently, however, this has been disputed as being an inadequate description and the

silvering process is currently being redefined by various authors although agreed nomenclature is still to agreed.

During silvering the eel pre-acclimates physiologically to seawater in preparation for the migration to the spawning grounds of the Sargasso Sea (Cutler and Cramb, 2001; Kirsch et al., 1975; Tesch and Greenwood, 1977). As eels reach maturity the undersides of the skin turn silver or bronze due to differentiation of pigment cells (Pankhurst, 1982). There is some proliferation of the gonads (Pankhurst, 1982), their eyes become bigger and the head takes on a more hydrodynamic form. A very recent study, profiling the level of circulating developmental hormones of silvering eels, has indicated that this process is associated with hormonal surges of testosterone and estradiol, whilst growth hormone and thyroid hormone do not appear to change between the two stages (van Ginneken, 2006).

It is postulated that in the late summer and autumn following silvering there is an environmental trigger which induces the migration back to the spawning grounds (Vøllestad et al., 1986). This process is not fully understood but has been attributed to many environmental cues in eel species including temperature (Boubée et al., 2000), atmospheric depressions (Okamura, 2002), lunar phase and river water levels (Cullen and McCarthy, 2003). Most likely there is a combination of factors involved which trigger downstream migration. The timing of migration appears to be sex dependent, with males departing up to two months prior to females (Tesch, 2003). This segregation between the sexes is thought to be based on body size, which is directly proportional to swim speed (Usui, 1991). Males start to mature at ~40 cm whilst the females grow to >60 cm before silvering (Svedäng 1996). Based on the average open ocean swim speed of 0.48 body lengths/s for migrating *Anguilla japonica* (Aoyama et al., 1999), a male eel 50 cm long would take ~289 day to make the 6000 km migration whilst a female eel, 80 cm long would take ~181 days (author's calculation). The eel is thought to migrate to the Sargasso Sea at great depth, having been photographed at 2000 m (Robins et al., 1979) and as the current of the Gulf Stream is negligible at this depth (Halkin and Rossby, 1985) these calculations should

be reasonably accurate, providing the eels take a direct route. The temporal coincidence of male and female sexually mature eels at the Sargasso Sea is implicit from the sex-dependent timing of migration and the difference in swimming speeds. Interestingly, the very action of performing this migration, and the change in body composition it causes, has been suggested as the trigger for the final sexual development of the eel (van Ginneken, 2006).

There has never been a study of the naturally occurring endogenous hormonal changes during the final sexual maturation because captive silver eels do not finally mature and there are only two published reports of migrating silver eels being caught at sea (Bast and Klinkhardt, 1988; Ernst, 1977). In teleosts, sexual development is under the control of the brain-hypophyseal-gonadal endocrine axis (Yaron and Sivan, 2006). Induced "natural" maturation by the administration of sexual steroids has been shown to promote luteinising hormone (LH) synthesis in the pituitary but this was not associated with a subsequent systemic release of LH and thus sexual maturation did not occur (Dufour et al., 1983). Treatment of silver eels with exogenous gonadotrophin has, however, been used to induce gonadal development (Fontaine, 1936) which indicates that there is inhibition of gonadotropin release or actions in captive silver eels. It has recently been suggested that dopamine prevents final sexual maturation of the eel by inhibiting release of LH (Vidal et al., 2004). This model involves a decrease in dopamine inhibition of gonadotrophin releasing hormone expression, which in turn stimulates LH synthesis and secretion to bring about ovarian development. How the external environment triggers these processes is not understood.

2.2 Introduction to osmoregulation

In freshwater, the epithelia of the eel are constantly challenged by the osmotic gradient created between the external medium (high osmotic potential/ low osmolality) and the internal plasma (low osmotic potential/ high osmolality). The physiological challenge is reversed in seawater as the external salinity induces water loss across epithelial surfaces as well as ion gain. To combat oedematous or dehydrating conditions, and maintain osmotic homeostasis, eels possess an arsenal of ion and water transport pathways. These are used in concert across the three main osmoregulatory tissues; kidney, intestine and gill, with the latter being responsible for the majority of ion movements to balance diffusional gains or losses (Evans, 1999; Petr, 1968).

The salt and water transporting systems are highly labile and rapidly upregulate or downregulate when the animal changes environmental salinity. In addition to regulation of expression, the distribution of ion transporters in key regulatory tissues can also be salinity dependent. The cystic fibrosis transmembrane conductance regulator, for example, will redistribute from the apical surface to the basolateral surface of epithelial tissues in the gill, kidney and gut when the eel adapts to freshwater from seawater (Marshall and Singer, 2002).

In freshwater, volaemic homoestasis is achieved principally by the excretion of large volumes of urine (Gaitskell and Jones, 1971). Even though the urine is very dilute, salts are lost in this process and the eel must actively absorb ions via branchial epithelial mitochondria-rich cells in the gill (Ando, 1981; Baldisserotto and Mimura, 1994) which supplements those obtained from ingested food and water. In the marine environment, the eel maintains a relatively stable blood plasma osmolality level by increasing drinking, secreting excess ions via epithelial surfaces in the gill and excreting low volumes of urine which is approximately isosmotic to the plasma (Beyenbach, 1995; Cutler and Cramb, 2001).

2.3 Osmoregulatory adaptations: Gill

The primary role of the gills in fish is one of gas exchange, for which there is a large epithelial surface area arranged over a complex series of branchial arches subdivided into multiple filaments which are then partitioned further into lamellae. With such a large surface area specifically adapted for rapid diffusion of gases, the gills are susceptible to water uptake and ion loss in freshwater whilst the converse is true in seawater. The eel gill physiology adapts physiologically, however, in order to absorb or secrete ions in freshwater and saltwater respectively. Differences in both osmotic membrane permeability and blood perfusion of the gill epithelia are also exhibited between the two environmental salinities.

The epithelia of the gill are made of three main cell types; pavement cells, which make up approximately 90% of the gill surface area; mitochondria-rich cells (also know as chloride cells) and accessory cells. The pavement cells are joined to each other and to mitochondria-rich cells by deep-tight junctions consisting of several multi-strand protein connections (e.g. claudins, occludins and junctional adhesion molecules), whilst links with accessory cells consist of fewer strands and are therefore deemed thin-tight junctions (Karnarky, 1992). The mitochondria-rich cells mediate the net loss or gain of ions via a suite of membrane ion transport mechanisms (Evans et al., 1999) but pavement cells have also been indicated to play a role in Cl^- uptake (Wood et al., 1998).

Trans-epithelial ion transport, cell volume and integrity are maintained by the chloride-cation-cotransporter family which is important during salinity adaptation (Cutler and Cramb, 2002b; Haas and Forbush III, 2000). This family includes NKCC1 which is found primarily on the basolateral membranes of secretory epithelia. Their role is to transport Na^+, K^+ and Cl^- ions across this membrane in an electrically neutral way with two Cl- ions being transported with one ion each of Na^+ and K^+ (Russell, 2000).

Freshwater adapted gill: During freshwater acclimation of the eel there is a net influx of chloride ions from the external medium across the gill epithelium. The dilute nature of freshwater and the inherent electrochemical gradients necessitate an active transport mechanism to facilitate Na^+ and Cl^- uptake. The basolateral membrane of the gill mitochondria-rich cell has extensive infoldings which produce a high surface area and extensive tubular system. Associated with this membrane are high numbers of mitochondria and the transport enzyme Na^+/K^+-ATPase (Karnaky et al., 1976), which uses ATP to drive $3Na^+$ from the mitochondria-rich cell into the extracellular compartment in exchange for $2K^+$. This process in addition to the action of K^+ channels sets up an electrochemical gradient from the extracellular fluid to the cytosol of the mitochondria-rich cell. When acclimated to seawater, Na^+ coupled to K^+ and Cl^- travel down the electrochemical gradient into the cell via a common basolateral transport protein, the NKCC1 isoform of the $Na^+/K^+/Cl^-$ cotransporter family (Degnan, 1985; Evans et al., 1999). Chloride ions then cross the apical membrane via anion channels such as the cystic fibrosis transmembrane conductance regulator (CFTR), whilst Na^+ exits via paracellular pathways through the thin-tight junctions between chloride and accessory cells.

Chloride uptake in freshwater acclimated yellow eels is thought to occur via $Cl^-/HCO3^-$ exchange, which also plays a role in acid-base regulation (Cutler and Cramb, 2001). This view is supported by the circumstantial evidence that acetazolamide and thiocyanate, $Cl^-/HCO3^-$ exchange inhibitors (Nguyen et al., 2004), cause a lowering of the Cl^- concentration in cultured *Salmo trutta* mitochondria-rich cells, as measured by X-ray microanalysis of frozen tissues (Morgan, 1994). The $Cl^-/HCO3^-$ exchanger has been localised to mitochondria-rich cells in gill epithelia of teleosts by localisation of the mRNA in the rainbow trout (*Oncorhynchus mykiss*) (Sullivan, 1996) and of the protein in freshwater tilapia (*Oreochromis mossambicus*) and mudskipper (*Periophthalmodon schlosseri*) (Wilson, 2000b). The precise involvement of pavement cells in this process remains unresolved; in vitro experiments assessing flux ratios of Na^+ and Cl^- across a cultured branchial epithelium from rainbow trout, thought to consist of pavement cells alone, showed active

chloride uptake at the apical surface and associated passive Na^+ transport (Wood et al., 1998). In separate experiments, however, acetazolamide and thiocyanate had no effect on intracellular Cl^- concentrations of brown trout (*Salmo trutta*) pavement cells (Morgan and Potts, 1995; Morgan, 1994).

Greg Goss and co workers illustrated that, in freshwater, the gill epithelium of rainbow trout (at least) exhibit two functioning sub-populations of mitochondria-rich cells (Goss, 2001). The morphologically identical subgroups were distinguished by their ability to bind peanut lectin agglutinin. The main function of mitochondria-rich cells that do not bind peanut lectin agglutinin (PNA^- cells) appears to be sodium uptake and acid secretion (Figure 2.3.1.a). They exhibit higher levels of H+-ATPase activity and acid stimulated Na+ uptake, the latter being sensitive to both phenamil and bafilomycin. H^+-ATPase is a H^+ pump which actively secretes protons to the external medium. This creates an electrochemical gradient with a net positive charge outside the cell and a negative charge within the cell. Conversely, the peanut lectin agglutinin binding (PNA^+) mitochondria-rich cells have a chloride uptake and base secretion function. These cells have high levels of Na^+,K^+-ATPase, half the level of H^+-ATPase and lack phenamil sensitive Na^+ transport (Figure 2.3.a).

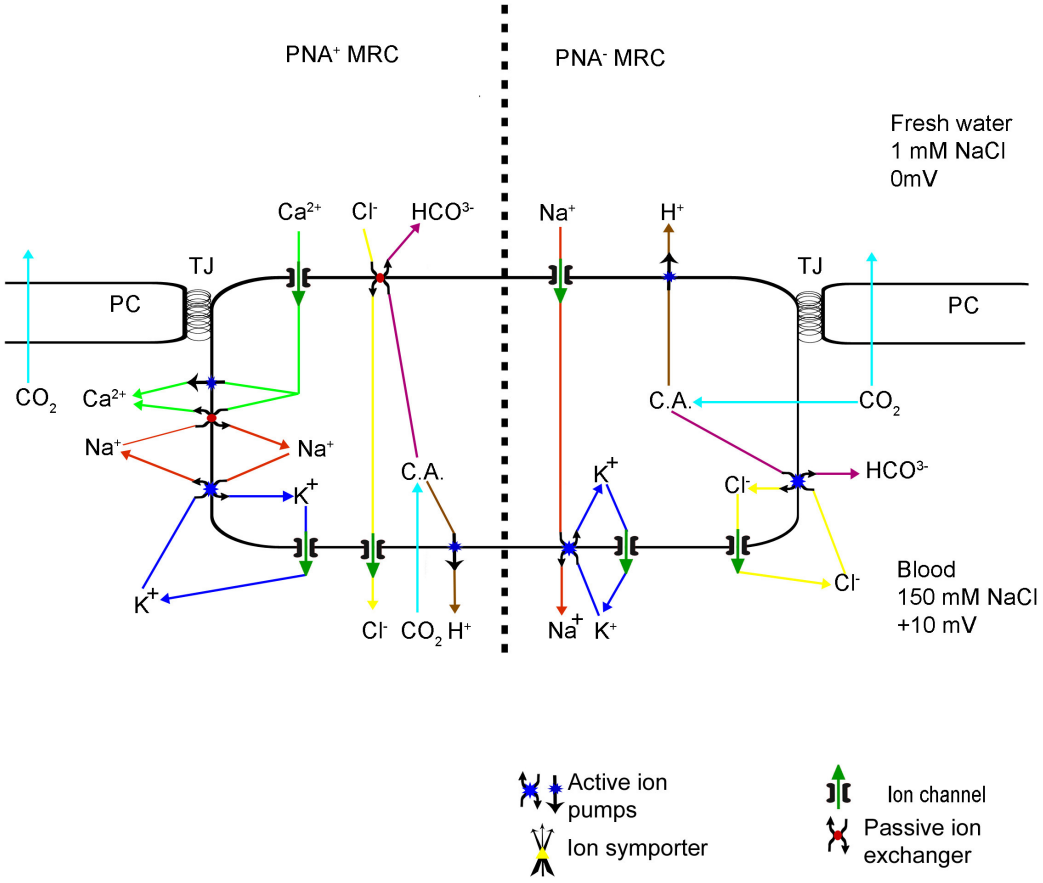

Figure 2.3.a. Freshwater adapted gill epithelial model. The morphologically identical mitochondria-rich cell subgroups, identified by their ability to bind peanut lectin, have distinct functions. PNA$^-$ mitochondria-rich cells have a chloride uptake/base secretion function which is driven by apical H+-ATPase activity. PNA$^+$ mitochondria-rich cells, however, have a sodium uptake/ acid secretion function driven by a basolateral proton pump. PNA: peanut agglutinin, MRC: mitochondria rich cell, TJ: tight junction, PC: pavement cell, C.A.: carbonic anhydrase.

Water transport across the gill epithelium occurs via simple diffusion through both the trans-cellular membranes and paracellular pathways. If these were the only pathways for water transport in eels then the epithelia of both freshwater and seawater acclimated fish would have a similar permeability to water but this is not the case. The branchial epithelial water permeability is ~6 fold higher in freshwater adapted eels compared to their seawater adapted counterparts (Isaia, 1984). Additional water transport

mechanisms must therefore be present and it is in this role that aquaporins (AQPs) are believed to play a part. Aquaporins are members of an ubiquitous family of channel-forming proteins, originally known as the major intrinsic protein (MIP) family, and function as molecular water channels that allow rapid osmotic water flow mainly in epithelial tissues (Deen and van Os, 1998). A cDNA homologue of the mammalian aquaporin 3, the first aquaporin to be cloned in the eel, was isolated from eel gill and subsequently shown to be expressed in the gill, eye, intestine and oesophagus with sporadic expression in the kidney (Cutler and Cramb, 2002). Expression of this protein is most prevalent in the freshwater adapted eel gill and a decrease in expression of up to 94% is seen following adaptation of the eel to seawater (Cutler and Cramb, 2002). The discovery of this peptide could explain the discrepancy between water permeability of membranes in eels adapted to different salinities.

Seawater adapted gill: The gill is the major site for salt secretion in the seawater-adapted eel. A typical mitochondria rich cell in seawater has an apical crypt and a basolateral tubular system. The tubular system is made of invaginations into the cell, toward the apical surface, which effectively brings the two membranes to within 2-5 µm of each other. This allows the membrane to function, essentially, as a thin NaCl pump. Salt secretion is driven by Na^+,K^+-ATPase which keeps intracellular Na^+ levels low (figure 2.3.b). This enzyme was localised to the basolateral membrane using the specific binding of tritiated ouabain (Karnaky et al., 1976), and more recently, TEM and immunogold studies have also shown it to be located specifically in the tubular system (Dang, 2004). Chloride ions can then enter across the basolateral membrane (via the Na^+,K^+,2Cl co-transporter) and they leave through apical CFTR type anion channels. This creates a membrane potential enabling sodium ions to follow by passive diffusion through a cation specific leaky paracellular shunt formed between the mitochondria rich and accessory cells.

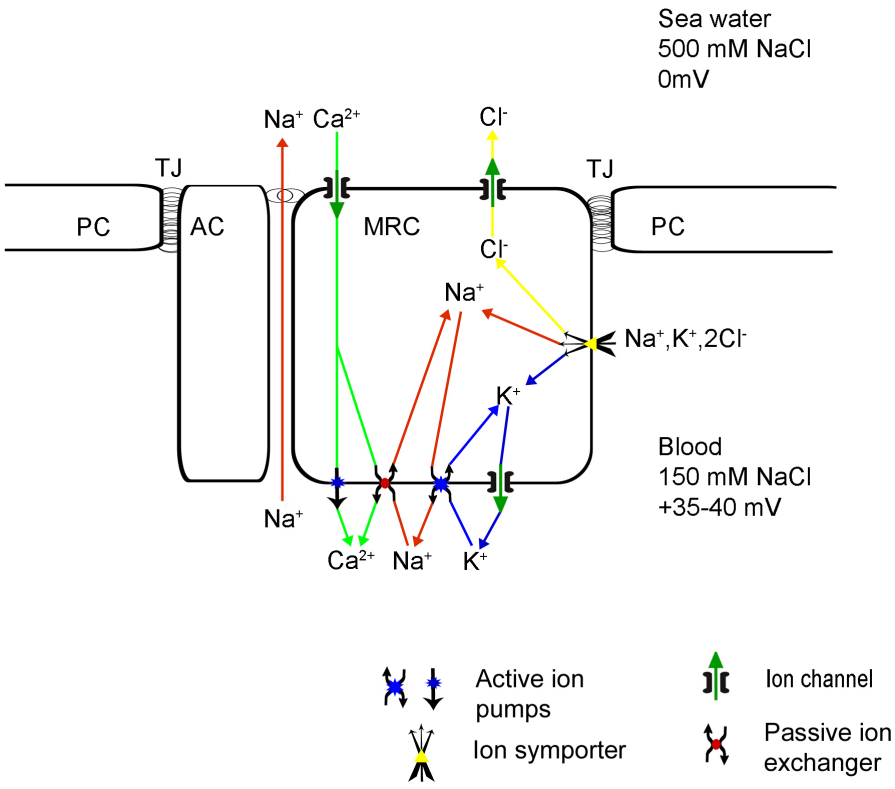

Figure 2.3.b. Ion transport across the seawater adapted gill epithelium. The basolateral membrane of the MRC is potentiated by Na^+,K^+-ATPase which drives Cl^- entry by $Na^+,K^+,2Cl^-$-ion symporter. Cl^- crosses the apical membrane through CFTR-like ion channels and Na^+ follows passively through paracellular routes. Also shown is Ca^{2+} absorption by a pathway independent to the secretion of NaCl. Not shown is the apical crypt or basolateral tubular system normally associated with the MRC. AC; accessory cell, MRC; mitochondria-rich cell, PC; pavement cell, TJ; tight junction.

2.4 Osmoregulatory adaptations: Renal system

The kidney of the eel is fully glomerular but it lacks the loop of Henlé found in mammals (Cleveland and Trump, 1969; Hentschel and Elger, 1989). The apical surface of the renal tubules is lined by an apical brush border which affords a large surface area for ion transport and fluid secretion/absorption depending on the salinity of the external habitat (Martinez et al., 2005).

Freshwater adapted renal system: In freshwater adapted eels, the glomerular filtration rate is high and nearly all filtered solutes are reabsorbed across the epithelia of the renal tubules; furthermore, ions are also reclaimed across the epithelia of the urinary bladder (Cutler and Cramb, 2000). In vertebrates the vast majority of these resorptive processes occur in the distal tubule but in teleosts (bar the lampreys) they occur in the proximal tubule (Dantzler, 2003). In the early distal tubule (figure 2.4.a) salt uptake is driven by basolateral Na^+,K^+-ATPase and facilitated by the apically located sodium, potassium, chloride co-transporter (NKCC2 isoform) (Dantzler, 2003). The latter mechanism is dependent on K^+ cycling through apical potassium channels and allows cellular Cl^- to accumulate and then exit passively down the concentration gradient via basolateral chloride channels and K^+:Cl^- cotransporters (Braun and Dantzler, 1997). Na^+:H^+ exchange and paracelluar routes may also contribute significantly to Na^+ transport. The transport mechanisms of the late distal tubule remain to be elucidated. The urinary bladder of freshwater adapted teleosts has a tight epithelium and is largely impermeable. Additional Na^+ and Cl^- are reclaimed from the urine as the urine is further diluted to ~2 mM (Marshall and Grossel, 2006).

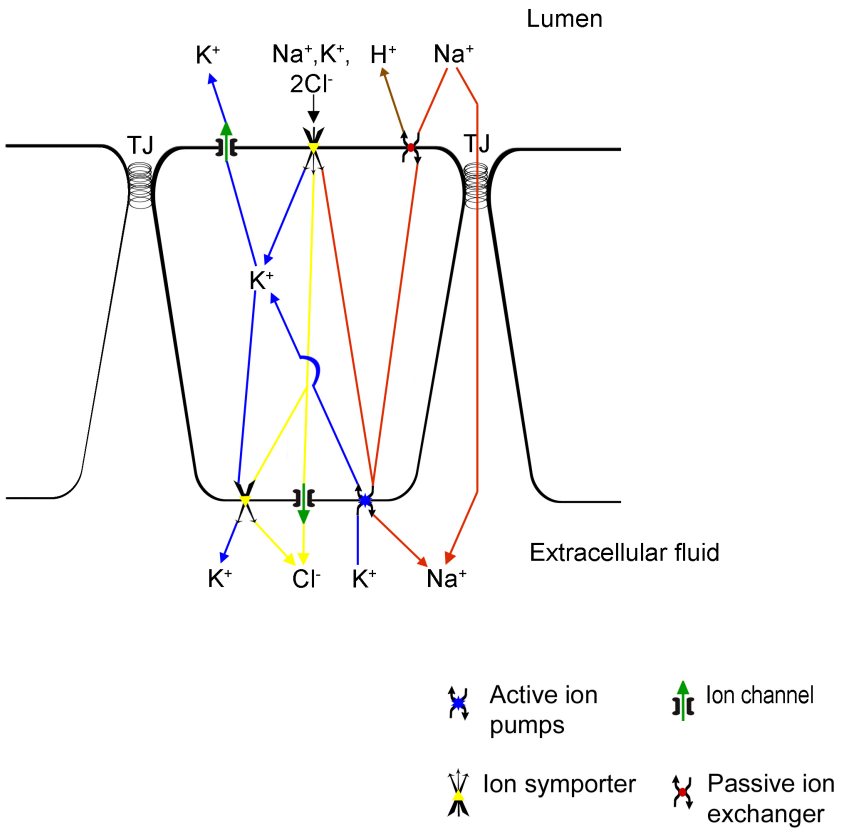

Figure 2.4.a. Ion transport mechanisms in the water impermeable epithelium of the early distal tubule of the freshwater eel. Basolateral Na^+,K^+-ATPase drives the process of salt reabsorption by creating gradients to allow apical import of Na^+, K^+ and Cl^-. K^+ is recycled apically through K^+ channels whilst Cl^- exits basolaterally through K^+:Cl^- cotansporters. Na^+ also crosses the membrane via paracellular routes and Na^+:H^+ exchange.

Seawater adapted kidney: In seawater adapted eels, the glomerular filtration rate is significantly reduced in order to conserve water, and tubular secretion of electrolytes and fluid contribute significantly to urine formation. Lacking a loop of Henlé, eels are unable to produce urine that is hypertonic to plasma but the kidney's osmoregulatory role in seawater is nonetheless essential, serving primarily as the main secretory route for absorbed Mg^{2+}, $Ca^{2+}$and SO_4^{2-} (Bone et al., 1995; Cleveland and Trump, 1969; Karnaky,

1998). The urine of seawater adapted eels has a tonicity similar to the extracellular fluid but with Mg^{2+}, SO_4^{2-} and Cl^- replacing Na^+ and Cl^- as the major electrolytes. Tubular secretion, which may exceed glomerular filtration by as much as four fold, occurs in the early proximal tubule (Beyenbach, 2004). Here, Cl^- is secreted by a secondary active process driven by basolateral Na^+,K^+ ATPase. Chloride ions enters basally through the NKCC1 $Na^+/K^+/2Cl^-$ cotransporter before exiting apically through CFTR-like anion channels (Figure 2.4.b). There is net secretion of Mg^{2+}, SO_4^{2-}, Na^+ and Cl^- in the early proximal tubule with the latter two ion types being largely reabsorbed in the late proximal tubule. Here, again, the driving force is basolateral Na^+, K^+ ATPase which creates a diffusion gradient allowing apical Na^+-glucose and Na^+-amino acid coupled transport.

Even before reaching seawater, freshwater adapted silver eels migrating downstream are thought to prepare physiologically for the impending change in salinity. The expression levels of the 1a isoform of $Na^+/K^+/2Cl^-$ cotransporter (NKCC1a) in the kidney increases during the silvering process but remains constant during seawater-acclimation of silver eels (Cutler and Cramb, 2002b). This suggests a pre-acclimation to seawater, controlled as part of a developmental process and occurring prior to leaving freshwater.

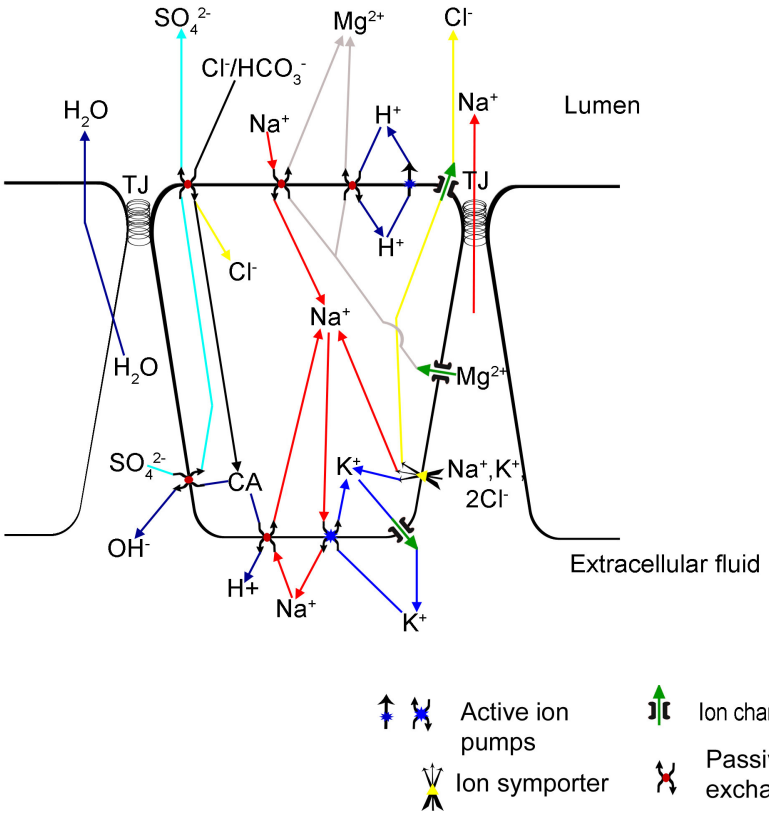

Figure 2.4.b. Ion transport mechanisms in the early proximal tubule of the seawater adapted eel kidney. There is net secretion of Mg^{2+} (via H^+ and Na^+ exchange), SO_4^{2-} (dependent on C.A.), Cl^- (driven by basolateral Na^+,K^+-ATPase) and Na+ (by electrically coupled paracellular pathways). K^+ enters the cell basally via Na^+,K^+-ATPase and $Na^+/K^+/2Cl^-$ cotransporter, and is recycled through basolateral K^+ channels. Na^+ is excreted via paracellular routes and Na^+:H^+ exchange. Water is lost down the resultant diffusion gradient. CA: carbonic anhydrase, TJ: tight junction.

2.5 Osmoregulatory adaptations: Intestine

The freshwater adapted eel drinks little, other than what is imbibed during feeding (Martinez et al., 2005). The ingested food provides the eel with a valuable source of salts, but otherwise the role of the intestine in freshwater osmoregulation is limited. Following seawater adaptation, however, drinking rates of the eel are markedly increased (> 10 fold) and the intestine takes on a key osmoregulatory role (Gaitskell and Jones, 1971). Ingested seawater is desalinated as it passes through the gut, largely by active transport of monovalent ions across the epithelia which starts in the oesophagus and continues throughout the intestine and rectum. The subsequent reduction in salinity of the luminal fluid allows water to be absorbed by passive osmosis (Skadhauge, 1969); a process facilitated by the large surface area of the brush border membranes of the luminal epithelial cells. The mechanism of Na^+ absorption from luminal fluids is powered by basolateral Na^+,K^+-ATPase which creates a diffusion gradient to drive apical Na^+ influx via Na^+/Cl^- and $Na^+/K^+/Cl^-$ co-transporters (Loretz, 1995). Cl^- uptake also occurs via bicarbonate transporters which secrete HCO_3^- in exchange for Cl^- (Ando, 1990). Thus far, cDNAs representing three chloride-bicarbonate exchanger isoforms have been found in the eel intestine (Cutler and Cramb, 2001). The bicarbonate is then rendered electrochemically inert by precipitation. A schematic summary of ion transport across this membrane is shown in figure 2.5.a. Upon initial examination this process could not drive water uptake but if the bicarbonate was derived from the osmotically inert cellular CO_2 then there would be a net influx of ions into the epithelial cells, thus aiding water uptake (Wilson et al., 2002).

Sodium/ bicarbonate co-transporter genes have also been isolated from eel intestine, as well as the gill and kidney tissues (Cutler and Cramb, 2001). The sodium/ bicarbonate co-transporter are thought to be located on the basolateral membrane of the luminal epithelial cells (Grossel et al., 2001) and may therefore provide extra HCO_3^- for the apical chloride-bicarbonate exchange. In addition, the process of transporting one sodium ion with two or

three bicarbonate ions from the extracellular fluid into the epithelial cell is electrogenic (Romero and Boron, 1999). This would hyperpolarize the cell membrane potential, thereby providing a driving force for basolateral Cl^- efflux via chloride channels (Cutler and Cramb, 2001).

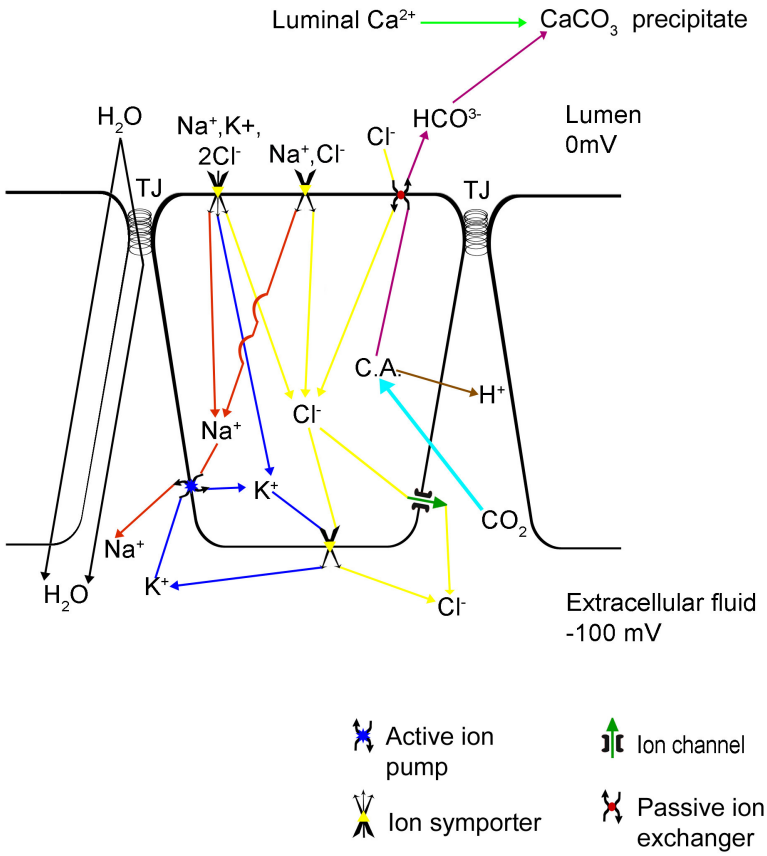

Figure 2.5.a. Ion transport across the seawater adapted intestinal membrane. Apical Na^+ uptake through co-transporters is driven by basolateral Na^+,K^+-ATPase. Apical Cl^- uptake occurs via HCO_3^-/Cl^- exchange and exits basolaterally through CFTR-like anion channels. Intracellular bicarbonate comes from hydration of dissolved CO_2 by carbonic anhydrase. Not shown are the basolateral sodium/ bicarbonate exchangers. TJ: tight junction, CA: carbonic anhydrase.

2.6 Introduction to brain function in osmoregulation and development.

Co-ordination of responses involves the reception of stimuli and subsequent reaction. Exogenous signals include day length, lunar phases, tides, water levels in rivers as well as external salinity. Endogenous signals include levels of energy stores (adiposity) and plasma osmolality and pH. Responses are mediated by the neuroendocrine and endocrine signalling pathways which invoke the appropriate responses from specific cells and tissues.

In the case of salinity adaptation there are various local and circulatory signalling systems and agents which modulate the expression and function of ion and water transporters in eel tissues (Evans, 2002).

When teleosts are faced with an osmoregulatory challenge there are two hormonal response types; the first is fast and short-acting whilst the second is slow and long-acting. The first type offer an immediate response to the osmoregulatory stress but are often cleared from the system within minutes (Takei and Hirose, 2002). They include oligopeptide hormones such as angiotensin II, arginine vasotocin, natriuretic peptides and urotensins which target specific epithelia where they modulate existing ion channels or transporters by phosphorylation or dephosphorylation of key residues. The long-acting response hormones show gradual increases to elevated levels for prolonged periods of several hours or longer. This group incorporates cortisol, growth hormone (GH), insulin-like growth factors (IGFs) and prolactin (PRL) and stimulate the synthesis of ion channels and transporters and induce structural reorganisation so that the animal can cope, long term, with its new environmental salinity.

The central control for many hormone secretions is the hypothalamus which regulates pituitary secretions through the actions of a variety of hormones which include; growth hormone-releasing hormone, pituitary

adenylate cyclase activating polypeptide, corticotropin-releasing hormone, somatolactin release-inhibiting hormones and thyrotropin releasing hormone. The tiered organisation of these systems is shown in context with their secretion sites, pathway induction and site of action (Figure 2.6.a).

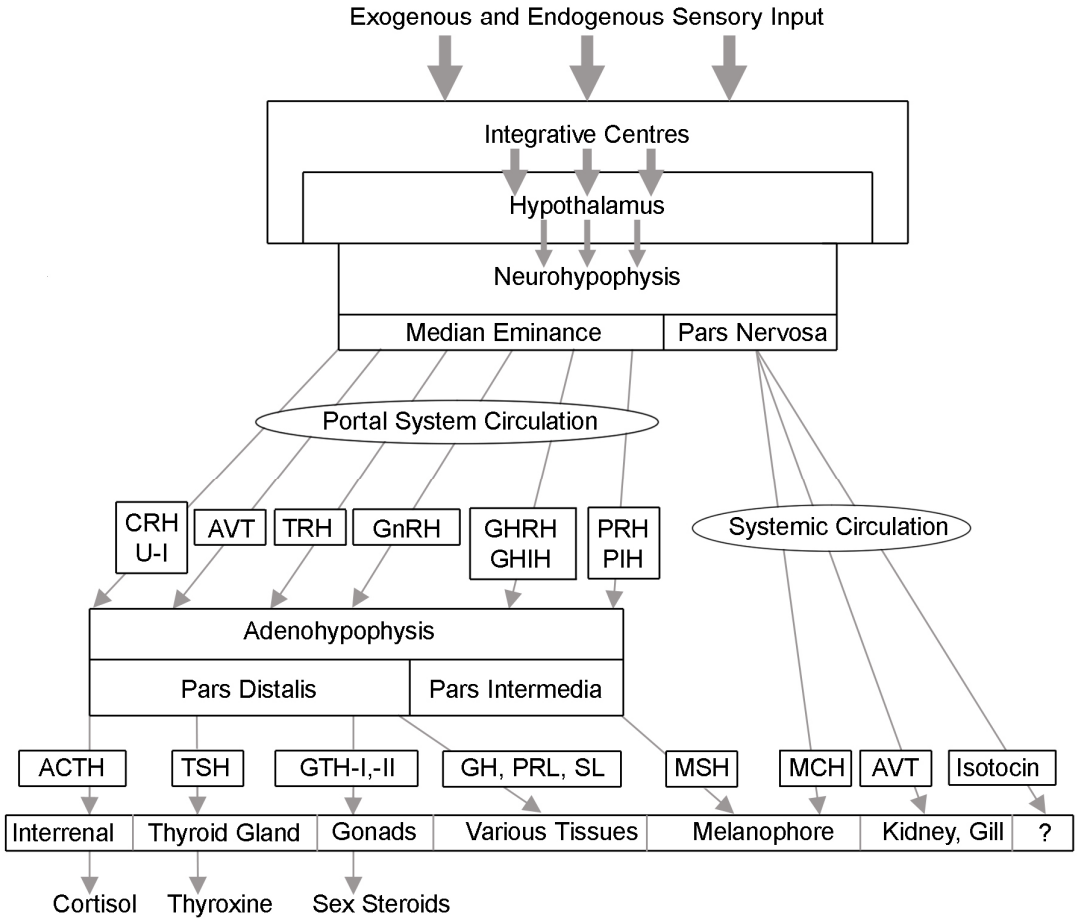

Figure 2.6.a. Hierarchical overview of the response to sensory input via the hypothalamo-hypophysial axis resulting in an endocrine cascade to peripheral glands and tissues. CRH: corticotropin-releasing hormone, U-I: urotensin-I, AVT: arginine vasotocin, TRH: thyrotropin-releasing hormone, GnRH: gonadotropin-releasing hormone, GHRH: growth hormone-releasing hormone, GHIH: growth hormone-inhibiting hormone, PRH: prolactin-releasing hormone, PIH: prolactin-inhibiting hormone, ACTH: adrenocorticotropic hormone, TSH: thyroid stimulating hormone, GTH-I and -II: gonadotropin-I and –II, GH: growth hormone, PRL: prolactin, SL: somatolactin, MSH: melanophore stimulating hormone, MCH: melanin concentrating hormone. Adapted from Takei and Loretz, 2006.

One of the principal sites of hormone secretion is the pituitary gland, which is subdivided into two functionally and anatomically distinct sections: the anterior pituitary and the posterior pituitary (neurohypophysis) (Figure 2.6.b.). The anterior pituitary (adenohypophysis) originates from the nasopharangeal epithelium and is subdivided into the rostral pars distalis and proximal pars distalis. It is responsible for the secretion of gonadotropin-I and –II (orthologous to follicle stimulating hormone and luteinising hormone respectively), thyroid stimulation hormone, growth hormone, prolactin, adrenocorticotropic hormone and somatolactin. The posterior pituitary is derived from neural tissue and comprises the pars intermedia and pars nervosa and secretes the neuroendocrine hormones; melanin concentrating hormone, arginine vasotocin and isotocin.

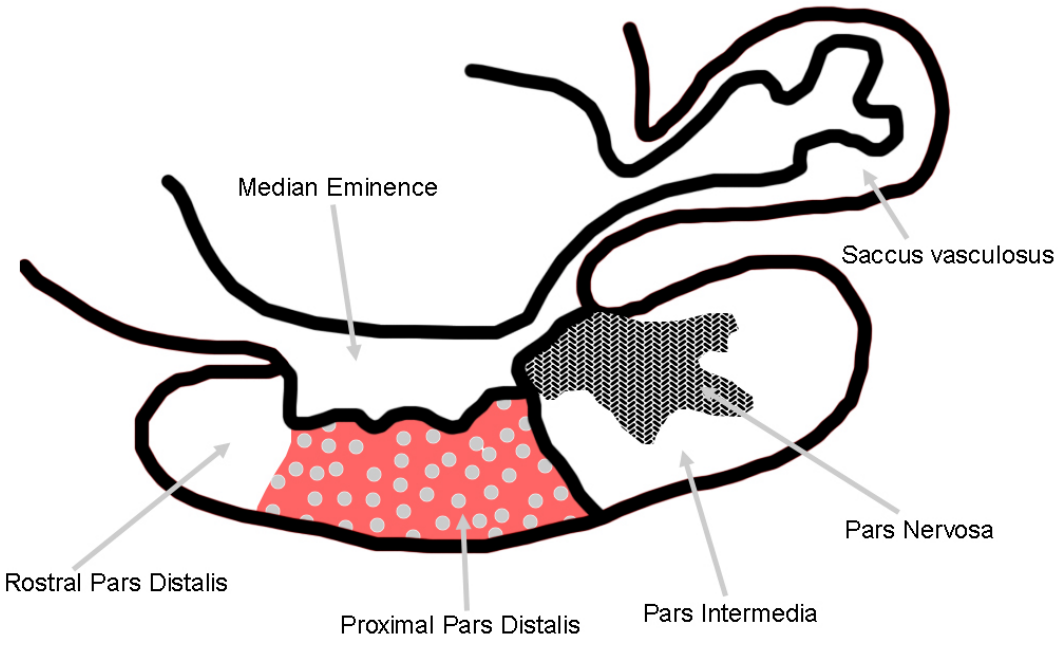

Figure 2.6.b. Hypothalamo-hypophysial structure of the eel.

Hormone secretions are not, however, restricted to those tissues laid out in Figure 2.6.a. Teleosts also possess a caudal neurosecretory system in the posterior section of the spinal chord comprised of Dahlgren cells and

responsible for urotensin-I and –II secretion, reviewed in Kobayashi et al (1986). Additionally, atrial natriuretic peptide, a seawater adapting hormone (Takei and Balment, 1993), is secreted by the heart whose release is stimulated by increases in plasma osmolality in teleosts (Kaiya and Takei, 1996) and by cardiac stretch in mammals (Farrell, 1999). Upon exposure to seawater the blood volume in the eel decreases (Kaiya, 1996b), which would normally inhibit ANP secretion in mammals. In teleosts, however, the increase in plasma osmolality has an overriding effect and ANP secretion increases. This in turn causes a dose dependent decrease in angiotensin II levels which inhibits both drinking (Tsuchida, 1998) and Na^+/Cl^- absorption by the intestine (Loretz, 1997). This appears, at first, to be counter intuitive as the eel in seawater must drink copiously to ensure adequate water uptake. Indeed, upon initial transfer to seawater the eel elevates its drinking rate substantially, a response which is initiated by external chloride receptors as it occurs prior to increases in plasma osmolality (Takei et al., 1998). Drinking rapidly abates, however, as the influence the plasma osmolality-stimulated increase in ANP secretion overrides these mechanisms. Increased ANP secretion and the associated anti-dipsogenic effects are transient, however, decreasing after 1-2 hours post seawater transfer (Kaiya and Takei, 1996b), at which point drinking rates become elevated once again. Therefore this system allows the eel a period of respite, during which, alimentary ion transport systems can adapt to seawater.

Following the work by Utida et al the traditional view was that, amongst teleosts, cortisol was *the* seawater adapting hormone and prolactin was *the* freshwater hormone (Utida et al., 1972). In the freshwater adapted killifish for example, *Fundulus heteroclitus*, plasma cortisol levels peak 1 hour post transfer to seawater, which coincides with the highest plasma Na^+ level (Marshall, 1999). More recent studies have now shown that cortisol may actually have a dual role as it is also implicated in ion uptake, whilst seawater acclimation also involves the growth hormone (GH)/ insulin like growth factor I (IGF-I) axis (McCormick, 2001). Salmonids treated long term with GH (Komourdjian et al., 1976) or transgenically over expressing the hormone (Saunders et al., 1998) show elevated levels of salinity tolerance. Although

larger fish will have an inherently greater salinity tolerance, the same effect has been noted just 48 hours following growth hormone injection, before any size effects could be implicated (Bolton et al., 1987). Several salinity related physiological changes induced by GH and IGF-I have been noted. Prunet et al (1994) found GH treated Atlantic salmon exhibited increased numbers of secretory mitochondria rich and accessory cells in the gill. *In vivo* Na^+,K^+-ATPase expression and activity are also raised in the gill mitochondria rich cells (Mancera and McCormick, 1998; Sakamoto et al., 1997), as is the Na^+-K^+-$2Cl^-$ cotransporter (Pelis and McCormick, 2001). Examining the system from the other side, elevated levels of GH and IGF-I have been shown in salmonids following salinity challenge (Sakamoto et al., 1993). Pertinent to the current study, however, is the lack of evidence which relates GH and IGF-I to osmoregulation within the anguillid eels. In cultured pituitary cells, an osmotic challenge had no effect on GH secretion levels (Suzuki et al., 1991; Suzuki et al., 1990). Additionally, eels have also been shown to survive in seawater without a pituitary, and therefore without growth hormone (Takei and Hirose, 2002).

In addition endocrine and neuroendocrine systems discussed, there must be also be pathway for sensing and coordinating environmental cues with endogenous factors to bring about eel silvering at a time to maximise reproductive success. Furthermore the eel must be able to react to additional environmental signals which dictate the timing of migration in a way that synchronises their arrival at the spawning grounds. One such mechanism for co-ordinating these responses in the eel could involve leptin (Zhang et al., 1994), which has been characterised as a signal peptide relating somatic energetic status to the reproductive system. Early leptin research focussed on the function of this adipocyte secreted peptide in relation to appetite regulation (Campfield et al., 1995). However, knockout mice, either incapable of producing leptin (*ob/ob*) or lacking the leptin receptor (*db*/*db*) were found to be infertile, suggesting a role in reproductive pathways. Subsequently, experiments showed that direct injection of human recombinant leptin could restore fertility of *ob*/*ob* mice mutants, cementing its place as a reproductive

signal peptide (Chehab et al., 1996). The first reported mechanism of interaction with reproductive pathways in mice was shown by direct injection of leptin which induced an increase in levels of circulating LH (Barash et al., 1996). Likewise, leptin has since been shown to influence follicle stimulating hormone in a similar way (Yu et al., 1997).

Leptin has recently been cloned in a number of teleost fish (Huising et al., 2006; Kurokawa et al., 2005) but the process of understanding its role is in its infancy. Some of the functions of teleost leptin appear to be conserved with other chordates, but the mechanisms involved remain unclear. In mammalian systems leptin appears to be antagonistic to neuropeptide Y, but this relationship is not immediately discernable in teleosts. Ammar *et al* (2000) showed that leptin is an appetite suppressant and stimulant of reproductive behaviour whilst neuropeptide Y stimulates eating and suppresses reproductive behaviour. The opposing roles of these two peptides is further highlighted by the direct inhibitory action of leptin upon neuropeptide Y synthesis in the hypothalamic arcuate nuclei (Baskin et al., 1999). As mentioned previously, leptin has been shown to cause an increase in LH secretion in mice but in teleosts, neuropeptide Y has also been shown to stimulate LH release. Two parallel studies, one on goldfish (Kah et al., 1989) and the other on rainbow trout (Bernard et al., 1989) both showed that porcine neuropeptide Y treatment of *in vitro* pituitary cell cultures induced a dose dependent increase in LH release. These findings are in agreement with a more recent *in vivo* study of seabass (*Dicentrarchus labrax*), which also showed that neuropeptide Y causes an increase in LH secretion (Cerda-Reverter et al., 1999). The effects of neuropeptide Y in this case, however, were dependent on nutritional state; stimulation of LH secretion was only seen in chronically fasted animals whilst the effects were suppressed in fed animals. One of the first leptin studies in teleosts treated cultured pituitary cells from carp (*Cyprinus carpio*) with purified mouse leptin and demonstrated an increase in secretion of LH; the amplitude of the response was dependent on the sexual maturation stage (Peyon et al., 2001). Therefore, at first glance the actions of leptin upon LH secretion appear to be complementary to those of neuropeptide Y. The situation is still unclear, however, as the stimulatory

effect on LH secretion seems to be nutritionally dependent for neuropeptide Y and developmentally dependent for leptin. These pathways are candidates for the regulation of sexual development in relation to energy stores in the eel, and may provide answers as to why, as in mammals, the onset of puberty is size not age dependent (Foster and Nagatani, 1999).

2.7 Introduction to Microarray Technology

There are many experimental approaches available which can be used to investigate biological systems. A hypothesis can be derived from known data of a model species and similar techniques can be reused to examine an unrelated organism. This approach has the advantage that tried and tested experimental techniques can be easily transferred to the system in question. It is, however, limited in the answers that it can provide and is unlikely to elucidate new and unexplored avenues of research. A different approach is to use screening tools which allow a wide range of potential targets to be studied simultaneously.

"Microarray Technology" describes a set of screening tools used to study the research fields which fall under the broad term "Genomics". These fields of research examine, in almost their entirety, a form of the genetic material or its derivatives of an organism. This ever broadening field now encompasses; genomics (study of all/most DNA), transcriptomics (study of all/most transcribed genes i.e. mRNA), proteomics (study of all/most proteins), metabolomics (study of metabolically relevant proteins), epigenomics (integrates disease modelling and genomics) and ecotoxicogenomics (integrates genomics and environmental toxicology). The present study will use transcriptomics by isolating and examining the mRNA. This has the advantage that mRNA lacks introns, promoters and non-transcribed DNA and a particular tissue will only express a subset of genes.

The challenge, however, when examining these fields is one of throughput; how to examine everything simultaneously. Microarrays provide one solution to this challenge and have revolutionised genomics. They allow the relative expression levels of thousands of features (DNA, mRNA or protein) to be simultaneously quantified. By comparing the expression of an experimental group with a control group, differences can be identified and subsequent expression profiles can be created. Such expression studies can provide insights into the function of genes and their products and to how they

are coordinated in a complicated and highly interlinked manner (Phimister, 1999). By clustering groups of seemingly co-regulated genes/proteins, previously unknown pathways can be highlighted and new lines of enquiry can be followed. Compared with traditional molecular biology experiments which examine genes or proteins in isolation, the use of microarray screening methods expedites the process of identifying possible relationships and finding novel genes.

The first published article to specifically use “microarrays” was Shena et al (1989) but the way in which a DNA microarray works has stemmed from the principles developed in Southern blotting techniques (Southern, 1975). These techniques use labelled nucleic acid molecules to interrogate nucleic acids attached to a solid medium via adenine-thymine and guanine-cytosine base hybridisation (Watson and Crick, 1953).

A cDNA microarray has the form of a regular microscope slide. The glass is of a higher quality, with fewer imperfections and a more uniform surface topology. The glass is coated so that the surface will bind cDNA strongly. Often a positively charged substance (e.g. poly-aminosilane) is used, which forms many interactions with the negatively charged cDNA to hold it in place. Amplicons are spotted onto the slide, traditionally using a pin spotter, so that each individual spot (~150 nm in diameter) comprises cDNA corresponding to a single gene transcript. This process is repeated so that up to ~ 20,000 features can be printed on a single slide to make the final microarray.

Two different probe sets (RNAs) isolated from an experimental and a control group are differentially labelled with fluorescent dyes (Cy3 and Cy5) and simultaneously co-hybridised to the cDNA microarray. The relative fluorescence (Cy3:Cy5) is quantified for each target by using a con-focal laser scanner. The Cy3:Cy5 ratio indicates which probe sequences have hybridised to the targets on the array and thus reflects the relative expression of individual genes in each sample. This method therefore quantitatively measures the relative amount of mRNA in a sample giving an indication as to

which genes are being up-/down-regulated. To imply a functional endpoint for a level of transcription for a particular gene requires the assumption that transcript copy number directly influences protein activity. This assumption ignores several biological processes (e.g. protein folding and post-translational modifications) which occur after transcription and before resultant performs its role. Despite this caveat the revealed data can be enlightening, to say the least.

Microarray techniques and genomic studies have traditionally been associated with model organism such as *H. Sapiens, D. melanogaster, C.elegans, M.musculus, A. thaliana* etc, but increasingly, non-model organisms are being investigated in this way (Cossins and Crawford, 2005). The European eel is one such non-model organism but as a fish it stands well placed to be of significant importance. Whilst most developmental and biological systems are common to all vertebrates, fish are by far the most specious, numbering over 28,000 extant species, which far outnumbers the mammals (~4600) or birds (~10,000) (Wilson and Reeder, 1993). Fish have managed to inhabit almost every piscine environment on the planet; hypersaline lakes, anoxic waters, highly pressured waters (<1000 Atm), the Arctic where ice fish rely on “anti-freeze” proteins to survive sub-zero temperatures and thermal springs where the temperatures can exceed 45 ºC. It has been suggested that the sheer diversity of fishes and their ability to adapt to niche habitats will, in conjunction with genomic studies, reveal some of natures most intriguing secrets (Oleksiak and Crawford, 2006). In addition, fish are unique in that their habitat is a medium in which they are immersed and effectively their environment is in direct contact with all bodily fluid compartments and tissues via the gills and gastrointestinal system (Randall et al., 2002). This has specific implications in the present study, as changes in environmental salinity will allow us to elucidate some of the important pathways involved in teleost osmoregulation.

There are already many fish genomic studies, the most advanced being the model oragnaisms zebrafish (*Danio rerio*), medaka (*Oryzias latipes*) and pufferfish (*Takifugu rubripes* and *Tetraodon nigroviridis*). Zebrafish is a

well-characterised developmental model species due in part to the transparent eggs and short reproduction cycle and has recently become the species of choice for gene knockdown studies for some of Sir David Lane's research groups. The pufferfish have some of the smallest known genomes and are thus a very attractive species for genomic studies. Non-model fish species are also increasingly under the genomic gaze. They include the the flounder (*Platichthys flesus*), killifish (*Fundulus heteroclitus*), rainbow trout (*Oncorhynchus mykiss*), several salmon species and the subject of the first genomic study of a non-model fish species which examined the hypoxic abilities of the goby (*Gillichthys mirabilis*, Gracey et al., 2001). Whilst model fish species certainly hold an important place in biological research, it will be the study of hyper-adaptable fishes such as the eel and those inhabiting extreme niches, along with subsequent comparative physiology that will facilitate the most fascinating discoveries over the coming years.

2.8 Hypothesis and aims.

The hypothesis to be investigated;

The brain is the central organ for the co-ordination of environmental cues (photoperiod, lunar cycle, temperature and environmental salinity) with the anatomical and physiological adaptations which accompany pre-migrational morphogenesis and the osmoregulatory plasticity seen in post-migrational, salinity-adapted fish.

The aims of the project;

Develop cDNA libraries for the brain, kidney, intestine and gill taken from eels adapted to both fresh and marine environments.
Use these cDNA libraries to create microarrays.
Determine gene expression profiles for yellow and silver eels adapted to freshwater and seawater.
Determine the cDNA sequence of potential genes of interest.
Validate the gene expression profiles using complementary techniques.

3.0 Materials and methods

The materials and methods chapter is presented in 27 sections.

Sections 3.1-3.4 detail the collection of eel tissues, RNA extraction and the preparation of messenger RNA.

Section 3.5 covers some commonly used techniques as well as buffer and oligonucleotide details.

Sections 3.6 – 3.23 detail the techniques used to create the cDNA libraries created during the project, the discursive timeline for this can be found in Results Sections 4.3 – 4.13.

Sections 3.23-27 detail the techniques associated with the microarray hybridisations and subsequent validation of results by real time quantitative PCR.

3.1 Animal treatment and tissue collection

Adult, sexually immature yellow and migrating, sexually maturing silver eels were captured in fresh water in the rivers and tributaries of the River Tay catchment area by a local supplier in Blairgowrie, Scotland. The occurrence of eels at the silver developmental stage is season dependent (Han et al. 2003) and as such the silver eels were caught in the autumn/winter during their downstream migration whilst yellow eels were caught all year round. Yellow eels were distinguished from silver eels on the basis of skin colour and head morphology and the independence between animal size and sexual maturation (Svedäng 1996; Vøllestad, 1992) was exhibited by a large weight range in both eel types (yellow=252

-540 g, silver=237-570 g). Eels were assumed to be all females as male eels tend to stop growing at ~150 g (Degani et al., 2003). Eels were kept in holding tanks (40 eels per 700 L tank) in the Gatty Marine Laboratory (St Andrews, Scotland) maintained on a 12h:12h light-dark cycle in fresh water (FW) at ambient temperature before experimentation until the experiments. Eels naturally undergo long periods of fasting as part of their natural life-cycle and as such, were not fed during the holding or acclimation periods.

Groups of eels (n=6) were transferred to experimental tanks (6 eels per 100 L tank) containing FW 2-3 days before experimentation. Salinity transfer was achieved by decreasing the water level to approx 5 % then re-filling back to initial levels over a 1 hour period with SW (salinity stressed) or FW (controls). Free flowing FW or SW was provided for each tank for the remainder of the acclimation period. Eels were concussed by striking the cranium and then killed by decapitation and pithed before removal of tissues. The groups of silver eels from the FW and SW tanks were killed at 6 hours, 2 days, 7 days and 5 months. Yellow FW and SW eels were killed at the 7 day time point. In total, 60 eels were used according to table 3.1.a below. Gill, intestine, brain, renal- and head-kidney tissues were collected from all eels.

Table 3.1.a. Eel acclimation groups.

Eel type	Condition	Acclimation time	Number of Fish
Silver	SW	6 Hours	6
Silver	FW	6 Hours	6
Silver	SW	2 Days	6
Silver	FW	2 Days	6
Silver	SW	7 Days	6
Silver	FW	7 Days	6
Silver	SW	5 Months (Longterm)	6
Silver	FW	5 Months (Longterm)	6
Yellow	SW	7 Days	6
Yellow	FW	7 Days	6

3.2 Metadata

Physiological data and biological observations, collectively known as metadata, were recorded for each fish used in the experiment; whole fish weight; tissue weight; presence of parasites and signs of disease (e.g., lesions on skin or internal organs); disturbance and kill times.

Additionally, blood samples from the silver eels were taken directly after decapitation and plasma properties (Figures 4.1.a - f) were recorded; plasma osmolality (assessed using a vapour pressure osmometer, Wescor Inc., Logan, US); plasma protein concentration; plasma cortisol concentration ; plasma angiotensin II; plasma Cl- (measured with a Chloride Analyser, Corning, Essex, UK); plasma Na^+ and K^+ concentrations (determined using flame photometry (Corning, Model 450).

3.3 Total RNA Extraction

The RNA extraction protocol was adapted from Chomczynski and Sacchi (1987). In brief, tissues were homogenised in 10 times volume:weight of Solution D (4 M guanadinium thiocynate, 10 % v/v β-mercapthoethanol, 1 mM EDTA, 10 mM Tris-HCl, pH 7.5) using a Polytron System PT3100 Homogeniser (Kinematica, Luzern, Switzerland) or using a syringe and 16 gauge needle. Following homogenisation the following solutions were added sequentially and votexed after each addition; 0.1 volume 2 M sodium acetate, pH 4; 0.5 volume phenol and 0.2 volume 1bromo-2chloropropane (BCP). Samples were centrifuged at 5020 g for 35 min at 0 ℃, (Beckman J6-M6, Rotor 4.2). The supernatant was transferred to a new tube and 0.2 volume BCP added, the mixture was then vortexed and centrifuged as before. The supernatant was mixed with 0.2 volume isopropan-2-ol and 0.2 volume High Salt Buffer (1.2 M NaCl, 0.8 M sodium citrate), vortexed and incubated at room temperature for 10 min before being centrifuged for 20 min at 5020 g at room temperature. The second BCP step was omitted to maximise the RNA yield from brain samples. The supernatant was removed and the remaining pellet was washed twice in 70 % ethanol and air dried before being resuspended in H2O (all water was distilled and purified >18mΩ (Milli-Q, Millipore, Waterford, UK)). The RNA concentration was calculated using spectrophotometric absorbance at 260 nm.

The quality of RNA was determined by visualising the 18 Svedberg unit (S) and 28S bands on a denaturing agarose gel (see Results 4.2). The denaturing agarose gel was made by suspending 1.2 g agarose (high pure, low EEO, BioGene, UK) in a mixture of H2O (65 ml) and 10 x MOPS buffer (10 ml, 0.5 M 3-(N-Morpholino)-propanesulfonic acid, pH 7.0; 50 mM sodium acetate; 5 mM EDTA) by boiling for several minutes and then cooled to 55 ºC. Fomaldehyde (18 ml) was added and the solution poured into a cast, a Teflon coated comb with the appropriate number of wells was inserted and the gel allowed to set at room temperature for 30 min. Gels were submersed in 1 x MOPS buffer. RNA samples (5 µl) were added to RNA loading buffer {28 µl;

formamide (62.5 % v:v), formaldehyde (9.25 % v:v), 1.25 x MOPS buffer, bromophenol blue (50 µg/ml)} and heated to 65 ºC for 15 min to denature the secondary structure of the RNA. The samples were cooled to room temperature and loaded into the wells and a current of 10 mV/cm applied until the bromophenol dye front had traveled ~2/3 of the length of the gel. The gel was washed for 30 min in H2O to remove formaldehyde followed by RNA staining by immersing the gel in a solution of ethidium bromide 10 µg/ml for 30 mins. Excess stain was removed by washing the gel three times in H2O for 30 min each.

Ratios of relative intensity of 18S:28S rRNA bands were determined by densitometric analysis using GeneSnap and GeneTools (Syngene, UK) and used to highlight degraded RNA samples; intact RNA should have an 18S:28S ratio of 1:2.

RNA quality was also verified with capilliary electrophoresis using a 2100 Bioanalyzer (Agilent Technologies, Palo Alto, California) carried out at Ninewells Hospital, Dundee, UK (see Results 4.2).

3.4 Messenger RNA Isolation

Messenger RNA (mRNA) for each tissue was isolated from total RNA pooled from each fish within a group. Each tissue pool contained 1.2 mg total RNA comprising 20 µg taken from each fish in each experimental (FW/ SW) and control (FW/ FW) group. mRNA was extracted from the total RNA by oligo (dT)-cellulose affinity column chromatography using an adaptation of a standard method (Berger and Kimmel, 1987). In brief, 0.25 g oligo (dT)-cellulose was resuspended in H_2O to remove fine particles and then stacked in a 3 ml clear syringe blocked with ashless cotton wool. Three column volumes (CV) of binding buffer (Tris-HCl 0.01 M, pH 7.5), NaCl (0.5 M), EDTA (1 mM, pH 8), 0.5 % SDS) were passed through the column. A peristaltic pump assisted the flow of liquid through the column and the final binding buffer was drawn through until level with the top of the cellulose. Total RNA (1.2 ml of 1 mg/ ml) was mixed with an equal volume of 2 x binding buffer and heated to 65 °C for 5 minutes, cooled on ice for 2 minutes, applied to the column and drawn through until level with the cellulose surface. The sample was left for 2 mins at room temperature and then the column was washed with 3 CV binding buffer. The entire eluate was collected, reheated to 65°C for 5 minutes, cooled on ice and reapplied to the column at room temperature. This was followed by a further 5 CV binding buffer and then 3 CV wash buffer (0.01 M Tris-HCl, 0.5 M NaCl, 1 mM EDTA, pH 7.5). The effluent was discarded and 9 ml elution buffer (0.01 M Tris-HCl, 1 mM EDTA, pH 7.5) was heated to 65 °C and passed through the column 1ml at a time and the eluate was collected in a 50 ml conical centrifuge tube. To precipitate the mRNA, 2.5 volumes 100 % ethanol and 0.1 volume 3 M sodium acetate (pH 5.2) were added to the eluate and the solution left overnight at 4 °C. The mixture was centrifuged at 5020 g for 40 min at 4 °C. The pellet was washed twice with 70 % ethanol at room temperature, allowed to air dry and then dissolved in 50 µl H_2O.

3.5 Commonly used techniques, buffers and oligonucleotides

The following techniques were used frequently during the development of the cDNA libraries (Sections 3.6 to 3.16). To minimise repetition the reader will be referred back to this section when standard protocols were used. Commonly used buffers and oligonucleotides are presented in Tables 3.5.a and 3.5.b respectively.

General PCR conditions: Reactions were carried out in a final volume of 25 µl containing 1 µl template DNA, 1 µl forward primer (10 mM), 1 µl reverse primer (10 mM), 5 µl betaine (5 M), 2.5 µl 10 x PCR buffer, 1 µl dNTPs (10 mM each), 3 µl magnesium acetate (25 mM), 0.5 U Accurase™ (Biogene, UK) and H_2O to 25 µl. Cycling parameters were 95 ºC for 2 min, followed by 40 cycles of 95 ºC for 10 s, X ºC (specific for each primer set) for 10 s, 68 ºC for 5 min (plus 20 s added incrementally per cycle), with final extension for 10 min.

DNA agarose gel electrophoresis: Agarose (1 g, high-pure low EEO, BioGene, Cambridge, UK) was suspended in 100 ml 1 x TAE buffer (4 mM Tris-acetate, 0.1 mM EDTA) and dissolved by boiling for several minutes. The solution was cooled to 40 ºC and ethidium bromide added to a final concentration of 1 µg/ ml before pouring into a mould and inserting a Teflon coated comb with the appropriate number of wells, and allowed to set at room temperature for 30 min. DNA samples were mixed 6:1 with 6 x DNA loading buffer {1 x TAE, bromophenol blue (1.2 %, w:v), glycerol (25 %, v:v)}. Gels were submersed in 1 x TAE buffer, DNA samples loaded and a current of 10 mV/cm applied until the bromophenol dye front had traveled ~2/3 of the length of the gel.

Spot blot: A 1 % agarose solution (15 ml) containing ethidium bromide was made as per DNA agarose gel method and poured into a 10cm diameter petri-dish and allowed to set at room temperature for 15 min. The underside of the petri-dish was marked out with a grid to localise samples.

DNA samples to be quantified were serially diluted and 1 µl of each dilution applied to the gel surface alongside serially diluted DNA solution of the plasmid pEXP7-tet (50 ng/µl, Invitrogen, Paisley, UK). DNA was visualised under UV light and comparatively quantified by eye.

DNA precipitation: Unless otherwise stated all DNA precipitation was performed by adding glycogen (1 µl, 20 µg/µl) to the DNA solution followed by 0.1 volume 7.5 M ammonium acetate and 2.5 volumes ice cold 100 % ethanol and incubated for at least 10 min at –20 ºC. DNA was pelleted by centrifugation at 15,000 g for 10 min, the supernatant removed and the pellet washed twice with 200 µl 70 % ethanol. The ethanol was aspirated, the pellet air-dried and resuspended in H_2O.

Table 3.5.a. Chemical details of commonly used buffers

1 x TE	Tris-HCl (10 mM), EDTA (1 mM)
1 x TAE	Tris-acetate (4 mM), EDTA (0.1 mM)
TEN buffer	10 mM Tris-HCl, pH 7.5; 0.1 mM EDTA; 25 mM NaCl)
1 x SSPE	180 mM NaCl, 1 mM EDTA, 10 mM NaH2PO4, pH 7.4)
10 x Black Buffer (Biogene, Cambridge, UK)	Tris-HCl (750 mM, pH 8.8), ammonium sulphate (200 mM) and Tween 20 (0.1%)
10 x Tris PCR Buffer	Tricine (150 mM), potassium acetate (200 mM), Tween 20 (0.1% v:v)
LB agar	Bacto-tryptone (10 g), bacto-yeast extract (5 g), NaCl (10 g), dissolved in 950 ml, pH adjusted to 7.0 with NaOH (~0.2 ml, 5 M), volume made up to 1 l with H20 and autoclaved.
Terrific Broth	Bacto-tryptone (12 g), bacto-yeast extract (24 g), glycerol (4 ml), dissolved in 900 ml, autoclaved, and added to a 100 ml sterile solution of KH_2PO_4 (0.17 M), K_2HPO_4 (0.72 M)
1 x SSPE buffer	150mM Sodium Chloride, 10mM Sodium Phosphate, 1mM EDTA
1 x SSC buffer	Sodium chloride (0.15 M), sodium citrate (0.015 M)
SOC	Bacto-tryptone (20 g), bacto-yeast extract (5 g), NaCl (0.5 g), dissolved in 950 ml,autoclaved and supplemeted with a sterile solution of KCl (10 ml. 250 mM, pH 7.0), a solution of $MgCl_2$ (5 ml, 2M) and a sterile solution of glucose (20 ml, 1 M)
mRNA isolation 1 x Binding Buffer	Tris-HCl (0.01 M, pH 7.5), NaCl (0.5 M), EDTA (1 mM), SDS (0.5% w:v)
mRNA isolation 1 x Wash Buffer	Tris-HCl (0.01 M, pH 7.5), NaCl (1 M), EDTA (1 mM)
mRNA isolation 1 x Elution Buffer	Tris-HCl (0.01 M, pH 7.5), EDTA (1 mM)
10 x MOPS buffer	10 ml, 0.5 M 3-(N-Morpholino)-propanesulfonic acid, pH 7.0; 50 mM sodium acetate; 5 mM EDTA
RNA loading buffer	Formamide (62.5 % v:v), formaldehyde (9.25 % v:v), 1.25 x MOPS buffer, bromophenol blue (50 µg/ml)

Table 3.5.b. Oligonucleotides and primers for PCR, QPCR, cDNA synthesis and RNA amplification. All sequences are 5' – 3' orientation. 14CSA = 14 carbon long spacer arm, P = phosphate group.

SMART™ cDNA PCR amplified library primers	
G-Super-Oligo-d(T)	5'-GGGGACCCACTTTGTACAAGAAAGCTGGGTAGGCGGCGCCACTCCTGGAGCCCGT(T)$_{26}$-3'
GSO2	5'-GGGGACAAGTTTGTACAAAAAAGCAGGCTAUGGCAGTGGTAACAACGCAGAGTACGCGGG-3'
SMART-*att*B1	5'-GGGGACAAGTTTGTACAAAAAAGCAGGCTAUGGCAGTGG-3'
SMART-*att*B2	5'-GGGGACCCACTTTGTACAAGAAAGCTGGGTAGG-3'
EnvGenIntOligo	5'-AGGCGGCGCCACTCCTGGAGCCCGT-3'
G-MCS2	5'-UGGCAGTGGTAACAACGCAGAGTACGCGG-3'
M13 Forward	5'-GTAAAACGACGGCCAG-3'
M13 Reverse:	5'-CAGGAAACAGCTATGAC-3'
CloneMiner Library Orignal primers	
Biotinylated Oligo d(T) *att*B2 Primer	5'-Biotin.GGCGGCCGCACAACTTTGTACAAGAAAGTTGGGT(T)$_{19}$-3'
*att*B1 adapter	5'-TCGTCGGGGACAACTTTGTACAAAAAAGTTGG-3' 3'-CCCCTGTTGAAACATGTTTTTTCAACC-P-5'
Biotinylated Random attB2 primer	5'-Biotin.GGCGGCCGCACAACTTTGTACAAGAAAGTTGGGT(N)$_6$TGCCTG-3'
2G CloneMiner Primers	
Biotinylated 2G Oligo d(T) attb2 Primer	5'-Biotin-GGCGGCCGCACAACTTTGTACAAGAAAGTTGGGTGGAACCGTCACGTAC(T)20-3'
Biotinylated 2G Random attB2 primer	5'-Biotin- GGCGGCCGCACAACTTTGTACAAGAAAGTTGGGTGGAACCGTCACGTAC(N)6TGCCTG-3'
2G attb1 adapter	5'-TCGTCGGGGACAACTTTGTACAAAAAAGTTGGGTGCATCAGCTGGACTAG-3' 3'-CCCCTGTTGAAACATGTTTTTTCAACCCACGTAGTCGACCTGATC-P-5'
NintpDONR222anti	5'-GTTGGGTGGAACCGTCACGTAC-3'
NpDONR222sense	5'-GTTGGGTGGAACCGTCACGTAC-3'
3G CloneMiner Primers	
Biotinylated 3G Oligo d(T) *att*B2 Primer	5'Biotin- 14CSA.GGCGGCCGCACAACTTTGTACAAGAAAGTTGGGTGGAACCGTCACTAGT(T)$_{19}$-3'
Biotinylated 3G Random *att*B2 primer	5'Biotin- 14CSA.GGCGGCCGCACAACTTTGTACAAGAAAGTTGGGTGGAACCGTCACTAGT(N)$_6$TGCCT-3'
3G *att*B1 adapter	5'-TCGTCGGGGACAACTTTGTACAAAAAAGTTGGGTGCATCAGCTGGACTAGT-3' 3'-CCCCTGTTGAAACATGTTTTTTCAACCCACGTAGTCGACCTGATCA-P-5'
3G Bi-directional Colony PCR primer	5'- GACTGATAGTGACCTGTTCGTTGCAACAAATTG-3'
Suppression Subtractive Hybridisation Primers	
Oligo d(T) cDNA synthesis primer	5'-TTTTGTACAAGCTT$_{30}$N$_1$N-3'
Adaptor 1	5'-CTAATACGACTCACTATAGGGCTCGAGCGGCCGCCCGGGCAGGT-3' 3'-GGCCCGTCCA-5'
Adaptor 2R	5'-CTAATACGACTCACTATAGGGCAGCGTGGTCGCGGCCGAGGT-3' 3'-GCCGGCTCCA-5'
Bi-directional PCR primer	5'-CTAATACGACTCACTATAGGGC-3'
SSH Nested PCR primer 1	5'-TCGAGCGGCCGCCCGGGCAGGT-3'
SSH Nested PCR primer 2	5'-AGCGTGGTCGCGGCCGAGGT-3'
RNA Amplification Primers	
Oligo dT(15)-T7 primer	5' AAACGACGGCCAGTGAATTGTAATACGACTCACTATAGGCGC(T)$_{15}$ 3'
Template Switch	5' AAGCAGTGGTAACAACGCAGAGTACGCGGG 3'

3.6 SMART cDNA PCR Amplified Library

SMART cDNA Synthesis. mRNA (1 µg) was combined in a 200 µl PCR tube with 1 µl G-Super-Oligo-dT (10 µM) and 1 µl GSO2 (10 µM), final volume 4 µl, and incubated at 65 ºC for 5 min to denature the nucleic acid and then cooled to 48 ºC. The temperature was maintained at 48 ºC during the addition of 2 µl 5x First Strand Buffer, 1 µl DTT (0.1 M) and 1 µl dNTPs (10 mM each). The solution was mixed by gentle pipetting before the addition of 1 µl RNAseOUT (40 U/µl, Invitrogen, Paisley, UK) and 1 µl Superscript III (200 U/µl, Invitrogen, Paisley, UK). The solution was mixed again and incubated at 48 ºC for 2 hours, cooled to 37 ºC and1 µl RNAse H (2 U/µl, Invitrogen, Paisley, UK) added and incubated at 37 ºC for 30 min.

SMART cDNA amplification. cDNA was amplified in 3 x 25 µl PCR reactions as detailed in Section 3.5 using SMART-ATTB1 (GGG GAC AAG TTT GTA CAA AAA AGC AGG CTA AGG CAG TGG) and SMART-ATTB2 (GGG GAC CCA CTT TGT ACA AGA AAG CTG GGT AGG) primers with an annealing temperature of 58 ºC. These primers bind to the nested sites in the *att*B adapters shown in Figure 3.7.a.

SMART cDNA Size selection. Following amplification, cDNA above 400 bp was size selected using SizeSep 400 Sepharose Columns (Amersham International, Little Chalfont, U.K). Columns were washed three times with 3 ml TAE buffer, pH 7.6 and centrifuged at 400 g for 2 min supported in 15 ml centrifuge tubes. The columns were transferred to fresh 15 ml centrifuge tubes and the cDNA samples were applied to the column. Following incubation at room temperature for 2 min the columns were centrifuged again as above to collect the cDNA. A small sample of the cDNA was placed in a well of a 1 % agarose gel containing 0.2 µg/ml ethidium bromide. In the adjacent well were DNA markers (1 kb DNA Ladder, NEB, Hitchin, UK) with the remainder of the cDNA in a separate well (Figure 3.6.d). Following electrophoresis, the gel was cut parallel to the lanes so that the small cDNA sample and DNA markers were in one section whilst the remaining cDNA was

in the other. The gel section containing the cDNA sample and markers was visualised with UV light and used as a template to excise the remaining cDNA from the other section of gel in size specific fractions. Therefore this portion of the cDNA was isolated without exposing it to UV light, reducing the likelihood of possible DNA nicking. The cDNA portion of the gel was cut into 5 sections containing cDNA fractions of 0.5-1.0 kb, 1.0-2.0 kb, 2.0-3.0 kb, 3.0-5.0 kb and >5 kb. The cDNA was extracted from the gel using Geneclean (Anachem Ltd, Luton, UK).

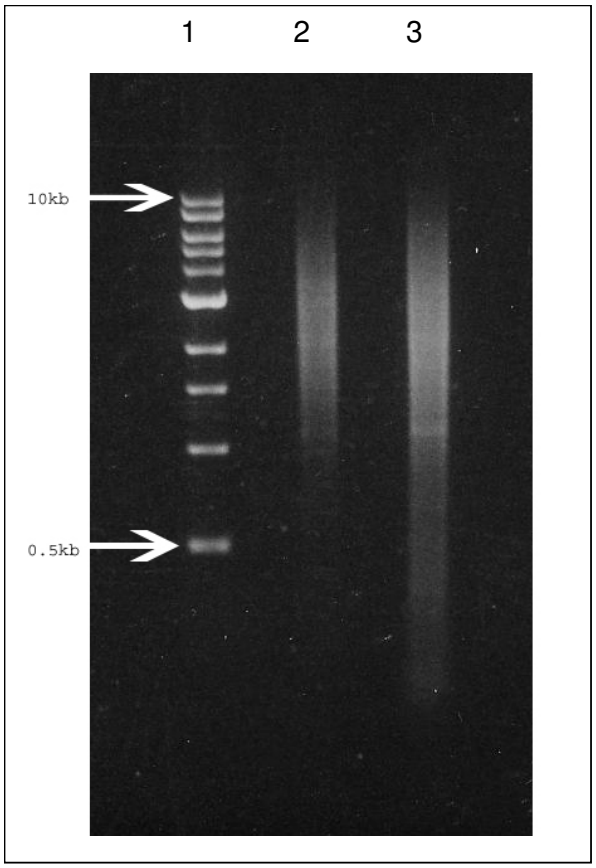

Figure 3.6.d. Lane 1: 1kb Ladder (Invitrogen), Lane 2: SMART cDNA Library after SizeSep Column treatment, Lane 3 Untreated SMART cDNA Library. cDNA presented here was exposed to UV light and as such not used for cloning.

Vector Transformation. A sample of size selected cDNA (2.5 µl) was combined with 0.5 µl pDONR221, 1µl 5 x BP Clonase™ reaction buffer and

1µl BP Clonase™ enzyme mix (proprietary, Invitrogen, UK) and incubated at room temperature for 2 days. The reaction was terminated by addition of 0.5 µl Proteinase K (2 µg/µl, Invitrogen, Paisley, UK) and incubation at 37 ºC for 10 min. cDNA was purified by precipitation by adding 2.5 vol isopropanol and placed on ice for 30min. cDNA was pelleted by centrifugation at ~15,000 g for 20 min, the pellet was washed once with 70 % ethanol and air dried.

Host Transfection. The cDNA pellet was resuspended in 5 µl H_2O and added to 50 µl GeneHog *E.coli*. (Invitrogen, Paisley, UK), transferred into a pre-cooled electroporation cuvette at 0 ºC and electroprated at 1600 v. Prewarmed SOC (450 µl, 37 ºC) was added and cells were incubated on a rotating wheel at 37 ºC for 45 min. Aliquots of the cell suspension (125 µl) were spread onto large (20 cm diameter) LB-agar plates containing kanamycin (50 µg/ml) and incubated at 37 ºC overnight. Individual colonies were randomly selected and grown in 200 µl Terrific Broth containing kanamycin (50 µg/ ml) in 96 well plates. Clones were verified for successful cDNA inserts by PCR amplification of 1 µl colony template with M13 forward and reverse primers (annealing temperature 58 ºC) and visualised on agarose gels.

3.7 CloneMiner™ cDNA library: Procedures

The procedures for the production of CloneMiner™ libraries are described briefly below. For a complete description of these protocols see Appendix 1 : CloneMiner™ cDNA Library Construction Kit Manual. All products mentioned in this section were manufactured by Invitrogen, Paisley, UK. The only deviation of note from the standard CloneMiner protocol was the creation of a second "random" cDNA library which was primed in the first instance by the degenerate CloneMiner™ Random attB2 primer. This primer was used at 20x the concentration of the standard CloneMiner™ oligo d(T) *att*B2 primer.

CloneMiner™ First strand cDNA synthesis: Reverse transcription was primed by 1 µl CloneMiner™ oligo d(T) *att*B2 primer (30 µM, 5′-Biotin. GGC GGC CGC ACA ACT TTG TAC AAG AAA GTT GGG T $(T)_{19}$ -3′) or CloneMiner™ Random *att*B2 primer (600 µM, 5′-Biotin. GGC GGC CGC ACA ACT TTG TAC AAG AAA GTT GGG T $(N)_6$ TGC CTG-3') and was combined with 2 µg mRNA and 2 µl dNTPs (10 mM each) in a volume of 9 µl and incubated at 65 ºC for 5 min, to denature any secondary RNA structure, and then cooled to 45 ºC for 2 min to allow primer annealing. The first strand master mix was prepared on ice containing 4 µl 5x First Strand Buffer (Invitrogen, UK), 2 µl DTT (0.1 M) and 1 µl H_2O, combined with the mRNA and incubated for 2 min at 45 ºC before adding 2 µl Superscript II RT and incubating for a further 60 min at 45 ºC to allow first strand cDNA synthesis to occur.

CloneMiner™ Second strand synthesis: The first strand reaction was placed on ice whilst adding the components of the second strand reaction; 92 µl DEPC-treated water, 30 µl 5X Second Strand Buffer, 3 µl dNTPs (10 mM each), 1 µl *E. coli* DNA Ligase (10 U/µl), 4 µl *E. coli* DNA Polymerase I (10 U/µl) and 1 µl *E. coli* RNase H (2 U/µl). This was incubated at 16 ºC for 2 hours, during which the second strand of cDNA was created. T4 DNA Polymerase (2 µl) was then added and incubated at 16℃ for 5

minutes to create blunt-ended cDNA. The reaction was stopped by adding 10 µl of 0.5 M EDTA, pH 8.0. The cDNA was separated from the proteins and any remaining RNA in the mix by adding 160 µl of phenol:chloroform:isoamyl alcohol (25:24:1) and shaking thoroughly by hand for approximately 30 seconds. This was then centrifuged at room temperature for 5 minutes at 14,000 rpm before carefully removing the upper aqueous phase to a fresh 1.5 ml tube. The cDNA was precipitated by adding 1 µl glycogen (20 µg/µl), 80 µl NH_4OAc (7.5 M) and 600 µl 100% ethanol and incubating at -80°C for 10 minutes. The cDNA was pelleted by centrifuging the sample at +4°C for 25 minutes at 14,000 rpm. The supernatant was carefully removed and the cDNA pellet was washed twice with 150 µl of 70% ethanol before aspirating all the ethanol and allowing the cDNA pellet to air-dry for 10 min. The cDNA pellet was then resuspended in 18 µl of DEPC-treated H_2O and placed in ice.

Ligation of the CloneMiner™ *att*B1 adapter: The CloneMiner™ *att*B1 adapter was blunt-end ligated to the non-biotinylated end of the cDNA by adding 10 µl 5X Adapter Buffer, 10 µl CloneMiner™ *att*B1 adapter (1 µg/µl), 7 µl DTT (0.1 M) and 5 µl T4 DNA Ligase (1 U/µl). The contents were mixed gently by pipetting and incubated at 16°C for 16-24 hours. The cDNA was then incubated at 70°C for 10 minutes to inactivate the ligase.

Size Fractionating CloneMiner™ cDNA by Column Chromatography: Column chromatography using Sephacryl® optimizes size fractionation of the cDNA and makes the cloning of larger inserts more probable. Sephacryl® particles are essentially hollow spheres (25-75 µm in diameter) with pores on their surface which allow molecules of a certain size to enter (up to 20,000 kDa MW). Therefore when the cDNA solution is passed through the column the largest molecules, including DNA over ~ 500 bp, elute first because they have less volume to traverse as they go around the particles. Conversely, the smaller molecules must travel a more convoluted route through the Sephacryl® particles and thus elute later allowing the two particle size fractions to be separated. A drip-column containing 1 ml of Sephacryl® S-500 HR resin suspended in ethanol (supplied with the CloneMiner kit) was mounted in a support stand and the ethanol

allowed to drain away. The column was then washed four times with 0.8 ml TEN buffer (10 mM Tris-HCl, pH 7.5, 0.1 mM EDTA, 25 mM NaCl) allowing all the buffer to drain away. TEN buffer (100 µl) was added to the cDNA solution which was then applied to the column. Two aliquots of 100 µl TEN buffer were then added to the column and the effluent discarded. Further aliquots of 100 µl TEN buffer were then added to the column and each of the next 20 individual droplets to come through the column were collected in pre-labelled 1.5 ml tubes.

CloneMiner™ cDNA quantification using spot blot analysis: The volume of each droplet was measured using a pipette and a spot blot was performed to measure the cDNA concentration. A 1 % agarose gel (15 ml) containing ethidium bromide (1 µg/µl) was made as per the DNA agarose gel method (Section 3.5) and poured into a 10cm diameter petri-dish and allowed to set at room temperature for 15 min. The underside of the petri-dish was marked out with a grid to localise samples. A 0.5 µl sample from each cDNA droplet was serially diluted to a 1:10 dilution and a 1:20 dilution. 1 µl from each of these dilutions was spotted onto the surface of the gel alongside five 1 µl samples of pEXP7-tet plasmid DNA diluted to 25 ng/µl,10 ng/µl, 5 ng/µl and 1 ng/µl. The samples were allowed to dry before the DNA was visualised with UV light. The concentration of each of the cDNA samples was determined by comparing their fluorescence to that of the pEXP7-tet DNA standards by eye.

Performing the CloneMiner™ BP Recombination Reaction: A pool of cDNA was collated comprising the first 150 ng to come through the column in the earliest drip fractions, this should contain the longest cDNA molecules. This cDNA was precipitated by adding 1 µl glycogen (20 µg/µl), 0.5 volumes NH_4OAc (7.5 M) and 2.5 volumes 100% ethanol and incubating at -80°C for 10 minutes. The cDNA was pelleted by centrifuging the sample at +4°C for 25 minutes at 14,000 rpm. The supernatant was carefully removed and the cDNA pellet washed twice with 150 µl of 70% ethanol before aspirating all the remaining ethanol and allowing the cDNA pellet to air-dry for 10 min. The cDNA was resuspended in 4.5 µl TE buffer and 0.5 µl was removed for spot

blot quantification as described above. In a final volume of 10 µl approximately 75-100 ng *att*B-flanked cDNA was combined with 1 µl pDONR222 plasmid (250 ng/µl), 2 µl 5 x BP Clonase™ reaction buffer and 3 µl BP Clonase™ enzyme mix. The BP reaction mixture was incubated at 25 °C for 20 hours.

Transformation of CloneMiner™ competent cells: The BP reaction was stopped by adding 2 µl of proteinase K (2 µg/µl) and incubating at 37 °C for 15 minutes and then at 75 °C for 10 minutes. The cDNA was precipitated by adding 90 µl H_2O, 1 µl glycogen (20 µg/µl), 50 µl NH4OAc (7.5 M) and 375 µl 100% ethanol and incubating at –80 °C for 10 minutes. The cDNA was pelleted by centrifuging the sample at +4 °C for 25 minutes at 14,000 rpm. The supernatant was carefully removed and the cDNA pellet washed twice with 150 µl of 70% ethanol before aspirating all the remaining ethanol and allowing the cDNA pellet to air-dry for 10 min. The cDNA was resuspended in 9 µl H_2O and then divided into six 1.5 µl aliquots. Each aliquot was mixed with 50 µl ElectroMAX™ DH10B™ T1 Phage Resistant Cells. These cells are not resistant to kanamycin but they are susceptible to the CcdB protein encoded by the *ccd*B gene found in the plasmid pDONR222. The cells must acquire a pDONR222 plasmid to be capable of growing on selective media containing kanamycin. The *ccd*B gene is removed completely from pDONR222 when replaced with an *att*B flanked cDNA molecule during the BP recombination reaction. Therefore, only the cells which are transfected by recombined plasmid will be viable. The cDNA/cell mixture was pipetted into an ice-cold electroporation cuvette and electroporated at 2000v using an Electroporator 2510 (Eppendorf, Cambridge, UK). Electroporation disrupts the cell membrane to allow the pDONR222 plasmid to enter. The cell suspension was quenched with 1ml SOC medium (see Table 3.5.a) and incubated on an orbital shaker for 1 hour at 37 °C to allow the kanamycin resistance gene to be expressed before plating onto LB agar containing kanamycin (50 µg/µl, see Table 3.5.a). Cells were allowed to grow overnight at 37 °C and then individual colonies were selected at random and grown overnight at 37 °C on an orbital shaker in Terrific Broth (200 µl, see Table 3.5.a) containing kanamycin (50 µg/µl). Clones were verified for successful

cDNA inserts by PCR amplification of 1 µl colony template with M13 forward and reverse primers (annealing temperature 58 ºC) and visualised on agarose gels (see Results, Figure 4.5.e).

3.8 Second generation (2G) CloneMiner™ libraries

Two cDNA libraries called “Oligo” and “Random” were made, following the CloneMiner™ protocol as described in Section 3.7, with the first strand cDNA synthesis primed by 2G oligo d(T) *att*B2 primer or 2G random *att*B2 primer respectively. The 2G *att*B1 adapter was used instead of the CloneMiner™ supplied adapter. In order to monitor the cDNA strands during subsequent normalisation and subtraction procedures, the second strand was radiolabelled as follows.

Radiolabelling of 2G CloneMiner™ Second Strand. Identical procedures were followed as detailed in Section 3.8 except that the second strand mixture contained; 20 µl first strand reaction kept on ice whilst adding 1 µl α^{32}P dCTP (~10µCi), 91 µl DEPC-treated water, 30 µl 5X Second Strand Buffer, 3 µl dNTPs (10 mM each), 1 µl E. coli DNA Ligase (10 U/µl), 4 µl E. coli DNA Polymerase I (10 U/µl) and 1 µl E. coli RNase H (2 U/µl). This was incubated at 16 ºC for 2 hours, during which the second strand of cDNA was created. Normal CloneMiner™ protocol was then resumed.

3.9 Normalisation

Due to experimental inefficiencies this protocol was never implemented fully (see Section 4.6).

*att*B flanked cDNA was made from kidney messenger RNA using the 2G Oligo d(T) *att*B2 primer and the 2G *att*B1 (see Section 3.5 for sequences) adapter as per the CloneMiner™ protocol detailed in Section 3.8. The first strand cDNA had a biotin label at the 5' end, as conferred by the first strand synthesis primers, and the second strand of the cDNA was radiolabelled with α^{32}P dCTP as described in Section 3.8. The cDNA (1 µg) was prepared in 100 µl 1 x SSPE buffer (150mM Sodium Chloride, 10mM Sodium Phosphate, 1mM EDTA) and 50 % formamide. The solution was heated to 95 ºC and then cooled to 65 ºC until ~50 % of the cDNA had annealed. The cDNA was then snap-cooled on ice. SA-PMPs (0.6 mg) were washed three times with 200 µl 1 x SSPE buffer. After the final wash the buffer was removed and the SA-PMPs resuspended with a solution of radiolabelled, biotinylated cDNA (1 µg) was diluted in 1 x SSPE buffer (100 µl). The suspension was incubated at room temperature for varying times between 30 min and 2 hours, following which the beads were removed using a magnet. The amount of radiolabelled cDNA either bound to the beads or remaining in the supernatants was determined by liquid scintillation counting (Cerenkov radiation).

3.10 Post-biotinylation of DNA

A 50 µl reaction was prepared containing 5 mg DNA, 5 µl 10 x Label IT Buffer, 5 µl Label IT biotinylating reagent, H2O to 50 µl. This was incubated for 1 hour at 37 ºC and then the DNA was purified by ethanol precipitation by addition of 1 µl glycogen (20 µg/µl), 0.1 volume NaCl (5 M) and 2 volumes ice cold ethanol (100 %) and incubated for 10 min at –20ºC. DNA was pelleted by centrifugation at 15,000 g for 10 min, the supernatant removed and the pellet washed once with 100 µl 70 % ethanol. The ethanol was aspirated, the pellet air-dried and resuspend in 20 µl H2O. Labelled DNA was denatured by adding 2 µl 3 M NaOH and incubated at 25ºC for 5 min then placed on ice for 2 min. The solution was neutralised by the addition of 2 µl N1 buffer (a proprietary buffer containing 3 M HCl, Mirus, WI, USA). The biotinylated, denatured DNA was then used in a variety of hybridisation reactions.

3.11 Cloning of 18S and 28S rRNA fragments

cDNA from the brain 2G random cDNA library was amplified using standard PCR conditions using *att*B1sense (TCGGGGACAACTTTGTACAAAAAA) and *att*B2anti (GGCGGCCGCACAACTTTGTACAAGAAA) primers , annealing temperature 58 ºC and run on a 1.5 % EtBr stained agarose gel. Two over-expressed bands at 500 bp and 1.5 kb were excised from the gel and purified using a GeneClean DNA purification kit (Anachem Ltd., Luton, UK) and cloned using TOPO TA Cloning Kit (Invitrogen, UK). PCR was performed on individual clones and the subsequent DNA was sequenced using BigDye™ (Applied Biosystems, Renton, USA).

3.12 Driver production

Clones (2000) were randomly selected from a library and grown individually in 200 µl Terrific Broth containing kanamycin (50 µg/µl) in 96 well plates overnight at 37 ºC. Clones were collated into a single 96 well plate containing 200 µl Terrific Broth (kanamycin 50 µg/ml) per well using a sterile replicator and grown overnight at 37 ºC. Colony PCR was performed for each well, containing ~20 clones, using 2G internal primers (NintpDONR222anti 5′-GTTGGGTGGAACCGTCACGTAC-3'and NpDONR222sense 5′-GTTGGGTGGAACCGTCACGTAC-3', annealing temperature 58 ºC) as per normal PCR conditions (Section 3.5) except that reaction volume was doubled to 50 µl. A sample (5 µl) from each PCR was collated into a Driver pool and amplicons were purified by ethanol precipitation as previously described (Section 3.5) and verified by visualisation on a 1 % ethidium bromide stained agarose gel (Figure 4.9.b).

3.13 Subtraction with pH directed hybridisation.

Driver cDNA (2 µg amplified kidney cDNA clones, 1.5 µg 18S cDNA and 1.5 µg 28S cDNA) was biotinylated using Label IT Biotin Labelling Kit (Mirus, WI, USA, see section 3.10) and ethanol precipitated (see section 3.5). Tester cDNA was prepared from intestine RNA using the CloneMiner™ kit with the non-biotinylated 2G CloneMiner™ 2G Random *att*B2 primers as per standard protocol (Section 3.8). Tester cDNA (150 ng) in 100 µl H_2O was used to resuspend the pellet of precipitated biotinylated driver. Tester and Driver DNA was denatured by adding 10 µl 3 M NaOH and heated to 65 ºC, immediately cooled to 30ºC. The solution was neutralised with 10 µl solution N1 (3 M HCl containing proprietary buffer, Mirus, WI, USA) and incubated at room temperature for 1 hour to allow rehybridisation of complimentary Tester and Driver cDNA strands. Biotinylated cDNA species were removed using SA-PMPs (0.6 mg) as described in Section 3.9. The remaining tester in the SA-PMP supernatant was ethanol precipitated and resuspended in 9 µl TE buffer and the cDNA concentration determined using a spot blot comparison. Tester cDNA was subsequently cloned into pDONR222 following standard CloneMiner™ protocol (see Section 3.8).

3.14 Temperature directed subtraction in the presence of formamide.

Tester cDNA (500 ng) was prepared from intestine RNA using the CloneMiner™ kit with the non-biotinylated 2G CloneMiner™ 2G Random attB2 primer. The cDNA was diluted in 16.7 µl H2O and then denatured by heating to 95 ºC for 2 min, snap-cooled on ice for 2 min before adding 100 µl ice-cold formamide and 5 µg biotinylated driver (2 µg kidney cDNA, 1.5 µg 18s cDNA and 1.5 µg 28s cDNA in 83.3 µl 1xSSPE, denatured following biotinylation as per Section 3.10). After overnight incubation at 42 ºC biotinylated cDNA was removed with 0.25 mg SA-PMPs as described in Section 3.9. The cDNA remaining after subtraction was quantified using a spot blot and standard CloneMiner™ cloning procedure ensued (Section 3.8).

3.15 Temperature directed subtraction in the absence of formamide.

Tester cDNA (500 ng) prepared from intestine RNA using the CloneMiner™ kit with the non-biotinylated 2G CloneMiner™ 2G Random attB2 primers was diluted in 29 µl 1xSSPE and then combined with 5 µg biotinylated driver (2 µg kidney cDNA, 1.5 µg 18s cDNA and 1.5 µg 28s cDNA in 10 µl 1 x TE). A thermal-cycler was used to heat the mixture to 95 ºC for 2 min and then to cool the sample gradually to room temperature at a rate of 5 ºC/min. Biotinylated species were removed using 0.25 mg SA-PMPs as described in Section 3.9. The cDNA remaining after subtraction was quantified using a spot blot and standard CloneMiner™ cloning procedure ensued (see Section 3.8).

3.16 Third generation (3G) CloneMiner™ libraries

Two cDNA libraries called “Oligo” and “Random” were made, following the CloneMiner™ protocol as described in Section 3.7. The only exceptions were that the first strand cDNA synthesis was primed by either the 3G oligo d(T) *att*B2 primer which incorporates a biotin molecule on a 14-carbon spacer arm (14CSA), (5′Biotin_14CSA.GGCGGCCGCACAACTTTGTACAAGAAAGTTGGGTGGAACCGTCACTAGT(T)19-3′) or 3G random *att*B2 primer (5′Biotin_14CSA.GGCGGCCGCACAACTTTGTACAAGAAAGTTGGGTGGAACCGTCACTAGT(N)6TGCCT-3’). The 3G *att*B1 adapter was used instead of the CloneMiner™ supplied adapter.;

```
5′-TCGTCGGGGACAACTTTGTACAAAAAAGTTGGGTGCATCAGCTGGACTAGT-3′
     3′-CCCCTGTTGAAACATGTTTTTTCAACCCACGTAGTCGACCTGATCA-P-5′
```

3.17 Investigation of SA-PMP non-specific binding

Two separate reactions were prepared, both contained 1 µl α^{32}P-labelled *A. anguilla* kidney cDNA (100 ng/µl, ~1000 cpm) and 3 µl H_2O with either 1 µl *C. leucas* cDNA (1000 ng/µl, non-biotinylated) or 1 µl *A. anguilla* kidney biotinylated cDNA (1000 ng/µl). NaOH (0.5 µl, 3 M) was added to each reaction followed by incubation at room temperature for 30 min before placing on ice. The pH of the reactions was neutralised by adding 0.5 µl ice cold 3 M HCl followed by 2.5 µl 20 x SSPE buffer and 2 µl H_2O and incubated at 70 ºC overnight to allow re-annealing of complementary cDNA strands. Two aliquots of 0.6 mg SA-PMPs were prepared as per Section 3.9 and finally re-suspended in 20 µl of 1 x SSPE. Each aliquot of SA-PMPs was resuspended with one of the two reactions and then incubated at room temperature for 10 min. The SA-PMPs were removed from the supernatants using a strong earth magnet. Unbound cDNA was washed from the SA-PMPs with six washes of 50 µl H_2O pre-warmed to 50 ºC. Radiolabelled DNA associated with each fraction was measured by liquid scintillation counting (Cerenkov radiation).

3.18 Solvent treatment of SA-PMPs to remove DNA.

Six separate, identical reactions were set up; each containing 1 µl α^{32}P-labelled *A. anguilla* kidney cDNA (100 ng/µl, ~1000 cpm) and 3 µl H_2O with 1 µl *A.anguilla* kidney biotinylated cDNA (1000 ng/µl). To each solution NaOH (0.5 µl, 3 M) was added followed by incubation at room temperature for 30 min before placing on ice. As in the previous experiment, the solutions containing the denatured cDNAs were neutralised by adding 0.5 µl ice cold 3 M HCl, 2.5 µl 20 x SSPE buffer and 2 µl H_2O and incubated at 70 ºC overnight to allow re-annealing. Six aliquots of 0.6 mg SA-PMPs were prepared as per Section 3.9 and finally re-suspended in 20 µl of 1 x SSPE. Each aliquot of SA-PMPs was resuspended with one of the six reactions and the resultant suspension was incubated at room temperature for 10 min. The SA-PMPs were removed from the supernatants using a magnet. SA-PMPs were washed twice with 50 µl H_2O pre-warmed to 50 ºC and then washed three times with 20 µl of one of the following solvents; 5 M NaCl; 3 M sodium acetate, pH 4.6; 70 % ethanol; 100 % ethanol; New Wash from the Geneclean kit (Anachem Ltd, Luton, UK); H_2O pre-warmed to 50 ºC (control). Radiolabelled DNA associated with each fraction was measured by liquid scintillation counting (Cerenkov radiation).

3.19 NeutrAvidin™ biotin binding protein agarose beads

α^{32}P-labelled tester *A. anguilla* kidney cDNA was incubated with a 10 or 100 fold excess of biotinylated *A. anguilla* kidney cDNA or a 100 fold excess of non-biotinylated *C. leucas* cDNA (as per table 3.19.a). Samples 1-3 were incubated at 70 ºC overnight and sample 4 was incubated for 2min at 95 ºC in order to denature the cDNA and then incubated at 70 ºC overnight. Twenty aliquots of NABs (20 µl each) were prepared by washing the beads three times in 1 x SSPE (centrifuged 20 µl NABs slurry at 3000 g for 30 sec, removed supernatant, added 20 µl 1 x SSPE and flicked gently to resuspend, repeated three times. NABs were never centrifuged at speeds >3000 g as this crushes the NABs, thereby reducing the active surface area available for biotin binding). Samples 1-4 were added to the individual NAB aliquots and then incubated on ice for 20 min with occasional agitation. The NAB suspensions were centrifuged at 3000 g for 30 sec and the supernatant removed to a fresh aliquot of NAB whilst the spent NAB were kept for analysis. The process was repeated for the remaining NAB aliquots, finally the supernatants containing DNA were transferred to a pony vial. All samples of NABs and supernatants were transferred to pony vials containing 3 ml H_2O and the radioactivity determined by liquid scintillation counting (Cerenkov radiation).

Table 3.19.a. Sample contents and incubation conditions to test how efficiently NAB bind biotinylated cDNA.

Sample	*A. anguilla* α^{32}P dCTP labelled kidney cDNA (ng)	*A. anguilla* Biotinylated Driver kidney cDNA (ng)	*C. leucas* non-biotinylated cDNA (ng)	Incubation conditions
1	10	0	1000	70 ºC Overnight
2	10	100	0	70 ºC Overnight
3	10	1000	0	70 ºC Overnight
4	10	100	0	95 ºC for 2 min followed by 70 ºC overnight

3.20 Inclusion of spin-columns to separate NeutrAvidin™ beads

Driver cDNA was prepared by PCR amplifying the 1536 brain SSH clones as per standard protocol with Nested PCR primers 1 and 2 (see Section 3.21). The amplicons were purified by ethanol precipitation (as described in Section 3.5) and then biotinylated using the Mirus method as described in Section 3.10. Two identical samples were prepared containing α^{32}P-labelled radiolabelled, biotinylated Driver cDNA (6 µg) in 1 x SSPE buffer (30 µl). These were added to 300 µl aliquots of NAB (pre-washed three times with 300 µl 1 x SSPE buffer) and incubated at room temperature for 1 hour. Samples were transferred to micro-centrifuge spin-columns, taken from a GeneClean kit (Anachem Ltd, Luton, UK). The spin-columns were mounted in a 1.5 ml tube to catch the eluate and centrifuged at 3000 g for 3 min. The NAB were washed by adding 140 µl H_2O to the spin column which was then centrifuged over the same tube as before to combine the wash fluid with the previous eluate. This solution was treated with a further two aliquots of NAB. The radioactivity in the eluate and all three used NAB aliquots was determined by liquid scintillation counting (Cerenkov radiation, Figure 4.11.b).

3.21 Suppression Subtractive Hybridisation.

The SSH protocols were carried out as described in the PCR-Select™ cDNA Subtraction Kit User Manual (Clontech, Basingstoke, UK) which can be found in appendix 2; brief details are provided below. Double stranded cDNA was produced for each tissue by oligo d(T) (5'-TTTTGTACAAGCTT$_{30}$N$_1$N-3') primed reverse transcription from messenger RNA (isolated as per Section 3.4). This was followed by second strand synthesis. The cDNA was then digested using *Rsa* I, a restriction endonuclease that recognises a four base sequence found in the oligo d(T) primer and randomly throughout the cDNA, and yields blunt ends. The cDNA of the tissue undergoing subtraction was divided into two Tester aliquots whilst the cDNAs from the three other tissues was combined to form the Driver. The two Tester cDNAs were ligated with different adapters, the ends of which do not have a phosphate group, so only one strand of each adaptor attaches to the 5' ends of the cDNA. The two adaptors have stretches of identical sequence to allow annealing of SSH PCR primer 1 after the recessed ends have been filled in (see Figure 4.12.a). The bi-directional SSH PCR primer 1 (5'-CTAATACGACTCACTATAGGGC-3') was used to amplify the subtracted cDNA. A secondary PCR amplification was then performed using nested primers (SSH Nested PCR primer 1: 5'-TCGAGCGGCCGCCCGGGCAGGT-3', SSH Nested PCR primer 2: 5'-AGCGTGGTCGCGGCCGAGGT-3') to further reduce any background PCR products and enrich for differentially expressed sequences. The cDNAs were inserted into the T/A cloning vector pCR4-TOPO (Invitrogen Ltd, Paisley, UK) and transformed by electroporation into DH5α *E. coli* (Eurogentec Ltd, UK).

3.22 Creation of a high quality subtracted *att*B brain library

Driver preparation. A 96 well plate was prepared with Terrific Broth (200 µl) containing kanamycin (50 µg/µl) in each well. Each well was transfected with a bacterial sample (1 µl) from 16 brain SSH clones so that all 1536 brain SSH clones were represented on the one plate. The bacteria were grown overnight on a shaking bed incubated at 37 ºC. A sample (1 µl) from each well representing 16 brain SSH clones was then used as template in one of 96 50 µl PCR reactions using the SSH Nested primer 1 TCGAGCGGCCGCCCGGGCAGGT and SSH Nested primer 2 AGCGTGGTCGCGGCCGAGGT using standard PCR protocol (Section 3.5) and an annealing temperature of 57 ºC. An additional PCR was performed to create a radiolabelled tracer to track the Driver using the same PCR conditions as before but with the addition of α^{32}P dCTP (10 µCi) using 16 SSH clones (1 µl) as template. The 97 PCRs were collated and the DNA purified by ethanol precipitation (see Section 3.5) and resuspended in H_2O (110 µl). This solution represented the Driver cDNA. A SizeSep 400 Spun column (Amersham Biosciences, UK) was prepared by washing 3 times with 2 ml TAE buffer (pH 7.6). The column was supported in 15 ml centrifucation tube and centrifuged at 400 g for 2 min at room temperature before the columns were transferred to fresh 15 ml centrifugation tubes. The Driver cDNA solution was applied to the SizeSep 400 column in order to purify it from the components of the PCR reaction, critically the α^{32}P dCTP. The PCR solution was allowed to sit in the column for 2 min at room temperature before centrifuging at 400 g for 2 min at room temperature to collect the cDNA. Size selected Driver DNA subsequently biotinylated using the Label IT Biotin Labelling Kit (Mirus, WI, USA) as described previously in Section 3.10.

Subtraction. A hybridisation was prepared in 1 x SSPE buffer (30 µl) containing Tester cDNA (600 ng) subtracted with a ten-fold excess of biotinylated Driver cDNA (6 µg, with α^{32}P tracer). The solution was incubated at 95 ºC for 2 min, 70 ºC for 10 min and then cooled to 20 ºC at a rate of 1 ºC/min. To remove the Driver from the hybridisation, the solution was added

to a 300 µl aliquot of NAB (pre-washed three times with 300 µl 1xSSPE buffer) and incubated at room temperature for 1 hour. The suspension of NAB was transferred to a micro-centrifuge spin-column (Anachem Ltd, Luton, UK), mounted in a 1.5 ml tube to catch the Tester eluate and centrifuged at 3000 g for 3 min. Unbound cDNA was washed from the NAB by resuspending the beads with 140 µl H_2O and centrifuging again, combining the wash fluid with the previous Tester eluate. The eluate, now in a volume of 170µl, was treated with a further two aliquots of NAB and the washes repeated each time so the final volume was 450 µl. The radioactivity in a 10 µl sample of the Tester eluate and all three used NAB aliquots was determined by liquid scintillation counting (Cerenkov radiation). All of the radiolabelled Driver cDNA was associated with the NAB confirming that only Tester cDNA was present in the eluate.

Cloning. The Tester cDNA was ethanol precipitated and resuspended in 4.5 µl TE buffer. The DNA concentration was determined using a spot blot analysis on EtBr stained agarose gel with DNA standards (see Section 3.5) and found to be 20 ng/µl. The Tester cDNA was cloned into pDONR222 in a reaction comprising Tester cDNA (4 µl), pDONR222 (1 µl, 250 ng/µl), 5 x Clonase ™ buffer (2 µl) and BP Clonase™ enzyme mix (3µl, proprietary), and incubated overnight at room temperature. The recombination reaction was stopped by adding proteinase K (2 µl, 2 µg/µl) and incubating at 37 ºC for 10 minutes before adding 90 µl H_2O. The DNA in the solution was precipitated as per Section 3.5 and resuspended in 9 µl H_2O, which is important in order that the recombined vector is in a salt free solution. Six samples of the recombined vector (1.5 µl each) were combined with ElectroMAX™ DH10β T1 phage resistant cells (50 µl) and transferred into a pre-cooled electroporation cuvettes at 0 ºC and electroprated at 1600 v. Prewarmed SOC (1 ml, 37 ºC) was added to each electroporation cuvette to quench the cells before transferring to a 1.5 ml micro-centrifuge tube and incubating on a rotating wheel at 37 ºC for 45 min. Aliquots of the cell suspensions (125 µl) were spread onto large (20 cm diameter) LB-agar plates containing kanamycin (50 µg/ml) and incubated at 37 ºC overnight. Individual colonies were randomly selected and grown in 200 µl Terrific Broth containing

kanamycin (50 µg/µl). The clones were grown overnight on a shaking bed incubated at 37 ºC. To verify the integrity and redundancy level of the library the inserts from 46 clones analysed. Colony PCR was performed using standard PCR conditions with the 3G bi-directional colony PCR primer (5'-GACTGATAGTGACCTGTTCGTTGCAACAAATTG-3') with an annealing temperature of 60 ºC. The amplicons were visualised on an agarose gel to check if all clones contained inserts and the size of inserts (Section 4.13). To test the redundancy level of the library the 46 clones were sequenced by Macrogen (South Korea). The sequences were edited from expression vectors and adaptors sequences, quality assessed by electrophoretogram and blasted against available databases using Trade2dBest (CIH, Oxford).

3.23 RNA Amplification

First strand cDNA synthesis: Reverse transcription is primed by and T7 Oligo dT(15) primer (1 µl, 30 µM, 5' AAA CGA CGG CCA GTG AAT TGT AAT ACG ACT CAC TAT AGG CGC T(15) 3') and was combined with 0.5 – 3 µg total RNA in 8 µl H_2O and incubated at 70 ºC for 4 min then cooled to 45 ºC for 2 min. The first strand master mix was prepared on ice containing 4 µl 5x First Strand Buffer (Invitrogen, UK), 1 µl template switch (TS) primer (100 µM, 5' AAG CAG TGG TAA CAA CGC AGA GTA CGC GGG 3'), 2 µl DTT (0.1 M), 1 µl RNAseIN (40 U/ µl), 2 µl dNTPs (10 mM each) and 2 µl Superscript II RT (200 U/µl, Invitrogen,UK). The first strand master mix was combined with the RNA and T7 oligo d(T) primer and incubated for 1 h 30 min at 45 ºC before placing on ice.

Second strand cDNA synthesis: The following was added to the first strand reaction, 89.25 µl H_2O, 15 µl Black Buffer {Tris-HCl (750 mM, pH 8.8), ammonium sulphate (200 mM) and Tween 20 (0.1%), BioGene, UK}, 9 µl magnesium actetate (25 mM), 3 µl dNTPs (10 mM each), 1 µl *E.coli* RNase H (2 U/µl, Invitrogen, UK), 0.75 µl Accurase DNA polymerase (5 U/µl, BioGene, UK), and then incubated at 37 ºC at 5 min to allow the RNase H to nick the RNA, 94 ºC for 2 min to denature the nucleic acid strands, 75 ºC for 1 min to allow primer annealing and 68 ºC for 30 min for Accurase to make the second strand. Following second strand synthesis a solution containing NaOH and EDTA (7.5 µl, 1 M NaOH, 2 mM EDTA) was added and the mixture incubated heated to 65 ºC for 10 min to degrade the RNA.

cDNA purification: cDNA was purified by phenol:chloroform extraction; 160 µl phenol:chloroform:isoamyl alcohol (25:24:1) was added to the second strand synthesis cocktail and shaken by hand thoroughly for 30 s. This was centrifuged at room temperature and 15,000 g for 5 min, and upper aqueous phase removed to a fresh tube and the DNA purified by ethanol precipitation (as per section 3.5).

***In vitro* transcription:** The T7 Megascript Kit (Ambion, UK) was used and the standard protocol followed. Briefly, a mixture containing 8 µl H_2O, 8 µl ribo-NTP Mix (A, G, C and UTP, 18.75 mM each) and 2 µl 10 x Megascript reaction buffer (proprietary, Ambion, UK) was prepared and used to resuspend the cDNA pellet. The solution was kept at room temperature to prevent the spermidine in the reaction buffer co-precipitating with the cDNA. To this was added Megascript enzyme mix (2 µl, proprietary, contains RNase inhibitor and T7 phage polymerase, Ambion, UK) and incubated for 6 hours at 37 ºC. The RNA was purified by ethanol precipitation and the RNA pellet was washed twice in 70 % ethanol, briefly air-dried (<5 min, do not over-dry the RNA pellet as it becomes insoluble) and resuspend in 30 µl RNase free H_2O. The RNA concentration was determined by spectrophotometric absorbance at 260 nm. The cDNA created during reverse transcription was left in the solution of amplified RNA. Compared to the RNA, the cDNA forms only a minute fraction and will not influence future reactions.

3.24 Microarray probes, labelling and hybridisation

For all microarray experiments, cDNAs used for hybridisation were prepared from 20 µg samples of total RNA from a single tissue type (gill, intestine, brain and renal kidney) either pooled from all animals in an experimental group (n=6) or from individual fish. Two cDNA samples from different eel groups were co-hybridised to a microarray, one sample being labelled with Cy3 and the other with Cy5. Experiments were replicated in dye-swap to address any labelling bias caused by differential incorporation rates between Cy3 and Cy5 (Churchill, 2002). Dye-swap replication involves repetition of the entire microarray experiment but swapping the cDNA labels so that the cDNA previously labelled with Cy3 is now labelled with Cy5 and vice versa. This controls for any bias which could be introduced if the Cy3 and Cy5 labelling reactions are not equally efficient.

Fluorescently labelled cDNA was created using the CyScribe Post-Labelling Kit (Amersham Biosciences, Little Chalfont, UK) according to the manufacturers instructions. CyScript™ reverse transcriptase is used to create first-strand cDNA incorporating a chemically reactive nucleotide analogue (amino allyl-dUTP) into the cDNA. The RNA is then degraded and the cDNA purified to remove free nucleotides and then labelled with the reactive forms of Cy3 or Cy5 NHS-esters that bind to the modified amino allyl-nucleotides. After a final purification, the labelled cDNA is ready for hybridisation.

cDNA production and labelling: Briefly, two first strand synthesis reactions were performed in parallel for the two samples to be hybridised to the microarray. Eel RNA (20 µg) was combined with random nonamer primers (1 µl, Amersham Biosciences) and/ or anchored oligo d(T) primer (1 µl) and the volume made up to 11 µl with H_2O. Both primer types were used for amplified mRNA but only the anchored oligo d(T) was used with total RNA to avoid non-messenger RNA being transcribed. Reactions were incubated at 70 °C for 5 min and then cooled and left at room temperature for 10 min to allow the primers to anneal to the mRNA. To the solution was added 5 x CyScribe™ buffer (4 µl, proprietary), DTT (2 µl, 0.1 M), CyScribe™ nucleotide

mix (1 µl, proprietary), CyScribe™ post -labelling amino allyl-dUTP (1 µl, proprietary) and CyScript™ reverse transcriptase (1 µl). The reaction was incubated at 42 ℃ for 90 min to allow reverse transcription to occur before cooling to 37 ℃ and adding NaOH (2 µl, 2.5 M). The reaction was incubated for 15 min to degrade the RNA and then neutralised by adding 10 µl HEPES (2 M, pH 6.6). The cDNA was purified by adding to a GFX glass fibre matrix purification column (Amersham Biosciences) containing 500 µl GFX capture buffer (proprietary) and centrifuging over a 1.5 ml micro-centrifuge tube at 13800 g for 30 seconds. The eluate was discarded and the column transferred to a fresh 1.5 ml tube. The cDNA was washed three times by adding 600 µl ethanol (80 %) and centrifuging at 13800 g for 30 seconds, discarding the eluate after each centrifugation. The column was centrifuged for an additional 10 s at 13800 g to remove residual ethanol and then transferred to a fresh 1.5 ml tube. To elute the cDNA, freshly made sodium bicarbonate (60 µl, 0.1 M, pH 9.0) was added to the column and incubated at room temperature for 5 min. The column was centrifuged again at 13800 g for 1 min to collect the purified amino allyl-labelled cDNA. The cDNA was post-labelled by using the amino allyl-labelled cDNA solution to resuspend an aliquot of Cy3 or Cy5 CyDye NHS-ester (Amersham Biosciences) and incubated in the dark at room temperature for 90 min. Unreacted CyDye NHS-ester was inactivated by adding hydroxylamine (15 µl, 4 M) and incubated in the dark at room temperature for a further 15 min. Unincorporated CyDye was immediately removed from the fluorescently-labelled cDNA by using a CyScribe GFX purification column as described above except that GFX wash buffer (Amersham Biosciences) was used instead of 80 % ethanol to wash the cDNA.

The two differentially labelled (Cy3 and Cy5) cDNA samples were mixed in a light-proof 1.5 ml tube, to which was added calf thymus DNA (20 µl, 200 ng/ ml) and poly A oligo-nucleotides (2 mg/ml, 20-mers). The solution was transferred to a Centricon concentrator column (Millipore, Watford, UK) supported in a 1.5 ml micro-centrifuge tube. Water was added up to the mark engraved on the column and then centrifuged at 14000 g for 5 min. The eluate was discarded and H_2O again added to the engraved mark and the column centrifuged at 14000 g for 8 min. Further centrifugations at 14000 g

were performed for 1 min until the remaining volume was 14.4 µl or less. The solution was collected by placing the column inverted in a fresh 1.5 ml micro-centrifuge tube and centrifuging for 1 min at 14000 g. The solution was transferred to a PCR tube, combined with 20 x SSC buffer (15 µl), formamide (30 µl), SDS (0.6 µl, 10% weight:volume) and the volume made up to 60 µl with H_2O. The solution was heated to 95 °C for 5 min to denature the DNA and then snap cooled on ice before being applied to a pre-hybridised microarray slide as described below.

Microarray pre-hybridisation: Microarrays were pre-hybridised for 1 hour at 45 °C in 50 ml pre-hybridisation solution containing to following final concentrations; formamide (50 % v/v); 5 x SSC buffer; SDS (0.1 %); bovine serum albumin (0.1 mg/ ml); denatured calf thymus DNA (200 ng/ ml) and yeast RNA (200 ng/ ml). Pre-hybridisation reduces background fluorescence signal which usually originates from non-specific hybridisation of the labeled samples or auto-fluorescence of the glass slide. Arrays were washed twice for 5 min in 0.1 x SSC for 5 min, dipped in H_2O and dried by centrifugation. Labelled cDNA probes were aliquoted onto the arrays and overlayed with an M-series lifterslip (Erie Scientific Company, Portsmouth, USA) which ensures equal distribution of probe across the printed surface as they have a raised perimeter edge on the underside. Arrays were placed in an airtight chamber to maintain humidity and incubated overnight at 44 °C to allow binding of the labelled cDNA with the complementary features on the microarray.

Microarray stringency washes: The microarray was placed vertically into a flask containing solution A (50 ml, 10 % SDS, 1 x SSC) at room temperature to allow the coverslip to come away from the microarray. The microarray was transferred to a cylindrical flask containing solution A (50 ml) at room temperature and placed on a roller for 5 min. The microarray was then transferred to a fresh flask containing solution B (50 ml, 1 % SDS, 1 x SSC) pre-warmed to 42 °C and placed on a roller inside an incubation oven at 42 °C for 5 min. The wash with solution B was repeated before the microarray was washed 5 times in solution C (50 ml, 0.1 x SSC) pre-warmed to 42 °C in rolling flasks for 5 min each. The array was washed once more

with solution D (50 ml, 0.01 x SSC) at room temperature by submerging for 10 s. The array was dried quickly by placing in a slide rack and centrifuging at 2000 g for 1 min and scanned immediately.

3.25 Sequencing analysis

Differentially expressed clones from the SSH array (400) and brain array experiments (100) were sequenced using M13 primers by Macrogen Ltd. (Seoul, South Korea) using dideoxy chain termination with BigDye™ and an ABI3730 XL DNA Analyser (Applied Biosystems, Renton, USA). The sequencing reaction involves an initial PCR of a clone using M13 forward (5′-GTAAAACGACGGCCAG-3′) and M13 reverse (5′-CAGGAAACAGCTATGAC-3') primers followed by purification of the amplicons. The second stage uses DNA polymerase to copy the amplicons primed by a single specific primer (M13 forward). Included in this reaction are four different fluorescently labelled dideoxy chain terminators, one for each of the four DNA bases. When one of these dyes is incorporated instead of the matching nucleotide base the extension is terminated. This occurs for every length of strand possible (as dictated by the template) and the dye at the end of each strand can be identified by the ABI3730 XL DNA Analyser to give the final DNA sequence.

Trade2dBest (CIH, Oxford) was used for sequence analysis. The software extracts the sequence from the original electrophoretogram data and then edits out expression vector and adaptor sequences. Sequences were compared to NCBI databases using two algorithms based on Basic Local Alignment Search Tools blastx and blastn (Altschul et al., 1997) before being assembled into contigs using ClustalX software (NCBI Toolkit, University of British Columbia, USA).

Putattive functions for selected genes were determined using the Gene Ontology database (http://www.geneontology.org/, Ashburner, 2000).

3.26 Microarray data acquisition, normalisation and analysis

Hybridised slides were scanned with a confocal laser scanner (ScanArray Lite, Microarray Analysis System, PerkinElmer Life Sciences, Beaconsfield, UK). The microarrays were first scanned at a laser output of 633 nm to detect Cy5 labelled cDNA first, as this dye is more sensitive to photo-bleaching. Scans were performed at 10 µm resolution and laser intensities and PMT gain ranging from 60-90 % and then saved as *TIFF files. The process was then repeated with a laser output of 543 nm to detect Cy3 labelled cDNA. One scan for each dye type was selected for analysis. The criteria for selection included; the scans with the highest average signal intensity; no saturated features (spots) and a low background signal. The fluorescent signal intensities of both dyes for each spot were measured using Quantarray Microarray Analysis software (PerkinElmer Life Sciences). Features were located with a 20 x 20 spot-grid with 224.5 nm spacing between spots, a 160 nm standard feature diameter, grid elasticity was set to 10 and feature elasticity was set to 50. The grid and feature elasticity is a feature of the Quantarray Microarray Analysis software, and allows automatic location of the sub-arrays (grids) and features which fall outside the expected location as dictated by the grid and feature spacing. Adaptive quantification, which allows the spots intensity to be measured from spots of different sizes, was performed with a maximum feature diameter of 190 nm with background measurements taken between 220 to 265 nm from the centre point (Figure 3.20.a).

Figure 3.20.a. Red area represents feature data area (variable 160-190 nm diameter), blue portion represents background area measured from 220-265 nm from the centre-point of the feature.

Data processing was performed using the web-accessible MicroArray Data Suites of Computed Analysis (MADSCAN) software (Le Meur et al., 2004). MADSCAN then follows a stepwise data processing method encompassing:

Filtration. Median background intensities (taken from the 220-265 nm reading) of replicate spots are subtracted from each of the corresponding foreground intensities (taken from the 160-190nm feature data area). Features which exhibited high diameter variance, signal below background level or signal above saturation level were removed from further analysis.

Normalisation. Genes showing the lowest variation in expression between the two conditions were selected by an iterative Rank Invariant Method algorithm (Tseng et al., 2001). This method ranks all of the spot intensities in the Cy3 and Cy5 channels and the spots where the difference in rank is less than 5 are deemed to be non-variant. The data for the remaining genes are subjected to an intensity dependent normalisation to the non-variant genes using the Lowess fitness algorithm (Dudoit et al., 2000). Lowess fitness stands for Locally weighted estimated and uses the geometrical mean (A) and a constant (k) to minimize signal-dependent non-linear bias between the two intensity levels, Cy3 (G) and Cy5 (R). Madscan performs a within-print tip (local) normalization with a smooth parameter (defined as the fraction of data used to smooth at each data point) $f = 0.40$.

Scaling. After normalisation, scaling procedures were applied to bring the variances of filtered and normalised expression values among replicate spots to the same variation level.

Outlier detection. Due to the small number of replicates available in microarray experiments, the use of modified statistical tests are required to evaluate the consistency of replicates within one array and between replicated arrays. A median absolute deviation test (modified z-test) and Grubb's test ($p = 0.01$) were used to detect outliers which in the case of microarray

experiments represent the genes showing significant changes in expression between the two conditions.

The median absolute deviation test is a measure of the spread of data, similar to standard deviation (Burke, 2001), and is expressed as;

$$MAD \equiv median\left\{\left|x_i - \tilde{x}\right|\right\} \quad (1)$$

$$z \equiv \frac{0.675\,(x_i - x_m)}{MAD} \quad (2)$$

$$if\ |zi| \geq 3.5\ then\ x_i\ is\ an\ outlier. \quad (3)$$

The Grubb's test specifically detects outliers in data. If the largest value in a data set is suspected of being an outlier then;

$$T_n \equiv \frac{x_n - \tilde{x}}{\sigma}, \quad (4)$$

but if the smallest value is suspected then;

$$T_i \equiv \frac{\tilde{x} - x_1}{\sigma}, \quad (5)$$

where x_n is the largest value, x_1 is the smallest value, x is the mean of all the n values and s is the sample standard deviation of all n values. The critical value for the test performed depends on the sample size n and the selected significance level

Data integration. The replicated data points are summarised using mean and coefficient of variation values per slide and between replicated slides. This step consolidates the data sets and allows the comparison between them.

Hierarchical clustering with Cluster and Tree View software 1.6.6 (Eisen et al., 1998) was performed with the SSH array data to obtain a good visual data representation. These programs permit the clustering of genes with similar expression profiles based on calculation of difference between gene expression levels.

Fold change method (Draghici, 2003) was used for selection of differentially expressed genes. Using the fold change method, genes were considered up-regulated if the ratio between salinity stress and control normalised expression values was reproducibly (including dye-swap) higher than 1.5 (mRNA more abundant in fish encountering salinity stress) and under expressed if the ratio was lower than 0.6 (mRNA is less abundant in fish encountering salinity stress).

Statistical analysis was performed using Student's t-test to determine the significance of inter-individual differences between gene expression in fish in the FW to SW acclimation experiments.

3.27 Real-time Quantitative PCR Assays

cDNA was synthesised separately for each eel using brain total RNA. Total RNA (1 µg) was combined in a PCR tube with 1 µl random hexamers (10 µM), 1 µl dNTPs (10 µM each) and made up to a final volume of 12 µl with H_2O. Random hexamers must be used when using RPL-P0 as the endogenous control as the encoding RNA does not have a poly (A) tail. The mixture was incubated at 65 ºC for 5 min to denature the nucleic acid and then cooled rapidly on ice for 2 min. To the mixture was added 4 µl 5 x Superscript II reaction buffer (Invitrogen, Paisley, UK), 2 µl DTT (0.1 M) and 2 µl RNAseOUT (40 U/µl, Invitrogen) and then incubated at 25 ºC for 2 min to allow primers to anneal. Superscript II reverse transcriptase was then added and the mixture incubated at 25 ºC for 10 min, then at 42 ºC for 50 min and finally at 70 ºC. RNA was removed by adding 1 µl *E. coli* RNAse H (2 U/µl, Invitrogen, Paisley, UK) and incubating at 37 ºC for 30 min. cDNA was purified by ethanol precipitation as per Section 3.5 and then resuspended in 20 µl H_2O.

QPCR Primers (Table 4.24.a) were synthesised (MWG Biotech, Ebersberg, Germany) and checked to see if they amplified a single product by visualising amplicons on ethidium bromide stained agarose gels (see Section 3.5) and by analysis of dissociation curves. To ensure that there was no amplification of non-specific products or amplification from genomic DNA, control QPCR reactions were performed for each primer set which contained no template or an RNA template. The spent reactions were analysed with gel electrophoresis and dissociation plot analysis and primer sets which gave multiple products were discarded and new primers designed.

Real time PCR reactions contained ABI SYBR Green Master Mix (12.5 µl, 2 x), forward and reverse primers at final concentrations of 70 – 300 nM, 1 µl cDNA template and made up to 25 µl with H_2O. Reactions were performed using the ABI Prism 7000 apparatus (Applied Biosystems, Warrington, UK). Identical cycling conditions were used for all primers (initial activation at 95 ºC 15 min, then 45 cycles of 95 ºC 15 s, 60 ºC 1 min) followed by a dissociation analysis from 60 ºC to 95 ºC. Reactions were performed in duplicate or triplicate.

4.0 Results

The results chapter is presented in 28 sections.

Sections 4.1 and 4.2 contains the metadata results and RNA quality analysis.

Sections 4.3 – 4.13 contain the results and experimental timeline for the creation of the various cDNA libraries created during the project.

The microarray hybridisations and data analysis are presented in Sections 4.14 - 4.17.

The identification of genes showing significant changes in expression and subsequent sequencing and gene ontology data are presented in Sections 4.18 – 4.21.

Sections 4.22 –4.29 contains results pertaining to the QPCR validation of microarray results and target gene characterisation.

4.1 Metadata

The following physiological data and biological observations, collectively known as metadata, were recorded for each fish used in the experiment; whole fish weight; tissue weight; presence of parasites and signs of disease (e.g., lesions on skin or internal organs); disturbance and kill times. Although these factors are not directly related to the microarray experiment this metadata may provide explanatory variables for anomalies in the results. Collection of this data is also a requisite for the MIAME standards (Brazma 2001), which detail the minimum information about a microarray experiments to be included in any publications. Additionally, blood samples from the silver eels were taken directly after decapitation and plasma properties (Figures 4.1.a - f) were recorded; plasma osmolality (assessed using a vapour pressure osmometer (Wescor Inc., Logan, US)); plasma protein concentration; plasma cortisol concentration ; plasma angiotensin II; plasma Cl^- (measured with a Chloride Analyser (Corning, Essex, UK); plasma Na^+ and K^+ concentrations (determined using flame photometry (Corning Model 450).

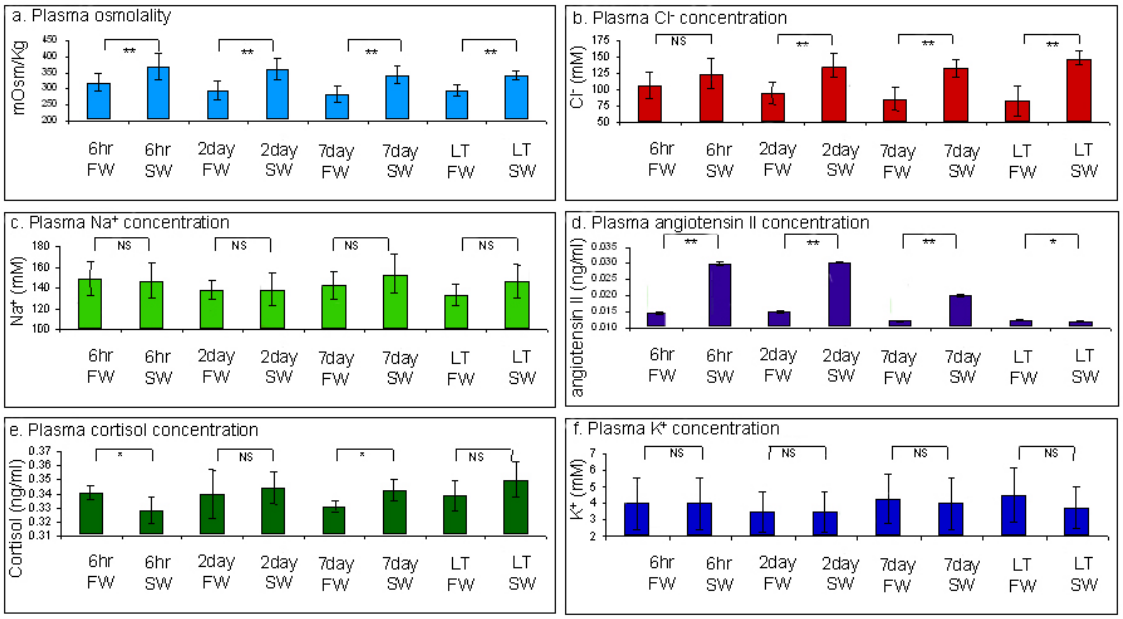

Figure 4.1.a - f. Plasma properties for silver eel groups. Bars represent mean values for groups of six identically treated fish. Error bars indicate standard deviation from the mean. Statistics are a pairwise t-test assuming heteroschedastic variation. NS = Non significant, * = 95 % significance level and ** = 99 % significance level.

4.2. RNA Quality Analysis

The quality of all RNA samples was verified using both denaturing gel electrophoresis (Figure 4.2.a) and by capilliary electrphoresis (Figure 4.2.b). Degraded RNA samples were discarded

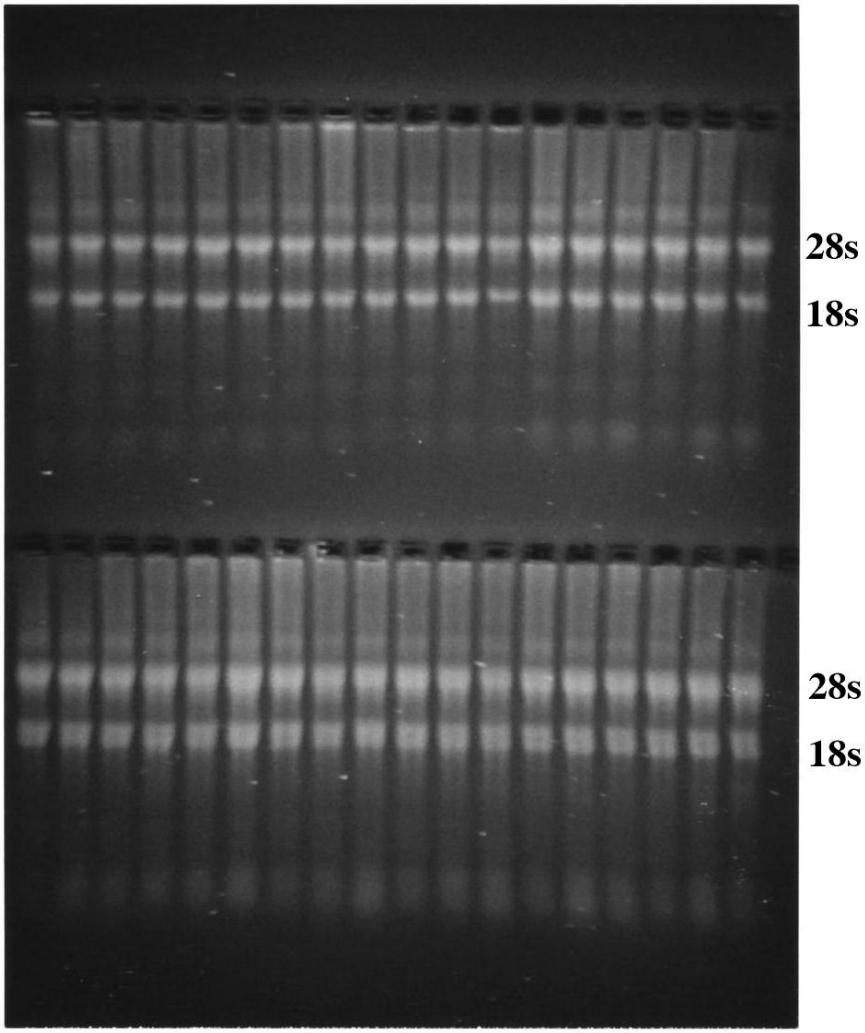

Figure 4.2.a. Total RNA run on a denaturing agarose gel. Top row; lanes 1-6 = renal kidney from yellow 7day FW acclimated eel, lanes 7-12 = renal kidney from yellow 7day SW acclimated eel, lanes 13-18 = gill from silver 7day FW acclimated eels. Bottom row; lanes 1-6 = gill from silver 7day SW acclimated eels, lanes 7-12 = gill from silver 5 month FW acclimated eels, lanes 13-18 = gill from silver 5 month SW acclimated eels.

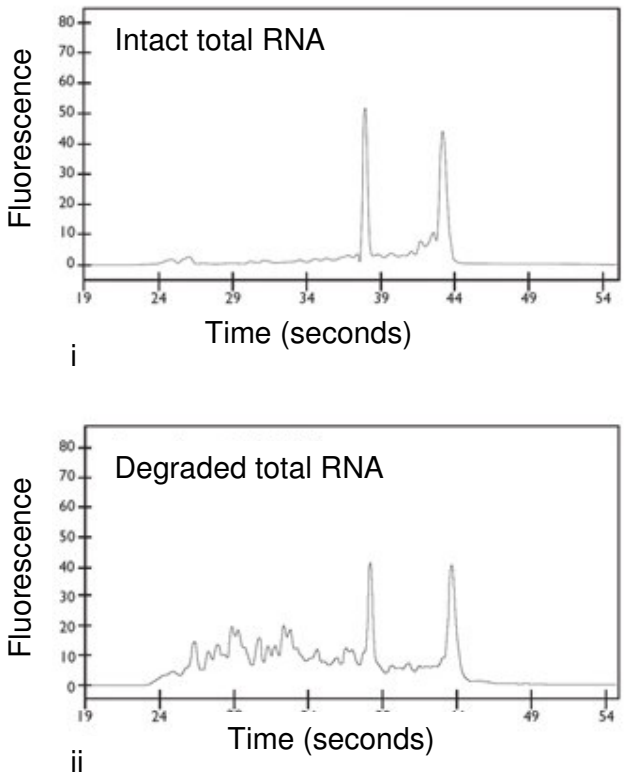

Figure 4.2.b. RNA analysis by Agilent Bioanyliser representing an intact (i) and a degraded (ii) total RNA sample.

4.3 Overview of cloning method evolution

A cDNA library refers to a complete, or nearly complete, set of all the transcribed genes contained within a particular organism or cell/tissue type. Genes are transcribed from genomic DNA as intronless mRNA but as all RNA is inherently fragile, being susceptible to ubiquitous RNases, reverse transcription is used to convert the mRNA into the more stable cDNA.

Genes are present in different frequencies in genomes and their transcription can vary by several orders of magnitude. The most prevalent mRNA species in a typical somatic cell comprises ~10 transcripts, each of which is represented by approximately 5000 copies whilst there are around 15,000 rare mRNAs that are represented by only 1-15 copies per cell (Bishop et al., 1974; Davidson and Britten, 1979). Rare mRNAs are even more under represented in the brain which exhibits very high transcript diversity (Hahn and Owens, 1988; Snider and Morrison-Bogorad, 1992). This can cause redundancy problems for microarray experimenters as the most abundant genes can be repeated many times on a single microarray whereas the rare genes might not be represented at all. Normalisation and subtraction procedures can be utilised to maximise the number of unique genes represented in a cDNA library (Bonaldo et al., 1996).

The creation of a high quality cDNA library with low redundancy is the cornerstone of a good microarray project and as such a large amount of effort was invested in optimising the procedure. The original goal was to create a full length cDNA library with low redundancy for each of the four tissues under examination (brain, gill, intestine and kidney). Making high quality cDNA libraries, however, proved difficult and a large amount of time was invested in developing a new method of producing cDNA libraries with a large average insert size and low redundancy. A library with low redundancy reduces the number of repeated clones, maximising mRNA representation on the array and minimising time and money wasted on characterisation of repeated

clones. The larger insert size allows easier identification and characterisation of each clone.

The Gateway™ system, based on the site specific recombination properties of bacteriophage lambda (Landy, 1989), was chosen as the basis for the protocol. The mRNA is first subjected to reverse transcription and second strand synthesis to create double stranded complementary DNA (cDNA). Primers and adapters used in this process confer an *att*B recombination site to each end of every cDNA created which is then inserted into a plasmid via an enzyme-mediated recombination, during which the *att*B sites recombine with two corresponding *att*P recombination sites in a plasmid (Figures 3.7.a and 3.7.b). The recombination site names, *att*B and *att*P, refer to attachment sites of bacteriophage lambda in the bacterial DNA and the corresponding site in the phage sequence and it was the biology of this system which inspired the current technique (Campbell, 1961). The recombined plasmid is then transfected into a host *Escherichia coli* by electroporation whereupon the bacteria can be spread on selective media and grown allowing individual colonies containing unique cDNAs to be selected.

The plasmids used also contain a *ccd*B gene between the two *att*P sites and a kanamycin resistance gene (Kan^R) outwith the *att*P sites (Figure 4.4.c and 4.5.d). Thus when the recombination reaction occurs the *ccd*B gene is replaced in the plasmid by the cDNA insert. This allows for both positive and negative selection of the donor vector in *E. coli* following recombination and transformation. Media containing kanamycin are used to positively select for transformants containing the plasmid. The *ccd*B gene encodes the CcdB protein which interferes with *E. coli* DNA gyrase thus inhibiting bacterial growth and allowing negative selection.

4.4 SMART cDNA PCR amplified library

The first attempt at creating a cDNA library was based around the cDNA preparation method known as SMART which stand for “Switching Mechanism At the 5' end of RNA”. Two primers were used during cDNA synthesis, G-Super-Oligo-d(T) and GSO2, which confer nested primer sites for PCR amplification of cDNA and *att*B1 and *att*B2 sites for recombination with the plasmid (Figure 3.7.a).

G-Super-Oligo-d(T)

GGG GAC CCA CTT TGT ACA AGA AAG CTG GGT AGG CGG CGC CAC TCC TGG AGC CCG T(T)$_{26}$

GSO2

GGG GAC AAG TTT GTA CAA AAA AGC AGG CTA AGG CAG TGG TAA CAA CGC AGA GTA CGC GGG

Figure 4.4.a. G-Super-Oligo-d(T) primer with the nested cDNA amplification primer site, EnvGenIntOligo, underlined and the SMART-*att*B2 recombination site highlighted in green. GSO2 primer with G-MCS2 nested primer cDNA amplification site underlined, the SMART-*att*B1 recombination site is highlighted in yellow and the GGG site which allows template switching during first strand synthesis is highlighted in red.

The mRNA, oligonucleotides, dNTPs and reverse transcriptase are mixed together and the G-Super-Oligo-d(T) primer binds to the poly A tail at the 3' end of mRNA, thus initiating reverse transcription. The poly A tail is a long sequence of adenine nucleotides (often several hundred) added to the "tail" or 3' end of the mRNA by polyadenylate polymerase (Higgs et al., 1983). Upon reaching the 5’ end of the RNA template the RT adds several cytosine residues to the 3’ end of the newly synthesised cDNA molecule, to which the complementary GGG section of GSO2 binds. The RT then switches templates from the mRNA to GSO2 and incorporates the complement of GSO2 at the 3’ end of the first strand cDNA molecule. The first strand cDNA

is therefore a complement of the mRNA but with *att*B1 and *att*B2 adapters at either end. Only full length cDNAs will be viable as both *att*B sites are required for the Gateway reaction. The cDNA is amplified by PCR using SMART-*att*B1and SMART-*att*B1primers which has the combined effect of making the second strand of cDNA and increasing the amount of cDNA. The whole process is shown schematically in Figure 4.4.b.

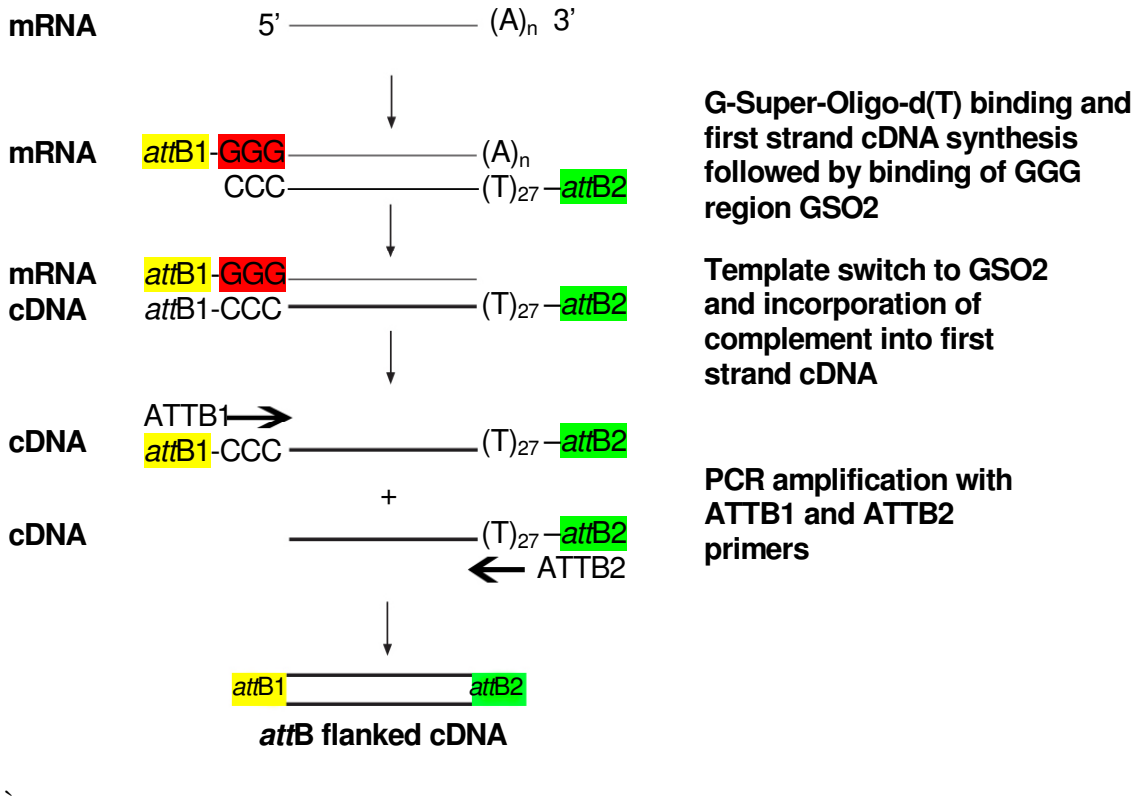

Figure 4.4.b. *att*B flanked cDNA synthesis using SMART™ cDNA PCR amplifiction method.

The resultant *att*B flanked cDNA was passed through a sepharose column to isolate the cDNA over 400bp in length. Size selected cDNA was then cloned into the plasmid pDONR221 by site specific recombination (*att*B x *att*P) (Figure 4.4.c). This process is mediated by the enzyme integrase and

host integration factor (Landy, 1989). *E. coli* (GeneHog, Invitrogen, Paisley, UK) were transfected with the recombined vector and grown on media containing kanamycin.

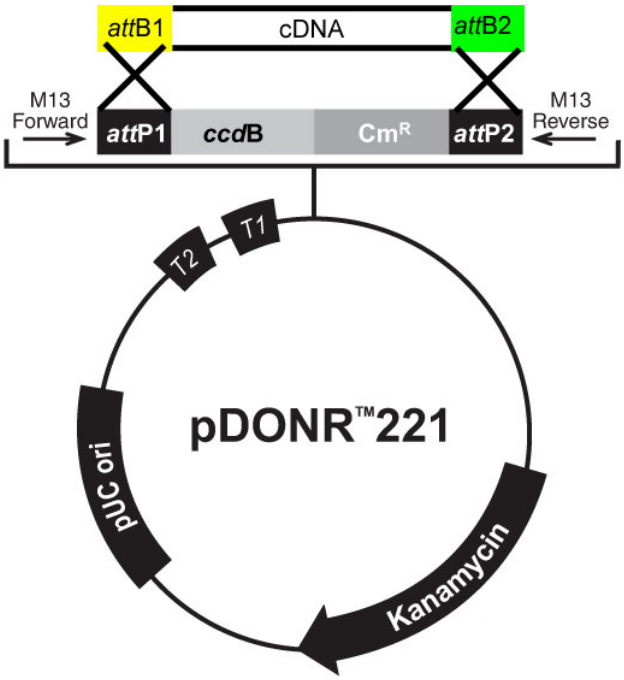

Figure 4.4.c. Insertion of *att*B flanked cDNA into pDONR221 via recombination with *att*P sites. The section of the plasmid encoding the *ccd*B and chloramphenicol resistance gene (Cm^R) genes is replaced with the *att*B flanked cDNA.

The libraries obtained with this method were characterised by small insert sizes (<1 kb) and, as only full length cDNA should be created, this suggests that only a fraction of the mRNA species present in each tissue was being represented. At this stage Invitrogen were consulted about the vector pDONR221, and it transpired that this vector was not intended for use in cDNA library creation. Although promoted as being capable of accepting cDNA inserts of up to 180 kb the vector consistently preferentially accepted the smallest clones available, a fact not presented in the pDONR221 product brochure. Invitrogen suggested utilising the CloneMiner™ kit which uses the

same basic protocol but with a new vector, pDONR222 which was designed specifically for cDNA library production.

4.5 CloneMiner™ cDNA library

The CloneMiner™ kit (Invitrogen, UK) uses the same principles as the SMART™ cDNA PCR amplified library detailed in Sections 3.6 and 4.4. The procedures differ in that the *att*B flanked cDNA is made in a different way and a different plasmid and *E. coli* strain are used. The CloneMiner oligo d(T) *att*B2 primer has a biotin molecule at the 5' end and the *att*B2 site is highlighted (Figure 4.5.a). The oligo d(T) section binds the poly A tail of mRNA, priming first strand synthesis by reverse transcriptase. Second strand synthesis is performed by *E. coli* DNA polymerase 1 before the cDNA is blunt-ended by T4 DNA polymerase. The *att*B1 adapter is double stranded and phosphorylated at the 5' blunt end (Figure 4.5.a). This allows it to be blunt-end ligated to the double stranded cDNA by *E.coli* DNA ligase. The *att*B1 adapter is only ligated at the 5' end of the sense strand of the cDNA as the biotin at the 5' end of the *att*B2 site prevents the *att*B1 adapter ligation at the 3' end of the cDNA.

CloneMiner™ Oligo d(T) *att*B2 primer

5'-Biotin.GGCGGCCGCACAACTTTGTACAAGAAAGTTGGGT$(T)_{19}$-3'

CloneMiner™ *att*B1 adapter

5'-TCGTCGGGGACAACTTTGTACAAAAAAGTTGG-3'

3'-CCCCTGTTGAAACATGTTTTTTCAACCp-5'

Figure 4.5.a. Biotinylated CloneMiner™ Oligo d(T) attB2 primer with *att*B2 site highlighted in green. Phosphorylated CloneMiner™ *att*B1 adapter with *att*B1 site highlighted in yellow.

The diversity of cDNA species produced in this way is potentially limited as the cDNA is only made from the 3' end of mRNA. Any mRNA species lacking a poly (A) tail, due to degredation or shearing during handling, would not be represented. In an attempt to address this potential bias an additional first strand primer (random *att*B2 primer) was created with a 6 base wobble (N_6) replacing the oligo d(T) sequence (Figure 4.5.b).

CloneMiner™ Random *att*B2 primer

5'-Biotin.GGCGGCCGCACAACTTTGTACAAGAAAGTTGGGT(N)$_6$TGCCTG-3'

Figure 4.5.b. CloneMiner™ Random *att*B2 primer containing a 6-base variable region highlighted in red, a 6-base anchor highlighted in blue and the *att*B2 site is highlighted in green.

The variable $(N)_6$ site has the potential to bind to any complementary site along the length of a particular mRNA. The $(N)_6$ site could, however, bind to any complementary site on contaminating, non-messenger RNA carried over during the mRNA extraction; such as ribosomal RNA. In an attempt to limit this, the bases TGCCTG were added to the 3' end of the primer. Statistically a sequence 6 bp long should occur every 4096 bp but on testing various eel gene sequences (CFTR, NKCCl, Na^+K^+-ATPase) it was found to occur approximately every 800 bp – 1 kb. The complement to the sequence TGCCTG was not found in 18S or 28S rRNA sequences available for *A. anguilla*, nor any other 18S or 28S sequences from teleost species. The random *att*B2 primer was used in parallel with the oligo d(T) *att*B2 primer to make two cDNA libraries as summarised below (Figure 4.5.c).

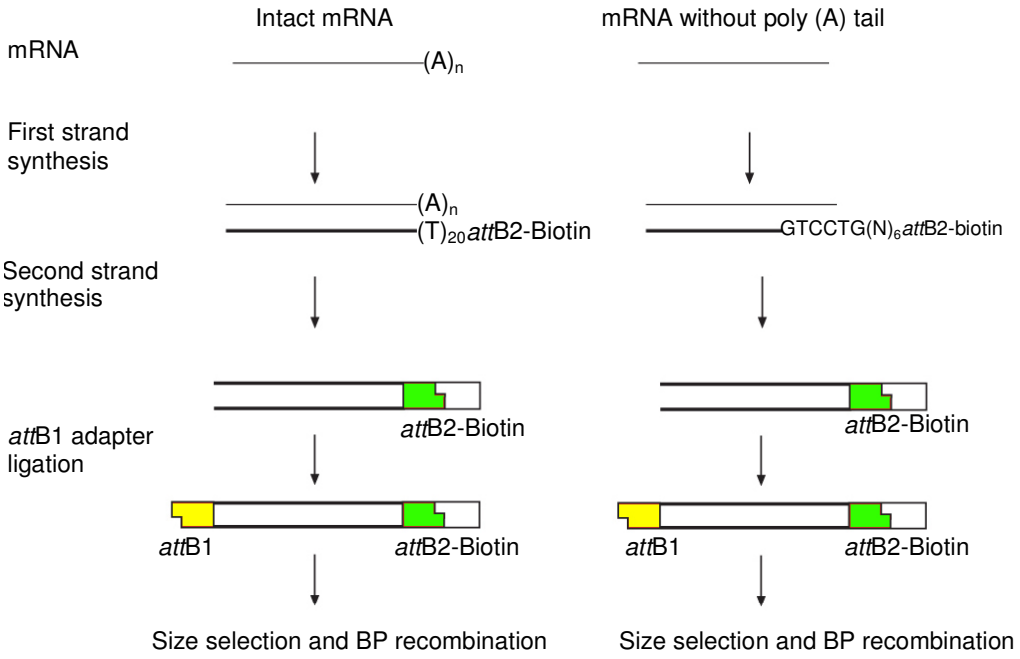

Figure 4.5.c. Production of *att*B flanked cDNA using CloneMiner™ Oligo d(T) *att*B2 or Random *att*B2 primers from mRNA with or without a poly (A) tail, respectively, using the CloneMiner™ protocol. The *att*B1 and *att*B2 sites are highlighted in yellow and green respectively.

The *att*B flanked cDNA made with the oligo d(T) and random primers was cloned into the plasmid pDONR222 (Figure 4.5.d) by recombination mediated by the enzyme Clonase™. As in the previous method the *att*B sites flanking the cDNA recombine with the *att*P sites in the plasmid, inserting the cDNA in place of the *ccd*B and chloramphenicol resistance (Cm^R) genes (figure 4.5.b).

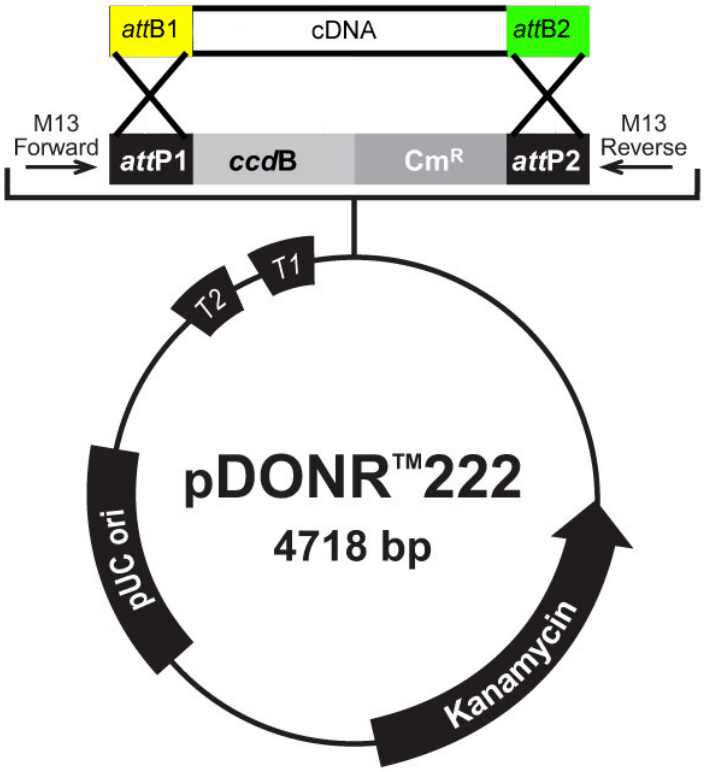

Figure 4.5.d. Insertion of *att*B flanked cDNA into pDONR222 via recombination with *att*P sites.

The two cDNA libraries created had a larger average insert size than the SMART™ cDNA PCR amplified library we prepared previously. Average size was approximately 1.2 kb for the Random primed library and ~2 kb for the Oligo primed library (Figure 4.5.e). This result confirmed that the CloneMiner™ protocol could be used to create cDNA libraries with an adequately large insert size. The protocol required to be adapted in order to allow normalisation and subtraction protocols to be applied at a later stage.

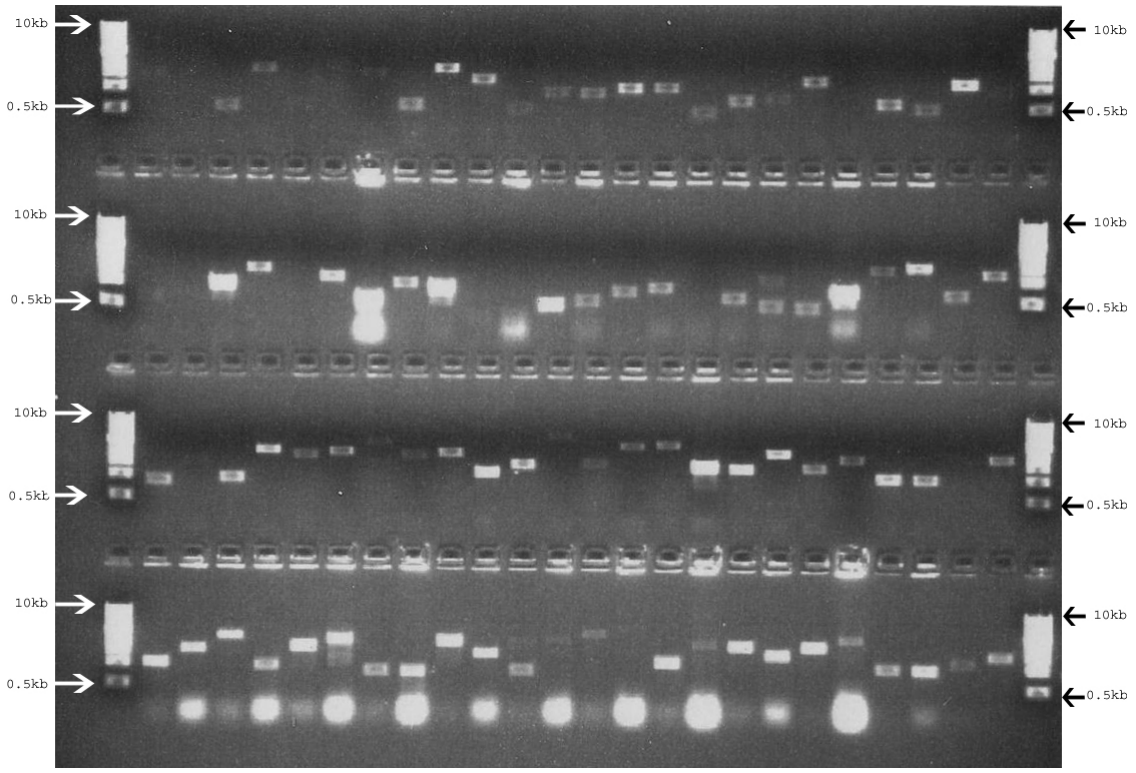

Figure 4.5.e. CloneMiner™ Library, 48 clones made with CloneMiner ™ random *att*B2 primer (top two rows), 48 clones made with CloneMiner ™ oligo d(T) *att*B2 primer (bottom two rows).

4.6 Second generation (2G) CloneMiner™ libraries

Second generation CloneMiner™ oligo and random libraries were made as detailed in section 3.8. The standard *att*B adapters from the CloneMiner™ kit which are conferred to the cDNA during reverse transcription and second strand synthesis, do not lend themselves to manipulations such as cDNA normalisation or subtraction. The sequences of the first strand synthesis oligo d(T) *att*B2 primer and *att*B1 adapter were altered to include internal primer sites (underlined portion) within the *att*B sites (highlighted portion) to give a set of second generation (2G) primers (Figure 4.6.a). The internal primer sites allow the cDNA to be amplified and the resulting amplicons will not have the sites necessary for *att*B x *att*P recombination and thus cannot insert into the pDONR222 plasmid.

2G Oligo d(T) *att*B2 Primer (N*att*B2dT primer)

5′-**B.**GGCGGCCGCACAACTTTGTACAAGAAAGTTGGGTGGAACCGTCACGTAC$(T)_{20}$-3′

2G Random *att*B2 primer (NInt*att*B2primer)

5′-**B.**GGCGGCCGCACAACTTTGTACAAGAAAGTTGGGTGGAACCGTCACGTAC$(N)_{6}$TGCCTG-3′

2G *att*B1 adapter (NInt*att*B1primer)

5′-TCGTCGGGGACAACTTTGTACAAAAAAGTTGGGTGCATCAGCTGGACTAG-3′

3′-CCCCTGTTGAAACATGTTTTTTCAACCCACGTAGTCGACCTGATC**p**-5′

Figure 4.6.a. Biotinylated 2G Oligo d(T) *att*B2 primer and biotinylated 2G Random *att*B2 Primer with *att*B2 sites highlighted in green and internal primer sites for NInt*att*B2primer underlined. Phosphorylated 2G *att*B1 adapter with *att*B1 site highlighted in yellow and internal primer site for NInt*att*B1primer underlined.

cDNA biotinylated on the first strand and radiolabelled on the second strand was created to monitor strand associations during the subsequent

normalisation protocol. The libraries were amplified by PCR as per standard protocol (see Section 3.5) using the internal primers (N*att*B2dT and NInt*att*B1 primers, annealing temperature 58 ºC) to examine the size of the cDNAs and to ensure both *att*B sites were present, as only cDNA with both *att*B adaptors at the ends would amplify. The cDNA from the Oligo and Random libraries was intact, in that it had both attB sites, and exhibited a large range of sizes from 0.5 to 10 kb (Figure 4.6.b). These cDNA libraries were subjected to normalisation procedures, as detailed in Section 4.7, to redress the imbalance in frequency of different genes.

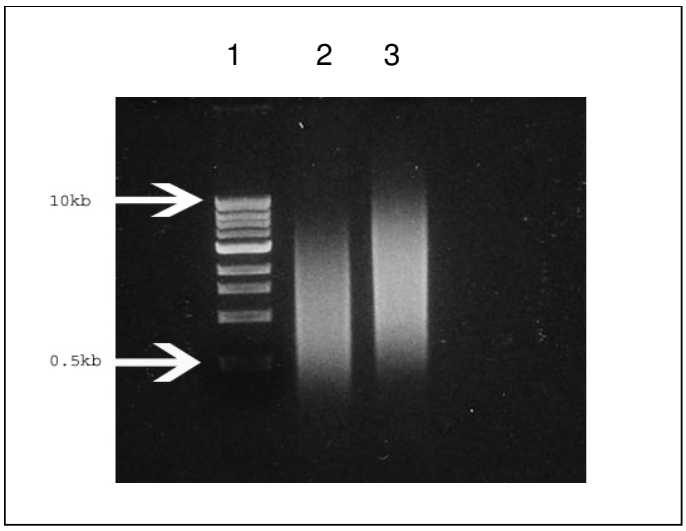

Figure 4.6.b. Lane 1, 1 kb DNA Ladder (NEB). Amplified cDNA from the Oligo (Lane 2) or Random (Lane 3) libraries made using the CloneMiner™ protocol with 2G primers and adapters.

4.7 Normalisation

Genes are present in different frequencies in genomes and similarly their transcription rates vary by several orders of magnitude. Normalisation aims to reduce this redundancy by removing a high proportion of the most abundant mRNAs without deleting any genes from the library.

One experimental procedure designed to accomplish this was to heat denature double stranded cDNA to create single stranded cDNA and then cool this down slowly in the presence of 50 % formamide. The rehybridisation is stopped once ~50 % of the cDNA has reannealed by snap cooling the cDNA. Re-association kinetics demand that when the cDNA rehybridises the most prevalent species will hybridise at a faster rate than those which are less abundant (James and Higgins, 1985; Ko, 1990; Patanjali et al., 1991; Weissman, 1987). The double stranded cDNA is then selectively removed and a normalised cDNA library remains. To remove a particular fraction of DNA from a solution, in this case the cDNA which has rehybridised, there must be a method of targeting only the desired species and the biotin label on the first strand of each cDNA provides such a target. Biotin binds to avidin and its homologues with a very high affinity (K_d=10^{15}M, (Green, 1975; Hiller et al., 1987) and solid supports coated in avidin can be used to bind and selectively remove biotin labelled compounds from a solution. Thus, avidin is used to remove all biotin-conjugated DNA which includes the double stranded cDNA and the first strand cDNA, leaving only the non-biotinylated, second strand of cDNA which did not rehybridise. The second strand cDNA is then converted into double stranded cDNA and cloned as described in Section 3.8. The resultant clone set should contain a library of cDNAs which are within approximately one order of magnitude of each other.

Initially, Streptavidin Magnesphere® Paramagnetic Particles (SA-PMPs, Promega, UK) were used to target and remove biotin-conjugated DNA molecules from the solution. The irregular shaped particles are coated with streptavidin, an avidin homologue isolated from *Streptomyces avidinii*, and are

promoted as being able to bind biotin-conjugated nucleic acid at a rate of 0.75-1.25 nmol biotinylated oligo(dT)/ mg particles. The SA-PMPs can be removed from a solution using a strong earth magnet as they exhibit a dipole moment when in a magnetic field. See section 3.9 for normalisation protocol details. This normalisation procedure was not used, however, as control experiments showed problems with the SA-PMPs as described below.

Before the normalisation protocol (Section 3.9) was implemented, a control experiment was performed to test the efficiency of the SA-PMPs and to see how long complete binding of the biotinylated cDNA would take. Three identical samples of biotinylated, radiolabelled kidney cDNA (1 µg) in a 100 µl solution containing 1 x SSPE were prepared (without formamide or heat denaturation). An aliquot of SA-PMPs (0.6 mg) pre-washed three times in 1 x SSPE was applied to each of the cDNA samples and incubated at room temperature either for 30 min, 1 hour or 2 hours, following which the beads were removed using a magnet. The amount of radiolabelled cDNA either bound to the beads or remaining in the supernatant was determined by liquid scintillation counting (Cerenkov radiation). The experiment showed, however, that the SA-PMP could not remove all the biotinylated, radiolabelled cDNA. The assay showed that the maximum amount of biotinylated cDNA that could be removed from a solution was ~30 % regardless of incubation time.

This had four possible meanings;

i. The streptavidin binding sites on the beads are saturated.

Only a fraction of the biotin-conjugated cDNA is available to the streptavidin due to steric hindrance.

The cDNA is not fully biotinylated suggesting that the reverse transcriptase primer may not be fully biotinylated.

The beads bind non-specifically to cDNA rather than to biotin.

To address the first possibility two identical biotinylated, radiolabelled cDNA samples (1 µg) in 100 µl 1 x SSPE were exposed to 50 µg and 100 µg SA-PMPs in otherwise identical conditions. The capture rates were 37 % and

31 % respectively suggesting that binding site saturation was not a plausible explanation.

The second possibility was investigated by heat denaturing the radiolabelled, biotinylated cDNA to release any secondary structure within the cDNA and to denature the two strands prior to binding with the streptavidin beads. Three identical samples (1 µg) of the same kidney radiolabelled, biotinylated cDNA prepared above were diluted in 1 x SSPE buffer (100 µl). Samples 1 and 2 were heated to 95 ºC for 2 min and then either cooled slowly to room temperature to allow strand annealing (Sample 1) or snap cooled on ice to maintain the cDNA in a denatured state (Sample 2). Sample 3 was a control and was maintained at room temperature. Samples were then combined with SA-PMPs (0.6 mg, pre-washed three times with 200 µl 1 x SSPE buffer) and incubated at room temperature (Samples 1 and 3) or at 0 ºC (Sample 2). SA-PMPs were separated from the supernatants using a strong earth magnet and the amount of radiolabelled cDNA either bound to the beads or remaining in the supernatants was determined by liquid scintillation counting (Cerenkov radiation). Samples were heated denatured and then cooled slowly to room temperature or snap cooled on ice followed by binding to SA-PMPs at room temperature or 0 ºC respectively. Relative capture rates were determined by liquid scintillation counting (Cerenkov radiation, Table 4.7.a).

Table 4.7.a. Biotinylated DNA capture rate by SA-PMP exposed to different heating regimes. The maximum capture rate was 32 %, regardless of incubation conditions.

Sample	Heat Treatment	Capture Rate (%)
1	95 ºC 2 min, cooled slowly to 25 ºC	**32**
2	95 ºC 2 min, snap cooled on ice	28
3	Control - No heating	25

The expected result was that sample 1 would show the highest capture rate as the radiolabelled second strand is allowed to re-anneal with the biotinylated first strand prior to binding to the SA-PMPs. Sample 2 was expected to show the lowest amount of radiolabelled cDNA associated with the beads as snap cooling and incubating the cDNA on ice throughout the incubation with the SA-PMP should keep the two strand of cDNA separate. Sample 3 was a control sample which was not heated. Comparing sample 1 to the control sample 3, only a small increase (7 %) was seen in capture rates after heat denaturation. An interesting result is shown when samples 1 and 2 are compared; there is only a 4 % decrease in capture rate following snap cooling of the cDNA. Snap-cooling should, however, have kept the cDNA single stranded and all of the radiolabelled, non-biotinylated second strand cDNA should have remained in the supernatant rather than binding to the SA-PMPs.

The third possible explanation for the poor binding efficiencies was that the cDNA is not fully biotinylated. This would suggest that the first strand cDNA reverse transctriptase primers may not be fully biotinylated. This was discussed with MWG Biotech, the manufacturers of the biotinylated primers. They explained that the primers were purified by HPLC and as such it was very unlikely that they were not fully biotinylated. The biotin molecule is, however, very close to the DNA backbone and steric hindrance may occlude it from the SA-PMP even in when the DNA strands are completely free from secondary structure. This does not explain why 28 % of the radiolabelled second strand cDNA is bound to the SA-PMPs even after full denaturation and dissociation from the biotinylated first strand. The possibility that the cDNA is not labelled with biotin could have serious consequences, as the main function of this is to block the ligation of the *att*B1 adapter, with follow on effects for the recombination reaction with the plasmid. To confirm whether the cDNA in the Random and Oligo libraries was flanked at either end by *att*B1 and *att*B2 sites, cDNA from each library was subjected to a standard PCR (see Section 3.5) with either NInt*att*B1primer the NInt*att*B2primer specific primers alone or together using an annealing temperature of 58 ºC

(Figure 4.7.a). If there was amplification with the NInt*att*B1primer alone then there must be an *att*B1 site at both ends of the cDNA molecules, which would imply that the cDNA did not possess the blocking biotin molecule on the first strand of cDNA.

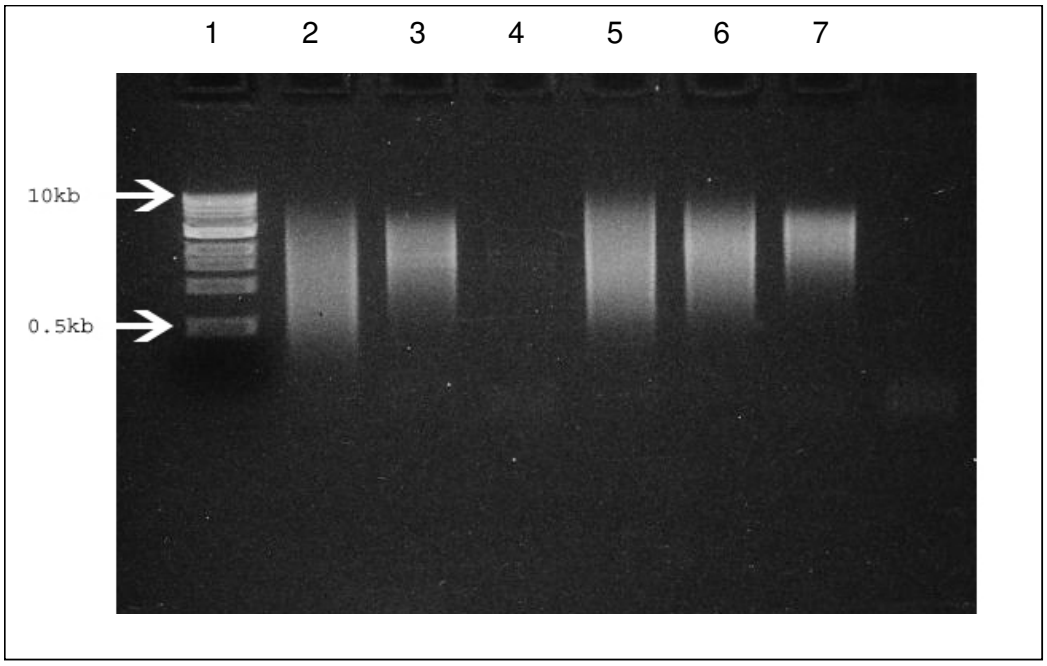

Figure 4.7.a. Lane 1:1 kb DNA Ladder (NEB). Lane 2: Oligo library cDNA amplified with NInt*att*B1primer and NInt*att*B2primer primers together, Lane 3: Oligo library cDNA amplified with NInt*att*B1primer alone, Lane 4: Oligo library cDNA amplified with NInt*att*B2primer primer alone, Lane 5: Random cDNA with NInt*att*B1primer and NInt*att*B2primer primers together, Lane 6: Random library cDNA amplified with NInt*att*B1primer alone, Lane 7: Random library cDNA amplified with NInt*att*B2primer primer alone.

The "random" and "oligo" library cDNAs amplify with both primers and Nint*att*B1primer primer alone (Figure 4.7.a). This implies there is an *att*B1 site at both ends of the cDNA indicating that some or all of the cDNA in both libraries does not have a biotin label which would otherwise block the *att*B1 adapter ligation. The Random cDNA also amplifies with the NInt*att*B2primer primer alone which could be a facet of the first strand primer as the $(N)_6$ portion of this primer could bind to the first strand cDNA during second strand synthesis, thus an *att*B2 site would be present at both ends.

Further tests were carried out to ascertain how much biotinylated cDNA could be removed using the SA-PMPs. First strand cDNA was made using the 2G Oligo d(T) *att*B2 primer as per normal protocol except for the inclusion

of 10μCi α^{32}P dCTP in the reaction mixture. Second strand synthesis and *att*B1 adapter ligation was not performed. The cDNA was heat denatured, snap cooled on ice and combined with the SA-PMPs and allowed to bind for 30 min. Less than 2% biotinylated, radiolabelled cDNA was bound to the beads. This result should have raised more suspicion than it did at the time. What it actually shows is that single stranded biotinylated cDNA is not bound by SA-PMPs. The poor binding was attributed to steric hindrance caused by occlusion of the biotin by the cDNA, a situation which has been previously described (Sabanayagam et al., 2000). To overcome the suspected steric hindrance new primers were created with a 14-carbon spacer arm linked to a biotin molecule at the 5' end of the nucleotide but no improvement in binding efficiency was observed (results not shown).

Other unsuccessful attempts to improve the binding efficency included using a heat stable reverse transcriptase (*C.therm.* RT) isolated from *Carboxydothermus hydrogenoformans* so that cDNA could be created at higher temperatures to limit creation of secondary structures which may have occluded the biotin (data not shown). Another protocol involved binding the biotinylated first strand cDNA synthesis primers to the SA-PMPs and making the cDNA *in situ* on the beads which was also unsuccessful (data not shown).

During the various attempts to optimise the efficiency of biotin captures by SA-PMPs discussions with members of collaborating group (Prof Balment, Manchester University, UK) showed that they too were having great difficulty in optimising the normalisation process using a similar procedure and the decision was subsequently taken to abandon it in favour of a subtraction protocol.

4.8 Post-biotinylation of cDNA

At the point of changing from normalisation to subtraction protocols there were still fundamental problems with the extraction of biotinylated DNA from a solution using SA-PMPs, fundamental to both processes. This issue was addressed by changing to post-biotinylation of the cDNAs after synthesis using Label IT Biotin Labelling Kit (Mirus, WI, USA) as opposed to the previous method of incorporation of biotin via the first strand cDNA synthesis primer. Post-biotinylation refers to the fact that the biotinylation occurs after the cDNA has been synthesised.

At this time our laboratory was undergoing a refurbishment and radioactive material handling facilities were not available so non-radiolabelled DNA was used and quantified by visualisation on ethidium bromide stained agarose gels.

The Label IT Biotin Labelling Kit (Mirus, WI, USA) was evaluated by preparing 5 mg biotinylated kidney cDNA (see section 3.10). This was then added to 0.6 mg SA-PMPs (previously washed three times with 300 µl 1 x SSPE buffer) and incubated for 15 min at room temperature. The SA-PMPs were isolated with a magnet and the supernatant was removed to a new tube. The beads were then washed three times with 200 µl H_2O and each wash was kept so that any DNA not aspirated with the supernatant and not bound to the SA-PMPs could be quantified. The supernatant and washes were separately subjected to DNA precipitation and the pellets resuspended and visualised on an agarose gel (Figure 4.8.a).

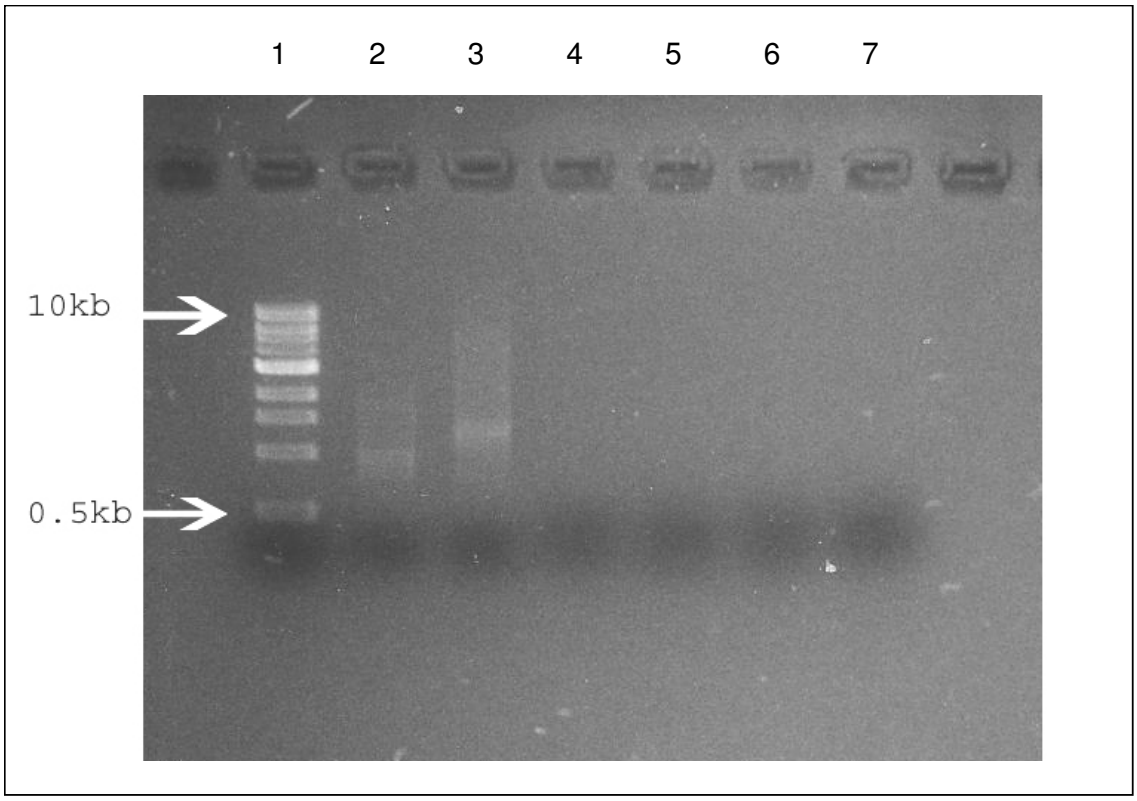

Figure 4.8.a. Lane 1 1kb DNA Ladder (NEB, Hitchin, UK), Lane 2 kidney cDNA prior to biotinylation, Lane 3 kidney cDNA post-biotinylation, Lane 4 Supernatant of biotinylated kidney cDNA treated with SA-PMPs, Lanes 5, 6 and 7 contain washes 1-3 respectively.

Successful biotinylation of the DNA is clearly shown by the gel shift (Lane 3, Figure 4.8.a) as biotin-labelled DNA runs slower than non-labelled DNA on the gel. This is a function of the biotin linkage group covalently bound at the N7 position on guanine bases along the length of the DNA molecules (Figure 4.8.b). Following incubation with the SA-PMPs the labelled DNA appears to have been completely removed from the solution (Lane 4) and no DNA is seen in the washes (Lanes 5-7). This indicated that this method can be used to separate biotinylated DNA from non-labelled DNA using a subtraction method.

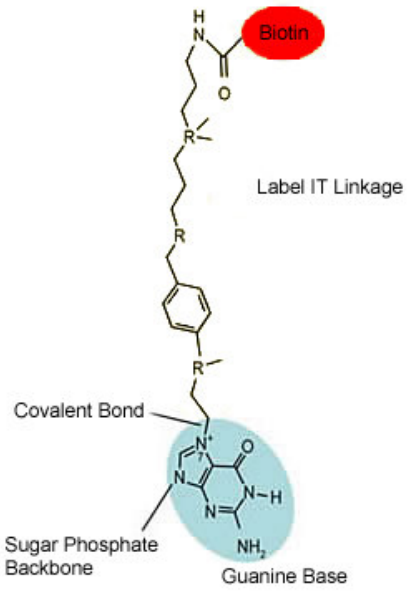

Figure 4.8.b. A guanine base following Mirus biotinylation.

4.9 Subtraction

The normalisation process proved too difficult to optimise and was thus superseded by a subtraction hybridisation protocol Subtraction has many similarities to normalisation; both processes aim to reduce redundancy in the library and both utilise the specific binding of cDNA strands. They differ because subtraction aims to totally remove a subset of cDNAs in a population but normalisation tries to minimise the huge differences in cDNA copy number without deleting any species from the library (Bonaldo et al., 1996). The subtraction protocol was based on a method described in Carninci et al., (2000).

Subtraction uses two pools of cDNA, Tester and Driver. The Tester is the cDNA library from which a fraction of the cDNAs has to be removed whereas the Driver represents the solution containing the cDNAs to be removed from the library. Driver is normally amplified from cDNA clones which have already been isolated and is biotinylated allowing it to be targeted and removed from a solution following hybridisation with the Tester cDNA. Tester is combined with excess amounts of the Driver. The cDNA is denatured to create single stranded DNA and then allowed to completely reanneal. The cDNA which is present in the Tester and also represented in the Driver will, due to reassociation kinetics (James and Higgins, 1985), be more likely to rehybridise with the excess complementary Driver strand than with the complementary Tester strand. Tester cDNA not represented in the Driver cDNA sample can only rehybridise with the complementary Tester strand. All biotin-labelled DNA is then removed from the solution; this includes heterologous cDNA with one strand each from Tester and Driver. The cDNA left in the solution is cloned and the resultant library contains only Tester cDNA not present in the Driver cDNA. Optimising subtraction should be easier than normalisation as an excess of Driver, containing genes already collected, can be hybridised with Tester and the binding reaction allowed to go to completion.

The aim was to create a cDNA library from one tissue and then sequentially subtract this tissue from the next, with each subsequent Driver pool containing the cDNA of clones already isolated from the previous libraries as outlined in the flowchart (Figure 4.9.a). The Driver pools were also supplemented with biotinylated amplicons of 18S and 28S rRNA fragments which had been isolated from the brain cDNA library.

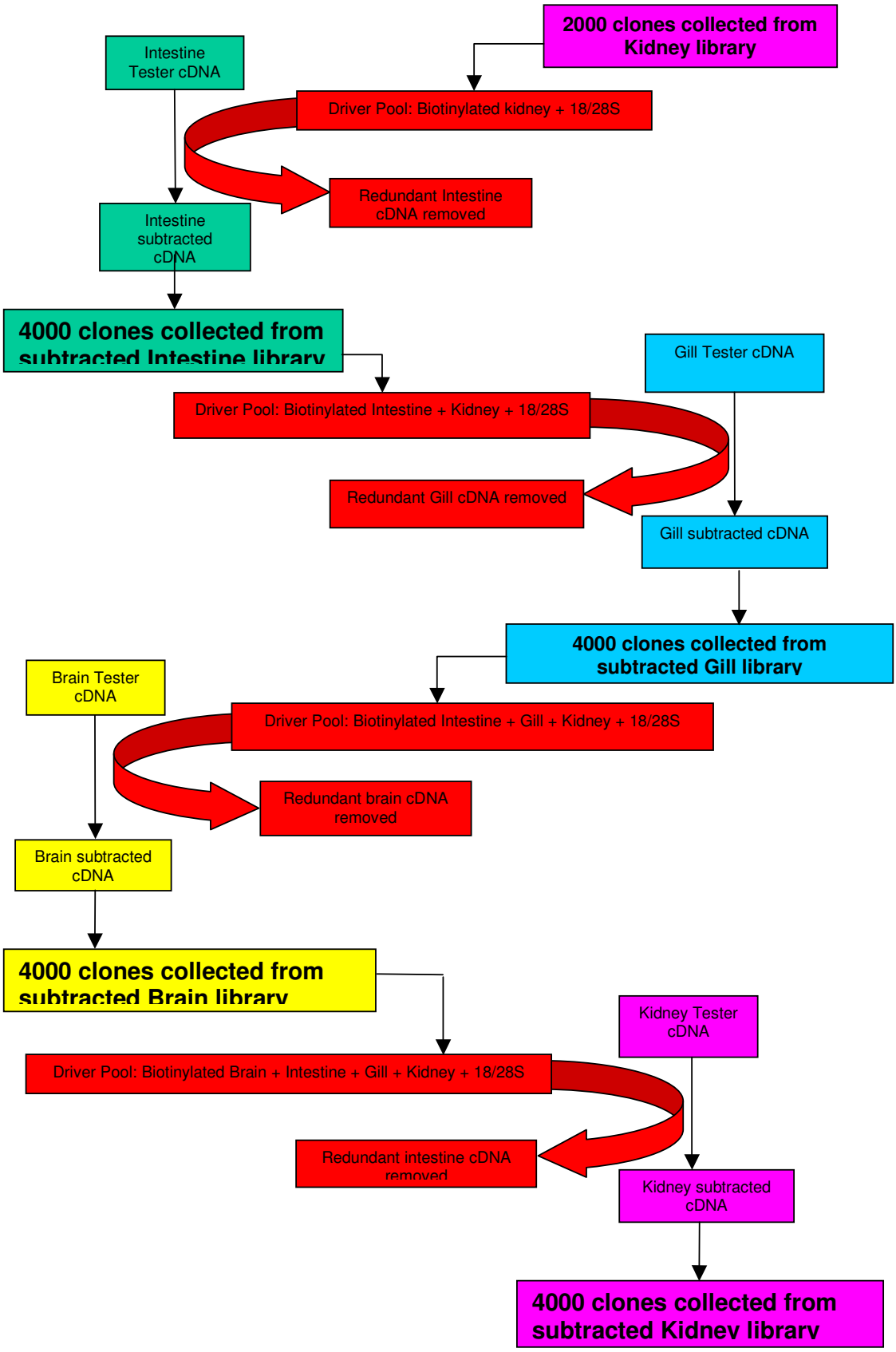

Figure 4.9.a. Flow chart summarising the sequential subtraction process.

Cloning of 18S and 28S rRNA fragments. When examining the *A. anguilla* brain 2G random cDNA library on an agarose gel, two over-expressed bands were found. In an attempt to remove these from the library during subtraction, the bands were cloned and subsequently found to be 18S and 28S rRNA gene fragments (see section 3.11). In an attempt to subtract these clones from subsequent libraries, amplicons for each were synthesised by colony PCR using 2G internal primers (NintpDONR222anti 5′-GTTGGGTGGAACCGTCACGTAC-3'and NpDONR222sense 5′-GTTGGGTGGAACCGTCACGTAC-3', annealing temperature 58 ºC) as per normal PCR conditions (Section 3.5). These amplicons were then used to supplement the Driver pools.

Driver production. Initially, a CloneMiner™ cDNA library was created from the first tissue (kidney) using the 2G Oligo d(T) *att*B2 primer. (Figure 4.9.b).

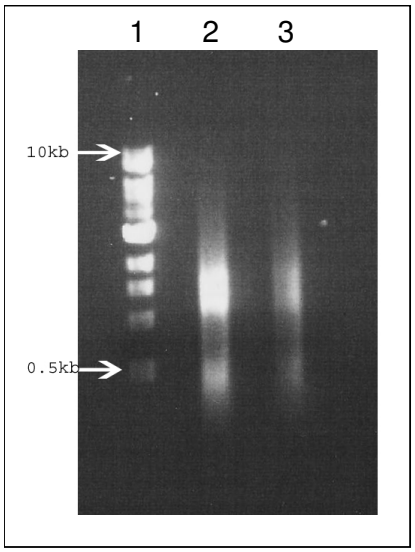

Figure 4.9.b. Lane 1 1kb DNA Ladder (NEB, Hitchin, UK); Lane 2 1µl kidney Driver cDNA solution; Lane 3 0.5µl kidney Driver cDNA solution.

The intestine– kidney subtraction process was attempted following three protocols where denaturation/re-annealing was mediated by either pH,

temperature with formamide or formamide alone (see Sections 3.13, 3.14 and 3.15 respectively)

This first, pH directed, subtraction used 150 ng intestine Random cDNA as Tester and 5 µg biotinylated Driver cDNA made from a 2G kidney CloneMiner library library using a pH directed hybridisation protocol in which strongly alkaline conditions were used to denature the DNA and re-annealing was brought about by neutralisation. Only 48 ng cDNA remained after subtraction which is lower than recommended (75 –100 ng) in the CloneMiner™ manual for cloning but nevertheless cloning was attempted. Less than 1/3 of the resultant clones which grew on LB agar containing kanamycin contained a vector with an insert (data not shown). The ElectroMAX™ DH10B™ T1 Phage Resistant Cells should not grow on media containing kanamycin as resistance is only conferred after transfection by an appropriate vector. The vector, however, contains a *ccd*B lethal gene which kills the *E.coli* unless it has been replaced during recombination with a cDNA. Thus, only cells containing a vector with an insert should grow. In practice there is always a percentage of cells which grow but do not show a positive insert because they have developed kanamycin resistance or had it conferred by transfection with a vector containing the resistance gene but lacking the *ccd*B gene. The low numbers of positive clones was attributed to the amount of Tester cDNA (48 ng) which remained after the subtraction being significantly less than the 150 ng recommended for efficient cloning by the CloneMiner™ protocol. It was suspected that the rapid pH change could allow non-specific binding of Driver and Tester, resulting in insufficient cDNA being left for cloning.

The second attempt at the intestine – kidney subtraction used temperature to denature the Driver and Tester cDNA, which was then snap-cooled on ice before the addition of formamide and warming of the solution to room temperature. The formamide was present to slow the rate of DNA re-annealing. A higher concentration of Tester DNA (500 ng) and the same amount of Driver (5 µg) was used to increase the likelihood that sufficient cDNA would remain after subtraction. After the subtraction there was ~80 ng

cDNA left, which should have been enough for successful cloning, but no colonies grew. This was possibly due to formamide being carried over with the cDNA into the cloning step and inhibiting the recombination reaction.

The intestine – kidney subtraction was thus repeated a third time, again using heat directed denaturation of Driver and Tester. No formamide was added, instead the Tester/Driver mix was cooled slowly from 95 ºC to 25 ºC at a rate of 5 ºC/min. Approximately 80 ng cDNA remained following subtraction and this protocol seemed to have proved successful in that a large number of colonies grew after cloning and the majority contained a vector with an insert (Figure 4.9.c). The majority of clones were ~500 bp, with the largest clones being ~ 2.5 kb which was smaller than anticipated and indicative of a poor quality cDNA library.

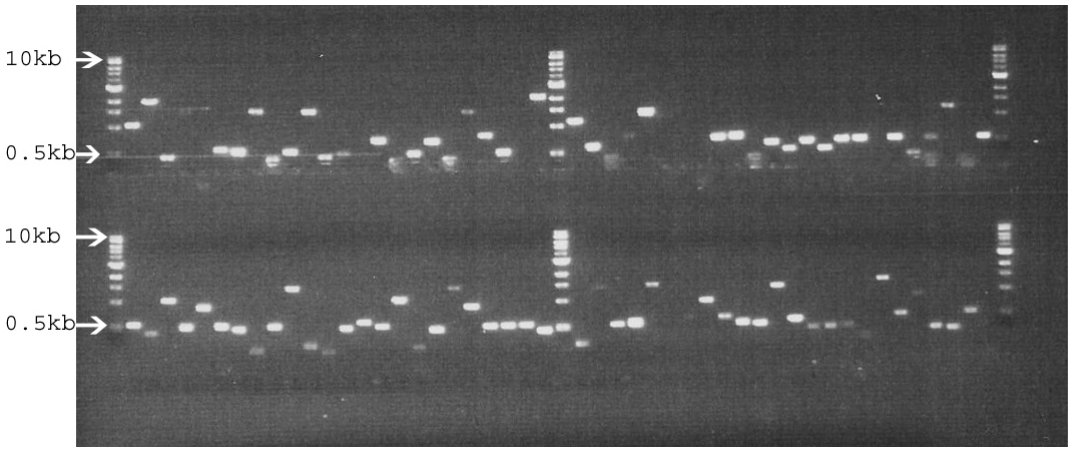

Figure 4.9.c. Colony PCR of 96 clones from the subtracted CloneMiner™ random intestine cDNA library made using the protocol: "heat directed hybridisation in the absence of formamide".

This experiment was replicated and in parallel to this, a second subtraction was performed using the same Driver cDNA (kidney cDNA, 18S and 28S rRNA amplicons) but the Tester was CloneMiner™ oligo intestine cDNA, which was prepared using non-biotinylated 2G oligo d(T) *att*B2 primers. It was hoped that the subtracted oligo library would have a larger average insert size but both of the resultant libraries were of a similar quality

to the library shown in Figure 4.9.c in that they had small inserts (data not shown).

One possible reason for the sub-optimal results of this protocol was the possible binding of biotinylated Driver cDNA to non-complementary strands of Tester which would then be removed during the extraction of biotinylated species. This could occur as the ends of the Driver and Tester are complementary as they had been amplified with the same primer sites. This could lead to removal of Tester cDNA not represented in the Driver cDNA pool, although why this would reduce the size of the cDNA library is not clear. This potential issue was addressed by the creation of third generation (3G) primers for library production with *Spe* I restriction sites (Figure 4.9.d) incorporated to allow complete adapter removal from Driver cDNA, therefore removing homologous sites shared by Tester and Driver which could facilitate binding of non-complimentary cDNA species. The nested internal primer sites, NintpDONR222anti and NpDONR222_sense (underlined portions) reflect incorporation of the restriction site but the *att*B sites remained unchanged (highlighted portion). A 3G bi-directional primer was designed for colony PCR purposes which binds outside the *att*B recombination site (Figure 4.9.d).

3G Oligo d(T) *att*B2 Primer (NpDONR222anti2)

5′-**14-CSA.**GGCGGCCGCACAACTTTGTACAAGAAAGTTGGGTGGAACCGTC**ACTAGT**(T)19-3′

3G Random *att*B2 primer (NpDONR222anti2)

5′-**14-CSA.**GGCGGCCGCACAACTTTGTACAAGAAAGTTGGGTGGAACCGTC**ACTAGT**$(N)_6$TGCCT-3′

3G *att*B1 adapter (NintpDONR222sense2)

5′-TCGTCGGGGACAACTTTGTACAAAAAAGTTGGGTGCATCAGCTGG**ACTAGT**-3′

3′-CCCCTGTTGAAACATGTTTTTTCAACCCACGTAGTCGACC**TGATCA**-**P**-5′

3G Bi-directional Colony PCR primer

5′-GACTGATAGTGACCTGTTCGTTGCAACAAATTG-3′

Figure 4.9.d. 3GOligo d(T) *att*B2 primer and 3G Random *att*B2 primers, both have a 5' 14-carbon spacer arm, an *att*B2 site highlighted in green and an internal primer site for NpDONR222anti2 primer which is underlined. Phosphorylated 3G *att*B1 adapter with *att*B1 site highlighted in yellow and an internal primer site for NpDONR222sense2 underlined. All 3G primers and adapters have an *Spe* I restriction site (ACTAGT) denoted in bold. The 3G Bi-directional Colony PCR primer binds to the pDONR222 vector outside the *att*B recombination sites on both sides of the cDNA insert.

4.10 Non specific DNA binding by SA-PMPs

The subtraction protocol initially used SA-PMP as they had been shown to remove all the DNA, labelled using the Mirus Label IT kit, from a solution (see Section 4.8). Following continued lack of success of the various subtraction processes, further investigation of the SA-PMPs was carried out and they were found to non-specifically bind substantial amounts of double-stranded cDNA. During these investigations, two hybridisation reactions were arranged, each containing α^{32}P dCTP labelled eel kidney cDNA subtracted with either excess *Carcharhinus leucas* (bull shark) rectal gland cDNA or excess biotinylated eel kidney cDNA. The bull shark rectal gland cDNA was used to make up the cDNA concentrations in both reactions to the same concentration. The cDNA strands in both reactions were dissociated by applying strongly alkaline conditions followed by neutralisation to allow re-annealing before the reactions were treated with SA-PMPs (see Section 3.17).

Theoretically the reaction containing the *C. leucas* rectal gland cDNA and radiolabelled eel cDNA should show no binding to the SA-PMPs as there is no biotinylated cDNA. In the other reaction, the radiolabelled eel cDNA should hybridise to the biotinylated cDNA and subsequently bind to the SA-PMP. In practice, 83 % non-biotinylated *A. anguilla* kidney radiolabelled cDNA bound to the SA-PMPs when hybridised to biotinylated *A. anguilla* kidney cDNA. In the absence of any biotinylated cDNA, however, 64 % of non-biotinylated radiolabelled *A. anguilla* kidney cDNA bound. Thus the SA-PMPs bound biotinylated cDNA but they also bound non-biotinylated cDNA non-specifically (Figure 4.10.a).

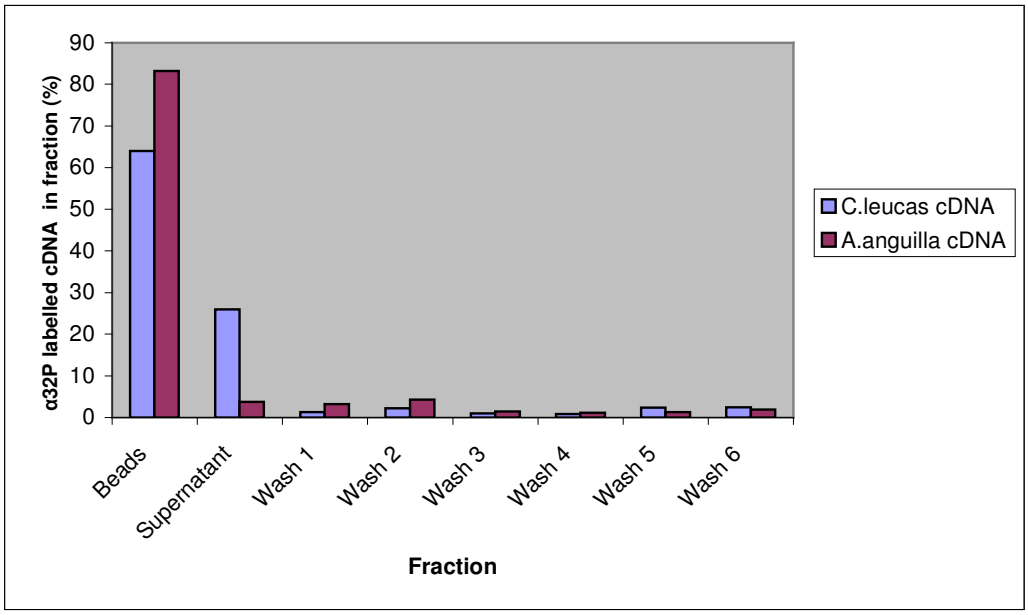

Figure 4.10.a. Non-specific cDNA binding by SA-PMPs shown as percent α^{32}P labelled kidney cDNA (non-biotinylated) bound to SA-PMPs after hybridisation with either complementary biotinylated *A. anguilla* kidney cDNA or non-complementary, non-biotinylated *C. leucas* rectal gland cDNA.

An additional experiment was performed to see if the non-biotinylated cDNA associated with the SA-PMPs could be recovered using various solvents (see Section 3.18). Only sodium acetate significantly reduced the amount of cDNA bound to the SA-PMPs but more than 30 % cDNA still remained bound indicating that the SA-PMPs were non-specifically binding cDNA (Figure 4.10.b).

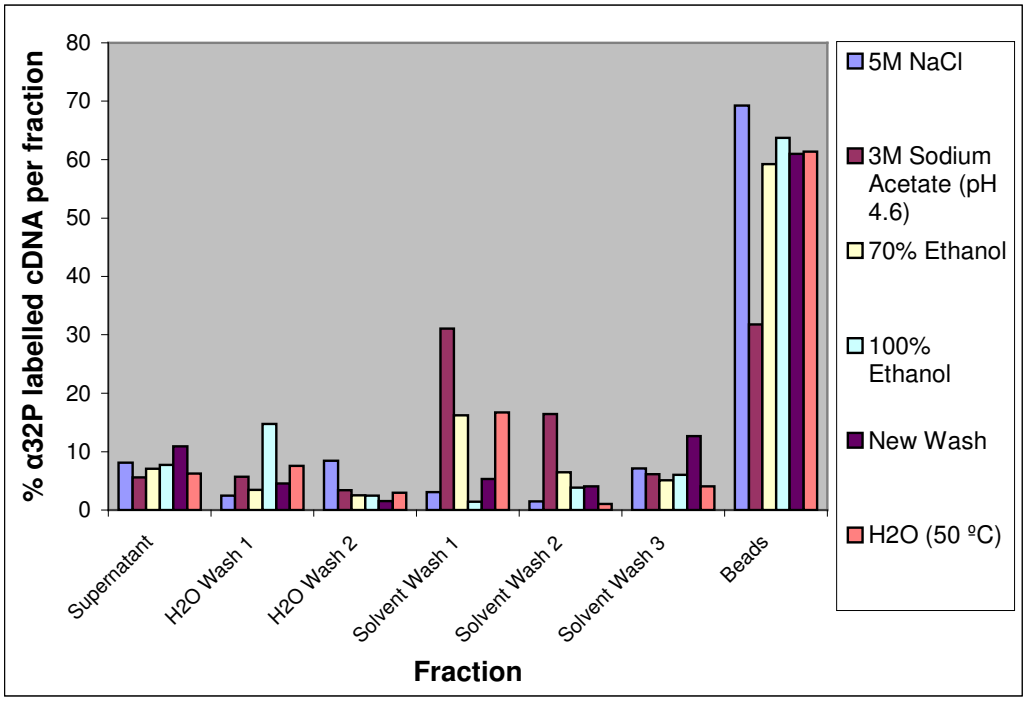

Figure 4.10.b. Removal of non-biotinylated α^{32}P-labelled cDNA non-specifically bound to SA-PMPs using various sovent washes; NaCl (5 M); sodium acetate (3 M, pH 4.6); 70 % ethanol; 100 % ethanol; New Wash (Anachem Ltd, Luton, UK) or H_2O.

Similar problems with SA-PMPs have been reported elsewhere (Murray, 2005). These problems include; low binding efficiency of biotinylated cDNA by SA-PMPs; non-linear relationships between levels of SA-PMP binding of biotinylated cDNA with either concentration of beads or length of incubation time; and limited removal of non-biotinylated cDNA non-specifically bound to SA-PMPs. Consequently, alternative avidin supports were sought.

4.11 NeutrAvidin™ biotin binding protein agarose beads: Specific and non-specific DNA binding capacity

Following the discovery that SA-PMPs bind DNA non-specifically, NeutrAvidin™ biotin-binding protein agarose beads (NABs) from Pierce Biotechnology (Perbio Science UK Ltd., Cramlington, UK) were tested as an alternative avidin support. A preliminary experiment tested the capacity of NABs for binding biotin labelled DNA and non-specific DNA binding. This was essentially a repeat of the experiment which showed non-specific DNA binding by SA-PMPs. Radiolabelled eel kidney cDNA was hybridised with excesses of biotinylated eel kidney cDNA or non-biotinylated cDNA from *C. leucas* before incubation with aliquots of Neutravidin™ (see Section 3.19). The NABs were shown to bind ~90 % of radiolabelled DNA which had been hybridised with a 10 or 100 fold excess of biotinylated cDNA (samples 3 and 4, figure 4.11.a). Losses of radiolabelled *A. anguilla* kidney DNA hybridised with non-biotinylated *C. leucas* rectal gland cDNA during the process were only ~18 % (sample 1, figure 4.11.a).

These results showed that the NABs could be used for removal of the majority (~90 %) of biotinylated DNA. At a Driver:Tester ratio of 10:1, heat denaturation at 95C for 2min prior to a reannealing period at 70 ºC overnight increased the efficacy of removal of Tester DNA from the solution by 26 %. In the control experiment 18 % of the radiolabelled *A. anguilla* kidney DNA remained associated with the NABs. During the application of this protocol to make a subtracted library this would be the equivalent of losing 18 % Tester cDNA. These losses would be acceptable and are probably due to the physical nature of the NAB slurry which makes it extremely difficult to remove all the supernatant following centrifugation.

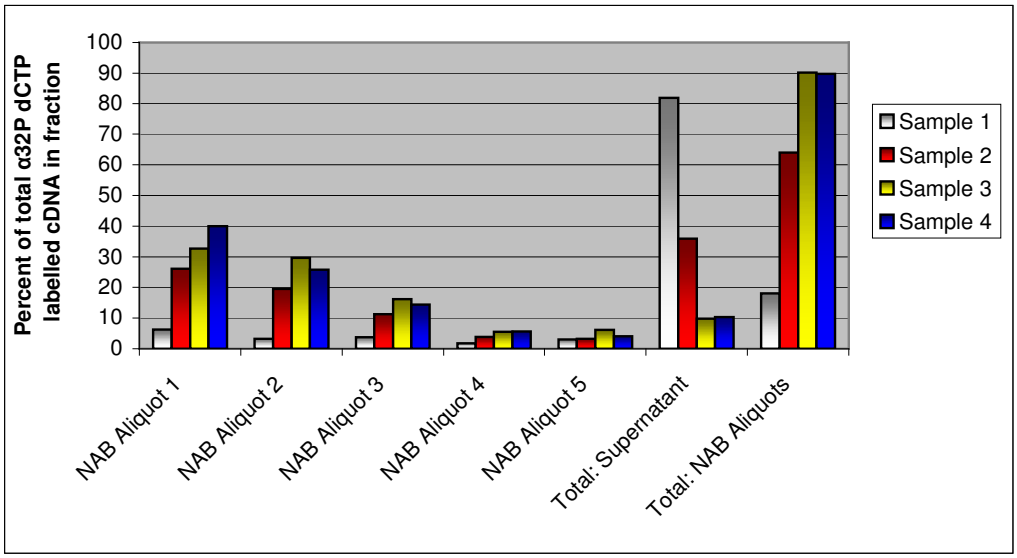

Figure 4.11.a. Tracking of α^{32}P labelled tester cDNA samples 1-4 (see table 3.14.a) after incubation with biotinylated eel kidney Driver cDNA or non-biotinylated *C. leucas* rectal gland cDNA. Samples 1-4 were exposed to five NAB aliquots in order to bind biotinylated cDNA. The Total: Supernatant column refers to total radiolabelled cDNA which remained in the supernatant after exposure to the five NAB aliquots. The Total: NAB Aliquots column represents the total amount of radiolabelled cDNA associated with all five NAB aliquots.

The protocol was adapted by the inclusion of spin-filters to separate the supernatant and NABs. This both streamlined the process and improved the efficiency (see Section 3.20). The two supernatants showed only trace levels of radiolabelled cDNA remaining after treatment with NABs (sample 1 = 0 cpm, sample 2 = 40 cpm, figure 4.11.b). The first aliquot of NAB bound the most radiolabelled, biotinylated cDNA (16624 and 17907 cpm for samples 1 and 2 respectively) with the second and third aliquots binding between 40.5 – 130.5 cpm.

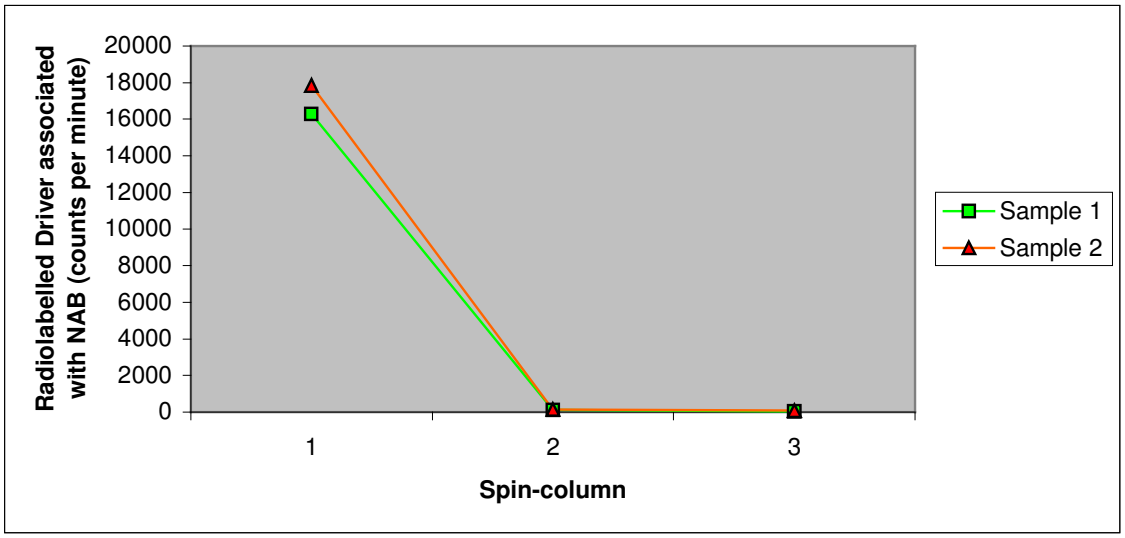

Figure 4.11.b. Binding of *A. anguilla* α^{32}P dCTP labelled kidney cDNA to NABs. Supernatant was subsequently removed using three spin-columns in series and the amount of *A. anguilla* α^{32}P dCTP labelled kidney cDNA associated with each NAB aliquot was quantified by liquid scintillation counting (Cerenkov radiation).

Thus far, no usable cDNA libraries had been created although good progress was being made in optimising the process. In addition to making the oligo and random libraries it was decided that a second, more established approach to making subtracted cDNA libraries would expedite results. The method chosen was suppressive subtraction hybridisation (SSH) cDNA libraries, a method that has been used for studies of osmoregulation in the teleost, tilapia (*Orechromis mossambicus*) (Fiol and Kultz, 2005).

4.12 Suppressive Subtraction Hybridisation cDNA libraries

The theory behind SSH libraries is similar to the subtraction protocols already described in Sections 4.3 and 4.4. Tester and Driver cDNAs are hybridised, and the hybrid sequences are then removed. Consequently, the remaining cDNAs represent genes that are expressed in the Tester yet absent from the Driver. SSH libraries were created for each of kidney, intestine, brain and gill in collaboration with Dr. S. Kalujnaia, University of St Andrews, UK.

For each library, three hybridisations were performed. In the first two hybridisations, an excess Driver cDNA was combined with each sample of Tester. The samples were heat denatured and cooled to allow to annealing, generating four potential strand arrangements; **a**, **b**, **c**, and **d** (Figure 4.12.b). The concentration of high- and low-abundance sequences is equalised among the type **a** molecules because re-annealing is faster for the more abundant molecules due to the second-order kinetics of hybridisation (James and Higgins, 1985; Ko, 1990). At the same time, type **a** molecules are significantly enriched for differentially expressed sequences while cDNAs that are not differentially expressed form type **c** molecules with the Driver. The first two hybridisations were combined to form the third hybridisation but the cDNA was not denatured this time. Only the remaining equalised and subtracted single-stranded Tester cDNAs can re-associate to form new type **e** hybrids. These new hybrids are double-stranded Tester molecules with different ends, which correspond to the sequences of Adaptors 1 and 2R. Fresh, denatured Driver cDNA was also added to further enrich fraction **e** for differentially expressed sequences. The adaptor ends were filled in by DNA polymerase, resulting in type **e** molecules with different annealing sites for the nested primers on their 5' and 3' ends. The sample, containing the entire population of molecules (**a-e**) was then subjected to PCR with PCR primer 1. During this PCR only type **e** molecules were exponentially amplified. Type **a** and **d** molecules are missing SSH PCR primer 1 annealing sites, and thus cannot be amplified. Most of the type **b** molecules form a pan-like structure

that prevents their exponential amplification, whilst type **c** molecules have only one primer annealing site and amplify linearly.

SSH Oligo d(T) cDNA synthesis primer

5′-TTTTGTACAAGCTT$_{30}$N$_1$N-3′

SSH Adaptor 1

5′-CTAATACGACTCACTATAGGGCTCGAGCGGCCGCCCGGGCAGGT-3′

3′-GGCCCGTCCA-5′

SSH Adaptor 2R

5′-CTAATACGACTCACTATAGGGCAGCGTGGTCGCGGCCGAGGT-3′

3′-GCCGGCTCCA-5′

SSH PCR primer 1

5′-CTAATACGACTCACTATAGGGC-3′

SSH Nested PCR primer 1

5′-TCGAGCGGCCGCCCGGGCAGGT-3′

SSH Nested PCR primer 2

5′-AGCGTGGTCGCGGCCGAGGT-3′

Figure 4.12.a. Sequences of the SSH Oligo d(T) cDNA synthesis primer, SSH Adaptor 1, SSH Adaptor 2R, Bi-directional SSH PCR primer, SSH Nested PCR primer 1 and SSH Nested PCR primer 2. There is a section in both SSH Adaptor 1 and 2R which allows annealing of the SSH PCR primer 1 to their complement once the recessed end have been filled in. When Adaptors 1 and 2R are ligated to *Rsa* I-digested cDNA, the Rsa I site is restored.

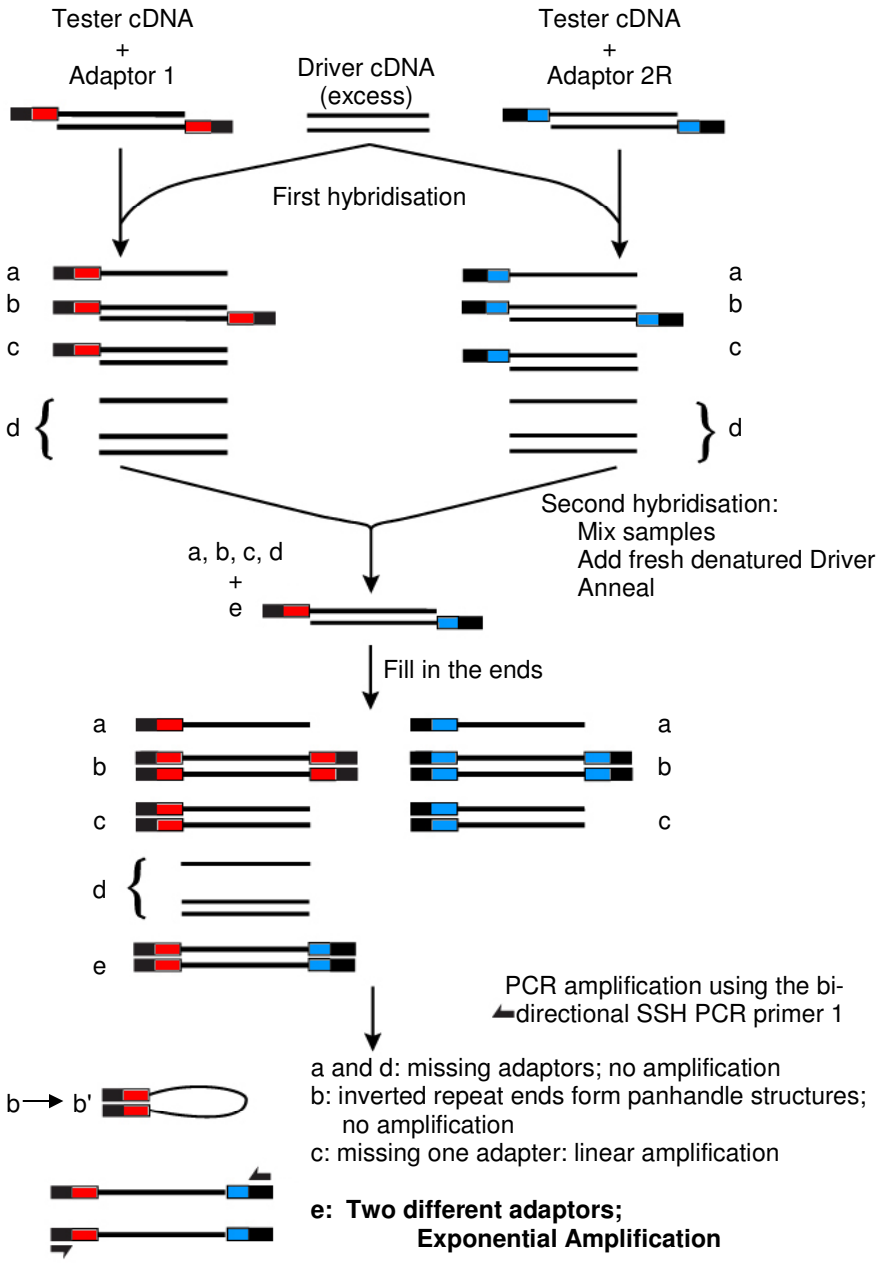

Figure 4.12.b. Schematic diagram of suppression subtractive hybridisation (SSH). Adapted from PCR-Select™ cDNA Subtraction Kit User Manual (Clontech, Basingstoke, UK) which is reproduced in appendix 2. See text for brief explanation.

Colonies (1536) were randomly picked from each tissue-subtracted library and 50 clones were randomly selected. Four subtracted cDNA libraries were constructed from brain, gill, intestine and renal plus head kidney based on the suppressive subtraction hybridization technique (Diatchenko et al., 1996) where cDNAs produced from each tissue (Tester) were subtracted against an excess of cDNA prepared from the three other tissues (Driver) to obtain the representative collection of tissue-specific expressed sequence tags (ESTs). The libraries were prepared from tissue specific pooled RNA samples collected at 6 hours, 2 and 7 days and 5 months from SW and FW acclimated silver eels. In total, 196 RNA samples (four tissues from 48 fish) were used in these studies. Clones (1536) were randomly selected from each of the four SSH libraries and amplified by high throughput colony PCR and amplicons visualised on large agarose gels. Colonies showed almost 100% positive inserts, ranging in size from 200-1300bp (Figure 4.1.a). Inserts were generally small because the cDNA was restriction digested with *Rsa*1 before cloning meaning that full-length clones were unlikely. Subsequently the amplified clones were sequenced to measure redundancy. The redundancy levels were found to be 26 %, 21 %, 11 % and 18 % for brain, intestine, gill and kidney libraries respectively.

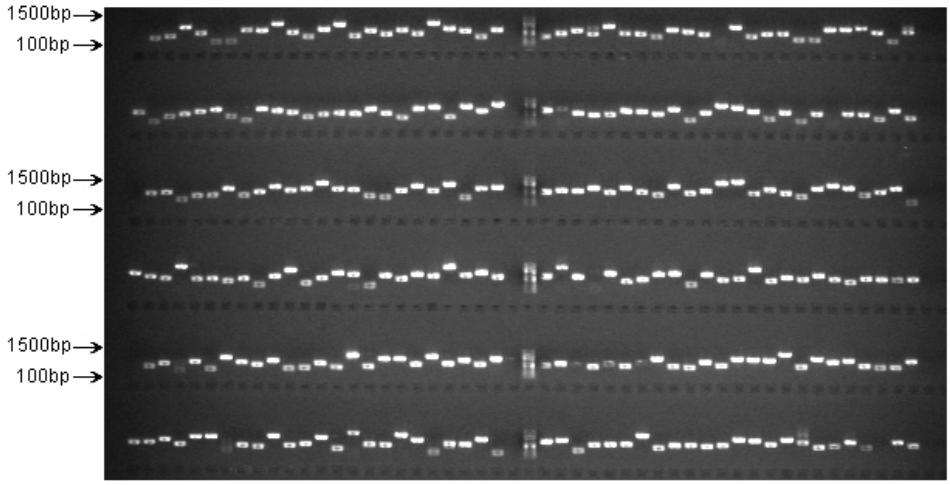

Figure 4.12.c. A representative sample of the SSH library. The samples are amplified from 96 samples from the brain SSH library using the bi-directional SSH primer (see section 3.5). Cloning efficiency is close to 100 % and inserts range from 200-1300 bp. The centre lane of each row contains DNA markers (100bp Ladder, NEB, Hitchin, UK) with size labels marked on alternate rows.

4.13 Creation of the high quality subtracted *att*B brain library

Tissue specific, subtracted cDNA libraries for gill, kidney, brain and intestine were created using SSH and as such the subtraction scheme described in Section 4.9 was no longer needed. Rather than abandoning the body of work which had been prepared during the development of these protocols, they were instead adapted to create a single brain cDNA library containing long/full-length clones exhibiting low redundancy levels.

The brain exhibits very high transcript diversity with rare mRNAs being represented very infrequently and as such, using a cDNA library containing more clones would increase the likelihood of finding interesting genes (Hahn and Owens, 1988; Snider and Morrison-Bogorad, 1992). In addition, if the clones in the new brain library were longer than those in the SSH library, it would be easier to identify them via homology with known genes from other species. By using the cDNA clones from the brain SSH library to create Driver to subtract the new brain library it was hoped that the redundancy level would be significantly lower than the 26 % achieved with the SSH brain library. A similar method was developed using SSH subtracted, biotinylated cDNA to enrich a *Gillichthys mirabilis* cDNA library for hypoxia-induced genes (Gracey et al., 2001). Combining a lower redundancy with a larger number and size of clones would lead to a high quality subtracted brain cDNA library. This new high quality library, now referred to as the "Subtracted *att*B Brain Library" was to be printed alongside the SSH brain cDNA library creating a brain microarray representing ~ 6000 genes to be used primarily for examining the differences in gene expression in the brains of yellow and silver FW eels.

A largely novel method (Section 3.22) was employed to produce the subtracted *att*B brain library, a high quality brain oligo d(T) primed library comprising a representative collection of long/full-length brain-specific ESTs. cDNAs produced from brain (Tester) using an adapted CloneMiner Gateway protocol (Invitrogen, Paisley, UK) were subtracted against an excess of cDNA

prepared from the SSH brain library (Driver) resulting in a library with low redundancy. The subtracted *att*B brain library was prepared from 48 brain RNA samples collected at 6 hours, 2 days, 7 days and 5 months from yellow and silver eels acclimated to SW and FW. Clones (4224) were randomly selected from the subtracted *att*B brain library (subtracted with SSH brain clones) amplified by high throughput colony PCR and amplicons visualised on 1 % agarose gels. Colonies showed almost 100% positive inserts ranging in size from 0.5kb to 10kb indicating that a large proportion were full length cDNAs (Figure 4.13.a).

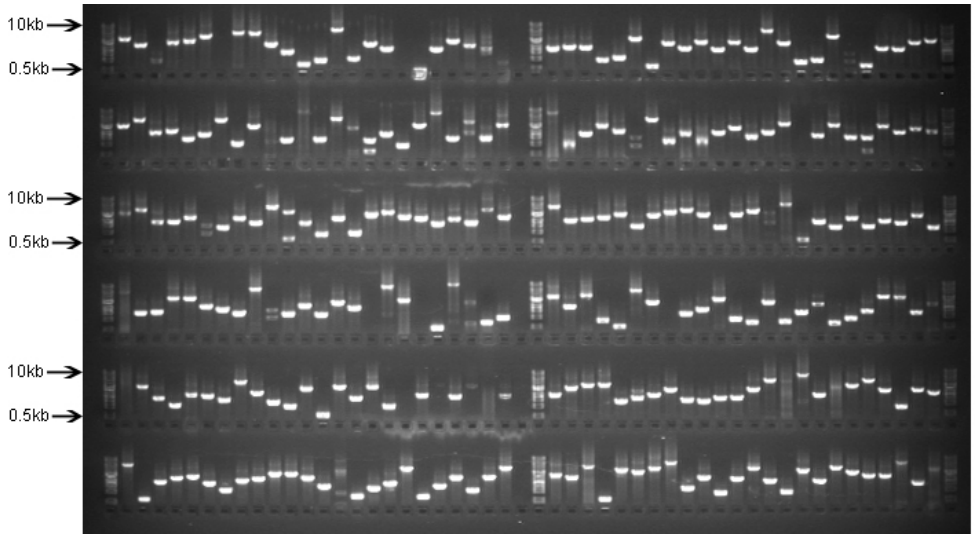

Figure 4.13.a. A representative sample of the subtracted *att*B brain library. The samples are amplified from 96 samples from the subtracted *att*B brain library using the 3G bi-directional SSH primer. Cloning efficiency is close to 100 % and inserts range from 0.5 – 10 kb. The centre lane of each row contains DNA markers (1 kb Ladder, NEB, Hitchin, UK) with size labels marked on alternate rows.

For each library created, the subtracted *att*B brain library and SSH brain, kidney, gill and intestine libraries, clones were randomly selected for sequencing to determine the approximate redundancy levels (Table 4.1.a). BLAST sequence analysis indicated the subtracted *att*B brain library had the lowest level of redundancy (4%) with only one clone being repeated twice, 33

clones with high homology to known genes, 7 clones with no known homology. The redundancy levels in the SSH libraries were higher (27.1 %, 20.8 %, 10.4 % and 18.8 % redundancy for brain, intestine, gill and kidney libraries respectively).

Table 4.13.a. Estimated library redundancy levels for the subtracted *att*B brain library and the four SSH libraries as calculated from sequences of a random, representative sample of clones taken from each library.

Library	Sequences analysed	Number of redundant clones	Redundancy (%)
Subtracted *att*B brain library	43	2	4.2
Brain SSH	48	13	27.1
Kidney SSH	48	9	18.8
Gill SSH	48	5	10.4
Intestine SSH	48	10	20.8

Amplicons from the 4224 clones from the subtracted *att*B brain library, the 1536 brain SSH clones and 96 control cDNAs comprising either known eel genes or coding regions of genes from other species (detailed in Table 4.2) were packed in dry ice and sent to the Liverpool Microarray Facility (The University of Liverpool) for printing onto microarrays.

4.14 RNA amplification for microarray hybridisation

The eel brains is small (<1 g) and as such the amount of extractable RNA per fish was very low (3-80 µg per brain). To compensate for the limited material a method of RNA amplification was employed to provide extra RNA for the microarray hybridisations. One method of RNA amplification uses T7 Phage polymerase to make multiple copies of RNA from a cDNA template in a linear reaction so that small quantities (<1 µg) of total RNA can be amplified several hundred fold yet maintaining the relative abundances of all mRNA species present (Eberwine et al., 1992; Phillips and Eberwine, 1996; Vangelder et al., 1990). Amplification of RNA can increase reproducibility and enhance gene discovery when using microarrays (Feldman et al., 2002). This protocol was applied to the brain RNA samples derived from the 5 month freshwater acclimated silver eel, and 7 day freshwater acclimated yellow eel groups (see Section 3.23 for experimental details).

The first strand synthesis follows the same procedure as the SMART cDNA synthesis described previously and is summarised in figure 4.14.b below. Reverse transcription is primed by the T7 oligo d(T) primer (Figure 4.14.a) to create first strand cDNA. Upon reaching the 5' end of the RNA template, reverse transcriptase (RT) adds several cytosine residues to the 3' end of the newly synthesised cDNA molecule, to which the complementary GGG section of the Template Switch primer binds (Figure 4.14.a). The RT then switches templates from the mRNA to the Template Switch primer and incorporates its complement at the 3' end of the first strand cDNA molecule.

Oligo $d(T)_{15}$-T7 primer

5' AAA CGA CGG CCA GTG AAT TGT AAT ACG ACT CAC TAT AGG CGC $(T)_{15}$ 3'

Template Switch primer

5' AAG CAG TGG TAA CAA CGC AGA GTA CGC GGG 3'

Figure 4.14.a. Oligo $d(T)_{15}$-T7 primer with the T7 nested RNA site highlighted in green. Template Switch primer with the GGG site which binds the 3' end of newly synthesised cDNA.

When the reverse transcriptase reaches the 5' end of the mRNA it switches template from the mRNA to the Template Switch primer, the complement of which is copied into the first strand of cDNA (Wang et al., 2000). Messenger RNA nicks created by RNase H and the Template Switch primer bound at the 3' end of the first strand cDNA primes the second strand cDNA synthesis. The RNA is then degraded by addition of NaOH which is followed by purification of the cDNA by ethanol precipitation (see section 3.5) before *in vitro* transcription of the cDNA by T7 phage polymerase. The end product is multiple copies of the mRNA present in the original total RNA sample.

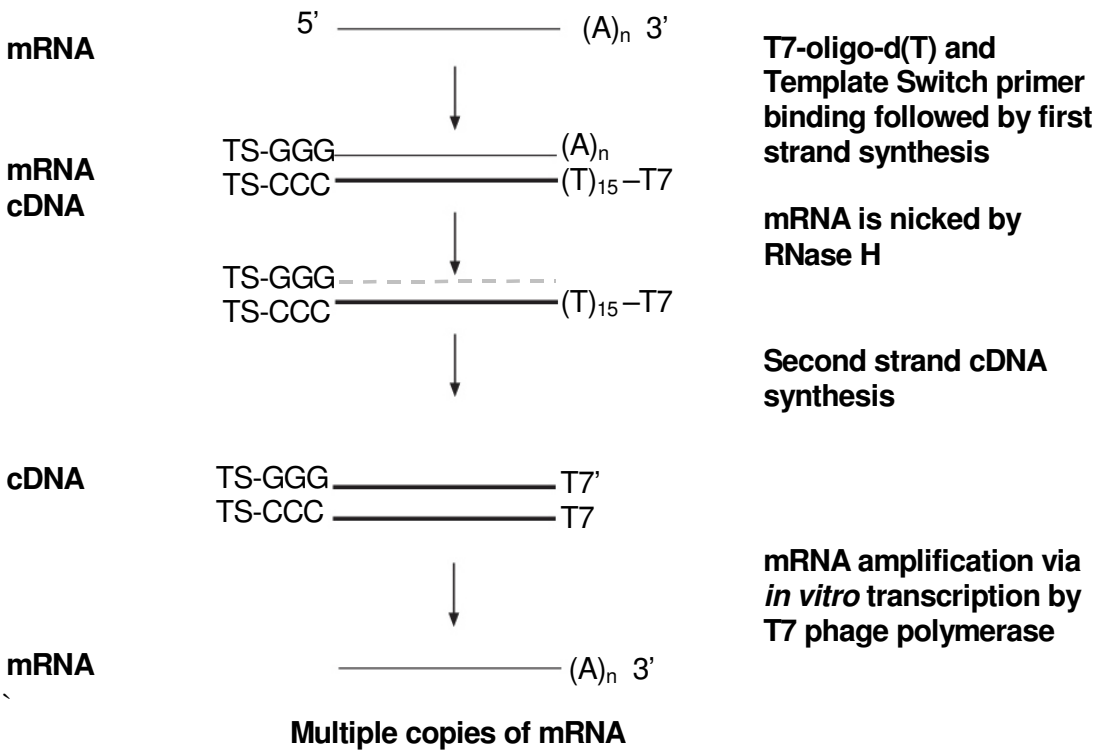

Figure 4.14.b. Schematic representation of the mRNA amplification protocol.

4.15 Microarray construction

Two types of microarray were constructed, one incorporated only brain cDNAs from the subtracted *att*B brain library clones (4224) and the SSH brain library (1536) whilst the other array type incorporated clones (6144) from the SSH arrays from the four tissues, kidney, brain, intestine and gill.

The brain array was created with 5896 cDNAs comprising 4224 clones from the subtracted *att*B brain library and 1536 clones from the SSH brain library. The multi-tissue SSH array was constructed with 6144 ESTs, 1536 from each of the subtracted libraries of brain, gill, kidney and intestine. Both array types were supplemented with an additional 96 control cDNAs comprising either known eel genes or coding regions of genes from other species (Table 4.15.a). These 96 genes, isolated from other fish or plant species, were used as controls to test the stringency and probe specificities under the hybridisation conditions used. For both arrays, each cDNA was printed in three locations to give three technical replicates per slide. Each replicate was divided into 16 sub-arrays, 19 spots wide and 20 spots tall, with landing lights (spots which fluoresce) placed at the corners of the replicate to aid spot location (Figure 4.15.a). The arrays were spotted onto GAPS II Coated Slides (Corning Incorporated, Corning, NY) by the Liverpool Microarray Facility (The University of Liverpool). Array experiments were replicated in dye-swap, meaning that the cDNA sample fluorescently labelled with Cy3 in the first (forward) experiment was labelled with Cy5 in the second (dye-swap) experiment, and vice versa for the other cDNA (Churchill, 2002).

Table 4.15.a. Control genes from plate Aa_BOS_61 incorporated onto every microarray used. Accession numbers are given for gene sequences published in public databases. AQP = aquaporin, CFTR = cystic fibrosis transmembrane conductance regulator, SERCA = sarco/endoplasmic reticulum Ca2^{+} ATPase, PMCA = plasma membrane Ca^{2+}-ATPase, MDR = multi drug resistance p-glycoprotein, EAE = epithelial anion exchanger, NHE = sodium/hydrogen exchanger, HSP = heat shock protein.

Well	Species	Gene isoform	Accession number	Colony PCR primers	Plasmid	Bacterial Resistance
A1	*Aspergillus nidulans*	Nitrate transporter	XP_658612	M13*	PCR 4	Km, Amp
A2	*Anguilla anguilla*	Na^+/K^+ ATPase α1	X76108	M13*	PCRII	Km, Amp
A3	*Anguilla anguilla*	Na^+/K^+ ATPase α3	Not published	M13*	PCRII	Km, Amp
A4	*Anguilla anguilla*	Na^+/K^+ ATPase α3	Not published	M13*	PCRII	Km, Amp
A5	*Anguilla anguilla*	Na^+/K^+ ATPase α3	Not published	M13*	PCRII	Km, Amp
A6	*Anguilla anguilla*	Na^+/K^+ ATPase α3	Not published	M13*	PCRII	Km, Amp
A7	*Anguilla anguilla*	Na^+/K^+ ATPase β1	AJ239317	M13*	pGEMT, Xl2bleu	Amp
A8	*Anguilla anguilla*	Na^+/K^+ ATPase β3	AJ239316	M13*	PCRII-INVF'	Km, Amp
A9	*Anguilla anguilla*	Na^+/K^+ ATPase β2	Not published	M13*	pGEMT, Xl2bleu	Amp
A10	*Anguilla anguilla*	Na^+/K^+ ATPase β2	Not published	M13*	pGEMT, Xl2bleu	Amp
A11	*Anguilla anguilla*	Na^+/K^+ATPase β4	Not published	M13*	PCRII-INVFalfa	Km, Amp
A12	*Anguilla anguilla*	Na^+/K^+ ATPase β2	Not published	M13*	PCRII-INVFalfa	Km, Amp
B1	*Anguilla anguilla*	CFTR	Not published	M13*	PCRII-INVFalfa	Km, Amp
B2	*Anguilla anguilla*	CFTR	Not published	M13*	PCR blue 2-1	Km, Amp
B3	*Anguilla anguilla*	MDR	Not published	M13*	PCR 2-1	Km, Amp
B4	*Anguilla anguilla*	SERCa	Not published	M13*	pGEMT	Km, Amp
B5	*Anguilla anguilla*	SERCa	Not published	M13*	PCRII-INVF'	Km, Amp
B6	*Anguilla anguilla*	PMCA	Not published	M13*	PCRII-INVF'	Km, Amp
B7	*Anguilla anguilla*	Golgi Ca^{2+} ATPase	Not published	M13*	pGEMT	Km, Amp
B8	*Anguilla anguilla*	$Na^+K^+2Cl^-$ cotransporter	CAD92101	M13*	pGEMT, Xl2-MRF'	Amp
B9	*Anguilla anguilla*	$Na^+K^+2Cl^-$ cotransporter	CAD92101	M13*	pGEMT, Xl2-MRF'	Amp
B10	*Anguilla anguilla*	$Na^+K^+2Cl^-$ cotransporter	CAD92101	M13*	pGEMT, Xl2-MRF'	Amp

Well	Species	Gene isoform	Accession number	Colony PCR primers	Plasmid	Bacterial Resistance
B11	*Anguilla anguilla*	$Na^+K^+2Cl^-$ cotransporter	CAD92101	M13*	PCR4 blunt	Km, Amp
B12	*Anguilla anguilla*	$Na^+K^+2Cl^-$ cotransporter	CAD92101	M13*	pGEMT, Xl2-MRF'	Amp
C1	*Anguilla anguilla*	$Na^+K^+2Cl^-$ cotransporter	CAD92101	M13*	pGEMT, Xl2-MRF'	Amp
C2	*Anguilla anguilla*	$Na^+K^+2Cl^-$ cotransporter	CAD92101	M13*	PCR4 blunt	Km, Amp
C3	*Anguilla anguilla*	Na^+K^+2Cl cotransporter	CAD92101	M13*	PCR4 blunt	Km, Amp
C4	*Anguilla anguilla*	Na^+K^+2Cl cotransporter	CAD92101	M13*	PCR4 blunt	Km, Amp
C5	*Anguilla anguilla*	Na^+K^+2Cl cotransporter	CAD92101	M13*	PCR4 blunt	Km, Amp
C6	*Anguilla anguilla*	KCl cotransporter	Not published	M13*	PCR4 blunt	Km, Amp
C7	*Anguilla anguilla*	$Na^+/Cl^-/HCO3^-$ exchanger	Not published	M13*	PCR4 blunt	Km, Amp
C8	*Anguilla anguilla*	$Na^+/Cl^-/HCO3^-$ cotransporter	Not published	M13*	PCR 2-1	Km, Amp
C9	*Anguilla anguilla*	NHE	AJ006917	M13*	PCR 2-1	Km, Amp
C10	*Anguilla anguilla*	EAE1	Not published	M13*	PCR 2-1	Km, Amp
C11	*Anguilla anguilla*	EAE2	Not published	M13*	PCR 2-1	Km, Amp
C12	*Anguilla anguilla*	EAE3	Not published	M13*	PCR 2-1	Km, Amp
D1	*Anguilla anguilla*	NKCC	CAD92101	M13*	PCR4 blunt	Km, Amp
D2	*Anguilla anguilla*	NKCC	CAD92101	M13*	PCR4 blunt	
D3	*Anguilla anguilla*	AQP1	AJ564420	M13*	PCR4 blunt	Km, Amp
D4	*Anguilla anguilla*	AQP1	AJ564420	M13*	PCR4 blunt	Km, Amp
D5	*Anguilla anguilla*	AQP3	AJ319533	M13*	PCR 2-1	Km, Amp
D6	*Anguilla anguilla*	AQP3a	AJ319533	M13*	PCR4	Km, Amp
D7	*Anguilla anguilla*	AQP3c	Not published	M13*	PCR4	Km, Amp
D8	*Anguilla anguilla*	AQP3f	Not published	M13*	PCR4	Km, Amp
D9	*Anguilla anguilla*	AQP4	Not published	M13*	PCR4	Km, Amp
D10	*Anguilla anguilla*	AQP1	AJ564420	M13*	PCR4	Km, Amp
D11	*Anguilla anguilla*	AQP1	AJ564420	M13*	PCR4	Km, Amp
D12	*Anguilla anguilla*	AQP3	AJ319533	M13*	PCR4	Km, Amp
E1	*Anguilla anguilla*	AQP3a	Not published	M13*	PCR4	Km, Amp
E2	*Anguilla anguilla*	AQP3c	Not published	M13*	PCR4	Km, Amp

Well	Species	Gene isoform	Accession number	Colony PCR primers	Plasmid	Bacterial Resistance
E3	*Anguilla anguilla*	AQP3e	AJ784153	M13*	PCR4	Km, Amp
E4	*Anguilla anguilla*	AQP3	AJ319533	M13*	PCR4	Km, Amp
E5	*Anguilla anguilla*	AQP4	Not published	M13*	PCR4	Km, Amp
E6	*Anguilla anguilla*	AQP8	Not published	M13*	PCR4	Km, Amp
E7	*Anguilla anguilla*	AQP8	Not published	M13*	PCR4	Km, Amp
E8	*Anguilla anguilla*	AQP8b	Not published	M13*	PCR4	Km, Amp
E9	*Anguilla anguilla*	AQP8b	Not published	M13*	PCR4	Km, Amp
E10	*Anguilla anguilla*	AQP3F'	Not published	M13*	PCR4	Km, Amp
E11	*Anguilla anguilla*	AQP3e'	AJ784153	M13*	PCR4	Km, Amp
E12	*Anguilla anguilla*	P-type flappase	Not published	M13*	PCR 2-1	Km, Amp
F1	*Anguilla anguilla*	GAPDH	AB075021	M13*	PCR 2-1	Km, Amp
F2	*Anguilla anguilla*	β-actin	DQ493907	M13*	PCR 2-1	Km, Amp
F3	*Anguilla anguilla*	Uroguanylin	Not published	M13*	PCR 2-1	Km, Amp
F4	*Anguilla anguilla*	Renoguanylin	Not published	M13*	PCR 2-1	Km, Amp
F5	*Anguilla anguilla*	Guanylin	AJ301673	M13*	PCR 2-1	Km, Amp
F6	*Anguilla anguilla*	PepT1	Not published	M13*	PCT II or 4	Km, Amp
F7	*Anguilla anguilla*	HSP 70	Not published	M13*	PGEMT	Km, Amp
F8	*Anguilla anguilla*	Antisecretory factor	Not published	M13*	PCT II or 4	Km, Amp
F9	*Anguilla anguilla*	Prolactin	X69149	M13*	PCT II or 4	Km, Amp
F10	*Anguilla anguilla*	Guanylase cyclas c	Not published	M13*	PGem	Km, Amp
F11	*Anguilla anguilla*	Uroguanylin	Not published	pET32 Xa/lic	pET32	Amp
F12	*Anguilla anguilla*	Renoguanylin	Not published	pET32 Xa/lic	pET32	Amp
G1	*Anguilla anguilla*	Guanylin	AJ301673	pET32 Xa/lic	pET32	Amp
G2	*Anguilla anguilla*	Phospholamban	Not published	M13	pDONR 222, Inv	Km
G3	*Anguilla anguilla*	Mitochondrial DNA	AP007233	M13	pDONR 222, Inv	Km
G4	*Anguilla anguilla*	Laminin receptor	Not published	specific	pDONR 222, Inv	Km
G5	*Anguilla anguilla*	18s rRNA	Not published	specific	pDONR 222, Inv	Km
G6	*Anguilla anguilla*	Ribosomal protein LS4a	Not published	M13	pDONR 222, Inv	Km

Well	Species	Gene isoform	Accession number	Colony PCR primers	Plasmid	Bacterial Resistance
G7	*Anguilla anguilla*	18s rRNA	Not published	specific	pDONR 222, Inv	Km
G8	*Anguilla anguilla*	HSP	Not published	specific	pDONR 222, Inv	Km
G9	*Anguilla anguilla*	18s rRNA	Not published	specific	pDONR 222, Inv	Km
G10	*Anguilla anguilla*	Na^+/K^+ ATPase α1	X76108	M13*	PCR 1000	Km
G11	*Anguilla anguilla*	18s rRNA	Not published	M13*	pDONR 222, Inv	Km
G12	*Anguilla anguilla*	28s rRNA	Not published	M13*, specific	pDONR 222, Inv	Km
H1	*Squalus acanthias*	Na^+/K^+ ATPase α1	AJ781093	M13*	PCR 4	Km, Amp
H2	*Carcharhinus leucas*	Na^+/K^+ ATPase α1	Not published	M13*	PCR 4	Km, Amp
H3	*Carcharhinus leucas*	Na^+/K^+ ATPase β1	Not published	M13*	PCR 4	Km, Amp
H4	*Carcharhinus leucas*	$Na^+K^+2Cl^-$ cotransporter	Not published	M13*	PCR 4	Km, Amp
H5	*Carcharhinus leucas*	AQP1e	Not published	M13*	PCR 4	Km, Amp
H6	*Scyliorhinus canicula*	$Na^+K^+2Cl^-$ cotransporter	Y18919	M13*	pGEMT	Amp
H7	*Scyliorhinus canicula*	$Na^+K^+2Cl^-$ cotransporter	Y18919	M13*	pGEMT	Amp
H8	*Scyliorhinus canicula*	CFTR	Not published	M13*	pGEMT	Amp
H9	*Salmo salar*	CFTR	AF161070	M13*	pGEMT	Amp
H10	*Pleuronectes flesus*	MDR-A	AJ344049	M13*	pGEMT	Amp
H11	*Pleuronectes flesus*	MDR-B	Not published	M13*	pGEMT	Amp
H12	*Arabidopsis thaliana*	Nitrate transporter	NM_114375	M13*	PCR4	Km, Amp

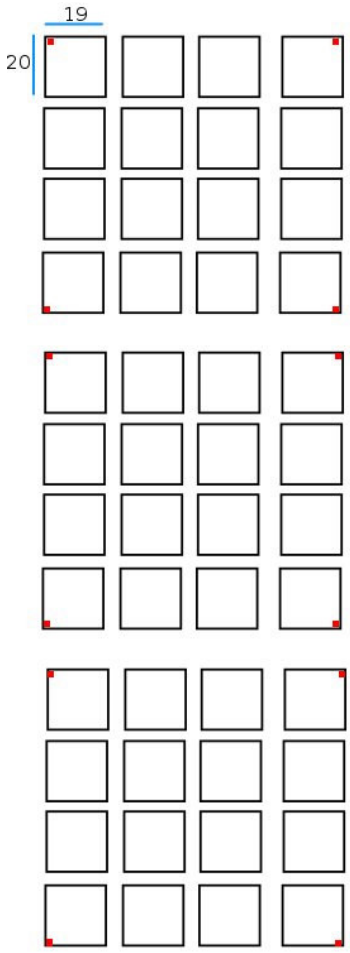

Figure 4.15.a. Microarrray printing design showing the three technical replicates per slide, each subdivided into 16 sub-arrays. Red spots indicate location of landing lights.

4.16 Optimising microarray print quality

Generally the quality of printing by the Liverpool Microarray Facility (The University of Liverpool) was very poor and batches of slides were regularly discarded as they were unusable. Initially, test microarrays were prepared using cDNA amplified from 96 clones from the brain oligo subtracted library. The cDNAs were printed repeatedly on the same array which was then hybridised with brain cDNA from a pool of samples. Analysis of a scanned slide at different levels of magnitude revealed various defects. Spot quality was poor at the top left of each replicate which was caused by a defective print tip (Figure 4.16.a i). Spots were also shown to be misaligned as shown by the kinks in the columns of spots (Figure 4.16.a ii). Although spot size was non-uniform (Figure 4.16.c iii) each replicate spot in the same position in each of the three replicates exhibited consistent size.

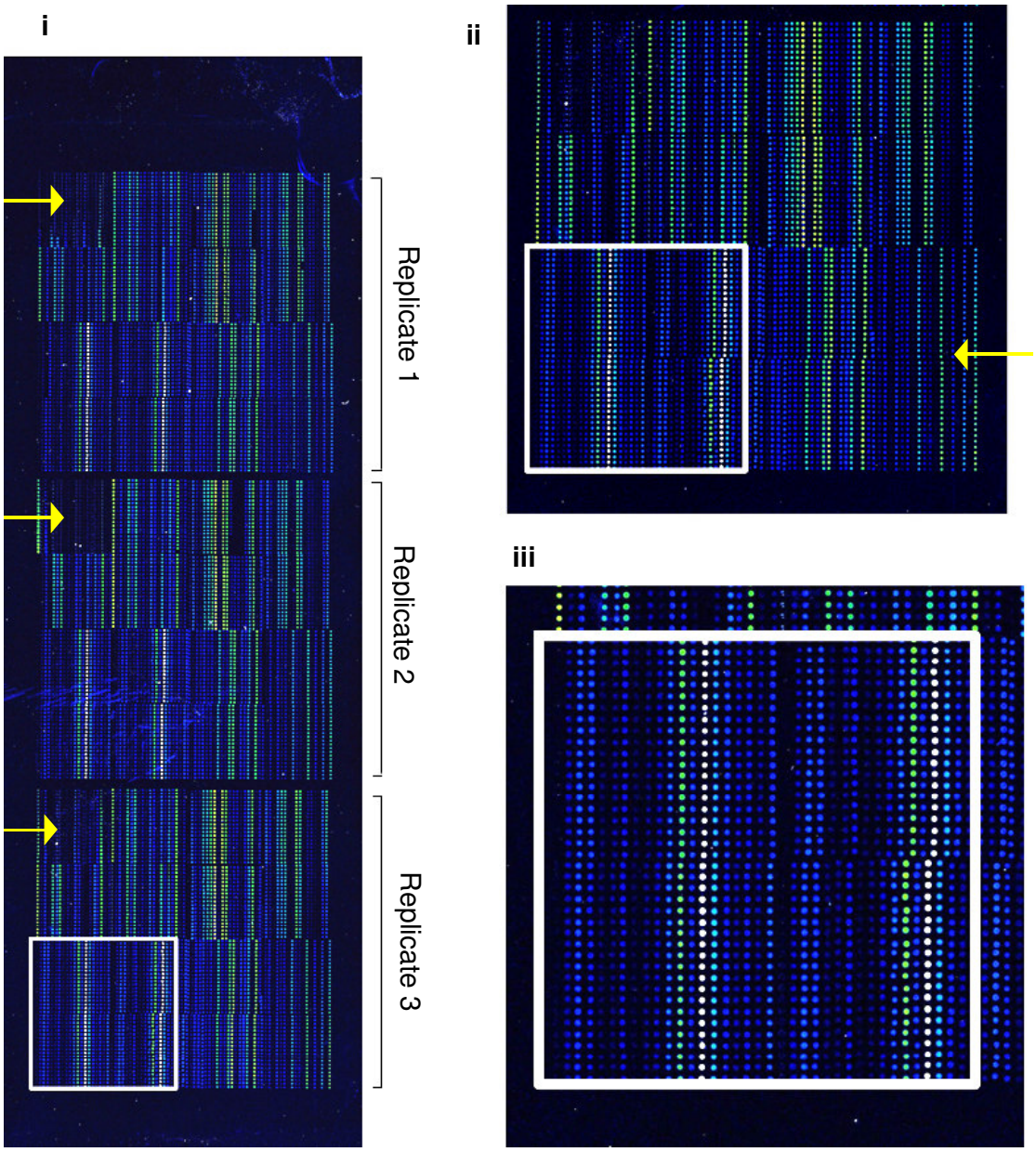

Figure 4.16.a. Test array, printed with 96 cDNAs viewed at three levels of magnification. Slide dimensions are 25 x 75 mm. At low magnification (i) the poor print quality of the top left sub-array of each replicate is indicated by the arrows. Medium magnification of the array (ii) shows misaligned columns of spots indicated by an arrow. Variability in spot size is shown at high magnification (iii).

Despite the imperfections in the spot printing, reasonable quality data could be expected from arrays of this standard. When the arrays were printed using the entire libraries, however, the print quality deteriorated further. Defects were diverse and included overlapping spots, inconsistent printing across the array, high or uneven background levels, and poor spot quality manifested as black-holes or doughnuts. Overlapping spots were found at the borders of adjacent sub-arrays (Figure 4.16.b). Spots with a doughnut conformation were found on some arrays (Figure 4.16.c). This normally occurs when the cDNA solution spotted onto the microarray dries too quickly following printing.

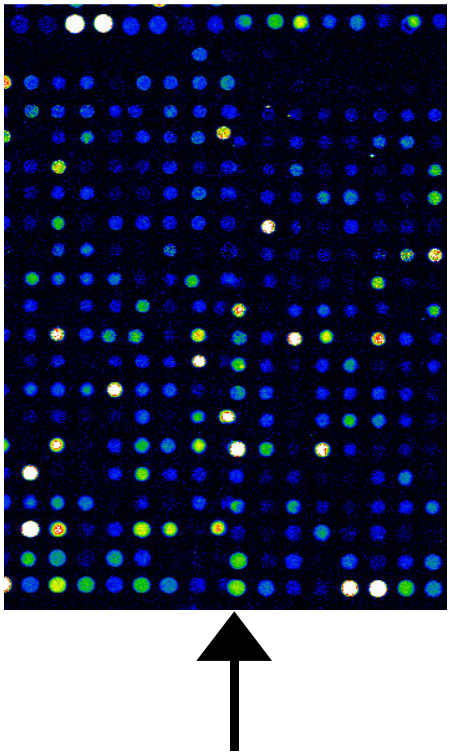

Figure 4.16.b. An example of overlapping spots shown at the border between two sub-arrays as indicated by arrow.

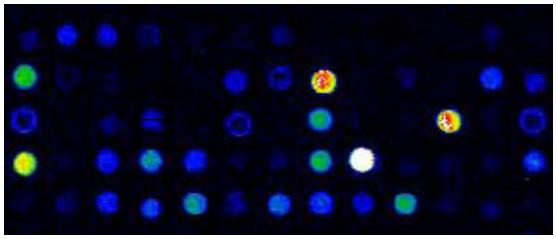

Figure 4.16.c. An example of spots on the brain array with a doughnut conformation. The row indicated by the arrow has three such spots.

The uneven printing was observed as banding across each row of sub-arrays on hybridised slides (Figure 4.16.d). The bands of higher fluorescence are comprised of spots which either have more material printed per feature, or the features have different binding properties. An investigation was undertaken to test whether the uneven banding shown in figure 4.16.d was due to the amount of cDNA printed per feature or if it could be attributed to variable binding characteristics across the array. A spot check was carried out to try and troubleshoot what the Liverpool Microarray Facility were doing wrong. A spot-check involves hybridising Cy3 labelled random 20-mers to a microarray, which will cause in turn cause all cDNA spots on the array to fluoresce. The array was not pre-hybridised before hybridisation to the fluorescent 20-mers and thus the array will show high background fluorescence. This is also useful as areas of differential background are highlighted. The scan of the spot-check array revealed a similar banding pattern to that shown in figure 4.16.d. Clear bands of low background fluorescence are visible on the scan of the spot-check array, indicated by arrows on Figure 4.16.e. These areas of low background contrast with the generally high background. These bands of low background fluorescence correspond to the areas of increased spot intensity shown in Figure 4.16.f.

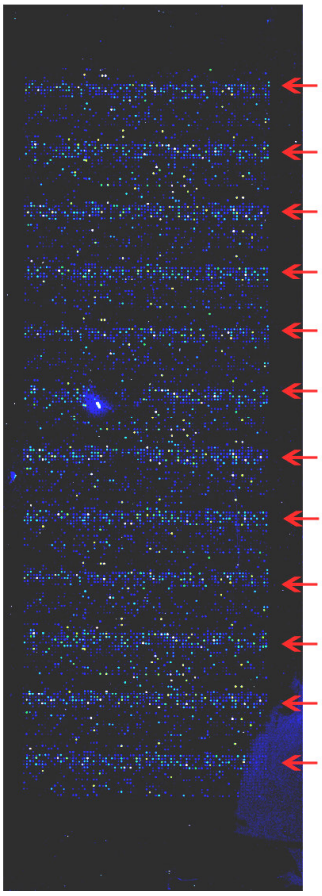

Figure 4.16.d. Uneven microarray printing on the brain array. The array was co-hybridised with fluorescently labelled eel brain cDNA from the 5 month silver FW and 7 day yellow FW groups. Arrows indicate bands of spots exhibiting higher levels of hybridisation to labelled material.

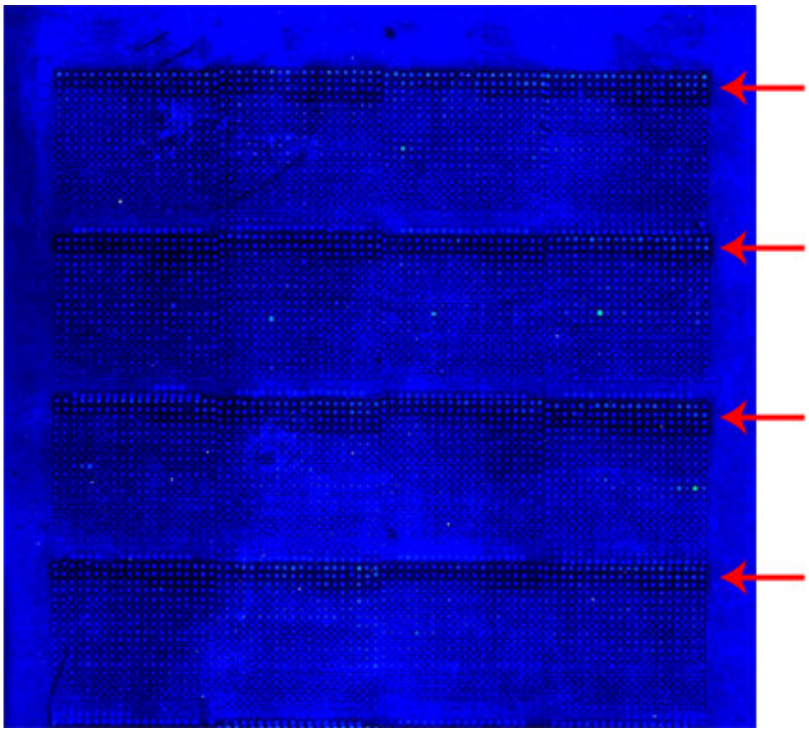

Figure 4.16.e. Scan showing a single replicate from the spot-check array. A brain array, not subjected to prehybridisation, was hybridised with fluorescently labelled (Cy5) random 20-mer oligonucleotides. The arrows indicate four horizontal bands of low background which correspond to the bands of high spot intensity shown in figure 4.3.d.

At higher resolution, three bands per sub-array are visible (Figure 4.16.f). The top 4 rows show high spot fluorescence and low background. The central 11 rows of each sub-array have spots which fluoresce at a slightly lower level but have a high background. The bottom 5 rows of each sub-array have spots which show low fluorescence combined with a high background.

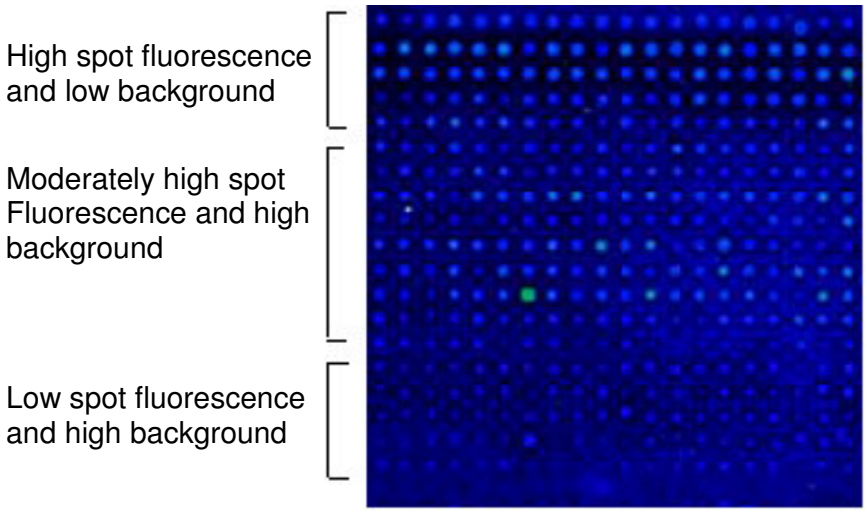

Figure 4.16.f. Sub-array from the brain array subjected to the spot-check. Three levels of print quality are visible

We communicated our findings to the Liverpool Microarray Facility who revealed that arrays were printed over the course of three days and that the three levels of banding would correlate to their spots printed on each of the three days. The disparity of quality between spots printed on separate days was attributed to the gradual degradation of the lysine coating of the slides which occurs once they are removed from the packaging which contains a protective atmosphere. Subsequently the arrays were remade with all spots being printed in a single day which improved quality to an adequate level (figure 4.16.g) and these arrays were used in the final hybridisation experiments. As a consequence of the various defects found with the printing the brain arrays were reprinted four times and the SSH arrays more than 10 times. Despite repeated attempts to aid the Liverpool Microarray Facility with troubleshooting problems the printing was never optimised. To keep the project progressing, sub-standard arrays were used which compromised the experiments as many spots were completely absent, reducing both the quantity and quality of data.

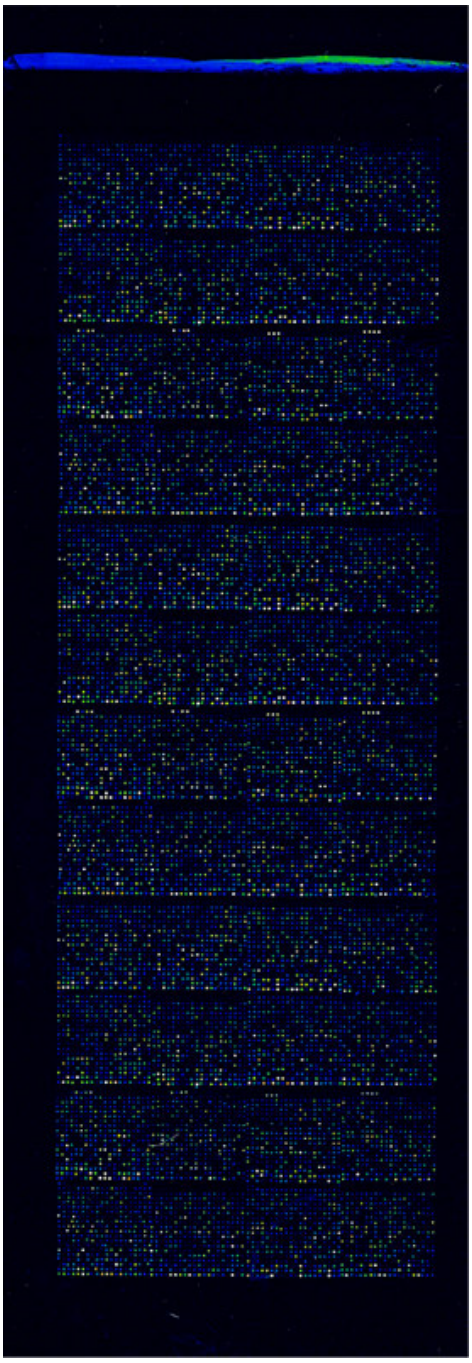

Figure 4.16.g. A brain oligo array exhibiting relatively even fluorescence across the slide. The array was co-hybridised with fluorescently labelled eel brain cDNA from the silver 5 month FW acclimated group and the yellow 7 day FW acclimated group. The array was printed in one continuous run on a single day.

4.17 Validation of array reproducibility

The reproducibility of successive array experiments was assessed by monitoring genes, including a number of known genes such as the Na,K,2Cl cotransporter (NKCC). Replicate microarrays were hybridised with the same cDNA samples over several days and the expression values across all the repeated NKCC features on the arrays was monitored. The average intensities from three triplicate spots recorded for each of seven NKCC clones across six replicate arrays showed that the results were reproducible between successive microarray experiments (figure 4.17.a).

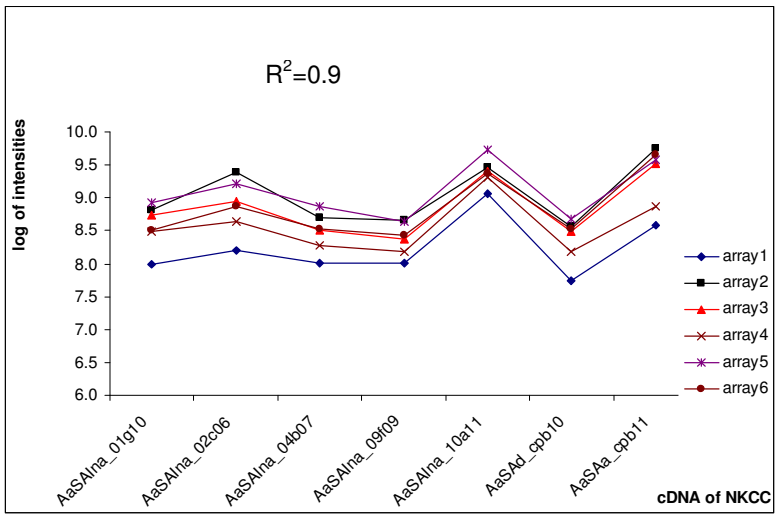

Figure 4.17.a. Assessment of the inter- and intra-array variability in levels of expression recorded for the Na, K, 2Cl-cotransporter (NKCC) mRNA in the intestine of FW-acclimated fish. cDNAs were pooled from 6 FW acclimated fish and on six separate days a sample of the pooled cDNAs was labelled, as detailed in section 3.17, before being hybridised to 6 independent microarrays which contained 7 different clones of NKCC. The Y axis represents the log of fluorescence intensity recorded and the X axis represents the average intensity values for the seven different cDNAs of NKCC spotted in triplicate across the microarrays.

4.18 Brain microarray results: Comparison of brain gene expression profiles between 7 day FW yellow and 5 month FW acclimated silver eels.

Ideally, gene expression in the 7 day FW acclimated yellow eels would have been compared to the 7 day FW acclimated silver eels but unfortunately the RNA for the latter samples was degraded and unsuitable for use. The RNA from the brains of 5 month FW adapted silver eels was chosen as a replacement. It was felt that modulation of gene expression in response to the eel being transferred from the holding tanks to the experimental tanks and to the disturbance experienced during draining and refilling of tanks would be minimised. The metadata (Section 4.1) did not reveal anything to suggest that the yellow and silver groups were significantly different, other than their developmental state. A non-paired t-test (assuming heteroskedastic variance) shows there to be no significant difference in circulating levels of the known stress response hormone, cortisol, between the yellow 7 day FW adapted and silver 5 month FW adapted eels ($p = 0.74$). Both groups were caught and killed at very similar times during the day, however the silver group was processed in April 2002, whilst the yellow group was processed in November 2002 (Table 4.18.a)

Table 4.18.a. Capture and kill times for the 7 day FW yellow and 5 month FW adapted silver eel groups.

Fish	Catch time		Kill time	
	Silver	Yellow	Silver	Yellow
1	2.39pm	2.39pm	2.47pm	2.42pm
2	3.07pm	3.07pm	3.09pm	3.09pm
3	3.30pm	3.28pm	3.35pm	3.31pm
4	3.54pm	3.48pm	3.58pm	3.51pm
5	4.16pm	4.09pm	4.23pm	4.11pm
6	4.40pm	4.34pm	4.46pm	4.36pm

The brain microarray was co-hybridised with fluorescently labelled cDNAs derived from amplified eel brain total RNA from the 7 day FW adapted yellow group and the 5 month FW adapted silver group. The yellow and silver eel cDNA was labelled with Cy3 and Cy5 respectively. Subsequently the experiment was repeated in dye-swap in which the exact procedure was repeated except the cDNA labels Cy3 and Cy5 were reversed.

At a given laser intensity and PMT gain, the signal intensity from Cy3 fluorescence is normally greater than that from the Cy5 fluorescence. In an attempt to compensate for this, the data for the yellow-silver comparison was analysed twice and will be referred to as “analysis 1” and “analysis 2”. Analysis 1 used identical scanning intensities in all instances, the laser output: PMT gain ratio was 68 %: 68 % for both forward and dye-swap experiments. For analysis 2, the Cy5 scans chosen had a higher laser intensity and PMT gain than the Cy3. Scan settings in analysis 2 for the forward experiment were; laser output: PMT gain ration Cy3 65 %: 65%, Cy5 68 %: 68 %, and for the reverse experiment, Cy3 63 %: 63%, Cy5 68 %: 68 %. These scans showed similar average fluorescence in an attempt to compensate for the difference fluorescence of Cy3 and Cy5. The calculated changes in expression level of genes were very similar between analysis 1 and 2 showing that the MADSCAN normalisation and data treatment gave consistent results with data obtained from scans at different intensities.

Data was analysed using MADSCAN. Initially the background fluorescence is subtracted from the foreground intensities from the Cy3 and Cy5 channels. Data then undergoes $\log_2$ transformation which uncouples the mean intensity from the

variance. Visualisation of the variance is much clearer following log_2 transformation and fold changes around low intensities become comparable to high intensities (figure 4.18.a).

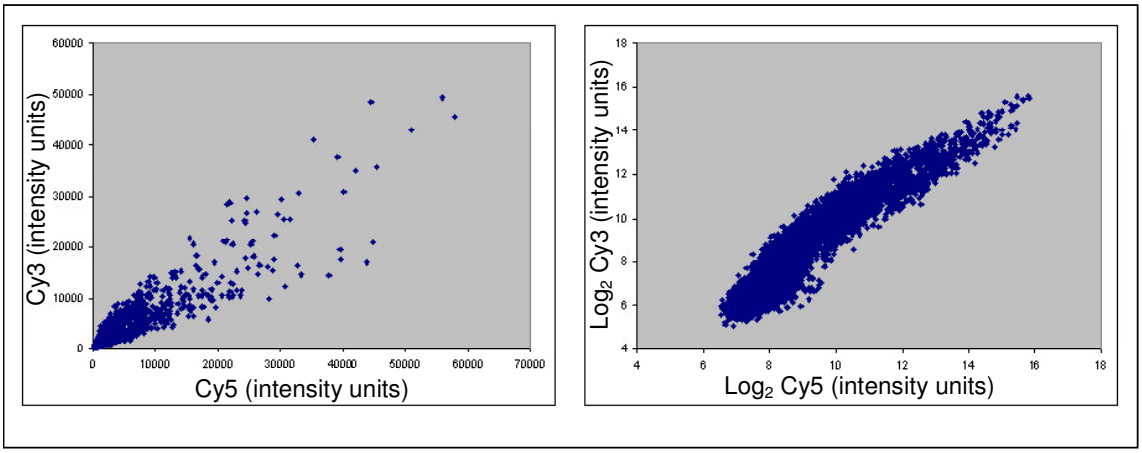

Figure 4.18.a. Cy5 intensities against Cy3 intensities before and after log_2 data transformation (analysis 1, non-normalised data, 7 day yellow FW brain vs 5 month silver FW brain, forward experiment). Before log_2 transformation the variance is directly correlated with intensity but following transformation the variance at all intensities becomes comparable.

M vs. A plots (Dudoit et al., 2000) were created to view ratios and fluorescence intensity at the same time (Figures 4.18.b and 4.18.c) in order to identify spot artefacts and detect intensity dependent patterns in the log ratios before and after normalisation. M stand for minus whilst A stands for add, a reference to the way in which they are calculated from the log fluorescence values;

M is the $\log_2$ intensity ratio for a given spot;
$M = \log_2 (Cy3 / Cy5) = \log_2 Cy5 - \log_2 Cy3$.

A is the mean $\log_2$ spot intensity in both the Cy3 and Cy5 channels;
$A = (\log_2 Cy5 + \log_2 Cy3) / 2$.

M vs A plots show non-linear unwanted dependence between ratios and fluorescence. The trendline in each M versus A plot is a *lowess* fitness curve which is applied to a selected set of non-differentially expressed genes. Non-differentially expressed genes were selected by an iterative Rank Invariant Method algorithm (Tseng et al., 2001). The algorithm is expressed as;

For the first loop:

$$S_0 \equiv \{g: \left| \text{rank}\,(Cy5_g) - \text{rank}\,(Cy3_g) \right| < p \times G \;\&\; I < \text{rank}[(Cy5_g + Cy3_g)/2] < G - I\}$$

For iteration ***i*** to the k^{th}

$$S_i \equiv \{g : g \varepsilon S_{i-1} \;\&\; \left| \text{rank}_{g \varepsilon Si-1}\, Cy5_g - \text{rank}_{g \varepsilon Si-1}\, Cy3_g \right| < p \times \left| S_{i-1} \right|\}$$

g is the gene being tested for rank variance, $Cy5_g$ and $Cy3_g$ are the fluorescent intensities, $p = 0.05$, *G* is the highest rank, *I* is the rank threshold = 10 (i.e. ± 5), S_{i-1} is the number of genes in set S_i. The iteration stops at the k^{th} step when $\left| S_k \right| \equiv \left| S_{k-1} \right|$, where the set of genes S_k is the rank invariant set.

This algorithm separately ranks all spots in the Cy3 and Cy5 channels according to the intensity. Spots in the highest (*G-I*) ranks are discounted as they

may be approaching saturation. A given spot (*g*) is selected for inclusion in the set of non-differentially expressed genes (S_k) if the assigned rank in Cy3 and Cy5 differs less than the rank threshold (± 5 ranks).

The *lowess* fitness curve, a local, non-parametric regression which stands for Locally Weighted Estimate, is fitted to this set of invariant genes. The remaining (variant) spot data are then normalised to this curve. This allows a differential normalisation factor to be applied to M depending on spot intensity, allowing the non-linear bias in the ratio to be accounted for. In addition, each sub-array in a microarray is printed with a different pin so there is an additional spatial variable in the normalisation equation which accounts for any variance in the data which is print-pin dependent. The normalisation curve function is intensity-dependent, using A, the geometric mean of the intensities.

$$\text{Log}_2\,\text{Cy5/Cy3} \longleftrightarrow \log_2\text{Cy5/Cy3} - c(A) = \log_2\text{Cy5}/[k(A)\text{Cy3}]$$

Where c(A) is the *lowess* fit to the M-A plot and k is a constant.

A span f is defined as the fraction of data used to smooth at each data point (f = 0.4, i.e., 40 % of data around a point). For the within-print tip group normalisation, *i.e.* spatial approach, the *lowess* fit simply becomes (print tip+A)-dependent.

$$\text{Log}_2\,\text{Cy5 / Cy3} \leftrightarrow \log_2\,\text{Cy5 / Cy3} - c_i(A) = \log_2\,\text{Cy5} / [k_i(A)\text{Cy3}]$$

Where *i* is the i_{th} sub-array. Finally the data is normalised according to:

$\equiv \tilde{f}(A)$ between $\min_{g \varepsilon S} A_g$ and $\max_{g \varepsilon S} A_g$

The transformation of data by the normalisation process is clearly visible; for analysis 1 see Figures 4.18.d and 4.18e; for analysis 2 see Figures 4.18.f and 4.18.g.

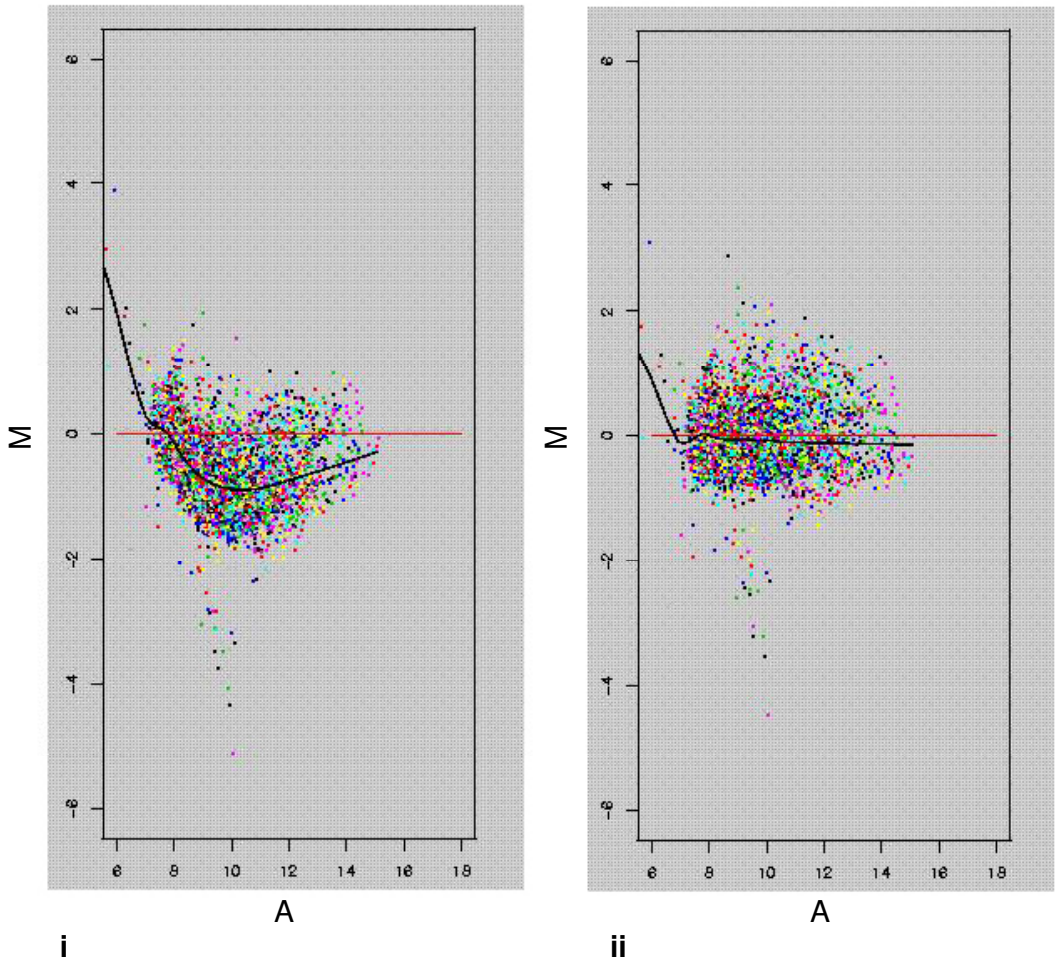

Figure 4.18.b. Representative MADSCAN generated M vs. A plots from analysis 1 before (i) and after (ii) data processing (analysis 1, 7 day FW acclimated yellow versus 5 month FW acclimated silver eel groups, brain, forward experiment). The curves are *lowess* fitness curves built on the set of non-variant genes to which the rest of the data is normalised. The different coloured spots correspond to the 48 sub-arrays printed by different print-tips. *M* is the $\log_2$ intensity ratio *= $\log_2$ (Cy3/Cy5)* and A is the mean $\log_2$ spot intensity = *($\log_2$ Cy5 + $\log_2$ Cy3) / 2.*

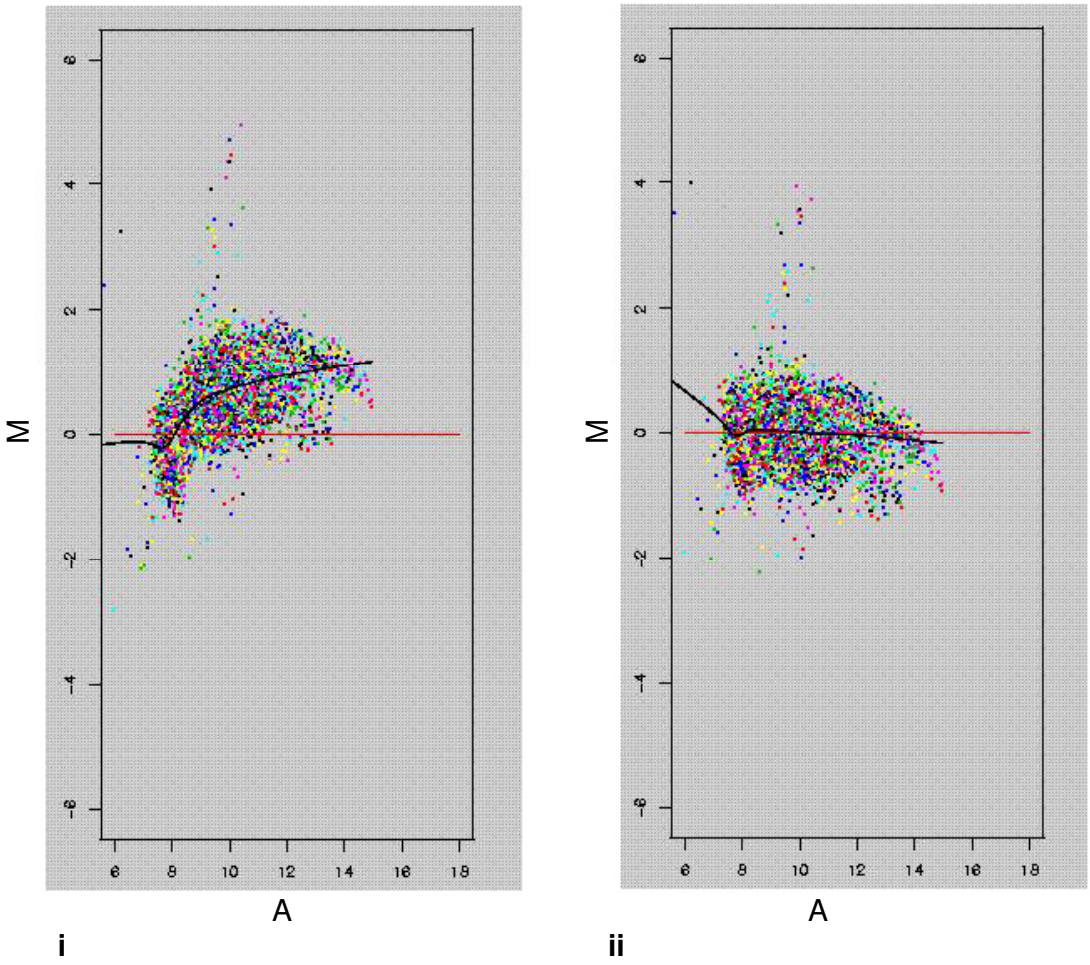

Figure 4.18.c. Representative MADSCAN generated M vs. A plots from analysis 2 before (i) and after (ii) data processing (analysis 2, 7 day FW acclimated yellow versus 5 month FW acclimated silver eel groups, brain, dye-swap experiment). The curves are *lowess* fitness curves built on the set of non-variant genes to which the rest of the data is normalised. The different coloured spots correspond to the 48 sub-arrays printed by different print-tips. *M* is the $\log_2$ intensity ratio = $log_2 (Cy3/Cy5)$ and A is the mean $\log_2$ spot intensity = $(log_2 Cy5 + log_2 Cy3) / 2$.

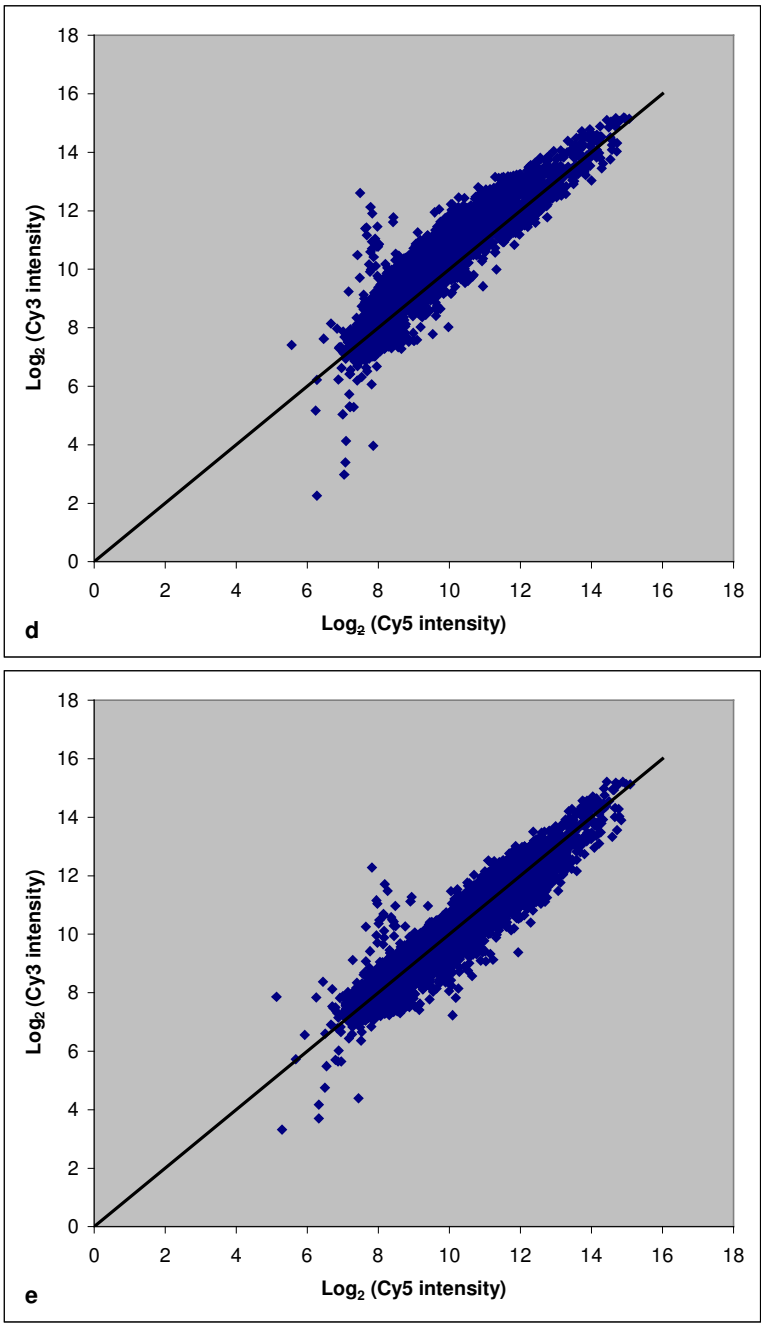

Figure 4.18.d and e. Plots of the log_2 Cy5 intensities against log_2 Cy3 intensities before (d) and after (e) normalisation (analysis 1, 7 day FW acclimated yellow eel (Cy3) vs 5 month FW acclimated silver eel (Cy5) groups, brain, forward experiment). Cy3 and Cy5 were scanned using identical laser intensity and PMT gain (65 % and 65 % respectively). There is a bias for Cy3 fluorescence intensity to be higher than Cy5 when scanned under identical conditions, as shown in the non-normalised plot in which the majority of the data points fall above the x = y regression. Following normalisation the variance is equally distributed about the regression.

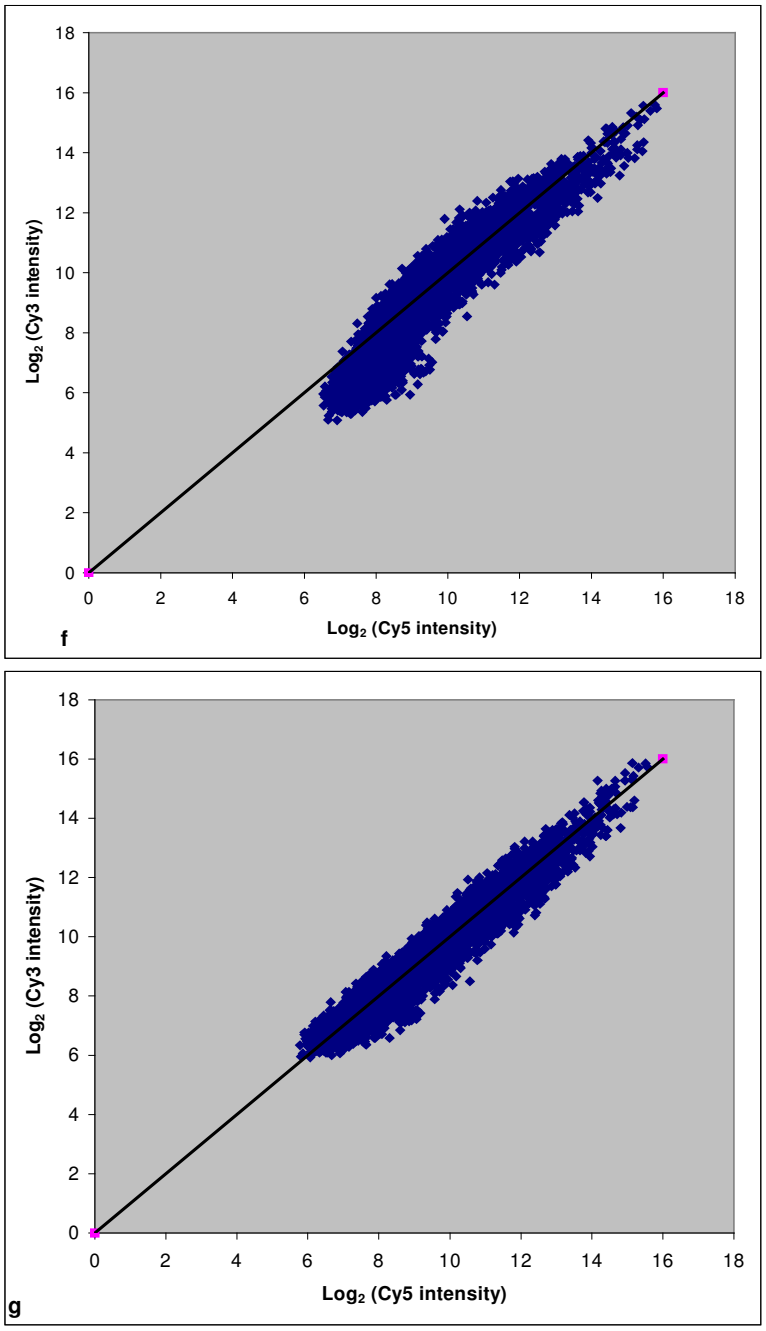

Figure 4.18.f and g. Plots of the log_2 Cy5 intensities against log_2 Cy3 intensities before (f) and after (g) normalisation (data from analysis 2, 7 day FW acclimated yellow eel (Cy3) vs 5 month FW acclimated silver eel (Cy5) groups, brain, forward experiment). Prior to normalisation the variance in analysis 2 is more centred around the x = y regression than in analysis 1. This was achieved by scanning the Cy3 and Cy5 channels using different laser intensity: PMT gain ratios (Cy3 65 %: 65%, Cy5 68 %: 68 % respectively) to accommodate for the higher natural of fluorescence of Cy3. The data in (d) is not linear but following normalisation (e) the variance is equally distributed about the regression showing a linear relationship.

Following *lowess* normalisation the data was scaled to bring the inter- and intra-slide variance to within the same range allowing separate slides to be compared directly. This is achieved using a function of the median absolute deviation and geometric mean (Yang et al., 2002).

Median absolute deviation $\equiv$ median $\{|x_i - \bar{x}_m|\}$ where $\bar{x}_m$ is the median of x_i

Geometric mean $= \text{prod}\,(MADx_{ij})^{(1/n)}$

Scaled $x_{ii} = (x_{ji} / MAD(x)_{ij}) * GM$

The scaling is visualised using whisker plots (Figure 4.18.h and 4.18.i) which show five statistical descriptors. The line in the box is the 50th percentile, i.e. the median, 50% of the data are contained below and above this line. The height of the box, i.e. the distance between the 25th and 75th percentiles, is known as the inter-quartile range or inter-quartile distance (IQD). The length of the tails or whiskers is usually 1.5 times the IQD. Data points that fall beyond the whiskers are normally considered outliers, or in the case of microarrays they represent potentially differentially expressed genes. Before data normalisation the IQD is large showing that the variance is also large. The 50th percentile, IQD and the whiskers are not aligned between the forward and dye-swap experiments which indicates that the data from these two experiment cannot be compared directly. Following data normalisation the intra-slide variance is much smaller as shown by the smaller IQD and shorter whiskers. Data normalisation scales the inter-slide variance so that it is now comparable, as shown by the alignment between IQD and whiskers, so that outliers (differentially expressed genes) can be accurately identified.

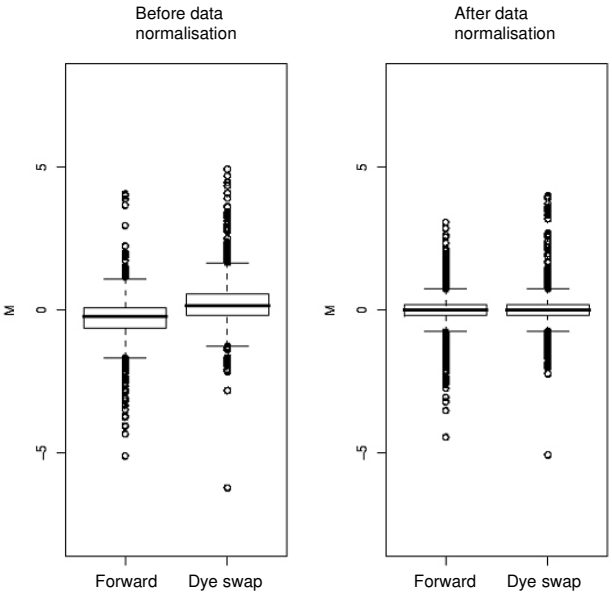

4.6.h

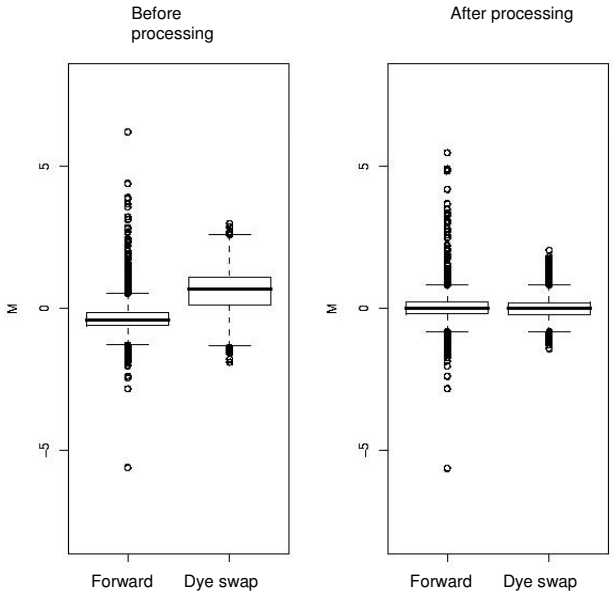

4.6.i

Figures 4.18.h and 4.18.i. Whisker plots before and after data processing {analysis 1 (4.18.h) and analysis 2 (4.18.i)}, yellow 7 day FW acclimated versus silver 5 month FW acclimated eel groups, brain). The height of the box represent the inter-quartile distance, the line within the box represents the 50th percentile and the length of the whiskers is 1.5 x the IQD. Outliers beyond the whiskers represent potentially differentially expressed genes.

Density plots of the intensity ratios for analyses 1 and 2 following all processing steps show the data have a distribution which is close to normal (Figure

4.18.j). There is a slight positive bias (skew = 0.35) in the distribution which is also apparent in the whisker plots indicating that more genes are up-regulated in silver eels than yellow eels.

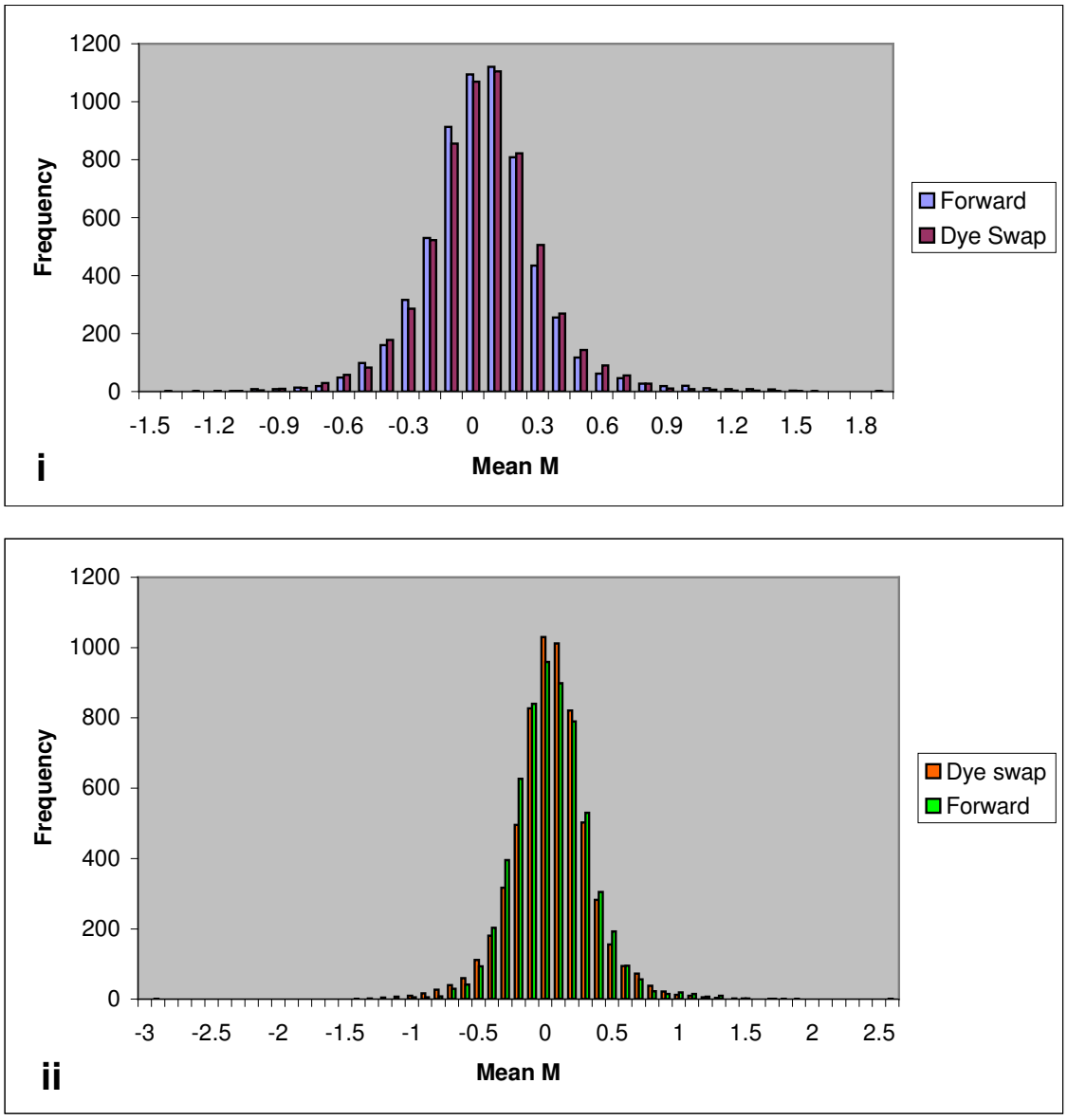

Figure 4.18.j. Frequency distributions showing near normal distribution of mean intensity ratios (M) of replicate spots following data normalisation in both analysis 1 (i) and analysis 2 (ii), (7 day FW acclimated yellow eel versus 5 month FW acclimated silver eel groups, brain). *M* is the log_2 intensity ratio = *log_2 (Cy3/Cy5)*

Genes were selected for further analysis if they showed consistent up or down-regulation in silver eels shown by expression ratios >1.5 or <0.67-fold respectively. Thresholds were set to select only the genes exhibiting the largest fold changes between conditions. Differences between experimental groups were considered consistent if replicated in each of the triplicate spots on each array and between separate arrays in the dye-swap experiment.

Genes (70) which showed consistent up or down regulation were selected for further analysis. Genes identified in analysis 1 always showed very similar expression ratios in analysis 2 and vice versa. All genes identified in analysis 1 and 2 were sequenced, trimmed for vector and adapter sequences using trace2dbest and compared to current NCBI protein and EST databases using blastx and. These sequences have been submitted to arrayexpress (http://www.ebi.ac.uk/aerep) and will be available online following publication of the results. The known biological functions for each clone was ascertained from the Gene Ontology database (http://www.geneontology.org/, Ashburner, 2000). Clones were then clustered, by the putative function of the protein they encode, into the following sub-groups; signal transduction (Table 4.18.b), development and morphogenesis (Table 4.18.c), membrane and structure (Table 4.18.d), metabolism (Table 4.18.e), immune/stress response (Table 4.18.f) and transcription and post-translational modification (Table 4.18.g). Some clones could not be placed into any of these clusters, or they have no known function or the sequencing failed (Table 4.18.h).

Table 4.18.b. Signal transduction cluster. Mean fold-change (FC) and standard deviation (SD) of brain transcripts from the 7 day FW acclimated yellow eel group and the 5 month FW acclimated silver eel during forward and dye-swap experiments. Blastx and blastn results from NCBI database searches show homologies to known proteins and genes respectively.

Clone ID	FC	SD	Blastx	Blastn	Biological process
Aa_BOS_01C01	2.05	0.57	gb|AAH23556.1| VRK3 protein [Homo sapiens] 260 4e-68	TC18156 similar to GB|AAH23556.1|23272127|BC023556 VRK3 protein {Homo sapiens;}	Regulation of extra-cellular signal regulated kinases via MAP kinase pathway. Phosphorylation of transcription factors.
Aa_BOS_17C12	0.65	0.04	emb|CAA48902.1| prolactin-precursor [Anguilla anguilla] 381 e-104	TC80284 UP|PRL_ONCMY (P21993) Prolactin precursor (PRL), complete 98 5e-19	Hormonal signalling
Aa_BOS_28G03	1.66	0.22	gb|AAI02765.1| Microtubule-associated protein 396 e-109	TC90114 similar to UP|Q7ZXP1 (Q7ZXP1) Mapre2-A protein, Microtubule-associated protein 611 e-173	Cell proliferation Cellular defense Signal transduction
Aa_BOS_35D04	1.52	0.05	gb|AAH64229.1| DnaJ (Hsp40) homolog, subfamily C, member 9 [Xenopus Laevis] 241 3e-62	>gi|109502119|ref|XM_001064040.1| Gene info PREDICTED: Rattus norvegicus DnaJ (Hsp40) homolog, subfamily 52.0 0.003	Small GTPase mediated signal transduction
Aa_BOS_38B06	0.66	0.05	emb|CAA48902.1| prolactin-precursor [Anguilla anguilla] 382 e-105	TC80284 UP|PRL_ONCMY (P21993) Prolactin precursor (PRL), complete 105 2e-21	Hormonal signalling
Aa_BOS_45C05	1.92	0.15	gb|AAH59577.1| Secretogranin III [Danio rerio] 133 9e-30	TC292724 UP|Q6PBU8 (Q6PBU8) Secretogranin III, complete 165 2e-39	Intercellular trafficking of storage components during granule maturation
Aa_BOS_49C01	1.74	0.34	gb|AAH59577.1| Secretogranin III [Danio rerio] 134 2e-30	TC292724 UP|Q6PBU8 (Q6PBU8) Secretogranin III, complete 165 2e-39	Intercellular trafficking of storage components during granule maturation
Aa_BOS_58A09	0.62	0.02	gi|1638811|dbj|D88022.1| Anguilla japonica mRNA for eel C-type natriuretic peptide 702 0.0	gi|1638811|dbj|D88022.1| Anguilla japonica mRNA for eel C-type natriuretic peptide 702 0.0	Blood pressure regulation
Aa_BOS_38B06	0.66	0.05	emb|CAA48902.1| prolactin-precursor [Anguilla anguilla] 382 e-105	TC80284 UP|PRL_ONCMY (P21993) Prolactin precursor (PRL), complete 105 2e-21	Hormonal signalling

Table 4.18.c. Development and morphogenesis cluster. Mean fold-change (FC) and standard deviation (SD) of brain transcripts from the 7 day FW acclimated yellow eel group and the 5 month FW acclimated silver eel during forward and dye-swap experiments. Blastx and blastn results from NCBI database searches show homologies to known proteins and genes respectively.

Clone ID	FC	SD	Blastx	Blastn	Biological processes
Aa_BOS_01C05	1.68	0.41	ref|NP_998310.1| tyrosine 3-monooxygenase/tryptophan 5-monooxygenase activation protein, beta polypeptide [Danio rerio]. 384 e-105	TC87178 UP|Q6UFZ9 (Q6UFZ9) 14-3-3B1 protein, complete 492 e-138	Ubiquitous phosphoprotein partner regulating many pathways including apoptosis, cell proliferation and salinity adaptation in teleost gill
Aa_BOS_03C09	1.77	0.11	gb|AAH65983.1| Vangl2 protein [Danio rerio] 76 1e-12	TC268919 Vangl2 protein [Danio rerio] 785 0.0	Cell morphogenesis Cell migration in hindbrain Convergent extension involved in gastrulation Establishment of cell polarity Negative regulation of frizzled signalling pathway Integral membrane protein Wnt signalling pathway regulation
Aa_BOS_02H05	1.58	0.15	gb|AAT64101.1| reticulon 4-N [Takifugu rubripes] 74 4e-12	TC86638 UP|Q6IEJ1 (Q6IEJ1) RTN4-M, complete 88 4e-16	Angiogenesis Negative regulation of axon extension Nervous system development Regulation of cell migration
Aa_BOS_18F06	0.63	0.03	***** No hits found *****	TC279868 UP|Q91430 (Q91430) Seven-up[40] protein, complete 127 5e-28	Nervous system development Eye development Phototaxis Cell fate determinant Heart development Synaptic transmission
Aa_BOS_28D03	1.59	0.04	gb|AAT44427.1| V-Fos transformation effector-like protein 455 e-127	TC17783 homologue to GB|AAD10201.1|3037139|AF056328 V-Fos transformation effector {Oryzias latipes;} 882 0.0	Nervous system development Regulation of transcription from RNA polymerase II promoter Inflammatory response DNA methylation
Aa_BOS_28G03	1.66	0.22	gb|AAI02765.1| Microtubule-associated protein 396 e-109	TC90114 similar to UP|Q7ZXP1 (Q7ZXP1) Mapre2-A protein, Microtubule-associated protein 611 e-173	Cell proliferation Cellular defense Signal transduction
Aa_BOS_30B01	2.50	1.14	ref|NP_084066.2| methyltransferase 5 domain containing 1 [Mus musculus] 240 5e-62	TC87451 similar to UP|Q7PR74 (Q7PR74) ENSANGP00000016999 (Fragment) 218 2e-55	Cell proliferation Peptidyl-arginine N-methylation
Aa_BOS_30D02	1.71	0.17	gb|AAH55246.1| Birc4 protein [Danio rerio] 215 1e-54	TC292658 UP|Q7SXU1 (Q7SXU1) Birc4 protein (Fragment), complete 48 4e-04	Anti-apoptosis Caspase inhibition
Aa_BOS_40F12	0.63	0.03	gb|AAH55653.1| Microspherule protein 1 [Danio rerio] 187 3e-46	TC4627 similar to GB|AAC52086.1|2384717|AF015308 nucleolar protein {Homo sapiens;} 76 2e-12	Protein modification Regulation of cell cycle progression
Aa_BOS_51F06	0.63	0.04	TC79092 similar to UP|SEP3_MOUSE (Q9Z1S5) Neuronal-specific septin 123 8e-27	***** No hits found ******	Cytokinesis
Aa_BOS_51H06	0.54	0.04	***** No hits found ******	TC79092 similar to UP|SEP3_MOUSE (Q9Z1S5) Neuronal-specific septin 123 8e-27	Cytokinesis
Aa_BOS_54B11	0.59	0.06	***** No hits found *****	TC79092 similar to UP|SEP3_MOUSE (Q9Z1S5) Neuronal-specific septin 123 8e-27	Cytokinesis
Aa_BOS_58D10	1.93	0.13	gb|ABC67288.1| midkine b [Carassius auratus gibelio] 108 7e-23	TC17948 similar to UP|Q9W767 (Q9W767) Pleiotrophin 1 (Midkine-related growth factor Mdk1)	Brain development Secretory pathway
Aa_BOS_59D06	0.63	0.05	***** No hits found ******	TC79092 similar to UP|SEP3_MOUSE (Q9Z1S5) Neuronal-specific septin 123 8e-27	Cytokinesis

Table 4.18.d. Membrane and structure cluster. Mean fold-change (FC) and standard deviation (SD) of brain transcripts from the 7 day FW acclimated yellow eel group and the 5 month FW acclimated silver eel during forward and dye-swap experiments. Blastx and blastn results from NCBI database searches show homologies to known proteins and genes respectively.

Clone ID	FC	SD	Blastx	Blastn	Biological processes as identified by Gene Ontology
Aa_BOS_30E02	1.87	0.24	gb|AAL00466.1| Nucleobase:cation symporter for xanthine 64 3e-09	CX066551 174 2e-42	Xanthine symport
Aa_BOS_40G07	1.75	0.31	gb|AAA21578.1| kainate receptor alpha subunit 325 1e-87	TC86160 similar to UP|Q90278 (Q90278) Kainate receptor beta subunit 113 8e-24	Extracellular-glutamate-gated ion channel activity
Aa_BOS_49G05	0.59	0.06	***** No hits found ******	TC78300 UP|Q68K22 (Q68K22) Gelsolin (Fragment), partial (12%) 101 3e-20	Actin filament assembly and disassembly
Aa_BOS_39H01	0.60	0.06	ref|NP_055723.1| transmembrane protein 15 [Homo sapiens] 223 6e-57	TC300781 weakly similar to UP|Q8R2Y3 (Q8R2Y3) Transmembrane protein 15 54 6e-06	Integral membrane protein
Aa_BOS_32G06	0.59	0.03	dbj|BAD93115.1| intercellular adhesion molecule 2 precursor 52 1e-05	***** No hits found ******	Intercellular adhesion
Aa_BOS_32E03	0.65	0.06	gb|AAQ97859.1| tubulin, beta, 2 [Danio rerio] 423 e-117	TC267911 UP|Q9DFT6 (Q9DFT6) Beta tubulin, complete 545 e-154	Cytoskeleton
Aa_BOS_29C12	0.51	0.04	ref|NP_570129.1| contactin associated protein-like 5 isoform 1 129 9e-29	***** No hits found ******	Cell adhesion Sensory perception of sound
Aa_BOS_01G06	1.55	0.20	gb|AAH62826.1| Tubulin, alpha 8 like 2 [Danio rerio] 380 e-104	TC268704 UP|Q6TNP4 (Q6TNP4) Tubulin, alpha 4, complete 591 e-168	Cytoskeleton

Table 4.18.e. Metabolism cluster. Mean fold-change (FC) and standard deviation (SD) of brain transcripts from the 7 day FW acclimated yellow eel group and the 5 month FW acclimated silver eel during forward and dye-swap experiments. Blastx and blastn results from NCBI database searches show homologies to known proteins and genes respectively.

Clone ID	FC	SD	Blastx	Blastn	Biological processes as identified by Gene Ontology
Aa_BOS_01E10	0.55	0.05	gb|AAH28818.1| Aldose 1-epimerase [Mus musculus] 186 7e-46	***** No hits found ******	Carbohydrate metabolism
Aa_BOS_06H03	1.50	0.09	emb|CAC83782.1| phosphoglucose isomerase-2 [Danio rerio] 375 e-103	TC291056 UP|Q7ZU30 (Q7ZU30) Glucose phosphate isomerase a, complete 163 7e-39	Glucose metabolism
Aa_BOS_13B10	0.65	0.04	gb|ABD38667.1| aldehyde dehydrogenase 4 family 207 3e-52	TC282238 similar to UP|Q96IF0 (Q96IF0) Aldehyde dehydrogenase 4A. 88 4e-16	Metabolic processes Proline catabolism Proline metabolism
Aa_BOS_28H10	1.81	0.27	gb|AAH53192.1| Aldolase c, fructose-bisphosphate [Danio rerio] 420 e-116	TC279277 UP|Q8JH70 (Q8JH70) Aldolase c, fructose-bisphosphate 470 e-131	Fructose metabolism
Aa_BOS_32G11	0.59	0.06	gb|AAA52646.1| hexokinase 1 [Homo sapiens] 431 e-119	TC269571 UP|Q6NX09 (Q6NX09) Zgc:77618 protein, complete 321 2e-86	Glycolysis
Aa_BOS_36A02	1.64	0.08	ref|XP_694230.1| PREDICTED: similar to Cytochrome P450 27, 390 e-107	CD599042 weakly similar to GB|AAH55637.1|3 LOC402831 protein 74 7e-12	Steroid hydroxylase for bile biosynthesis
Aa_BOS_33G03	0.60	0.06	gb|AAD34062.1| CGI-67 protein [Homo sapiens] 396 e-109	TC281312 homologue to UP|Q6PCB6 (Q6PCB6) LOC58489 protein (Fragment) 398 e-110	Peptidase
Aa_BOS_39A05	1.55	0.09	ref|NP_653355.1| calcium activated nucleotidase 1 [Rattus norvegicus] 54 3e-06	TC20399 similar to UP|Q8K4Y7 (Q8K4Y7) Apyrase , partial (54%) 58 4e-07	Ribonucleoside diphosphate catabolism Inhibition of blood coagulation
Aa_BOS_45C11	1.59	0.06	ref|YP_164025.1| NADH dehydrogenase subunit 2 [Anguilla rostrata] 144 9e-34	***** No hits found ******	Mitochondrial electron transport, NADH to ubiquinone
Aa_BOS_51C09	0.63	0.03	***** No hits found ******	TC69979 UP|Q7YXL7 (Q7YXL7) Glutathione S-transferase 115 2e-24	Glutathione metabolism
Aa_BOS_51D04	0.62	0.05	***** No hits found ******	TC69979 UP|Q7YXL7 (Q7YXL7) Glutathione S-transferase 115 2e-24	Glutathione metabolism
Aa_BOS_52E03	1.95	0.19	gb|AAD15625.1| lactate dehydrogenase [Anguilla rostrata] 68 3e-10	***** No hits found ******	Lactate metabolism
Aa_BOS_53C09	0.61	0.02	***** No hits found ******	TC69979 UP|Q7YXL7 (Q7YXL7) Glutathione S-transferase 115 2e-24	Glutathione metabolism
Aa_BOS_59C12	0.63	0.07	***** No hits found ******	TC69979 UP|Q7YXL7 s Glutathione S-transferase 115 2e-24	Glutathione metabolism
Aa_BOS_57E01	0.59	0.10	***** No hits found ******	TC69979 UP|Q7YXL7 (Q7YXL7) Glutathione S-transferase 115 2e-24	Glutathione metabolism

Table 4.18.f. Immune/stress response cluster. Mean fold-change (FC) and standard deviation (SD) of brain transcripts from the 7 day FW acclimated yellow eel group and the 5 month FW acclimated silver eel during forward and dye-swap experiments. Blastx and blastn results from NCBI database searches show homologies to known proteins and genes respectively.

Clone ID	FC	SD	Blastx	Blastn	Biological processes as identified by Gene Ontology
Aa_BOS_10F10	0.61	0.08	ref|NP_862671.1| aminoglycoside phosphotransferase 142 1e-32	***** No hits found ******	Response to antibiotic
Aa_BOS_27C04	1.82	0.30	gb|AAH54250.1| Xcirp2 protein [Xenopus laevis] 147 3e-34	TC91409 similar to UP|Q9DED4 (Q9DED4) Cold-inducible RNA binding protein 2 (Xcirp2 protein) 254 3e-66	Response to cold
Aa_BOS_28G03	1.66	0.22	gb|AAI02765.1| Microtubule-associated protein 396 e-109	TC90114 similar to UP|Q7ZXP1 (Q7ZXP1) Mapre2-A protein, Microtubule-associated protein 611 e-173	Cell proliferation Cellular defense Signal transduction
Aa_BOS_40G01	0.56	0.04	gb|AAL58575.1| invariant chain-like protein 14-1 [Oncorhynchus mykiss] 131 3e-29	TC78880 UP|Q8JFN5 (Q8JFN5) Invariant chain S25-7 (MHC class II) 68 4e-10	Association with major histocompatibility complex
Aa_BOS_60A02	1.77	0.14	ref|XP_854311.1| PREDICTED: similar to C-type lectin superfamily... 74 9e-12	***** No hits found ******	Immune response

Table 4.18.g. Transcription and post-translational modification cluster. Mean fold-change (FC) and standard deviation (SD) of brain transcripts from the 7 day FW acclimated yellow eel group and the 5 month FW acclimated silver eel during forward and dye-swap experiments. Blastx and blastn results from NCBI database searches show homologies to known proteins and genes respectively.

Clone ID	FC	SD	Blastx	Blastn	Biological processes as identified by Gene Ontology
Aa_BOS_02E06	1.53	0.14	ref|NP_956549.1| DNA methyltransferase 1 associated protein 1 96 8e-19	gi|33988721|gb|BC002855.2| Homo sapiens DNA methyltransferase 56.0 2e-04	Negative regulation of transcription
Aa_BOS_20H11	0.60	0.03	gb|AAH03896.2| Rpl17 protein [Mus musculus] 342 7e-93	TC86629 homologue to UP|Q80V08 (Q80V08) Ribosomal protein l17 (Fragment) 648 0.0	RNA binding
Aa_BOS_25B08	1.91	0.26	ref|NP_001026330.1| DEAH (Asp-Glu-Ala-His) box polypeptide 251 3e-65	TC267948 homologue to GB|AAH35974.1|23273556|BC035974 DHX15 protein (Homo sapiens) 293 4e-78	RNA splicing factor
Aa_BOS_31H01	1.87	0.22	gb|AAP20146.1| 40S ribosomal protein S2 [Pagrus major] 206 3e-52	TC3361 homologue to UP|Q6NWC3 (Q6NWC3) Zgc:85824, partial (97%) 492 e-138	Transcription
Aa_BOS_33G04	0.61	0.05	gb|AAH03896.2| Rpl17 protein [Mus musculus] 342 6e-93	TC86629 homologue to UP|Q80V08 (Q80V08) Ribosomal protein l17 (Fragment) 648 0.0	RNA binding
Aa_BOS_37F08	1.57	0.09	gb|AAS78677.1| transcriptional intermediary factor 1 delta 119 9e-26	TC282163 transcriptional intermediary factor 1 alpha; tripartite 52 2e-05	Negative regulation of transcription
Aa_BOS_39G11	0.46	0.05	gb|ABA95861.1| retrotransposon protein 34 4.7	TC87740 similar to GB|AAC51339.1|1888538|HSU89354 CREB-binding protein {Homo sapiens;} 56 2e-06	Positive regulation of transcription factor activity Transcription factor
Aa_BOS_42G09	1.70	0.24	gb|AAH10370.1| Tumor suppressor candidate 3, isoform b [Homo sapiens] 385 e-105 722 0.0	TC81556 homologue to GB|AAH10370.1|14714487|BC010370 tumor suppressor candidate 3, isoform b {Homo sapiens;}	Protein amino acid N-linked glycosylation via asparagine

Table 4.18.h. Other/no known function and failed sequencing clones. Mean fold-change (FC) and standard deviation (SD) of brain transcripts from the 7 day FW acclimated yellow eel group and the 5 month FW acclimated silver eel during forward and dye-swap experiments. Blastx and blastn results from NCBI database searches show homologies to known proteins and genes respectively.

Clone ID	FC	SD	Blastx	Blastn	Biological processes as identified by Gene Ontology
Aa_BOS_31F05	0.64	0.10	ref|NP_080003.1| kelch-like 10 [Mus musculus] 197 3e-49	TC72471 similar to UP|KH10_MOUSE (Q9D5V2) Kelch-like protein 10 94 7e-18	Striated muscle contraction
Aa_BOS_13E10	1.76	0.14	gb|AAH59675.1| Wu:fd42g01 protein [Danio rerio] 458 e-128	TC72100 similar to UP|Q91YM1 (Q91YM1) AW549877 protein, partial 613 e-174	No known function
Aa_BOS_25F06	1.75	0.05	***** No hits found ****** 52 2e-05	TC89335 similar to UP|Q8NH31 (Q8NH31) Seven transmembrane helix protein	Non known function
Aa_BOS_28H06	1.59	0.15	gb|AAH44166.1| Male sterility domain containing 2 [Danio rerio] 444 e-123	gi|7024432|emb|AJ272073.1|TMA272073 Torpedo marmorata mRNA for male sterility protein 2-like protein... 230 6e-57	No known function
Aa_BOS_49F03	1.62	0.09	***** No hits found ******	***** No hits found ******	
Aa_BOS_53A11	1.67	0.13	***** No hits found ******	***** No hits found ******	
Aa_BOS_53B11	1.76	0.32	***** No hits found ******	***** No hits found ******	
Aa_BOS_55E11	1.97	0.53	***** No hits found ******	***** No hits found ******	
Aa_BOS_58D11	0.63	0.05	Sequencing failure	Sequencing failure	
Aa_BOS_19C09	1.79	0.41	Sequencing failure	Sequencing failure	
Aa_BOS_31H06	0.50	0.05	Sequencing failure	Sequencing failure	
Aa_BOS_19G02	0.64	0.04	Sequencing failure	Sequencing failure	

4.19 Brain microarray results: Comparison of brain expression profiles between 2 day freshwater acclimated and 2 day seawater acclimated silver eels

Fluorescently labelled cDNAs from brain total RNA derived from the 2 day FW acclimated silver eel group and the 2 day SW acclimated silver eel group were co-hybridised to a brain microarray. Subsequently the experiment was repeated in dye-swap in which the exact procedure was repeated except the cDNA labels Cy3 and Cy5 were reversed Sufficient RNA was available for these samples and as such the RNA was not amplified. For both the forward and dye-swap experiments the laser output: PMT gain ratios were 73 %: 73% for Cy3 and 75 %: 75 % for Cy5. Data was processed using the MADSCAN method in the same manner as the yellow-silver experiment described previously. Unlike the yellow:silver data analysis described in section 4.18, only one analysis was performed only at the laser/ PMT gain settings stated. Background was subtracted from foreground spot intensities and non-variant genes were again selected by iterative rank invariant method algorithm. A *lowess* fitness model was applied to the selected genes and all data were normalised to the model. Data transformations following processing and normalisation are shown in the M versus A plots (Figures 4.19.a and 4.19.b).

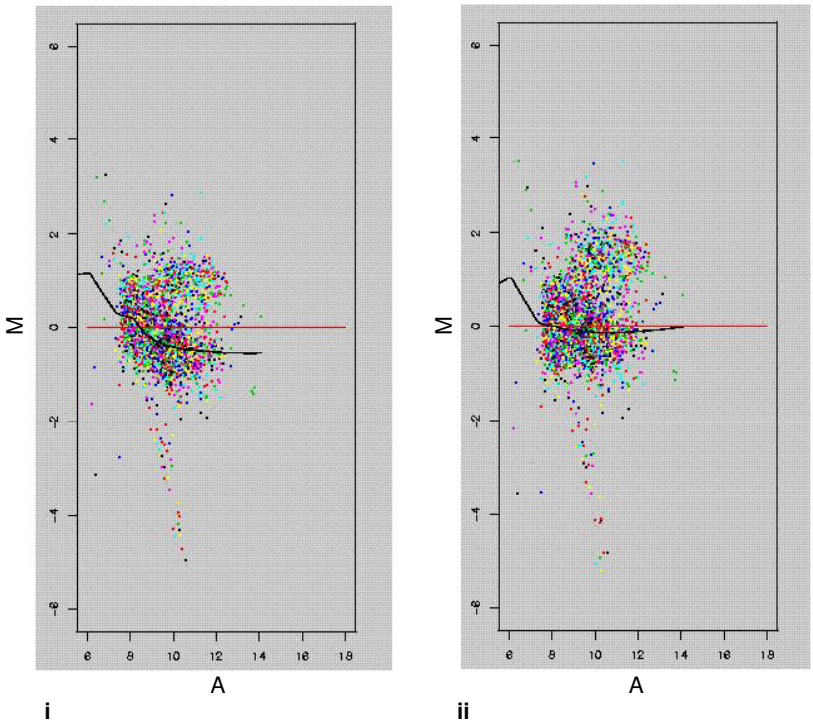

Figure 4.19.a. MADSCAN generated M vs. A plots from (i) before and (ii) after data normalisation (forward experiment, 2 day FW versus 2 day SW acclimated silver eel groups, brain). The curves are *lowess* fitness curves built on the set of non-variant genes to which the rest of the data is normalised. The different coloured spots correspond to the 48 sub-arrays printed by different print-tips. *M* is the $\log_2$ intensity ratio *= log_2 (Cy3/Cy5)* and A is the mean $\log_2$ spot intensity = *(log_2 Cy5 + log_2 Cy3) / 2*

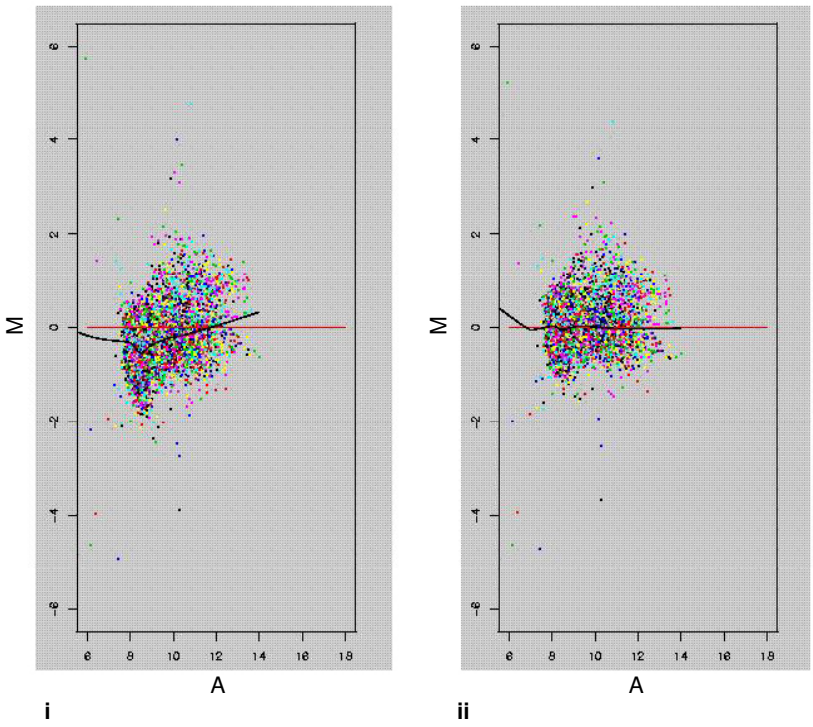

Figure 4.19.b. MADSCAN generated M vs. A plots from (i) before and (ii) after data processing (dye-swap experiment, 2 day FW versus 2 day SW acclimated silver eel groups, brain). The curves are *lowess* fitness curves built on the set of non-variant genes to which the rest of the data is normalised. The different coloured spots correspond to the 48 sub-arrays printed by different print-tips. *M* is the $\log_2$ intensity ratio *= $\log_2$ (Cy3/Cy5)* and A is the mean $\log_2$ spot intensity = *($\log_2$ Cy5 + $\log_2$ Cy3) / 2*

Data were scaled to median absolute deviation and geometric means of the forward and dye-swap experiments and visualised by whisker plots (Figure 4.19.c).

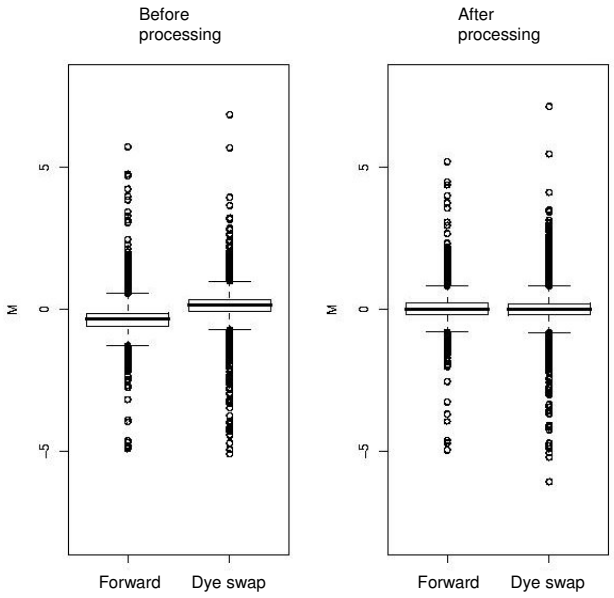

Figure 4.19.c. Whisker plots before and after data normalisation (2 day FW versus 2 day SW acclimated silver eel groups, brain).

Density plots of the intensity ratios of the normalised data show a distribution close to normal (Figure 4.19.d). There is a slight bias (skew = 1.59) in the distribution indicating more genes were being up-regulated following FW to SW transfer.

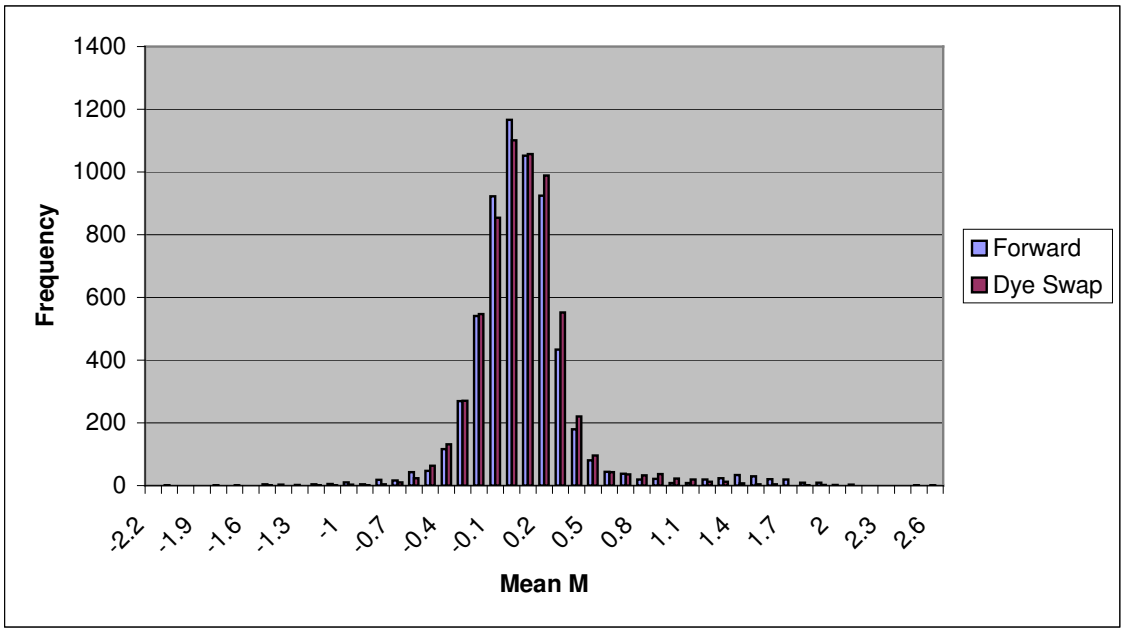

Figure 4.19.d. Frequency distribution showing near normal distribution of mean intensity ratios (M) of replicate spots following data normalisation (2 day FW versus 2 day SW acclimated silver eel groups, brain).

Genes (42) which showed consistent up or down regulation were selected for further analysis. Half (20) of these clones had also been previously identified from the 2 day FW acclimated yellow eel brain versus 5 month FW acclimated silver eel brain experiment (section 4.18). All genes identified were sequenced, trimmed for vector and adapter sequences using trace2dbest and compared to current NCBI protein and EST databases using blastx and blastn (Table 4.19.a). As with the Yellow: Silver analysis (Section 4.18), clones were then clustered according to their known biological function as deterimined from the Gene Ontology database (Ashburner, 2000). The vast majority of clones could be placed into the following clusters; signal transduction (Table 4.19.a), development and morphogenesis (Table 4.19.b), membrane and structure (Table 4.19.c), metabolism (Table 4.19.d), and transcription and post-translational modification (Table 4.19.e). Some clones

could not be placed into any of these clusters, or they have no known function or the sequencing failed (Table 4.19.f).

Table 4.19.a. Signal transduction cluster. Mean fold-change (FC) and standard deviation (SD) of brain transcripts from the 2 day FW and 2 day SW acclimated eel groups during forward and dye-swap experiments. Blastx and blastn results from NCBI database searches show homologies to known proteins and genes respectively.

Clone ID	FC	SD	Blastx	Blastn	Biological processes as identified by Gene Ontology
Aa_BOS_17G10	2.27	0.37	gb|AAA73877.1| thyroid hormone receptor interactor TRIP6 52 2e-05	TC291100 similar to UP|Q8UW12 (Q8UW12) Thyroid receptor interactor 40 0.091	Regulation of transcription, DNA dependent Electron transport Focal adhesion formation Positive regulation of cell migration Release of cytoplasmic sequestered NF-kappaB
Aa_BOS_21C08	2.50	0.81	emb|CAA48902.1| prolactin-precursor [Anguilla anguilla] >gi|4175... 381 e-104	TC80284 UP|PRL_ONCMY (P21993) Prolactin precursor (PRL), complete 105 2e-21	Hormonal signalling
Aa_BOS_22F09	2.60	0.04	dbj|BAE72666.1| bHLH protein DEC1 [Danio rerio] >gi|47086679|ref... 233 4e-60	TC94256 similar to UP|BHB2_MOUSE (O35185) Class B basic helix-loop helix protein 2...228 2e-58	Integrin-mediated signalling pathway Negative regulation of cell adhesion
Aa_BOS_35D04	1.99	0.55	gb|AAH64229.1| DnaJ (Hsp40) homolog, subfamily C, member 9 [Xeno... 241 3e-62	gi|109502119|ref|XM_001064040.1| Rattus norvegicus DnaJ (Hsp40) homolog, subfamily 52.0 0.003	Small GTPase mediated signal transduction
Aa_BOS_45C05	2.73	0.59	gb|AAH59577.1| Secretogranin III [Danio rerio] >gi|41152165|ref|... 133 9e-30	TC292724 UP|Q6PBU8 (Q6PBU8) Secretogranin III, complete 165 2e-39	Intercellular trafficking of storage components during granule maturation Secretion regulation

Table 4.19.b. Development and morphogenesis cluster. Mean fold-change (FC) and standard deviation (SD) of brain transcripts from the 2 day FW and 2 day SW acclimated eel groups during forward and dye-swap experiments. Blastx and blastn results from NCBI database searches show homologies to known proteins and genes respectively.

Clone ID	FC	SD	Blastx	Blastn	Biological processes
Aa_BOS_02H05	2.44	0.16	gb|AAT64101.1| reticulon 4-N [Takifugu rubripes] >gi|42601268|tp... 74 4e-12	TC86638 UP|Q6IEJ1 (Q6IEJ1) RTN4-M, complete 88 4e-16	Angiogenesis Negative regulation of axon extension Nervous system development Regulation of cell migration
Aa_BOS_03C09	2.73	0.84	gb|AAH65983.1| Vangl2 protein [Danio rerio] 76 1e-12	TC268919 Vangl2 protein [Danio rerio] 785 0.0	Cell morphogenesis Cell migration in hindbrain Convergent extension involved in gastrulation Establishment of cell polarity Negative regulation of frizzled signalling pathway Integral membrane protein Wnt signalling pathway regulation
Aa_BOS_15E12	2.08	0.13	ref|XP_696568.1| PREDICTED: similar to cerebellin 1 precursor pr... 91 6e-17	TC285223 similar to UP|CBN2_HUMAN (Q8IUK8) Cerebellin 2 precurso... 76 2e-12	Nervous system development Synaptic transmission
Aa_BOS_30C09	2.62	0.44	ref|NP_998388.1| myristoylated alanine-rich C kinase substrate 2... 66 2e-09	TC14418 weakly similar to UP|AAH66915 (AAH66915) MARCKS-like protein, Myristoylated alanine-rich (Kinase?)... 101 3e-20	Cell motility
Aa_BOS_17G10	2.27	0.37	gb|AAA73877.1| thyroid hormone receptor interactor TRIP6 52 2e-05	TC291100 similar to UP|Q8UW12 (Q8UW12) Thyroid receptor interactor 40 0.091	Regulation of transcription, DNA dependent Electron transport Focal adhesion formation Positive regulation of cell migration Release of cytoplasmic sequestered NF-kappaB
Aa_BOS_22F09	2.60	0.04	dbj|BAE72666.1| bHLH protein DEC1 [Danio rerio] >gi|47086679|ref... 233 4e-60	TC94256 similar to UP|BHB2_MOUSE (O35185) Class B basic helix-loop helix protein 2...228 2e-58	Integrin-mediated signalling pathway Negative regulation of cell adhesion
Aa_BOS_30E04	2.19	0.25	dbj|BAA90775.1| type II brain 4.1 minor isoform [Rattus norvegicus] 248 2e-64	CK025783 similar to SP|Q9WV92|E4L3 Band 4.1-like protein 3 (4.1B) (Differentially expressed inadenocarcinoma of the lung protein 1), ... 159 1e-37	Negative regulation of cell proliferation
Aa_BOS_35H07	0.65	0.18	sp|Q5XHG6|TS31A_XENLA Tetraspanin-31 A (Tspan-31 A) (Sarcoma amplified sequence) 268 1e-70	TC280466 UP|Q6TGU5 (Q6TGU5) Sarcoma amplified sequence, complete 174 2e-42	Positive regulation of cell proliferation
Aa_BOS_37H03	2.15	0.30	gb|AAH26335.1| Coronin, actin binding protein, 2B [Homo sapiens] 307 3e-82	TC82999 similar to UP|CO2B_HUMAN (Q9UQ03) Coronin-2B 464 e-129	Actin cytoskeleton organization and biogenesis

Table 4.19.c. Membrane and structure cluster. Mean fold-change (FC) and standard deviation (SD) of brain transcripts from the 2 day FW and 2 day SW acclimated eel groups during forward and dye-swap experiments. Blastx and blastn results from NCBI database searches show homologies to known proteins and genes respectively.

Clone ID	FC	SD	Blastx	Blastn	Biological processes
Aa_BOS_01G06	2.94	0.04	gb|AAH62826.1| Tubulin, alpha 8 like 2 [Danio rerio] 380 e-104	TC268704 UP|Q6TNP4 (Q6TNP4) Tubulin, alpha 4, complete 591 e-168	Cytoskeleton
Aa_BOS_29F05	2.67	0.06	gb|AAL00466.1| Nucleobase:cation symporter for xanthine [Strepto... 64 3e-09	gi|15903705|ref|NP_359255.1| Nucleobase:cation symporter for xanthine [Streptococcus pneumoniae R6] 64.3 4e-09	Xanthine symport
Aa_BOS_09E04	2.42	0.64	gb|AAR84618.1| beta actin [Acanthopagrus schlegelii] 427 e-118	TC290348 UP|ACTB_CTEID (P83751) Actin, cytoplasmic 1 (Beta-actin) 959 0.0	Cytoskeleton Muscle contraction Cell motility Cytokinesis Cell signalling Organelle transport
Aa_BOS_37H03	2.15	0.30	gb|AAH26335.1| Coronin, actin binding protein, 2B [Homo sapiens] 307 3e-82	TC82999 similar to UP|CO2B_HUMAN (Q9UQ03) Coronin-2B 464 e-129	Actin cytoskeleton organization and biogenesis
Aa_BOS_51H06	0.71	0.09	*** No hits found ***	TC79092 similar to UP|SEP3_MOUSE (Q9Z1S5) Neuronal-specific septin 123 8e-27	Cytokinesis

Table 4.19.d. Metabolism cluster. Mean fold-change (FC) and standard deviation (SD) of brain transcripts from the 2 day FW and 2 day SW acclimated eel groups during forward and dye-swap experiments. Blastx and blastn results from NCBI database searches show homologies to known proteins and genes respectively.

Clone ID	FC	SD	Blastx	Blastn	Biological processes
Aa_BOS_06H03	2.54	0.01	emb|CAC83782.1| phosphoglucose isomerase-2 [Danio rerio] 375 e-103	TC291056 UP|Q7ZU30 (Q7ZU30) Glucose phosphate isomerase a, complete 163 7e-39	Glucose metabolism
Aa_BOS_17F01	2.50	0.17	gb|AAH59511.1| Enolase 1, (alpha) [Danio rerio] 419 e-116	TC79739 homologue to UP|Q6IQP5 (Q6IQP5) Enolase 1, (Alpha) 652 0.0	Glycolysis
Aa_BOS_32F12	0.57	0.11	*** No hits found ***	gi|56565288|dbj|AP00 7233.1| Anguilla anguilla mitochondrial DNA, 1376 0.0	Mitochondria synthesis
Aa_BOS_36A02	3.01	0.74	ref|XP_694230.1| PREDICTED: similar to Cytochrome P450 27, mitoc... 390 e-107	CD599042 weakly similar to GB|AAH55637.1|3 LOC402831 protein {Danio rerio} 74 7e-12	Steroid hydroxylase for bile biosynthesis
Aa_BOS_38E03	2.35	0.14	gb|AAH66694.1| Ubiquitin specific protease 5 [Danio rerio] 406 e-112	gi|67514530|ref|NM_2 14755.2| Danio rerio ubiquitin specific protease 95.6 2e-16	Ubiquitin specific proteolytic cleavage mRNA catabolism
Aa_BOS_59C12	0.71	0.02	*** No hits found ***	TC69979 UP|Q7YXL7 (Q7YXL7) Glutathione S-transferase (Fragment) 115 2e-24	Glutathione metabolism
Aa_BOS_38G02	2.52	0.83	*** No hits found ***	>gi|75811931|gb|DQ0 19116.1| Pseudomys australis voucher ABTC35951 cytochrome c oxidase subunit 44.1 0.66	Electron transport

Table 4.19.e. Transcription and post-translational modification. Mean fold-change (FC) and standard deviation (SD) of brain transcripts from the 2 day FW and 2 day SW acclimated eel groups during forward and dye-swap experiments. Blastx and blastn results from NCBI database searches show homologies to known proteins and genes respectively.

Clone ID	FC	SD	Blastx	Blastn	Biological processes
Aa_BOS_02E06	3.025	0.13435	ref|NP_956549.1| DNA methyltransferase 1 associated protein 1 [Danio rerio] 96 8e-19	gi|33988721|gb|BC002855.2| Homo sapiens DNA methyltransferase 56.0 2e-04	Negative regulation of transcription
Aa_BOS_17G10	2.27	0.37	gb|AAA73877.1| thyroid hormone receptor interactor TRIP6 52 2e-05	TC291100 similar to UP|Q8UW12 (Q8UW12) Thyroid receptor interactor 40 0.091	Regulation of transcription, DNA dependent Electron transport Focal adhesion formation Positive regulation of cell migration Release of cytoplasmic sequestered NF-kappaB
Aa_BOS_37F08	2.94	1.12	gb|AAS78677.1| transcriptional intermediary factor 1 delta short 119 9e-26	TC282163 transcriptional intermediary factor 1 alpha; tripartite 52 2e-05	Negative regulation of transcription

Table 4.19.f. Other/no known function and failed sequencing clones. . Mean fold-change (FC) and standard deviation (SD) of brain transcripts from the 2 day FW and 2 day SW acclimated eel groups during forward and dye-swap experiments. Blastx and blastn results from NCBI database searches show homologies to known proteins and genes respectively.

Clone ID	FC	SD	Blastx	Blastn	Biological processes
Aa_BOS_60A02	2.37	0.38	ref|XP_854311.1| PREDICTED: similar to C-type lectin superfamily... 74 9e-12	*** No hits found ***	Immune response
Aa_BOS_13E10	3.09	0.42	gb|AAH59675.1| Wu:fd42g01 protein [Danio rerio] 458 e-128	TC72100 similar to UP|Q91YM1 (Q91YM1) AW549877 protein, partial ... 613 e-174	No known function
Aa_BOS_25F06	2.15	0.45	*** No hits found ***	TC89335 similar to UP|Q8NH31 (Q8NH31) Seven transmembrane helix ... 52 2e-05	No known function
Aa_BOS_28H06	1.95	0.73	gb|AAH44166.1| Male sterility domain containing 2 [Danio rerio] ... 444 e-123	gi|7024432|emb|AJ272073.1|TMA272073 Torpedo marmorata mRNA for male sterility protein 2-like protein... 230 6e-57	No known function
Aa_BOS_33A03	2.48	0.53	*** No hits found ***	*** No hits found ***	
Aa_BOS_46G06	2.70	0.91	*** No hits found ***	*** No hits found ***	
Aa_BOS_49F03	2.50	0.47	*** No hits found ***	*** No hits found ***	
Aa_BOS_53A11	2.66	0.89	*** No hits found ***	*** No hits found ***	
Aa_BOS_58D11	2.08	0.47	Sequencing failure	Sequencing failure	
Aa_BOS_01C07	2.47	0.79	Sequencing failed	Sequencing failed	
Aa_BOS_20E06	2.54	0.82	Sequencing failed	Sequencing failed	
Aa_BOS_31H06	0.66	0.08	Sequencing failed	Sequencing failed	

4.20 SSH multi-tissue array results

In the initial SSH array experiments, labelled cDNAs derived from pools of 6 FW acclimated eel samples for each tissue and time point were compared with the equivalent labelled, time and tissue-matched cDNAs made from RNA pooled from 6 SW acclimated eels. Maximum differences in gene expression were mainly found between the long-term acclimated, 5-month, FW and SW groups. The inter-fish variability was investigated in the 5 month FW/FW and FW/SW acclimated eel groups using reference design methodology (Churchill, 2002). Labelled cDNAs were prepared from the gill and intestine of 6 individual FW/SW transferred fish and then hybridised along with a common (for each tissue) reference obtained from a pool of 6 FW/FW fish RNAs.

4.21 Online Holdings Database

In collaboration with the NERC Environmental Bioinformatics Centre, a database was created outlining the holdings generated during the course of the project. The online holdings comprise details of: tissue samples, meta-data, RNA samples, clone sets, sequence data, microarrays and publications. The database can be viewed at;

http://envgen.nox.ac.uk/cgi-bin/view_dataset_secure.cgi?dsname=000011

4.22 Validation of the brain microarray results

Six genes were selected for further analysis to both validate the microarray results and to learn more about their involvement in biological process (Table 4.22.a). Using a gene ontology database (The Gene Ontology, http://www.geneontology.org) their general biological roles were elucidated.

Microarray results were validated using real-time quantitative PCR (QPCR) to quantify two genes identified during the yellow-silver experiment and one from the FW-SW acclimation experiment. This method was applied to each fish in all experimental groups, allowing inter-fish variability to be examined. Six genes were initially selected as candidates for real-time quantitative PCR (QPCR) validation of the yellow FW acclimated eel versus silver FW acclimated eel experiment using the brain microarray (Table 4.22.a). These genes were selected based on the quality of sequence obtained, and whether the putative gene identity suggested involvement in important developmental or osmoregulatory pathways.In addition, prolactin was chosen to validate the silver eel 2 day FW versus SW experiment. Prolactin was selected as its expression changed significantly in this instance and had also been shown to vary significantly in other tissues as identified by the SSH multi-tissue array and thus setting up this quantitative PCR experiment would expedite results elsewhere in the project.

Table 4.22.a. Gene candidates selected for validation of the brain array by QPCR. Known functions presented are from The Gene Ontology.

Clone ID	Analysis 1 (fold change from yellow to silver)		Analysis 2 (fold change from yellow to silver)		Putative identity as determined by homology to known genes using blast x and blastn	Known functions from gene ontology database
	Forward	Dye-swap	Forward	Dye-swap		
01e01_Aa_BOS_01C01	2.71	1.54	1.60	2.35	Vaccinia related kinase 3 protein (VRK3)	Regulation of extra-cellular signal regulated kinases via MAP kinase pathway. Phosphorylation of transcription factors.
01e09_Aa_BOS_01C05	2.25	1.28	1.66	1.53	Tyrosine 3-monooxygenase/ tryptophan 5-monooxygenase activation protein, β polypeptide (14-3-3)	Ubiquitous phosphoprotein partner regulating many pathways including apoptosis, cell proliferation and salinity adaptation in teleost gill
15a18_Aa_BOS_58A09	0.62	0.65	0.60	0.61	C-type natriuretic peptide	Vasorelaxant cGMP stimulant
08e23_Aa_BOS_29C12	0.46	0.53	0.48	0.55	Contactin associated protein	Part of the neurexin family Cell adhesion Contain EGF repeats
10n14_Aa_BOS_40G07	2.06	1.40	1.57	1.95	Kainate receptor alpha subunit	Ligand gated ion channel
12e09_Aa_BOS_45C05	1.97	1.69	2.01	2.01	Secretogranin III	Binds to secretory granule membrane and targets chromogranin A to secretory granules in pituitary and pancreatic cells

4.23 Real Time Quantitative PCR (QPCR) Assays

QPCR enables accurate quantification of mRNA transcription levels from small biological samples. The QPCR assay uses the intercalating dye SYBR Green to detect the DNA created during each round of PCR. In solution, the unbound dye fluoresces at a very low level but in the presence of double stranded DNA it binds the minor groove of DNA and its fluorescence is greatly elevated. This method of DNA quantification is simple and negates the need for expensive, sequence specific, fluorescently labelled probes. Its accuracy and sensitivity have lead to it being the most emerging method for mRNA transcription analysis (Bustin, 2002) and as a consequence was used in this instance as the amounts of starting material (RNA) required are much lower than for other methods such as Northern blotting. Using QPCR allows quantification of the expression level of a gene in relation to an endogenous reference gene, which allows different samples to be compared directly. The reference gene is usually a “housekeeping” gene whose transcription is not regulated or influenced by the experimental procedure under examination (e.g., salinity transfer) and is used to normalise for differing amounts of amplifiable material available between samples.

mRNA is first converted into cDNA, by reverse transcription, which is then used as a template for two separate PCR amplifications of the gene of interest and the endogenous reference gene. Included in the PCR mixture is a reporter dye which fluoresces when bound to double stranded DNA. The amount of target and control DNA synthesised during the PCR is quantified at the end of each PCR cycle by measuring the fluorescence emitted by the reporter dye which represents the DNA concentration. The fluorescence from all the samples is then plotted against the cycle number and a threshold is set within the exponential phase of the reaction (figure 4.23.a). This threshold is used to determine the Ct value for each sample. The Ct value is the cycle number at which the fluorescence emitted from the reaction crosses the threshold and it is used for the quantification calculations of target and reference genes.

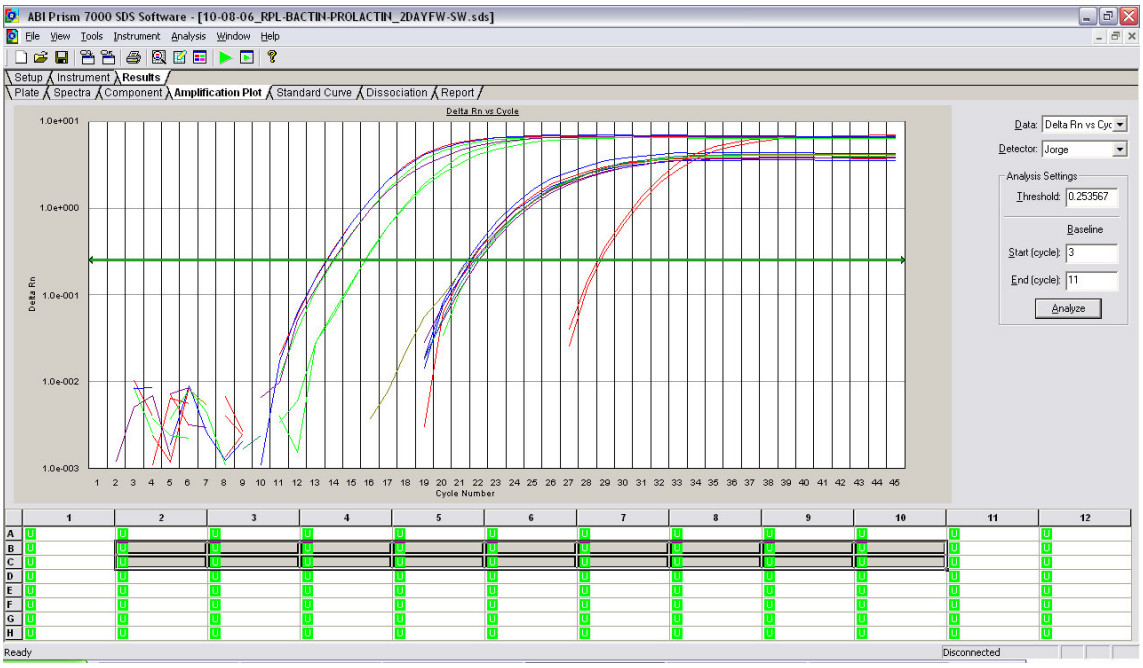

Figure 4.23.a. Screenshot from the QPCR analysis software (ABI Prism 7000 SDS, Applied Biosciences, Warrington, UK). Plots indicate the fluorescent signal emitted from each sample in each successive round of amplification which is equivalent to the DNA concentration. The green horizontal line represents the threshold which the user sets within the exponential phase of the reaction, the Ct values for each sample are taken at the point the fluorescence crosses this threshold.

Non-specific detection using SYBR Green was chosen as the initial set-up of the experiment was simpler and cheaper than specific detection systems which require the design and production of expensive fluorescently labelled probes (e.g., TaqMan QPCR). SYBR Green is an asymmetrical cyanine intercalating dye incorporated into the PCR reaction which binds any double stranded DNA generated during PCR and emits enhanced fluorescence (Ishiguro et al., 1995). Although any double stranded DNA created during PCR will give a fluorescent signal, well designed primers should only give a single product and this can be verified by gel electrophoresis or more specifically by DNA dissociation curve analysis (Ririe et al., 1997). The DNA dissociation curve is generated after the QPCR reaction has taken place. The spent QPCR reaction is slowly heated from 60 ºC to 95 ºC and the fluorescence emitted is measured every 0.35 ºC. The derivative of the fluorescence (d(F)/dt) is then plotted against temperature, the derivative of the fluorescence being used rather than the raw fluorescence data as it allows easier visual analysis. Only

primer sets which prime the synthesis of single products can be used for the SYBR green QPCR assay, as indicated by a single peak (figure 4.23.b).

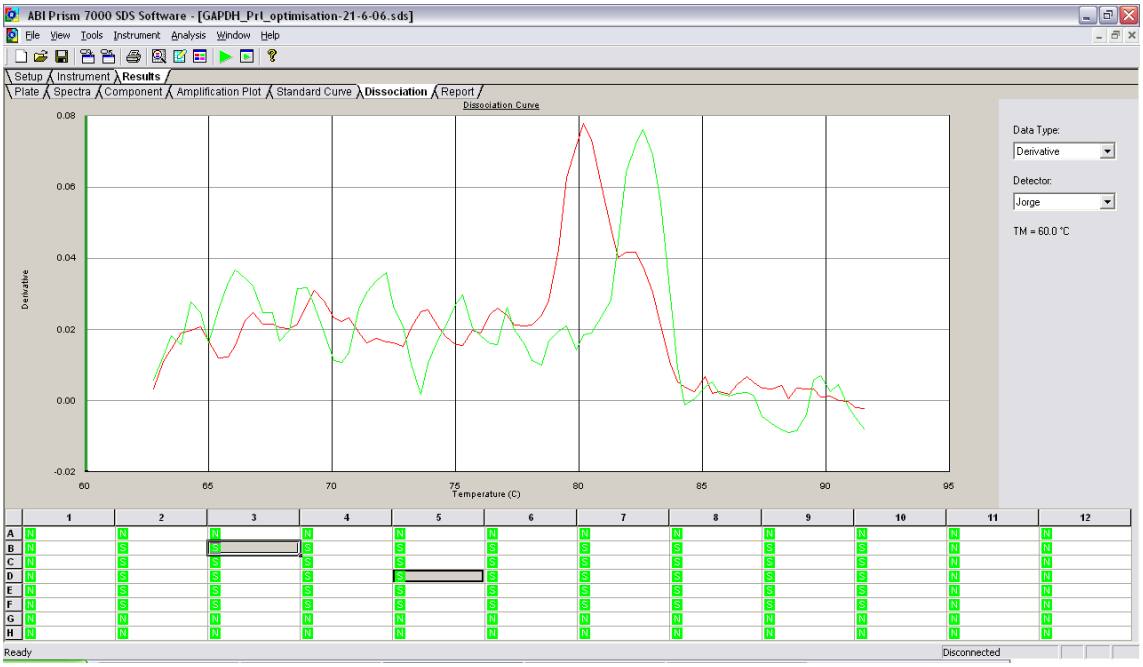

Figure 4.23.b. Screenshot taken from ABI Prism 7000 SDS software showing two dissociation plots. The green line, representing the dissociation plot for the prolactin amplicons, has a well-defined single peak indicating only one product has been formed. The red line, representing the dissociation of product synthesised with the first set of GAPDH primers, exhibits two peaks suggesting that two different products have been made during the QPCR reaction and that these primers are not suitable for use.

The delta-delta Ct ($2^{-\Delta\Delta Ct}$) method (Livak and Schmittgen, 2001) was chosen to analyse the QPCR data. Other methods available for analysing QPCR results such as the Relative Expression Software Tool (REST) (Pfaffl, 2001; Pfaffl et al., 2002) or the Data Analysis for Real-Time PCR (DART-PCR) method (Peirson et al., 2003) were not considered appropriate for use in this instance. Both the REST and DART methods calculate the mean Ct for the target and reference genes for each of the two experimental groups being examined and subsequently the expression of the target relative to the reference gene is calculated. These approaches require that all initial RNA samples under examination are at the same concentration and assumes that all reverse transcriptase reactions are equally efficient in order that the template cDNA is the same between the two experimental groups. If these assumptions do not hold true then large variability can be introduced into the results, which can

effectively mask subtle changes in expression. The advantage of using the REST or DART methods is that they can accommodate differences in efficiencies of the target and control reactions whilst the $2^{-\Delta\Delta Ct}$ method demands that both reaction types are equally efficient. The $2^{-\Delta\Delta Ct}$ method calculates the target gene expression relative to a reference gene for each individual fish. Mean averages of relative expression of the target gene in the two experimental groups are taken and compared. The key difference between the REST/DART and the $2^{-\Delta\Delta Ct}$ method is the point at which the mean expression values are taken. Thus the $2^{-\Delta\Delta Ct}$ method allows for variability in the starting RNA concentrations and between reverse transcription reactions as each individual sample is normalised for concentration by its own internal control. The amount of RNA available after the extensive work optimising the cDNA libraries and performing the microarray hybridisations was severely limited and as such it was decided that the $2^{-\Delta\Delta Ct}$ method would be used to avoid wasting RNA during the quantifications.

To understand the $2^{-\Delta\Delta Ct}$ method it is useful view the series of equations which define it. Starting with the exponential amplification of the target DNA during QPCR which can be described by the equation;

$$X_n = X_0 \times \left(1 + E_X\right)^n \qquad \textbf{i}$$

; where X_n is the number of target molecules at cycle n, X_0 is the starting number of target molecules and E_X is the efficiency of the target amplification reaction.

The threshold cycle (Ct) is the cycle number at which the amount of synthesised target reaches the threshold set by the user and is described as;

$$X_T = X_0 \times \left(1 + E_X\right)^{Ct_X} = K_X \qquad \textbf{ii}$$

; where X_T is the threshold number of target gene molecules, X_0 is the starting number of target gene molecules, Ct_X is the cycle number required for the target gene amplification to reach the threshold value and K_X is a constant. The equivalent equation for the reference gene is;

$$R_T = R_0 \times \left(1 + E_R\right)^{Ct_R} = K_R \qquad \textbf{iii}$$

; where R_T is the threshold number of reference gene molecules, R_0 is the starting number of reference gene molecules, Ct_R is the cycle number required for the reference gene amplification to reach the threshold value, E_R is the efficiency of the reference gene amplification reaction and K_R is a constant. The number of target molecules relative to reference molecules at the threshold can be calculated by dividing X_T by R_T;

$$\frac{X_T}{R_T} = \frac{X_0 \times \left(1 + E_X\right)^{Ct_X}}{R_0 \times \left(1 + E_R\right)^{Ct_R}} = \frac{K_X}{K_R} = K \qquad \textbf{iv}$$

Assuming the efficiencies of target gene and reference gene amplification are equal, equation **iv** can be simplified;

$$\text{If} \quad E_X = E_R = E, \qquad \textbf{v}$$

$$\text{then} \quad \frac{X_0}{R_0} \times (1 + E)^{Ct_X - Ct_R} = K. \qquad \textbf{vi}$$

X_0/R_0 represents the number of starting target gene molecules normalised to the number of starting reference gene molecules (X_N) and Ct_X-Ct_R is the difference in threshold cycles between target and reference (ΔCt). Thus, equation **vi** can be further simplified to;

$$X_N \times (1+E)^{\Delta Ct} = K, \qquad \textbf{vii}$$

and then rearranged to give;

$$X_N = K \times (1+E)^{-\Delta Ct}. \qquad \textbf{viii}$$

Equation **viii** can then be used to find the number of normalised target gene molecules in an experimental sample ($X_{N,es}$) relative to a control sample ($X_{N,cs}$);

$$\frac{X_{N,es}}{X_{N,cs}} = \frac{K \times (1+E)^{-\Delta Ct,es}}{K \times (1+E)^{-\Delta Ct,cs}} = (1+E)^{-(\Delta Ct_{es} - \Delta Ct_{cs})}. \qquad \textbf{ix}$$

The reaction efficiency (E) for an optimised PCR amplification of short amplicons (<150 bp) is close to one (*i.e.*, the amount of DNA in the reaction doubles every cycle). The expression -(ΔCt_{es}- ΔCt_{cs}) is shortened to –$\Delta\Delta Ct$. Thus, the amount of normalised target gene in an experimental sample relative to a control sample is expressed as;

$$amount\ of\ normalised\ target = 2^{-\Delta\Delta Ct}. \qquad \textbf{x}$$

4.24 QPCR Primer Design and Optimisation

The binding of SYBR green to double stranded DNA is not sequence-specific and as such, stringent controls were used to ensure only the desired DNA amplicons were amplified as non-specifically amplified DNA would have invalidated results. To ensure only desired DNA was being amplified, exon spanning primers were made for each control and target gene so only cDNA made from mRNA could be amplified. Additionally the amplicons were examined crudely by agarose gel electrophoresis and also by the more stringent method of analysing the dissociation plot of derivative fluorescence values of target and control amplicons. Genes to be analysed with QPCR were selected because of significant changes in expression shown by the microarray data and also because of sequence homology to known genes. The genes analysed and the QPCR primers are shown below (Table 4.24.a).

Table 4.24.a. Genes analysed with respective primers used for QPCR analysis. Primers spanning splice sites are shown in mixed black and red text.

Gene	Forward Primer	Reverse primer
Prolactin	ACGACCTGGACACCCATTTC	GATTCCGGCACTCTCAAAGC
VRK3	TGCCGAATACTGGACGTGC	GCAGTATCCCGCCAGGTACA
14_3_3	AGAAGACCGAGGGCAACGA	AGGAGTCCCAGCACGTCCT
Beta Actin	GGATCCGGTATGTGCAAAGC	CATCACACCCTGATGTCTGGG
RPL-P0	TGAAGTCTTGAGCGATGTGCA	GGAGAAGGGCGAGATGTTCAG
GAPDH1	GGAGGTGCCAAGAGGGTCAT	GCAGGAGGCATTGCTGACA
GAPDH2	CAATGCCTCCTGCACAACC	AACGGTGGTCATGAGCGC
18s rRNA	ACGGCCGGTACAGTGAAACT	CGCTCGTCGGCATGTATTAG

In order to attain reaction efficiencies close to 1 for target and reference gene primer sets, which is an assumption for the $2^{-\Delta\Delta Ct}$ method to hold true, stringent experimental design was necessary which included rigorous primer design and subsequent optimisation of reactions. The primers were designed using Primer Express 2.0 (Applied Biosystems, UK) with an annealing temperature (Tm) between 58 ºC and 60 ºC and an amplicon size ranging from 95 bp to 110 bp. The narrow Tm range allows standard cycling parameters to be used for all primers. A longer DNA

fragment will bind more molecules of dye and give a greater signal than a short fragment, thus all amplicons were kept within 15 bp of each other. There is a possibility that the isolated mRNA could contain traces of genomic DNA. To ensure that only cDNA complementary to intronless mRNA is amplified during QPCR, one primer from each pair was designed to span a splice site where an intron would have been present in the genomic DNA. This primer cannot bind to any contaminating genomic DNA, which would contain introns, and is therefore not amplified. The exon-intron boundaries were determined using a combination of Clustal X Multiple Sequence Alignment Program (version 1.8, June 1999) and Spidey (http://www.ncbi.nlm.nih.gov/spidey/) to align *A. anguilla* cDNA sequences with the corresponding cDNA and genomic DNA sequence from *D. rerio* or *T. rubripes*. cDNA sequences for *A. anguilla* were obtained from NCBI (http://www.ncbi.nlm.nih.gov/) or from the clones sequenced from the cDNA libraries used to make the microarrays. cDNA and genomic DNA information for *D. rerio* and *T. rubripes* was taken from the Ensembl database (Hubbard et al., 2005).

An example of the process of selecting a pair of primers, where one primer spans an intron, is shown below using the sequence of an eel clone (01e09_Aa_BOS_01C05) which is homologous to *D. rerio* tyrosine 3-mono-oxygenase/tryptophan 5-mono-oxygenase activation protein, beta polypeptide (14-3-3). Firstly, Primer Express 2.0 was used to generate a range of potential optimal primer pairs and then these were compared to the splice sites in the sequence. The fragment of *A. anguilla* 14-3-3 cDNA to be amplified was aligned with the corresponding cDNA and genomic DNA sequences from *D. rerio* using ClustalX with the primer sites highlighted (Figure 4.24.a). The alignment between the three sequences using ClustalX and the location of the donor and acceptor splice sites was then verified using Spidey (Figure 4.24.b). The intron-exon boundaries (splice sites) match in both the ClustalX alignment and the Spidey alignment. A pair of primers, one of which spans an intron, was selected from the Primer Express generated set. For 14-3-3 the forward primer is located within an exon whilst the reverse primer spans a 654bp intron between exons. In the unlikely event that amplification was also primed from genomic DNA there would be two products created, 103bp and 757bp in length, amplified from the cDNA and genomic DNA respectively which would be identified by gel electrophoresis or on the dissociation plot.

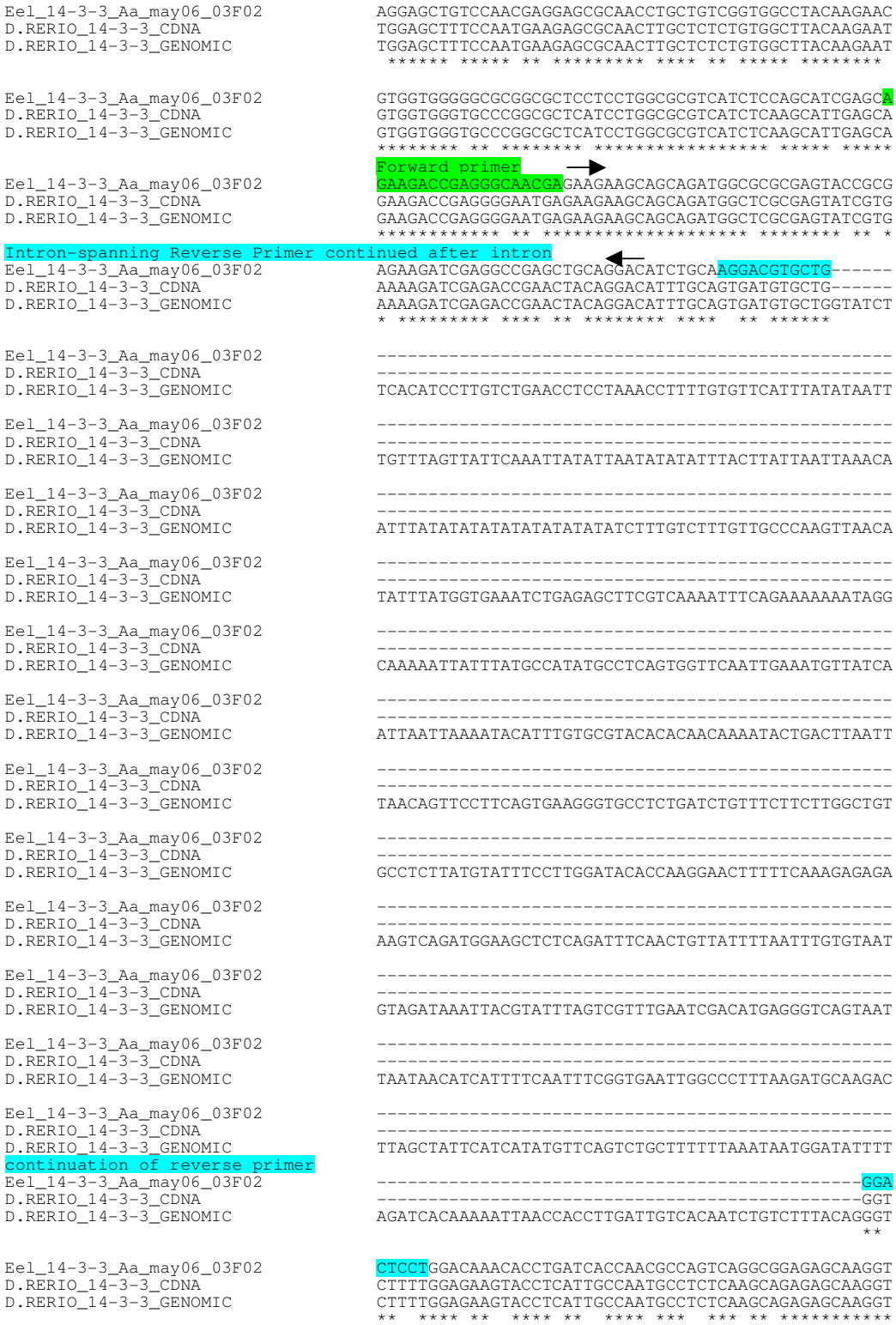

Figure 4.24.a. ClustalX alignment of *A. anguilla* 14-3-3 cDNA sequence flanking exons 1 and 2 with the corresponding cDNA and genomic DNA sequences from *D. rerio* (Ensembl gene ID: ENSDARG00000015382). Forward and intron-spanning reverse primers are highlighted in green and blue respectively.

Figure 4.24.b. Spidey (NCBI) alignment of the genomic region of *D. rerio* encompassing the 14-3-3 gene (above, Ensembl gene ID: ENSDARG00000015382) with the corresponding cDNA from *A. anguilla* (below) with nucleotide mismatches shown in red. The forward and intron-spanning reverse QPCR primers are highlighted in green and blue respectively.

In order to compensate for potential differences in binding or extension initiation between primers, test experiments were carried out for each primer pair using a standard amount of cDNA template with varying concentrations of each primer between 50 nM and 900 nM (final concentration). The lowest primer concentrations which gave the highest reaction efficiency were selected. For a PCR reaction optimised for Mg^{2+} and amplifying short amplicons the reaction efficiency should be close to 1. The reaction efficiencies of each primer set were compared over a 3125 dilution series of template to verify that primers worked equally efficiently over a range of template concentrations. Amplification efficiencies were calculated for each primer set using the equation below (slope is calculated as the linear regression coefficient of Ct versus log RNA input).

$$\text{QPCR Efficiency} = 10^{-(1/\text{slope})} - 1$$

For each primer set, the plots of Ct versus log RNA input, the reaction efficiencies (E) and the fit (R^2) of the fitted regressions are presented (Figure 4.24.c).

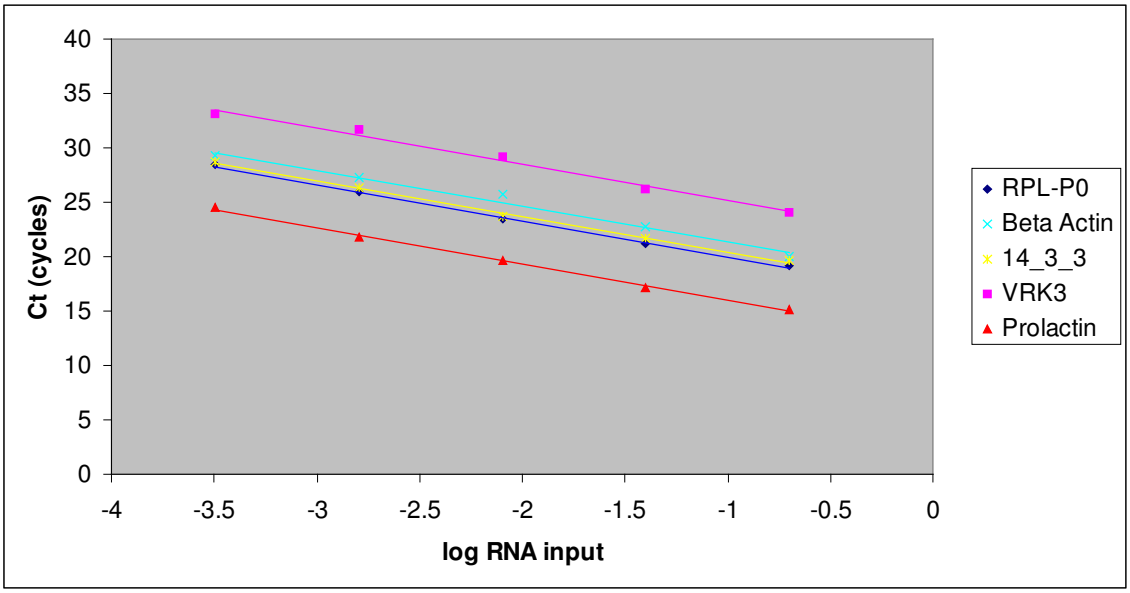

Figure 4.24.c. QPCR efficiency plots. QPCR was performed in triplicate for each primer set at 5 different template concentrations over a large (3125-fold) dilution series. A linear regression was applied to the mean Ct values for each primer set at each RNA concentration, the slope of which was used in the equation "Efficiency = $10^{-(1/slope)} - 1$" to give the reaction efficiencies. RPL-P0 (*E*= 1.00, R^2= 1.00); β-actin (*E*= 1.01, R^2= 0.99); VRK3 (*E*= 1.02, R^2= 0.99); 14-3-3 (*E*= 0.99, R^2= 1.00); prolactin (*E*= 0.99, R^2= 1.00).

Endogenous reference genes: GAPDH, 18s rRNA, acidic ribosomal phosphoprotein P0 (RPL-P0) and β-actin were chosen as candidates for endogenous control genes as they have been shown to have stable expression across a wide range of organisms under various treatments. The expression level of a target gene is compared to an endogenous control gene to give a relative expression level. This allows different samples to be compared directly whilst minimizing the effect of differences between samples caused by experimental inaccuracies such as the amount of starting RNA in the initial sample or RT efficiency.

The first set of GAPDH primers (see Figure 4.24.d and Table 4.24.a) designed as based on the above principles were not suitable for use in the QPCR assay as analysis of the dissociation curve revealed two distinct peaks around the 80 ºC mark (Figure 4.23.b). When viewed on a gel there was, however, only a single band at ~114 bp. A mis-prime from genomic DNA would have given a second product of 427 bp which would have been clearly visible on the gel and would have a significantly higher Tm than the 114 bp product. The two products were probably due to priming

of GAPDH and a similar isoform or pseudogene in the cDNA samples. New primers were designed to span a different intron (Figure 4.24.d) but these primers also gave multiple products and as such GAPDH was ruled out as a potential reference gene candidate.

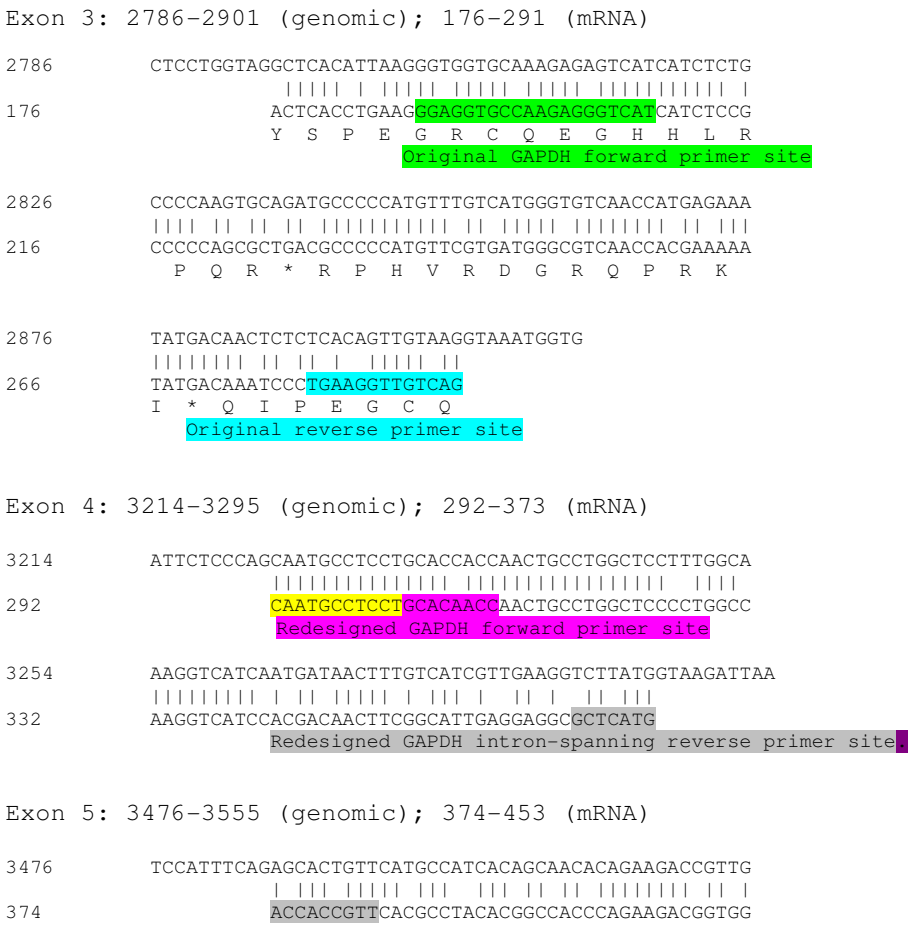

Figure 4.24.d. Spidey alignment of *A. anguilla* GAPDH cDNA (below) with *D. rerio* genomic DNA (above, Ensembl ID: ENSDARG00000043457) with nucleotide mismatches shown in red. The original forward and intron-spanning reverse GAPDH primer sites are highlighted in green and blue respectively. The second, redesigned intron-spanning forward and reverse GAPDH primer sites are highlighted in pink and grey respectively. There is an overlap between the original reverse and redesigned forward primer sites which is highlighted in yellow. Neither pair of primers was suitable to amplify a control gene for QPCR.

The 18S rRNA primers (Figure 4.24.e and Table 4.24.a) were also deemed to be unsuitable to amplify a control gene as the Ct of the control experiment containing RNA template was too near (<8 Ct) that of the cDNA. The ubiquitously abundant 18S rRNA gene comprises only one exon so primers cannot be designed to span an intron, thus genomic DNA is also amplified. This effect can be minimised by DNase treating the RNA before the RT step but as the amount of RNA was limited, the number of manipulation steps was kept to a minimum to preserve the integrity of the RNA. Contamination of solutions used in PCR is also common when using 18S rRNA primers as it is very highly conserved between species and a single stray cell or spore could erroneously influence a result.

TACACACGGCCGGTACAGTGAAACTGCGAATGGCTCATTAAATCAGTTATGGTTCCTTTGATCGCTCCAACGTTA
CTTGGATAACTGTGGCAATTCTAGAGCTAATACATGCCGACGAGCGCTGACCCTCCCAGGGGATGCGTGCATTTA
TCANACCCAAAACCCATCCGGGGTGCCTCGTGCGCCCCGGCCGCTTTGGTGACTCTAGATAACCTCGGGCCGATC
GCACGCCCTCCGTGGCGGTGACGTCTCA

Figure 4.24.e. *A. anguilla* 18s rRNA which is an intron-less gene, showing forward and reverse QPCR primer sites highlighted in green and red respectively. 18 S rRNA sequence derived from eel brain cDNA cloned in Section 3.12.

Actin is a major component of the protein scaffold that supports the cell and determines its shape, and is the most abundant intracellular protein in eukaryotic cells. The β isoform of actin has been widely used as a reference gene for QPCR studies, however, some studies have shown its expression to be regulated under certain experimental conditions suggesting that as a reference gene it should be used with caution (Dheda et al., 2004; Selvey et al., 2001). β-Actin has, however, been previously used as the endogenous reference gene for QPCR studies examining the yellow to silver developmental processes of the Japanese eel, Anguilla japonica (Han et al., 2003) which is one of the closest relatives of the European eel. β-Actin was also shown by the microarray results in the present study to have a very stable expression in the brain of both yellow and silver freshwater-adapted eels. β-Actin primers (Figure 4.24.f and Table 4.24.a) were also designed using the *D. rerio* genomic sequence (Ensembl ID: ENSDARG00000037746) to find the splice sites. These primers were only suitable as a control for the Yellow to Silver development

experiment as a significant increase in expression (2.42 fold) was shown during FW to SW transfer were shown during the microarray experiments (see Table 4.19.a).

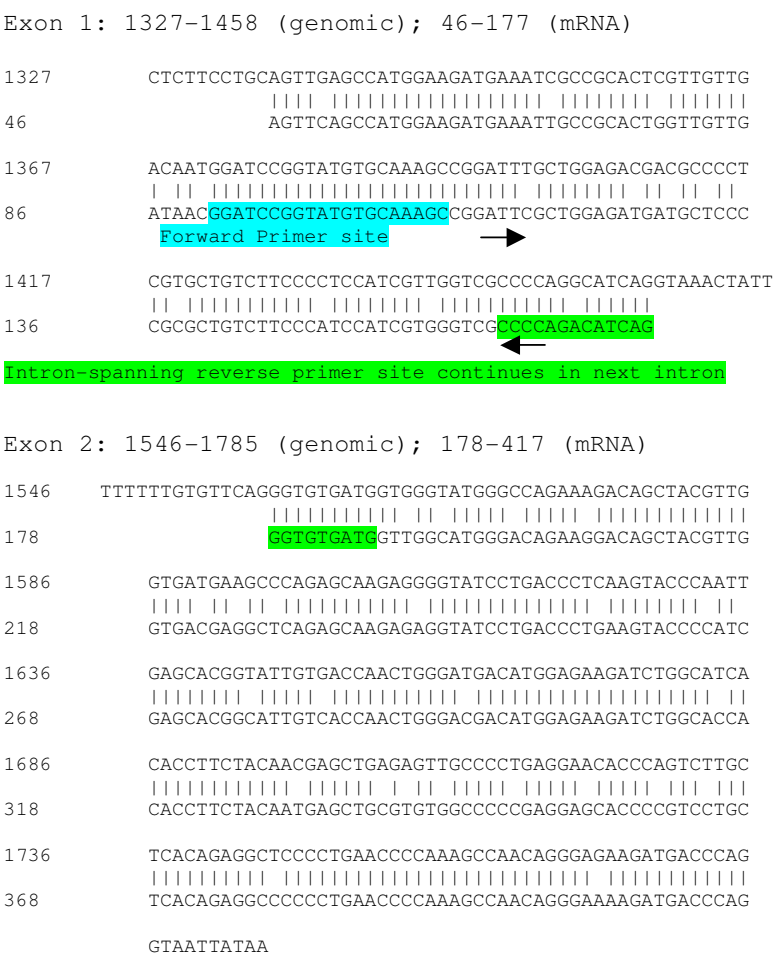

Figure 4.24.f. Extract from a Spidey (NCBI) alignment of the genomic region of *D. rerio* encompassing β-actin (upper sequence, Ensembl ID: ENSDARG00000037746) with the corresponding cDNA from *A. anguilla* β-actin (lower sequence). Forward and intron-spanning reverse QPCR primer sites are highlighted in blue and green respectively.

RPL-P0 is a ribosomal protein which is a component of the 60S ribosome subunit and the encoding gene (AY763793) has been used previously in QPCR studies for *A. anguilla* (Pierce et al., 2004b, Weltzien et al., 2005). Unlike some other ribosomal genes such as 18S and 28S, RPL-P0 contains introns which enable intron-spanning primers to be generated (Pierce et al., 2004a). Splice sites in *A. anguilla* predicted by Spidey correlated with *D. rerio*. The forward primer spans the splice site between two exons (Figure 4.24.g).

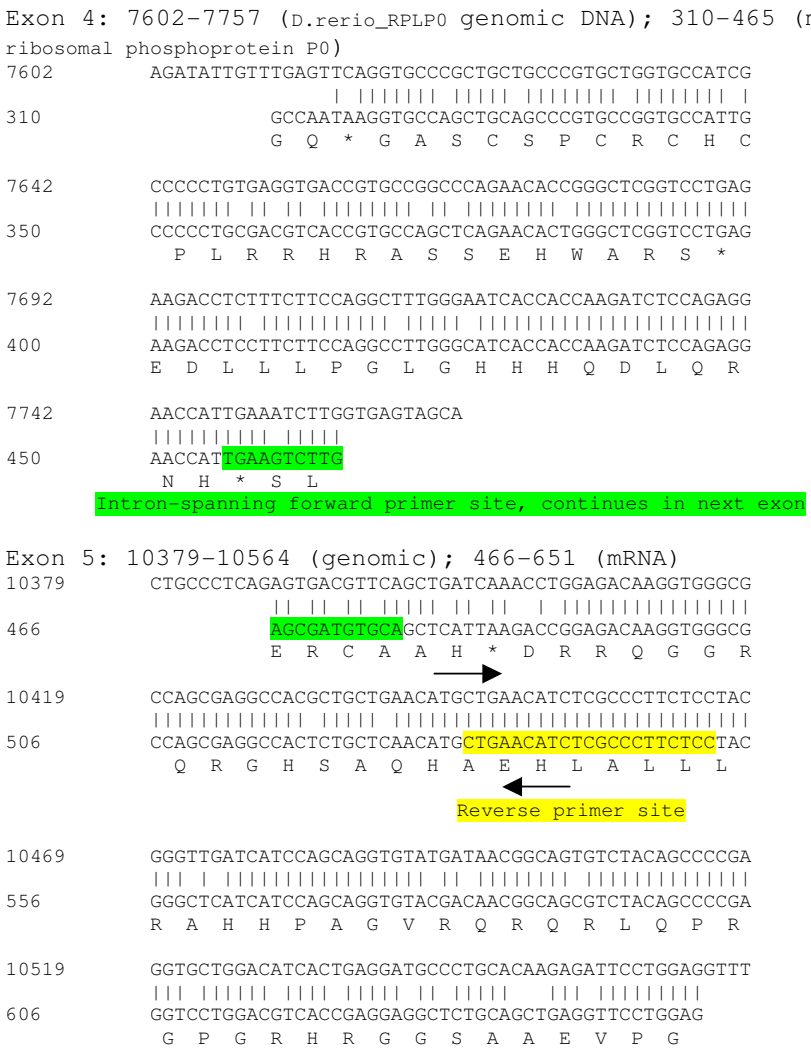

Figure 4.24.g. Extract from a Spidey (NCBI) alignment of the genomic region of D. rerio encompassing the RPL-PO gene (upper sequence, Ensembl gene ID: ENSDARG00000051783) with the corresponding cDNA from A. anguilla (lower sequence). The intron-spanning forward and reverse QPCR primers are shown in green and yellow respectively.

Optimal QPCR primers were sought for each gene but this was not always possible. For example, secretogranin III is comprised of only one exon so intron spanning primers were not possible. Predicted intron-exon boundaries for the homologues to kainate receptor, contactin and c-type natriuretic peptide genes were not reliable due to insufficient sequence information or significant divergence from known sequences at the nucleotide level. Optimal intron spanning primer sites were found for clones 01e01_Aa_BOS_01C01 and 01e09_Aa_BOS_01C05 and as such they were selected as the genes used to validate the array. The former shows strong homology (blastx score = 260, e = 4e-68) to human vaccinia related kinase 3 (VRK3). The latter is homologous to the β-subunit of *D. rerio* tyrosine 3-monooxygenase/ tryptophan 5-monooxygenase activation protein (blastx score = 384 e-105) which is a member of the 14-3-3 family, and hereon will be referred to as 14-3-3 protein.

14-3-3 proteins are ubiquitous phosphoprotein partners and very potent master regulators that control the activity of many signal transduction pathways in response to a changing environment (Fu et al., 2000). Interestingly, many molecular phenomena involved in salinity adaptation of euryhaline fish are regulated by 14-3-3 proteins. Examples are the activation of H^+-ATPase (Kultz et al., 2001), the regulation of cell proliferation and apoptosis (Fu et al., 2000), modulation of Na^+/K^+-ATPase activity via protein kinase C (PKC) regulation (Crombie et al., 1996), the regulation of ion transport and transporters (Chan et al., 2000), and the regulation of the cytoskeleton (Roth et al., 1999).

VRK3 is a member of the relatively uncharacterized VRK family which also includes VRK1 and VRK2 (Nichols and Traktman, 2004). The nucleolar protein VRK1 is known to phosphorylate various transcription factors including p53 (Vega et al., 2003), AFT2 and c-Jun (Sevilla, 2004; Sevilla et al., 2004). VRK2 localises in the endoplasmic reticulum and the human form has been shown to interact with BHRF1, an Epstein–Barr virus encoded protein resulting in an anti-apoptotic effect. VRK3 is expressed in the nucleus and over-expression and knockdown studies have shown it to be involved in the negative regulation of the extracellular signal regulated kinases ERK1 and ERK2 (Kang and Kim, 2006).

4.25 QPCR assay of *A. anguilla* 14-3-3 and VRK3 expression in yellow 7 day FW and silver 5 month FW acclimated eel brain.

A validated QPCR assay which could be used for 14-3-3, VRK3 and prolactin was established using the control genes ribosomal protein large P0 (RPL-P0) or β-actin. Specific primer pairs were made for each gene with at least one primer from each pair spanning an intron. Amplicon identity was assessed using gel electrophoresis and dissociation curves analysis (Figure 4.25.a).

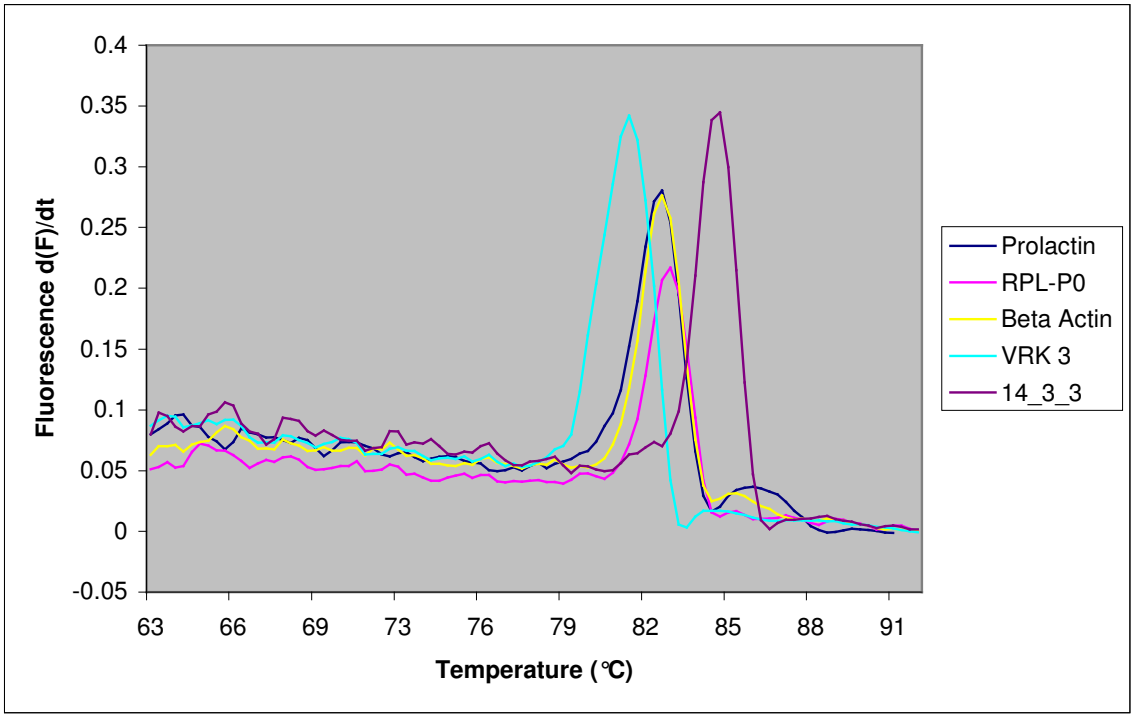

Figure 4.25.a. Dissociation plot of derivative fluorescence values of target and control amplicons. Following amplification the fluorescence is measured as the QPCR solution is gradually heated to separate the double stranded DNA. A single peak indicates that a single product has been created with no primer dimers.

Reactions were optimised using various primer concentration combinations to obtain efficiencies of 2 +/- 0.02 (equivalent to a doubling in DNA concentration for each round of PCR) so that the $2^{-\Delta\Delta Ct}$ data analysis method could be employed (see section 3.31) (Livak and Schmittgen, 2001). Ct measurements for each QPCR were taken for each sample at the point the fluorescence, which represents the DNA

concentration, reached a threshold set in the exponential phase of the reaction (see figure 3.31.a). In the $2^{-\Delta\Delta Ct}$ method of analysis data are presented as the fold change in target gene expression normalised to the endogenous control (β-actin or RPL-P0) and relative to the untreated control. For the untreated control sample, the expression of the target gene is treated as a constant in relation to the control gene, so ΔΔCt equals zero and as 2^0 equals one, so the fold change in gene expression of the target gene relative to the control gene equals one by definition. For the treated samples, evaluation of $2^{-\Delta\Delta Ct}$ indicates the fold change in gene expression relative to the untreated control.

The relative expression of 14-3-3 and VRK3 in the brain was measured in duplicate experiments with samples taken from each fish in the 7 day FW acclimated yellow (n = 6) and 5 month FW acclimated silver (n = 6) eel groups. β-actin was selected as the control gene as this had been shown in the microarray results to have stable expression in the brain of both yellow and silver FW acclimated eel brains [fold change from yellow to silver = 1.13 ± 0.11 (mean ± standard deviation)] and has been used previously as a reference gene when examining the yellow to silver development of anguillid eels (Han et al., 2003).

Relative expression of 14-3-3 normalised to β-actin as determined by QPCR was an average 1.61 fold higher in the brain of silver eels (p-value <0.05, Table 4.25.a). This concurred with the microarray determined relative expression change of 1.68.

Relative expression of VRK3 normalised to β-actin was an average 1.52 fold higher in the brains of silver eels (p-value <0.005, Table 4.25.a). This was similar to the microarray determined relative expression change of 2.05.

Table 4.25a. Expression of 14-3-3 and VRK3 in the brain relative to β-actin in yellow 7 day FW acclimated and silver 5 month FW acclimated eel brains. P-value calculated using a non-paired T-test assuming heteroskedastic variance and 10 degrees of freedom.

Target	Control	Ct difference between target and control gene (ΔCt mean +/- standard deviation)		Relative expression of target gene normalised to control gene (ΔΔCt)	Fold expression change from Yellow to Silver ($2^{-\Delta\Delta Ct}$)	T test p-value
		Yellow	Silver			
14-3-3	β-actin	1.39 ± 0.594	0.70 ± 0.081	0.69	1.61	0.035
VRK3	β-actin	7.85 ± 0.293	7.25 ± 0.084	0.60	1.52	0.003

4.26 QPCR assay of prolactin expression in silver 2 day FW and silver 2 day SW acclimated eel brain.

Prolactin was selected to validate the microarray experiment examining the effect of salinity change on gene expression in the brain. Prolactin was shown to be up-regulated in the silver 2 day SW in comparison with the corresponding FW group. β-Actin (used in the yellow-silver QPCR assay) was deemed unsuitable as the endogenous reference gene for the salinity change QPCR assay as the present microarray study had shown it to be up-regulated in the brain following SW adaptation of silver eels (fold change from FW to SW = 2.42 ± 0.63 standard deviations (Table 4.19.a). Therefore RPL-P0 was selected as an alternative endogenous reference gene as it was shown to have a constant expression in the brain of both FW and SW adapted silver eels.

The relative expression of prolactin in the brain was measured in duplicate experiments with samples taken from each fish in the silver 2 day FW acclimated (n = 6) and silver 2 day SW acclimated (n = 6) eel groups. β-actin was discounted as a control gene as the microarray result showed a significant increase in expression of this transcript in the brain following FW to SW transfer (fold change from yellow to silver = 2.42 ± 0.63 standard deviations, see table 4.7.a). Gene expression was instead normalised to RPL-P0 (accession number: AY763793) a housekeeping ribosomal protein which, unlike 18S rRNA, contains introns. RPL-P0 encodes a ribosomal protein that is a component of the 60S subunit (Weltzien et al., 2005). This gene was shown to have a constant expression in the brains of both FW and SW adapted silver eels (FW Ct = 23.94 ± 0.35 standard deviations, SW Ct = 24.25 ± 0.25 standard deviations).

Relative expression of prolactin normalised to RPL-P0 as measured by QPCR was an average 77 fold higher in the brain of silver eels acclimated to SW for 2 days than silver eels acclimated to FW for 2 days (Table 4.26.a).

Table 4.26.a. Expression of prolactin in the brain relative to RPL-P0 in silver eels acclimated for 2 days to FW or SW. P-value calculated using a non-paired T-test assuming heteroskedastic variance and 10 degrees of freedom.

Target	Control	Ct difference between target and control gene (ΔCt mean ± standard deviation)		ΔΔCt	Fold expression change (Yellow to Silver, $2^{-\Delta\Delta Ct}$)	P-Value
		FW	SW			
Prolactin	RPL-P0	2.18 ± 7.79	8.44 ± 0.19	6.26	76.64	0.11

The difference in expression (Δ Ct) between prolactin and the control gene RPL-P0 in SW was relatively consistent (Mean Δ Ct = 8.44, standard deviation = 0.19) but the FW group exhibited high variance (Mean Δ Ct = 2.18, standard deviation = 7.79). Thus, despite the large average increase in prolactin expression in 2 day SW acclimated silver eels the difference between the groups was not statistically significant (T-test p-value = 0.11) due to the high variability within the FW acclimated group. The average changes in expression levels of prolactin shown by QPCR, however, concur with the microarray expression data.

The large variance in prolactin expression in the FW group was investigated further by comparing it with the meta data. A linear regression using fish weight as the explanatory variable gave a model which appeared show correlation with the prolactin expression and explained most of the variance in the group ($y = -0.1016x + 44.477$, $R^2 = 0.724$) (Figure 4.26.a). Correlations were also sought between prolactin expression and plasma properties (angiotensin II, cortisol, protein content, osmolality, NA^+, K^+, Cl^-) collected as meta-data (see section 4.1) but none were found.

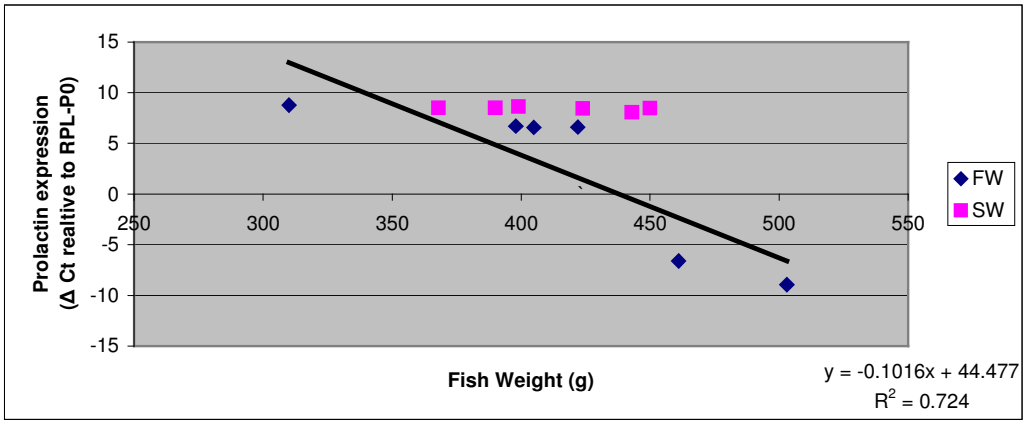

Figure 4.26.a. Fish weight and prolactin expression in the brain of the 2 day FW acclimated and 2 day SW acclimated, silver eel groups. A negative correlation between fish weight and prolactin expression in the FW group is shown by the fitted linear regression (y = -0.1016x + 44.477, R^2 = 0.724).

QPCR to assess the prolactin expression in silver 2 day FW adapted eel brain was repeated alongside brain RNA samples taken from the silver 6 hour FW and silver 5 month FW acclimated groups. The same linear relationship which correlated the prolactin expression with fish weight was seen again in the silver 2 day FW acclimated group (R^2 = 0.60) but there was no correlation between prolactin expression and fish weight in either the 6 hour or 5 month FW acclimated groups (R^2 = 0.05 and 0.20 respectively) nor when all the FW eels tested were treated as one group (R^2 = 0.026, figure 4.26.b).

The use of prolactin to validate the microarray results revealed the importance of examining the gene expression in individuals rather than relying solely on pooled samples as pooling data can mask variation. The correlation between prolactin expression in the 2 day FW silver eel brain and fish weight was not mimicked across all FW acclimated eels indicating the importance of examining a large sample size before drawing conclusions about possible correlations.

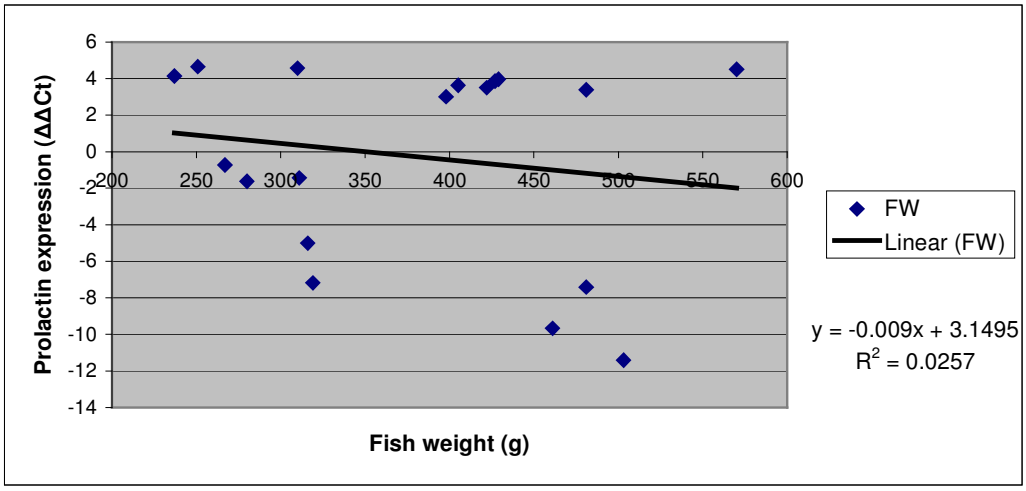

Figure 4.26.b. Prolactin expression plotted against fish weight. The fitted linear regression (y = -0.009x + 3.1495) is not significant (p > 0.5) and explains only a fraction of the variance (R^2 = 0.0257).

The SW acclimated eels from both the 6 hour and 2 day groups all exhibited high prolactin expression except for one fish in the 6 hour group which expressed the lowest prolactin expression of all fish tested. Prolactin expression in the brains of all the FW and the 5 month SW acclimated eels tested showed high variance in expression levels and there was no correlation with fish weight (figure 4.26.c).

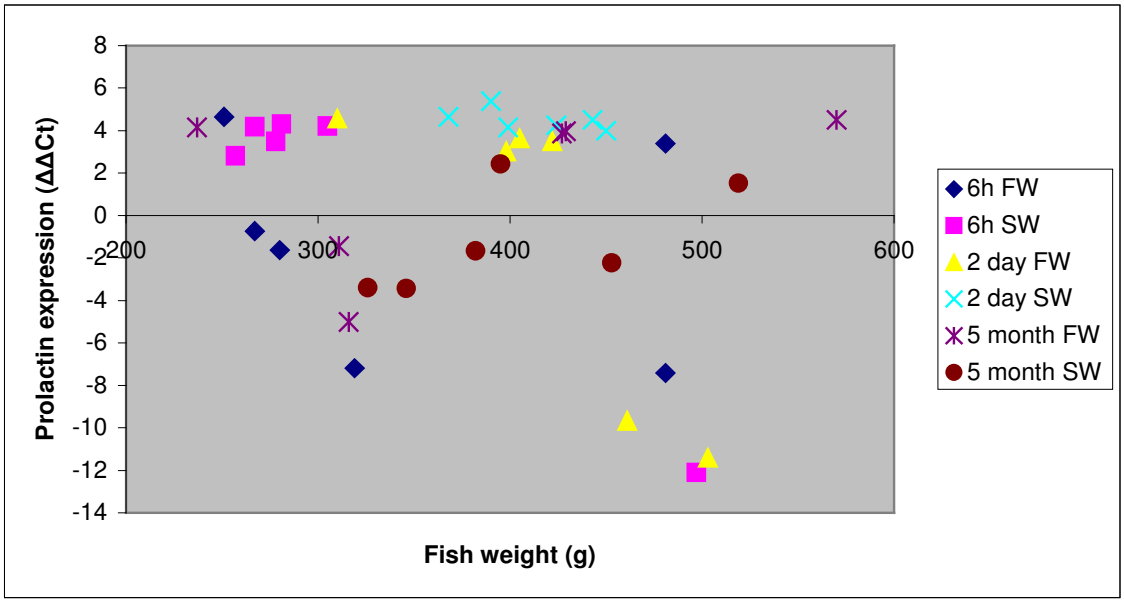

Figure 4.26.c. Prolactin expression in the brains of silver eels acclimated to FW or SW for 6 hours, 2 days or 5 months.

4.27 Confirmation of 14-3-3 protein clone identity.

The initial blastn and blastx searches likened the *A. anguilla* clone 01e01_Aa_BOS_01C01 to the beta isoform of the 14-3-3 protein from *D. rerio.* Initial sequencing of this clone from the subtracted *att*B brain library gave almost the entire 14-3-3 protein coding sequence with only 10 amino acids remaining to be determined. The level of sequence conservation of 14-3-3 maintained across isoforms and species is extremely high with human and yeast sharing 70 % homology (figure 4.27.b). The clone is probably the beta isoform as suggested by the Neighbour-Joined phylogram (figure 4.27.a). Members of the 14-3-3 family of proteins play a role in most cellular functions including regulation of protein kinase C, exocytosis, apoptosis, several metabolic processes, redox regulation. They are able to bind discrete phosphoserine/ threonine-binding motifs and in mammals the 14-3-3 family consists of seven homologues but no single conserved function has been assigned (Kjarland et al., 2006). Teleosts often exhibit high numbers of isoforms owing to evolutionary genome duplication events and this appears to be the case with 14-3-3 where nine isoforms have already been isolated in *D. rerio* alone. This is the first 14-3-3 protein isolated from *Anguilla anguilla.*

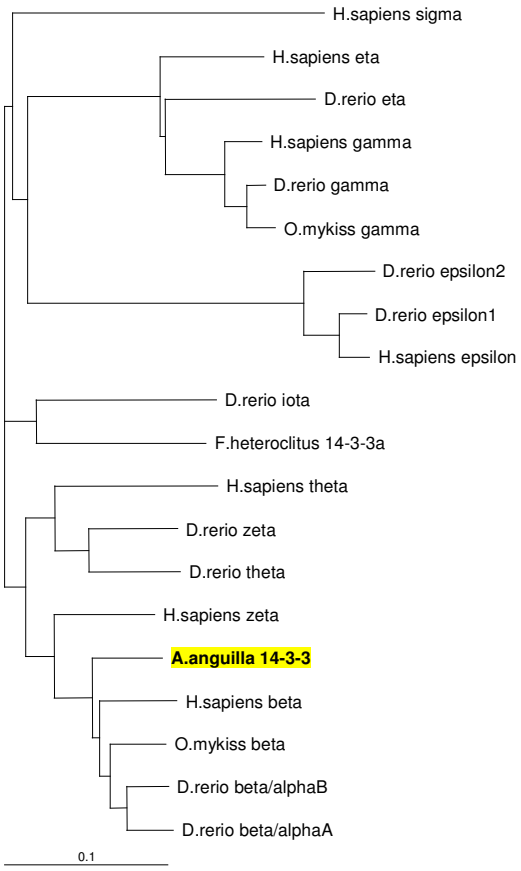

Figure 4.27.a. Cross-species Neighbour-Joined phylogram of 14-3-3 isoforms. The scale bar in the phylogram represents branch length (number of amino acid substitutions/site).

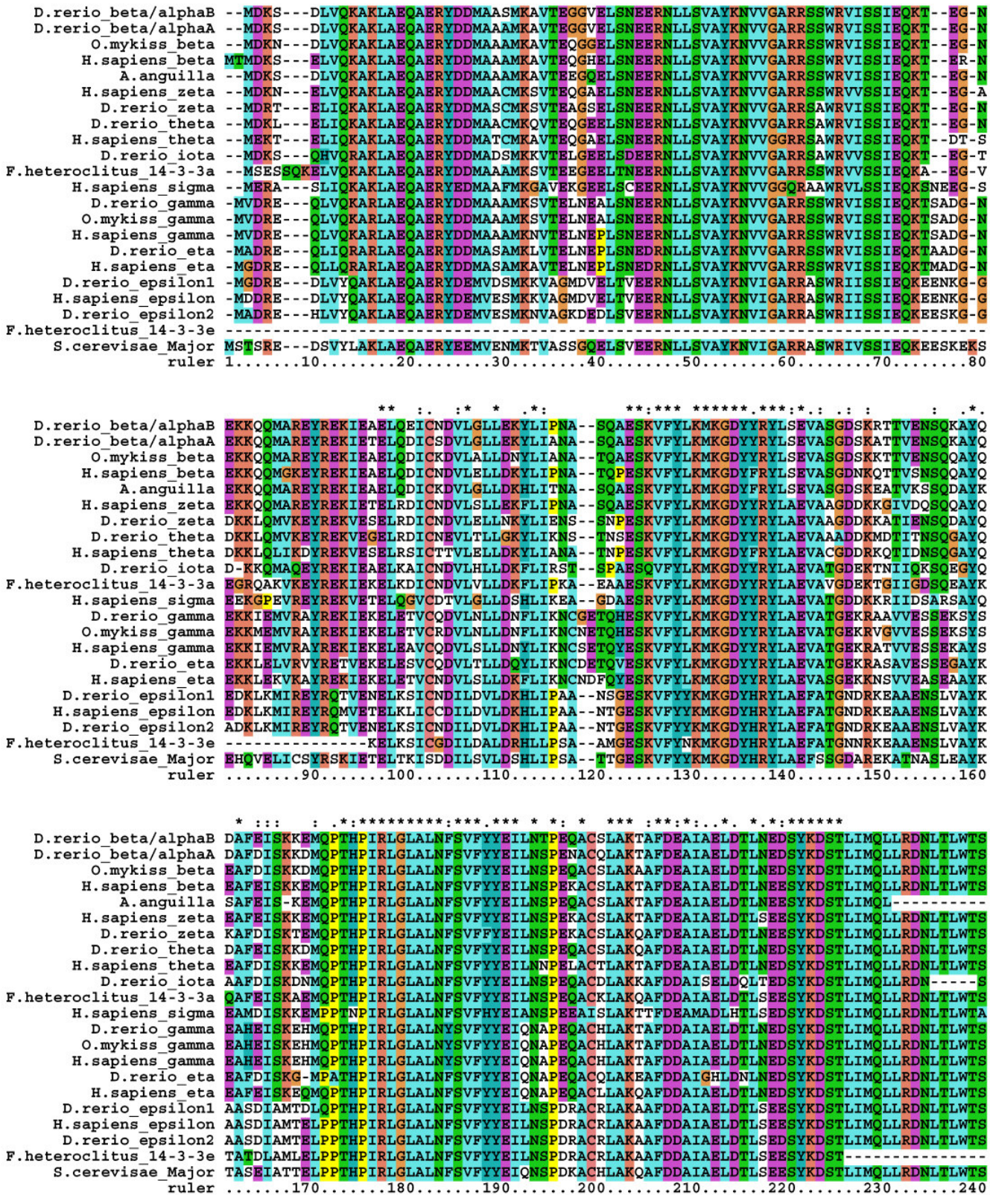

Figure 4.27.b. ClustalX alignment of vertebrate and *S. cerevisae* 14-3-3 isoforms with the *A. anguilla* clone 01e01_Aa_BOS_01C01.

4.28 Confirmation of Vaccinia related kinase 3 protein clone identity

The initial blastn and blastx searches likened the 01e09_Aa_BOS_01C05 *A. anguilla* clone to VRK3 from *H. Sapiens.* The closest teleost match from blastx was with VRK3 from *T. rubripes* but good matches were also found with VRK1 and VRK2 from *D. rerio* (VRK3 has not been isolated in *D. rerio*). This is the first member of the VRK protein family to be isolated in *Anguilla anguilla* or any other anguillid species. The VRK family of proteins have several characterised functions including the regulation of p53 by VRK1 and VRK2 (Blanco et al., 2006; Vega et al., 2004), phosphorylation of Barrier to Autointegration Factor by VRK1 and VRK2 (Nichols et al., 2006) and the suppression of ERK activity by VRK3 (Kang and Kim, 2006).

To confirm the identity of the *A. anguilla* clone a ClustalX alignment was done and a NJ phylogram was produced (figures 4.28.b and 4.28.a respectively). The VRK isoforms align well but the level of conservation is not as pronounced as with the 14-3-3 protein. The NJ phylogram concurs with the blast searches, grouping the *A. anguilla* clone with other VRK3 isoforms rather than VRK1 or VRK2.

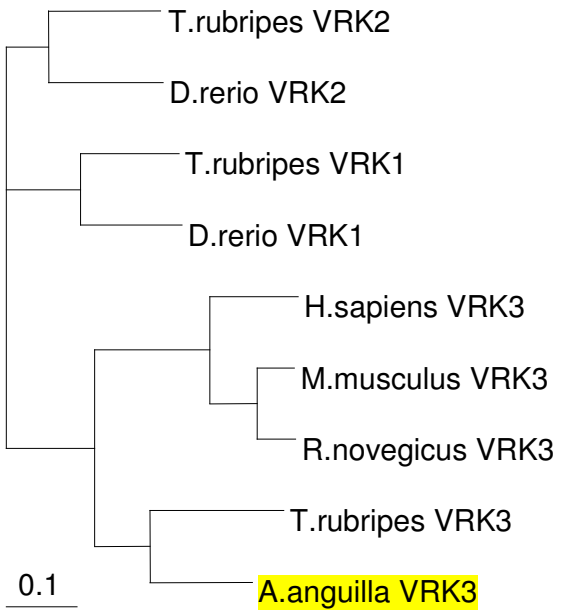

Figure 4.28.a. Cross-species NJ phylogram of VRK isoforms. The scale bar in the phylogram represents branch length (number of amino acid substitutions/site).

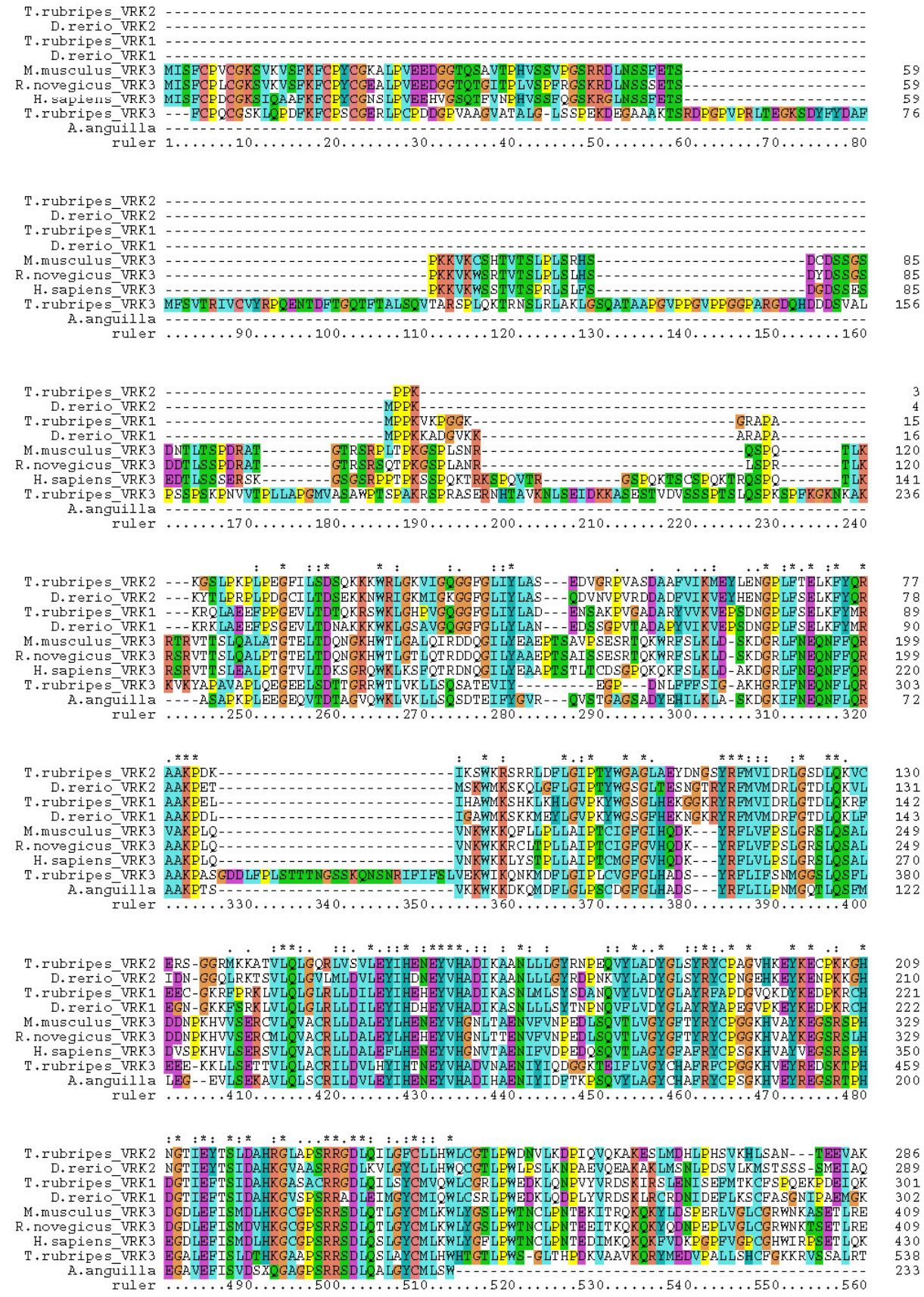

Figure 4.28.b. ClustalX alignment of vertebrate VRK isoforms with the *A. anguilla* clone 01e09_Aa_BOS_01C05.

4.29 Confirmation of prolactin precursor protein clone identity

The prolactin clone 06e15_Aa_BOS_21C08 aligns almost perfectly with the four previously published *A. anguilla* sequences of the prolactin precursor (figure 4.29.a). This clone, from the subtracted *att*B brain library contains the full-length sequence. Two other clones, 05e23_Aa_BOS_17C12 and 10c12_Aa_BOS_38B06, also contain the full length prolactin sequence but on the microarray these clones are spotted poorly and their fluorescence is not significantly enough above background to be reliable.

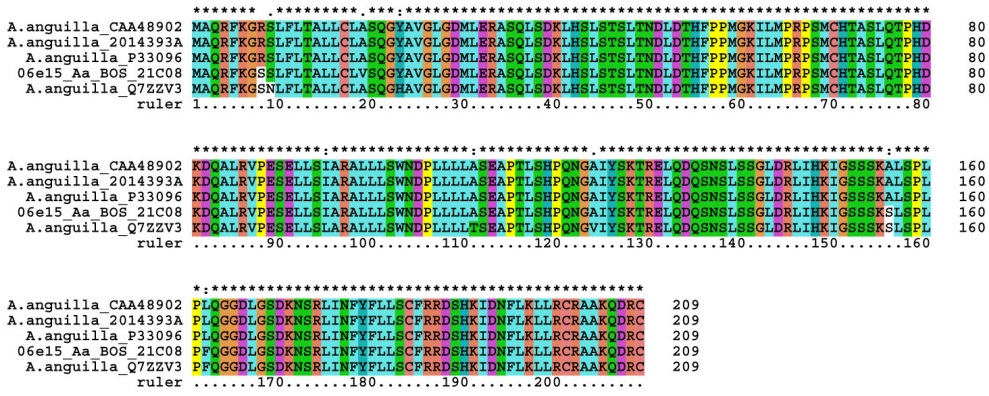

Figure 4.29.a. ClustalX alignment of published *A. anguilla* prolactin precursor sequences with clone 06e15_Aa_BOS_21C08.

5.0 Discussion

The European eel, *Anguilla anguilla* undergoes several remarkable developmental transformations during its fascinating life cycle which involves extraordinary migrations across the globe and across extreme physiological barriers. This life cycle presents researchers with an interesting model organism to study osmoregulation and development. To date, osmoregulatory research on the eel has focussed on its ability to rapidly adapt to changes in external salinity by modulating the epithelial expression of ion and water channels in the gills, kidney and intestine via the action of hormones, reviewed in Cutler and Cramb, 2001. Research into the sexual development of the eel has predominantly examined the effects and interactions of endocrine pathways involving dopamine and luteinising hormone (Vidal et al., 2004), follicle stimulating hormone (Degani et al., 2003), growth hormone (Marchelidon et al., 1996), thyroid-stimulating hormone(Han et al., 2004) and prolactin (Han et al., 2003). The population of European eels has declined rapidly since the early 1970s and in 2005 was classified as critically endangered by the Swedish Species Information Centre. As such, the importance of research into this species, especially with regards to its breeding, is becoming increasingly poignant.

This study set out to investigate the hypothesis;

The brain is the central organ for the co-ordination of environmental cues (day length, photoperiod, temperature and environmental salinity) with the anatomical and physiological adaptations which accompany pre-migrational morphogenesis and the osmoregulatory plasticity seen in post-migrational, salinity-adapted fish.

To create the tools to test this hypothesis, the following aims were defined;

i. Develop cDNA libraries for the brain, kidney, intestine and gill taken from eels adapted to both fresh and marine environments.
ii. Use these cDNA libraries to create microarrays.
iii. Determine gene expression profiles for yellow and silver eels adapted to fresh- and seawater.
iv. Determine the cDNA sequence of potential genes of interest.
v. Validate the gene expression profiles using complementary techniques.

All of the initial aims were achieved. Subtracted cDNA libraries were successfully created for the kidney, gill, intestine and brain of the eel, and used to create microarrays. A microarray, specific for the brain was used to determine brain gene expression profiles to examine two aspects of eel biology;

a. The transition from juvenile yellow to the adult sexually maturing, migrating silver eel; and
b. salinity adaptation during the migration from freshwater to seawater.

The microarrays created represent the first such study for the European eel *Anguilla anguilla* or for any eel species and enabled a wide range of genes to be simultaneously monitored.

The validity of the observed changes in gene expression determined using the microarrays was then confirmed using real-time quantitative PCR (QPCR) analysis. QPCR assays were developed for the quantification of three selected genes, which showed differential expression on the microarrays;

i. Tyrosine 3-mono-oxygenase/tryptophan 5-mono-oxygenase activation protein
ii. Vaccinia related kinase 3
iii. Prolactin

Quantification was normalised to an endogenous reference gene, either acidic ribosomal protein P0 or β-actin.

The cDNA libraries and microarrays produced in this project will provide the base to facilitate the discovery of important genes involved in many aspects of eel biology. In addition, the QPCR assays developed will be useful in validating gene expression profiles.

5.1 Gene expression changes during the life cycle of the eel.

We examined the changes in the gene expression profile of the eel brain which occur during one of the key developmental stages of the eel, the yellow to silver metamorphosis. The genes whose expression showed the greatest difference between the two developmental stages were selected for sequencing analysis. The sequencing results confirmed that the majority of clones in the *att*B subtracted brain library were very long or full-length and that the level of redundancy in the library was very low (Table 4.13.a). These sequences have been submitted to arrayexpress (http://www.ebi.ac.uk/aerep) where they will be freely available online once the data have been published.

The sequenced clones were then assigned putative biological functions by comparison with the Gene Ontology database (http://www.geneontology.org/, Ashburner, 2000). Clones whose functions were related were then clustered into six sub-groups; Signal Transduction; Development and Morphogenesis; Membrane and Structure; Metabolism; Immune/Stress Response; and Transcription and Post-Translational Modification (Tables 4.18.b-g respectively). Unsurprisingly the largest cluster was Development and Morphogenesis indicating that there are significant changes which occur in these pathways during the yellow to silver transition. The second largest cluster was Metabolism, suggesting that there may be significant changes in the metabolic pathways employed following silvering, perhaps in preparation for the long migration ahead.

Within the Membrane and Structure cluster, intercellular adhesion molecule 2 was down regulated by 0.59-fold. Inter-cellular adhesion and the formation of tight-junctions are key to the permeability of membranes and would seem an unlikely candidate to be up-/down-regulated within the brain. The expression of related genes (claudins) involved in membrane permeability are known to be down-regulated in eel gill following transfer to seawater (Kalujniaia 2007b). Whilst the membranes of the eel gill are known to undergo extreme phenotypic changes following salinity transfer, little has

been reported on the membranes which protect the brain and changes which may occur during osmoregulation and development. As discussed below, 14-3-3 proteins have been implicated as having a role in membrane integrity and the possibility that there are osmotically regulated changes to the brain from salinity fluctuations is intriguing. It would be interesting to follow up these results using immunohistochemistry or in situ hybridisation techniques to localise the expression of these membrane specific genes and elucidate what role they may be playing.

Two genes, 14-3-3 and VRK3, were selected for more detailed analysis by QPCR. This enabled the microarray results to be validated and the inter-fish gene expression variability to be examined.

The brain expression of 14-3-3 in the silver, 5 month FW acclimated eel group was 1.61 fold higher than in the yellow, 7 day FW acclimated group when assayed with QPCR, which is very similar to the 1.68 fold change quantified for the same gene when using the microarray. Inter-fish variability of brain 14-3-3 expression was lower within the silver group (mean $\Delta Ct = 0.70 \pm 0.08$ SD) than in the yellow group (mean $\Delta Ct = 1.39 \pm 0.59$ SD) and the result was statistically significant (t-test p-value = 0.035).

The 14-3-3 family of proteins was originally identified in 1967 as an abundant cytosolic protein in the bovine brain with the numerical nomenclature arising from their fraction number on DEAE-cellulose chromatography and migration position on starch gel electrophoresis (Moore and Perez, 1967). The 14-3-3 proteins are small acidic soluble proteins with a native size of 28-33 kDa that are found in all eukaryotic organisms. Speculative functions were suggested as the 14-3-3s kept cropping up associated with biologically important proteins (early 14-3-3 work reviewed in Aitken et al., 1992) but it was almost 30 years after their initial discovery when the first functional evidence showed that 14-3-3 proteins bind discrete phosphoserine/threonine motifs (Muslin et al., 1996).

14-3-3 proteins are now known to be ubiquitous regulators of cellular physiology and biochemistry that control the activity of many signal transduction pathways by their ability to bind a wide range of functionally diverse signaling proteins, including many protein kinases, phosphatases and other phosphoproteins in response to external stimuli (Fu et al., 2000). They operate by binding to specific phosphorylated sites on over 300 known target proteins, thereby forcing conformational changes or influencing interactions between their targets and other molecules leading to the description that they 'finish the job' when phosphorylation alone lacks the power to drive changes in the activities of intracellular proteins" (Mackintosh, 2004). It is difficult at this stage to pinpoint the role this protein is playing in the brain of the silver eel as 14-3-3s have been implicated in a wide range of cellular pathways including signal transduction, regulation of metabolism, cell cycle and checkpoint control, apoptosis, gene transcription, chromosome remodeling, intracellular protein trafficking and stress response. Large numbers of 14-3-3 isoforms have been isolated from other species; seven in mammals and thirteen in Arabidopsis thaliana (Ferl et al., 2002). Coupled with the genome duplication events specific to teleosts (Taylor et al., 2003) one can assume that the presently described 14-3-3 isoform in eel will not be a singular occurrence. What is not clear from the microarray result, however, is which 14-3-3 proteins are being elevated in the silver eel brain. This is an important aspect as 14-3-3 isoforms have been shown to be differentially expressed in mammalian (Nakanishi et al., 1997) and teleost (Koskinen et al., 2004) species suggesting different roles for each. The sequence homology between the 14-3-3 clone used on the microarray and other 14-3-3 isoforms from other species was examined using ClustalX which suggested that it was the beta isoform (Section 4.27). With such high sequence homology between the known 14-3-3 isoforms, however, it remains to be confirmed if the microarray technique was specific enough to measure whether it was 14-3-3 beta transcripts alone that were binding to the 14-3-3 beta cDNA clone on the array.

An interesting reported function of 14-3-3 is its involvement in salinity adaptation of the euryhaline teleost, F. heteroclitus (Kultz et al., 2001) where

an up-regulation of 14-3-3 was shown in the gills following SW to FW transfer. This has been linked with the increased activity of P-type H+-ATPase which has been seen in response to 14-3-3 binding (Babakov et al., 2000; Chelysheva et al., 1999). Increased P-type H+-ATPase activity mediated by 14-3-3 in response to external hypo-osmolality would thus drive out protons across the gill epithelial membrane, creating a gradient for the absorption of Na+ through sodium channels. Conversely, when F. heteroclitus 14-3-3 was expressed in Xenopus oocytes it was shown to have a protective effect from the effects of hyper-osmolality of the external medium leading to increased survival of the oocytes. The mode of action in this case was speculated to be the inhibition of membrane chloride channels (Kohn et al., 2003). Eels are euryhaline but the average plasma osmolality for all eels examined was higher in SW (354.16 ± 31.67 mOsm/L) than in FW (299.83 ± 27.83 mOsm/L), a significant salinity change ($p<0.0005$) from which the animal may need to protect itself. The up-regulation of 14-3-3 in the brain of silver eels could, therefore, be part of the pre-adaptation of silver eels to the hyper-osmotic environment of SW (Tesch and Greenwood, 1977). Other reported preadaptations of silver eels to SW include decreased gill osmotic permeability (Kirsch et al., 1975) and decreased NKCCIa expression in the kidney compared to yellow eels (Cutler and Cramb, 2001). Whether 14-3-3 directly influences P-type H+-ATPase expression in the brain of silver FW adapted eels is not apparent but during the current study, V-type H+-ATPase expression in the brain was up-regulated (mean M = 1.48, ± 0.10 SD, see Table 4.18.b) during yellow to silver transition of the eel. Although originally associated with vacuoloar proton transport, V-type H+-ATPase is now known to be expressed in a wide variety of plasma membranes where it is involved in energizing transport across cell membranes and entire epithelia (Beyenbach and Wieczorek, 2006). This proton pump has also been shown to associate with 14-3-3 proteins (Klychnikov et al., 2006) and although the nature of this interaction has not been clarified, increased expression of V-type H+-ATPase would provide more targets for the simultaneously up-regulated 14-3-3.

14-3-3 isoforms are also known to bind to and activate protein kinase C (PKC) (Isobe et al., 1992; Van Der Hoeven et al., 2000) which in turn has

been shown to inhibit the activity of Na+/K+ ATPase in the gill epithelium of teleosts, e.g. Atlantic cod (Crombie et al., 1996). The microarray results from this study show that Na+/K+ ATPase α1 (clone 16m19_Aa_BOS_61G10) was consistently down regulated in the brain of silver eels (mean M = 0.77, ± 0.03). The second clone of Na+/K+ ATPase α1 was removed from the analysis as the fluorescence fell below background level; this appears to be because of poor quality spotting. Other clones on the microarray representing the Na+/K+ ATPase α3 isoform and the Na+/K+ ATPase representing β-subunit isoforms did not change their expression significantly between the two developmental conditions. Recently, the differential expression of Na+/K+ ATPase isoforms in response to salinity challenge has been demonstrated in teleosts which could account for the differences seen between Na+/K+ ATPase isoforms here (Richards et al., 2003). Several lines of evidence indicate, however, that Na+/K+ ATPase α and β-subunit synthesis is simultaneously regulated (Emanuel et al., 1987) which calls into question the differences in expression of the Na+/K+ ATPase subunits seen in silver eel brain. As with all results from microarrays, it would be prudent for the expression of the various isoforms of Na+/K+ ATPase subunits in the brains of yellow and silver eels to be verified by a second method such as QPCR.

A role of 14-3-3s which is related (indirectly) to the simultaneously up-regulated VRK3 is the stabilising effect 14-3-3 have on the inactive form of Raf-1 (Jirakulaporn and Muslin, 2004). Binding of Raf-1 by 14-3-3 prevents it from phosphorylating and activating the mitogen activated protein kinase (MAPK) family members ERK1 and ERK2. Negative regulation of ERK1 and ERK2 are also known functions of VRK3 (Kang and Kim, 2006) and are discussed further in section 5.3.

A final role to be mentioned in relation to the silvering process is 14-3-3's role linking photoreception, neurotransmission, signal transduction and the synthesis of melatonin from tryptophan in relation to the regulation of pineal photo-neuroendocrine transduction (Klein et al., 2003). The pineal gland of teleost fish is a photosensory organ whose primary role is the rhythmical release of melatonin, as dictated by ambient photoperiod, or by an

endogenous circadian oscillator entrained by diurnal photoperiod (Asaoka et al., 2002). The pineal organ transduces light-dependent neural inputs into a hormonal output by modulating the activity of arylalkylamine N-acetyltransferase (AANAT), which catalyses the production of N-acetylserotonin as part of the melatonin pathway (serotonin →N-acetylserotonin → melatonin) (Ganguly et al., 2005; Korf et al., 1996). At night, elevated cyclic adenosine monophosphate (cAMP) levels cause the phosphorylation of two sites on AANAT, S205 and T31, by protein kinase A. This post-translational modification of AANAT creates phosphorylated target sites for 14-3-3 binding which facilitate the formation of a complex between the two proteins. Binding of AANAT by 14-3-3s both increases and prolongs melatonin production; firstly by decreasing the Km for serotonin and secondly by protecting AANAT from degradation. This protection is manifested as physical shielding of susceptible amino acids from proteolytic enzymes and dephosphorylation of the S205 and T31 sites (Pozdeyev et al., 2006; Schomerus and Korf, 2005).

Melatonin has been shown to down regulate prolactin expression in cultured pituitary cells of rainbow trout (Falcon et al., 2003) which would correlate with the simultaneous down-regulation of prolactin in the brain of silver eel as indicated by two of the prolactin clones (mean fold change = 0.65 ± 0.05) in the present microarray experiments. This provides further circumstantial evidence that elevated expression of 14-3-3 in freshwater-adapted silver eel brains could be causing an increase in circulating melatonin levels.

It is not, however, only sunlight that can influence melatonin production. There is a lunar-related rhythmicity of melatonin production in cultured pineal cells of the teleost, Siganus guttatus, exposed to natural light conditions, including moonlight, which is suggested to direct the timing of spawning of these species (Park et al., 2006; Takemura et al., 2006). The link between lunar phase and spawning has also been reported in the gilt-head sea bream, Sparus aurata (Saavedra and Pousão-Ferreira, 2006) and has been specifically linked with the down-stream migration of silver eels at the

start of their journey to the Sargasso Sea where they spawn (Cullen and McCarthy, 2003). Eel spawning in the Sargasso Sea could be timed with lunar phase and thus the increased stability of melatonin production could be linked with this rhythm. The timing and amplitude of melatonin secretion can also be affected by temperature (Barrett and Takahashi, 1999; Ekstrom and Meissl, 1997; Underwood, 1990); an environmental variable which has also been linked with the timing of seaward migration of the eel (Boubée et al., 2000; Sloane, 1984).

A recently described function of melatonin could provide a clue to way in which these systems are regulated in the eel. Gaildrat and Falcón (2000) showed that melatonin inhibits cAMP accumulation in cultured pike (Esox lucius) pituitary cells. As previously mentioned, cAMP accumulation is directly involved in the phosphorylation of AANAT which, in turn, catalyses the penultimate step in melatonin production. The inhibition of cAMP, by 14-3-3 induced melatonin production could, therefore, provide the basis of a negative feedback system in the eel.

The injection of melatonin into rainbow trout has been shown to suppress hypothalamic-pituitary dopamine metabolism (Hernández-Rauda et al., 2000). Following the treatment there was a subsequent drop in DOPAC and a reduction of the DOPAC:DA ratio. Subsequently, Sylvie Dufour's group showed that dopamine inhibits gonadotrophin releasing hormone (GnRH) stimulated LH synthesis and release. Linking these two finding one can infer that increased melatonin would thus reduce the level of inhibition LH synthesis and thus allow puberty to progress. In a further twist, melatonin synthesis has also been shown to be under the influence of dopamine receptors, with different effect depending on the receptor isoform in question (Zawilska and Luvone, 1989).

When the VRK3 expression was assayed by QPCR, the results aligned well with the microarray results. QPCR showed the brain expression of VRK 3 in the silver, 5 month FW acclimated eel group to be 1.52 fold higher than in the yellow, 7 day FW acclimated group. This is slightly lower than the 2.05

fold change which was implied by the microarray experiments but both results are very comparable. The QPCR assay of VRK3 revealed inter-fish variability to be greater within the yellow group than the silver group which was consistent with the variability of 14-3-3 seen in the same eels. Within the yellow group the inter-fish variability (SD = ± 0.293) was almost three times greater than the silver group (SD = ± 0.084). The QPCR result showing the increase in VRK3 expression was statistically significant (t-test p-value = 0.003).

VRK3 is a member of the relatively uncharacterized VRK family which also includes VRK1 and VRK2 (Nichols and Traktman, 2004). The nucleolar protein VRK1 is known to phosphorylate various transcription factors including p53 (Vega et al., 2003), AFT2 and c-Jun (Sevilla, 2004; Sevilla et al., 2004). VRK2 has two known isoforms; VRK2A which localises in the endoplasmic reticulum and the VRK2B which is cytoplasmic (Blanco et al., 2006). Functionally, the human form of VRK2 has been shown to interact with BHRF1, an Epstein–Barr virus encoded protein resulting in an anti-apoptotic effect (Li et al., 2006).

VRK3 is expressed in the nucleus and over-expression and knockdown studies have shown it to be involved in the negative regulation of the extracellular signal regulated kinases ERK1 and ERK2 (Kang and Kim, 2006). In this situation VRK3 acts by activating a mitogen activated protein kinase (MAPK) phosphatase called vaccinia H1-related phosphatase which specifically dephosphorylates and inactivates ERK in the nucleus (Todd et al., 1999). ERK1 and ERK2 play a pivotal role as one of the four main groups of MAPKs which also include c-jun N-terminal kinase (JNK), p38 and a group of atypical MAPKs including ERK3, ERK5 and ERK8 (Lewis et al., 1998). ERKs are involved in a variety of physiological responses including in cell proliferation, differentiation, development and death, as well as in synaptic plasticity in the brain (Chang and Karin, 2001; Pouyssegur et al., 2002).

It would seem appropriate for a signalling peptide such as VRK3 to be up-regulated following silvering of the eel as there are a multitude of major

physiological changes which occur during silvering and also there may also be preadaptations for the impending seawater migration.

5.2 Gene Expression Changes During Osmoregulation

The analysis of 2 day FW/SW acclimation microarray results revealed a multitude of genes exhibiting marked up-/down-regulation. As for the yellow:silver analyses, the genes exhibiting the greatest changes in expression were sequenced. Once again the sequencing results underlined that the *att*B subtracted brain library has low redundancy and long clones. Through comparison with the Gene Ontology database, the clones were assigned a biological function and similar functional groups were clustered together into five sub-groups; Signal Transduction, Development and Morphogenesis, Membrane and Structure, Metabolism and Transcription and Post-translational modification (Tables 4.19.a-e respectively). As was seen during the yellow to silver experiments, the Development and Morphogenesis cluster was the most populous, possibly reflecting the multitude of adaptations at the cellular and organ structure level which are required following an osmoregulatory challenge.

Prolactin was selected for further analysis using QPCR in order to validate the silver eel 2 day FW/SW acclimation microarray results and to test the gene expression for each individual fish adapted to the different salinities. Exon-spanning primers were developed for *A. anguilla* prolactin and for the endogenous control RPL-P0.

When the brain prolactin expression of 2 day FW and SW eels was assayed using QPCR, the inter-fish variability FW acclimated group was so large (mean $\Delta Ct = 2.18 \pm 7.8$ SD) that the mean expression between the two groups was statistically indistinguishable (t-test p-value = 0.11). The standard deviation of 7.8 ΔCt is equivalent to a 222-fold variability in expression and as the variability in the SW group was so much lower (mean $\Delta Ct = 8.44 \pm 0.19$ SD), it raised the question as to whether the QPCR assay was performed incorrectly or if the brain RNA samples of the silver eel 2 day FW acclimated group had been incorrectly diluted or had become degraded. Replication of the experiment, however, revealed near identical results suggesting the

experiment had been performed correctly. The RNA samples used in the QPCR assay were all diluted to the same concentration and an equal aliquot of each was used for both target and control gene quantification. Thus any large variability in the Ct of the endogenous control gene, which should remain relatively constant would indicate possible sources of experimental error such as dilution mistakes or RNA degradation. The variability in brain expression of the endogenous control gene (RPL-P0) for the 2 day FW silver eel group RNA samples was, however, very low (Ct = 23.94 ± 0.35) indicating that the RNA was correctly diluted and that the RNA was not degraded. Therefore, these results indicate a possibly interesting phenomenon that SW acclimated eels exhibit high prolactin expression during the initial stages of SW acclimation. All but one of the eels in the 6 hour SW and all of the 2 day SW acclimated groups showed high prolactin expression whereas the corresponding FW groups showed large variation in prolactin expression (Figure 4.26.b).

Variation in prolactin expression was not restricted to the QPCR results; the microarrays also have an anomaly. On the microarray there are four prolactin clones, one from the control plate and a further three from the brain *att*B subtracted library. The prolactin clone from the control plate (16k17_Aa_BOS_61F09) did not show significant up- or down-regulation during the yellow to silver transition (mean fold change = 0.99 ± 0.2 SD) or during FW to SW adaptation (mean fold change = 0.93 ± 0.36 SD). During the FW-SW acclimation experiment one prolactin clone (06e15_Aa_BOS_21C08) from the brain *att*B subtracted library showed significant up-regulation after SW acclimation (mean fold change = 2.81 ± 1.26) but the same clone showed no significant difference during yellow to silver development (mean fold change = 1.06 ± 0.08 SD). The remaining two clones (05e23_Aa_BOS_17C12 and 10c12_Aa_BOS_38B06) showed no significant up-regulation in SW adapted eels, if anything they showed a slight decrease (mean fold change = 0.8 ± 0.08). Interestingly though, these two clones showed a significant down-regulation in silver eel brain, relative to their yellow counterparts (mean fold change = 0.65 ± 0.05), a phenomenon which has previously been identified in *Anguilla japonica* (Han et al., 2003).

Prolactin is known to be under the inhibitory control of dopamine in mammals (Ben-Jonathan and Hnasko, 2001) and has been reported in some teleosts (Chan et al., 2006; Wigham and Ball, 1976). Dopamine has been identified as the neuroendocrine "lock" which prevents final sexual maturation of silver eels until they are at sea (Vidal et al., 2004). Dopamine expression in the eel is thought to decrease during the final stages of maturation during the migration at sea causing an increase in luteinising hormone (LH) as implicated by dopamine antagonists which promote sexual maturation (Vidal et al., 2004). Therefore, dopamine would presumably be maintained at high levels in the silver eels used in the current study and could be inhibiting prolactin expression, possibly explaining the low expression in the brain of silver eels. Extrapolating this theory further, there would be a corresponding increase in prolactin expression during the final sexual maturation of the eel when dopamine expression decreases. A possible role for prolactin in this hypothetical situation could be the regulation of gonadal steroidogenesis. This pathway has been implicated in two other euryhaline teleosts; testosterone production in the goby (*Gobius niger*) is stimulated by treatment with mammalian prolactin (Bonnin, 1981) and similar results were found in a mummichog, *Fundulus heteroclitus*, when it was treated with purified salmon prolactin (Singh et al., 1988).

With such apparent disparity between the prolactin spots on the array, however, the expression first needs to be validated before making further speculative conclusions. This has already been done in this study for the prolactin expression in FW and SW adapted silver eels but remains to be done in future experiments for the yellow-silver transition.

5.3 Development of a new microarray platform for a non-model species.

Two types of microarray were created for *A. anguilla*, a first for this or any anguillid species. This provides a new resource for the fish research community to supplement similar projects which include, amongst others; *T.rubripes, O.latipes, T.nigroviridis P.flesus , F.heteroclitus*, *O.mykiss* and*, S.salar*. It is hoped that the results from future experiments with these microarrays, as well as those presented here will help to steer research in novel directions.

The first microarray constructed was specific for the brain and contained clones (5760) from the brain alone which were taken from the brain *att*B subtracted library (4224 clones) and the brain SSH library (1536 clones). The second microarray type was a multi-tissue SSH microarray that contained clones (6144) from the four SSH cDNA libraries from brain, gill, kidney and intestine (1536 clones from each). The results from the SSH array experiments were gathered by Dr S. Kalujnaia and as such are not presented in this thesis. The SSH array results can, however, be found in appendices 1 and 2 which refer to the published journal articles (Kalujnaia, McWilliam et al, 2006 and Kalujnaia, McWilliam et al, 2007).

Both array types were supplemented with an additional 96 cDNAs comprising known eel genes or coding regions of genes from other species were used as controls to test the stringency and probe specificities under the hybridisation conditions used. For both arrays, each cDNA was printed in three different locations to give three technical replicates per slide. The arrays were spotted onto GAPS II Coated Slides by the Liverpool Microarray Facility (LMF, The University of Liverpool).

Extensive problems with the quality of the printing carried out by the LMF were encountered, they included poor spot quality (black holes, doughnuts, unequal spot sizes), misaligned printing (overlapping spots, kinks

in rows) and inconsistent printing (manifested as banding across hybridised microarrays). The Liverpool Microarray Facility was a relatively new unit when they were printing the eel microarrays and it may have been beneficial to use a more experienced group. The contractual obligations of the NERC grant meant that funding for this part of the project had already been allocated to the LMF. Nevertheless, through extensive dialogue and troubleshooting with the LMF, microarrays of an acceptable quality were produced.

Many of the problems we encountered with the microarray printing can be attributed to the spotting robot used which spots the features using pins which first dip into the PCR amplicons and then makes contact with the surface of the array. This contact does not provide an accurate and reproducible feature and also can damage the delicate surface coating of the array. Recent advances in microarray printing technology, however, could circumvent many of the problems we encountered. By marrying inkjet technology to microarray production, bespoke arrays can now be produced using non-contact printing (Hall, 2006). The LMF have already invested in an Arrayjet inkjet spotter and the *A.anguilla* microarrays may see the benefit of this in the future.

The differences in brain gene expression between yellow, juvenile sexually immature eels and silver, sexually maturing, migrating eels were examined using the brain microarray. cDNA made from amplified brain total RNA taken from the yellow, 7 day FW-acclimated and silver, long term FW-acclimated eel groups was co-hybridised to a brain array, and the experiment repeated in dye-swap to obtain consistent results. Two sets of microarray data were obtained from these experiments. The first data-set used identical scanning intensities for Cy3 and Cy5 channels in both forward and dye-swap experiments whilst the second data-set represented Cy3 and Cy5 channels scanned under different laser intensities in an attempt to compensate for intrinsic differences of Cy3 and Cy5 fluorescence. Both data-sets were normalised using the MADSCAN process (Le Meur et al., 2004) and differences in gene expression between the two developmental conditions were recorded as fold changes. The fold changes in both data sets were very

similar indicating that the normalisation process worked well. A relatively small number of genes (70) showed a greater than 1.5 fold up- or down-regulation in the eel brain following the transition from the yellow to silver developmental stage. Of the 70 genes identified, 47 were from the *att*B subtracted brain library and they represented 43 different genes, with only one gene being represented twice and an additional three genes that were unidentifiable due to sequencing failure. There were 23 genes identified from the SSH brain library but these represented only 9 potentially different genes and one gene which was unidentifiable due to sequencing failure. The remaining 13 genes comprised 4 genes that were unidentifiable by either blastx or blastn due to limited sequence information, and 9 redundant clones which included 5 copies of a glutathione S-transferase homologue and 4 copies of a neuronal-specific septin homologue, a GTPase enzyme with multiple roles in cytokinesis, cell polarity and exocytosis (Xue et al., 2004). These results echo the preliminary redundancy sequencing results which indicated that the SSH brain library had a high (~26 %) redundancy level whilst the *att*B subtracted brain library had a very low (~4 %) redundancy level. The longer clones of the *att*B subtracted brain library permitted successful identification of all genes for which good sequencing results were obtained, whilst the shorter clones in the SSH brain library meant that some genes (18 %) were not identifiable by homology searches.

The differences in brain gene expression during salinity adaptation of silver eels were also examined. cDNA made from mRNA from the silver, 2 day, FW- and SW-acclimated groups was co-hybridised to the brain microarray with dye-swap replication of the experiment. Microarray data was extracted and analysed at only one laser intensity as the previous yellow-silver experiment showed near identical results in both analyses. The genes (37) with the largest changes in expression were selected for sequencing analysis. Of these genes, 29 were from the *att*B subtracted brain library which represented 26 different genes, the sequencing of two of the clones failed and one could not be identified by blastx or blastn sequence analysis. The remaining 9 genes were from the SSH brain library, of which 4 were identified as different genes, 4 could not be identified by either blastx or blastn

and one sequencing reaction failed. The brain *att*B subtracted library is again shown to have a low level of redundancy and the longer clones of which it comprises offer easier clone identification that those in the brain SSH library.

5.4 Future studies

There appear to be any number of directions in which this project could now be directed. Firstly, with regards to the protocol for making subtracted *att*B cDNA libraries; this could be applied to the other tissues in the eel to create a single highly representative library and used to create a microarray to be used to look at the majority of eel genes simultaneously. Special efforts could also be made to ensure all genes of interest, including those involved in the pathways mentioned above are represented.

To elaborate on the current microarray findings, several lines of investigation could be followed. Further QPCR analysis is necessary to validate other genes of interest from the microarray; especially addressing the prolactin expression in the brain of yellow and silver FW adapted eels. Elucidating the potential seasonality and lunar rhythmicity of systems associated with sexual maturation would require biologically relevant sampling of eels exposed to light and temperature conditions mimicking the natural environment. QPCR assays could also be applied to RNA extracted from dissected brains to localise the expression of particular genes to specific areas, such as the pineal organ. Immunohistochemistry could also be used for more precise localisation of expressed genes of interest.

As well as providing a valuable tool for research into eel development and osmoregulation, it is hoped that the protocols developed here, especially the method for cDNA library production, can be applied to other questions in other species.

6.0 References

Adams and John, v. C.-R. R. M., 1999. 191. (1999). Ocean Currents: Redmond: Microsoft.

Aitken, A. (1995). 14-3-3 proteins on the MAP. *Trends Biochem Sci* **20**, 95-7.

Aitken, A., Collinge, D. B., van Heusden, B. P., Isobe, T., Roseboom, P. H., Rosenfeld, G. and Soll, J. (1992). 14-3-3 proteins: a highly conserved, widespread family of eukaryotic proteins. *Trends Biochem Sci* **17**, 498-501.

Alonso, A. (2003). Tyrosine phosphorylation of VHR phosphatase by ZAP-70 (kinase). *Nature Immunol.* **4**, 44-48.

Altschul, S. F., Madden, T. L., Schaffer, A. A., Zhang, J., Zhang, Z., Miller, W. and Lipman, D. J. (1997). Gapped BLAST and PSI-BLAST: a new generation of protein database search programs. *Nucl. Acids Res.* **25**, 3389-3402.

Ammar, A. A., Sederholm, F., Saito, T. R., Scheurink, A. J., Johnson, A. E. and Sodersten, P. (2000). NPY-leptin: opposing effects on appetitive and consummatory ingestive behavior and sexual behavior. *Am J Physiol Regul Integr Comp Physiol* **278**, R1627-33.

Ando, M. (1981). Effects of ouabain on chloride movements across the seawater eel intestine. *Journal of Comparative Pysiology* **145**, 73-79.

Ando, M. (1990). Effects of bicarbonate on salt and water transport across the intestine of the seawater eel. *Journal of Experimental Biology* **150**, 367-379.

Ando, M. and Subramanyam, M. (1990b). Bicarbonate transport systems in the intestine of the seawater eel. *Journal of Experimental Biology* **150**, 381-394.

Aoyama, J., Hissmann, K., Yoshinga, T., Sasai, S., Uto, T. and Ueda, H. (1999). Swimming depth of migrating silver eels *Anguilla japonica* released at seamounts off the West Mariana Ridge, their estimated spawning sites. *Marine Ecology Progress Series* **186**, 265-269.

Aplin, A. E., Stewart, S. A., Assoian, R. K. and Juliano, R. L. (2001). Integrin-mediated adhesion regulates ERK nuclear translocation and phosphorylation of Elk-1. *J. Cell. Biol.* **153**, 273-281.

Appelbaum, L., Vallone, D., Anzulovich, A., Ziv, L., Tom, M., Foulkes, N. S. and Gothilf, Y. (2006). Zebrafish arylalkylamine-N-acetyltransferase genes - targets for regulation of the circadian clock. *J Mol Endocrinol* **36**, 337-347.

Aristotle. (350 B.C.). The History of Animals. Adelaide: eBooks@Adelaide.

Asaoka, Y., Mano, H., Kojima, D. and Fukada, Y. (2002). Pineal expression-promoting element (PIPE), a cis-acting element, directs pineal-specific gene expression in zebrafish. *Proc Natl Acad Sci U S A* **99**, 15456-61.

Ashburner, M., Ball, C. A., Blake, J. A., Botstein, D., Butler, H., Cherry, J. M., Davis, A. P., Dolinski, K., Dwight, S. S., Eppig, J. T. et al. (2000). Gene Ontology: tool for the unification of biology. *Nat Genet* **25**, 25-29.

Babakov, A. V., Chelysheva, V. V., Klychnikov, O. I., Zorinyanz, S. E., Trofimova, M. S. and De Boer, A. H. (2000). Involvement of 14-3-3 proteins in the osmotic regulation of H+-ATPase in plant plasma membranes. *Planta* **211**, 446–448.

Baldin, V. (2000). 14-3-3 proteins and growth control. *Prog Cell Cycle Res* **4**, 49-60.

Baldisserotto, B. and Mimura, O. M. (1994). Ion transport across the isolated mucosa of *Anguilla anguilla*. *Comparitive Biochemistry and Physiology* **108A**, 297-302.

Barash, I. A., Cheung, C. C., Weigle, D. S., Ren, H., Kabigting, E. B., Kuijper, J. L., Clifton, D. K. and Steiner, R. A. (1996). Leptin is a metabolic signal to the reproductive system. *Endocrinology* **137**, 3144-3147.

Barrett, R. K. and Takahashi, J. S. (1999). Temperature compensation and temperature entrainment of the chick pineal cell circadian clock. *Journal of Neuroscience* **15**, 5681–5692.

Baskin, D. G., Schwartz, M. W., Seeley, R. J., Woods, S. C., Porte, D., Jr., Breininger, J. F., Jonak, Z., Schaefer, J., Krouse, M., Burghardt, C. et al. (1999). Leptin Receptor Long-form Splice-variant Protein Expression in Neuron Cell Bodies of the Brain and Co-localization with Neuropeptide Y mRNA in the Arcuate Nucleus. *J. Histochem. Cytochem.* **47**, 353-362.

Bast, H. D. and Klinkhardt, M. B. (1988). Catch of a silver eel (*Anguilla anguilla* (L., 1758)) in the Iberian Basin (Northeast Atlantic) (Teleostei: Anguillidae). *Zool. Anz.* **221**, 386-398.

Ben-Jonathan, N. and Hnasko, R. (2001). Dopamine as a Prolactin (PRL) Inhibitor. *Endocr Rev* **22**, 724-763.

Berger, S. and Kimmel, A. (1987). Guide to molecular cloning techniques. In *Methods in Enzymology*, vol. 152 (ed. J. N. a. S. Abelson, M.I.), pp. 256-258. San Diego: Academic Press.

Bernard, B., Tomasz, M., Jean-Michel, D., Francis, G., Serge, S.-P. and Hubert, V. (1989). Neuropeptide Y (NPY) modulates in vitro gonadotropin in release from rainbow trout pituitary glands. *Fish Physiology and Biochemistry* **V7**, 77-83.

Berson, D. M., Dunn, F. A. and Takao, M. (2002). Phototransduction by retinal ganglion cells that set the circadian clock. *Science* **295**, 1070-3.

Beyenbach, K. (1995). Secretory electrolyte transport in renal proximal tubules of fish. San Diego: Academic Press.

Beyenbach, K. W. (2004). Kidneys sans glomeruli. *American Journal of Physiology* **286**, F811-827.

Beyenbach, K. W. and Wieczorek, H. (2006). The V-type H+ ATPase: molecular structure and function, physiological roles and regulation. *J Exp Biol* **209**, 577-589.

Bhalla, U. S., Ram, P. T. and Iyengar, R. (2002). MAP kinase phosphatase as a locus of flexibility in a mitogen-activated protein kinase signaling network. *Science* **297**, 1018-1023.

Bini, E., Dikshit, V., Dirksen, K., Drozda, M. and Blum, P. (2002). Stability of mRNA in the hyperthermophilic archaeon Sulfolobus solfacatrius. *RNA* **8**, 1129-1136.

Bishop, J., Morton, J., Rosbash, M. and Richardson, M. (1974). Three abundance classes in HeLa cell messenger RNA. *Nature Biotechnology* **250**, 199–204.

Blanco, S., Klimcakova, L., Vega, F. M. and Lazo, P. A. (2006). The subcellular localization of vaccinia-related kinase-2 (VRK2) isoforms determines their different effect on p53 stability in tumour cell lines. *Febs J* **273**, 2487-504.

Bolton, J. P., Collie, N. L., Kawauchi, H. and Hirano, T. (1987). Osmoregulatory actions of growth hormone in rainbow trout (*Salmo gairdneri*). *Journal of Endocrinology* **112**, 63-68.

Bonaldo, M. F., Lennon, G. and Soares, M. B. (1996). Normalization and subtraction: two approaches to facilitate gene discovery. *Genome Res.* **6**, 791-806.

Bone, Q., Marshall, N. B. and Blaxter, J. H. S. (1995). Biology of Fishes. London: Blackie Academic and Professional.

Bonga, S. (1997). The stress response in fish. *Physiological Reviews* **77**, 591-625.

Bonnin, J.-P. (1981). Effect de la prolactine ovine sur la testosterone plasmatique et le tractus genital male chez *Gobius niger* L. . *C R Acad Sci Paris* **292**, 319-322.

Borgnia, M., Nielsen, S., Engel, A. and Agre, P. (1999). Cellular and molecular boilogy of the aquaporin water channels. *Annual Review of Biochemistry* **68**, 425-458.

Boubée, J., Mitchell, C., Chisnall, B., West, D., Bowman, E. and Haro, A. (2000). Factors regulating the downstream migration of mature eels (*Anguilla* spp.) at Aniwhenua Dam, Bay of Plenty, New Zealand. *New Zealand Journal of Marine and Freshwater Research* **35**, 121-134.

Braun, E. J. and Dantzler, W. H. (1997). Vertebrate renal system.

Brazma, A., Hingamp, P., Quackenbush, J., Sherlock, G., Spellman, P., Stoeckert, C., Aach, J., Ansorge, W., Ball, C., Causton, H. et al. (2001). Minimum information about a microarray experiment (MIAME) - toward standards for microarray data. *Nature Genetics* **29**, 365-371.

Bridges, D. and Moorhead, G. B. G. (2005). 14-3-3 Proteins: A Number of Functions for a Numbered Protein. *Sci. STKE* **2005**, re10-.

Brondello, J. M., Pouyssegur, J. and McKenzie, F. R. (1999). Reduced MAP kinase phosphatase-1 degradation after p42/p44MAPK-dependent phosphorylation. *Science* **286**, 2514-2517.

Burke, S. (2001). Missing Values, Outliers, Robust Statistics & Nonparametric Methods. : LC.GC.

Bustin, S. A. (2002). Quantification of mRNA using real-time reverse transcription PCR (RT-PCR): trends and problems. *Journal of Molecular Endocrinology* **29**, 23-39.

Campbell, A. M. (1961). Episomes. *Adv. Genet* **11**, 101-145.

Campfield, L. A., Smith, F. J., Guisez, Y., Devos, R. and Burn, P. (1995). Recombinant mouse OB protein: evidence for a peripheral signal linking adiposity and central neural networks. *Science* **269**, 546-549.

Camps, M. (1998). Catalytic activation of the phosphatase MKP-3 by ERK2 mitogen-activated protein kinase. *Science* **280**, 1262-1265.

Camps, M., Nichols, A. and Arkinstall, S. (2000). Dual specificity phosphatases: a gene family for control of MAP kinase function. *FASEB J.* **14**, 6-16.

Carninci, P., Shibata, Y., Hayatsu, N., Sugahara, Y., Shibata, K., Itoh, M., Konno, H., Okazaki, Y., Muramatsu, M. and Hayashizaki, Y. (2000). Normalization and subtraction of cap-trapper-selected cDNAs to prepare full-length cDNA libraries for rapid discovery of new genes. *Genome Research* **10**, 1617-1630.

Castelli, M. (2004). MAP kinase phosphatase 3 (MKP3) interacts with and is phosphorylated by protein kinase CK2[alpha]. *J. Biol. Chem.* **279**, 44731-44739.

Castonguay, M., Hodson, P. V., Moriarty, C., Drinkwater, K. F. and Jessop, B. M. (1994). Is there a role of ocean environment in American and European eel decline? *Fish Oceanography* **3**, 197-203.

Cerda-Reverter, J. M., Sorbera, L. A., Carrillo, M. and Zanuy, S. (1999). Energetic dependence of NPY-induced LH secretion in a teleost fish (*Dicentrarchus labrax*). *Am J Physiol Regul Integr Comp Physiol* **277**, R1627-1634.

Chan, H. C., Wu, W. L., So, S. C., Chung, Y. W., Tsang, L. L., Wang, X., F., Y., Y. C., Luk, S. C., Siu, S. S., Tsui, S. K. et al. (2000). Modulation of the Ca^{2+}-activated Cl^- channel by 14-3-3e. *Biochem. Biophys. Res. Commun.* **270**, 581-587.

Chan, K. M., Tse, M., Xiao, P., Wong, G. K.-P. and Cheng, C. H. F. (2006). Prolactin gene regulations in goldfish (*Carassius auratus*). *Personal communication- presented at 23rd Conference of European Comparative Endocrinologists 2006*.

Chang, L. and Karin, M. (2001). Mammalian MAP kinase signalling cascades. *Nature* **410**, 37-40.

Chehab, F. F., Lim, M. E. and Lu, R. (1996). Correction of the sterility defect in homozygous obese female mice by treatment with the human recombinant leptin. *Nat Genet* **12**, 318-20.

Chelysheva, V. V., Smolenskaya, I. N., Trofimova, M. C., Babakov, A. V. and Muromtsev, G. S. (1999). Role of the 14-3-3 proteins in the regulation of H+-ATPase activity in the plasma membrane of suspension-cultured sugar beet cells under cold stress. *FEBS Lett* **456**, 22-6.

Chenchik A, Zhu, Y. Y., Diatchenko, L., Li, R., Hill, J. and Siebert, P. D. (1998). Gene Cloning and Analysis by RT-PCR. Natick, MA, .

Chomczynski, P. and Sacchi, N. (1987). Single step method of isolation by acid guanidinium thiocynate-phenol-chloroform extraction. *Analytical Biochemistry* **162**, 156-159.

Churchill, G. A. (2002). Fundamentals of experimental design for cDNA microarrays. *Nature Genetics Supplement.* **32**, 490-495.

Cleveland, J., P.H. and Trump, B. F. (1969). Excretion, Ionic Regulation and Metabolism: The kidney. New York: Academic Press.

Cocquet, J., Chong, A., Zhang, G. L. and Veitia, R. A. (2006). Reverse transcriptase template switching and false alternative transcripts. *Genomics* **88**, 127-131.

Cossins, A. R. and Crawford, D. L. (2005). Fish as Models for Environmental Genomics. *Nature Reviews Genetics* **6**, 324-333.

Cramb, G., Martinez, A.-S., McWilliam, I. S. and Wilson, G. D. (2005). Cloning and Expression of Guanylin-like Peptides in Teleost Fish. *Annals of the New York Academy of Sciences* **1040**, 277-280.

Crombie, H. J., Bell, M. V. and Tytler, P. (1996). Inhibition of sodium-plus-potassium-stimulated adenosine-triphosphatase (Na+-K+-ATPase) by protein kinase C activators in the gills of Atlantic cod (Gadus morhua). *Comparitive Biochemistry and Physiology* **B 113**, 765–772.

Cullen, P. and McCarthy, T. K. (2003). Hydrometric and Meteorological Factors Affecting the Seaward Migration of Silver eels (*Anguilla anguilla*, L.) in the Lower River Shannon. *Environmental Biology of Fishes* **67**, 349-357.

Cutler, C. P. and Cramb, G. (2000). Water transport and aquaporin expression in fish. New York: Kluwer Academic/ Plenum Publishers.

Cutler, C. P. and Cramb, G. (2001). Molecular physiology of osmoregulation in eels and other teleosts: the role of transporter isoforms and gene duplication. *Comparative Biochemistry and Physiology Part A* **130**, 551-564.

Cutler, C. P. and Cramb, G. (2002). Branchial expression of an aquaporin 3 (AQP3) homologue is downregulated in the European ell *Anguilla anguilla* following seawater acclimation. *Journal of Experimental Biology* **205**, 2643-2651.

Cutler, C. P. and Cramb, G. (2002b). Two isoforms of the Na+/K+/2Cl- cotransporter are expressed in the European eel (*Anguilla anguilla*). *Biochimica et Biophysica Acta* **1566**, 92-103.

Dang, Z., Balm, P.H., Flik, G., Wendelaar Bonga, S.E., Lock, R.A. (2004). Cortisol increases Na^+,K^+-ATPase density in plasma memebranes of gill chloride cells in the freshwater tilapia *Oreochromis mossambicus*. *Journal of Experimental Biology* **203**, 2349-2355.

Dantzler, W. H. (2003). Regulation of renal proximal and distal tubule transport: sodium, chloride and organic anions. *Comparitive Biochemistry and Physiology* **136A**, 453-478.

Davidson, E. and Britten, R. (1979). Regulation of gene expression: possible role of repetitive sequences. *Science* **204**, 1052–1059.

de Pedro, N., Martinez-Alvarez, R. and Delgado, M. J. (2006). Acute and chronic leptin reduces food intake and body weight in goldfish (*Carassius auratus*). *J Endocrinol* **188**, 513-520.

Deelder, C. (1981). On the age and growth of cultured eels (*Anguilla anguilla* Linnaeus)). *Aquaculture* **26**, 13-22.

Deen, P. M. T. and van Os, C. H. (1998). Epithelial Aquaporins. *Current Opinion in Cell Biology* **10**, 435-442.

Degani, G., Goldberg, D., Tzchor, I. I., Hurvitz, A., Yom Din, S. and Jackson, K. (2003). Cloning of European eel (*Anguilla anguilla*) FSH-β subunit, and expression of FSH-β and LH-β in males and females after sex determination. **136**, 283-293.

Degnan, K. J. (1985). The role of K+ and Cl- conductances in chloride secretion by the opercular epithelium. *Journal of Eperimental Zoology* **236**, 19-25 (Cited in Marshall, W.S., 1995).

Dekker, W. (2003). Worldwide decline of eel resources necessitates immediate action. *Fisheries* **28**, 28-30.

Dheda, K., Huggett, J. F., Bustin, S. A., Johnson, M. A., Rook, G. and Zumla, A. (2004). Validation of housekeeping genes for normalizing RNA expression in real-time PCR. *Biotechniques* **37**, 112-4, 116, 118-9.

Diatchenko, L., Lau, Y. F. C., Campbell, A. P., Chenchik, A., Moqadam, F., Huang, B., Lukyanov, S., Gurskaya, N., Sverdlov, E. D. and Siebert, P. D. (1996). Suppression subtractive hybridization: a method for generating differentially regulated or tissue-specific cDNA probes and libraries. . *Proceedings of the National Academy of Sciences of the United States of America* **93**, 6025-6030.

Draghici, S. (2003). Data Analysis Tools for DNA Microarrays. . Florida: Chapman & HallBoca Raton.

Dudoit, S., Yang, Y. H., Callow, M. and Speed, T. P. (2000). Statistical methods for identifying differentially expressed genes in replicated cDNA microarray experiments. *Statistics* **578**.

Dufour, S., Burzawa-Ge´rard, E., Le Belle, N., Sbaihi, M. and Vidal, B. (2003). Reproductive endocrinology of the European eel, Anguilla anguilla. Tokyo: Springer Verlag.

Dufour, S., Delerue-Le Belle, N. and Fontaine, Y. A. (1983). Effects of steroid hormones on pituitary immunoreactive gonadotropin in European freshwater eel, *Anguilla anguilla* L. *Gen Comp Endocrinol* **52**, 190-197.

Eberwine, J., Yeh, H., Miyashiro, K., Cao, Y. X., Nair, S., Finnell, R., Zettel, M. and Coleman, P. (1992). Analysis of Gene-Expression in Single Live Neurons. *Proceedings of the National Academy of Sciences of the United States of America* **89**, 3010-3014.

Eisen, M. B., Spellman, P. T., Brown, P. O. and Botstein, D. (1998). Cluster analysis and display of genome-wide expression patterns. *Proceedings of the National Academy of Sciences* **95**, 14863-14868.

Ekstrom, P. and Meissl, H. (1997). The pineal organ of teleost fishes. *Reviews in Fish Biology and Fisheries* **V7**, 199-284.

Ellerby, D., Spierts, I. and Altringham, J. (2001). Slow muscle power output of yellow- and silver-phase European eels (Anguilla anguilla): changes in muscle performance prior to migration. *Journal of Experimental Biology* **204**, 1369-1379.

Emanuel, J. R., Garetz, S., Stone, L. and Levenson, R. (1987). Differential expression of Na^+,K^+-ATPase a- and a-subunit mRNAs in rat tissues and cell lines (a-subunit isoforms/development). *Proceedings of the National Academy of Sciences USA: Cell Biology* **84**, 9030-9034.

Ernst, P. (1977). Catch of an eel (*Anguilla anguilla*) northeast of the Faroe Islands. *Ann. Biol.* **32**, 175.

EU-Communication:IP/03/1332. (2005). Commission proposes EU action to protect European eels: European Union.

Evans, D. (2002). Cell signalling and ion transport across the fish gill epithelium. *Journal of Experimental Zoology* **293**, 336-347.

Evans, D. H., Piermarini, P. M. and Potts, W. T. W. (1999). Ionic transport in the fish gill epithelium. *Journal of Experimental Zoology* **283**, 641-652.

Falcon, J., Besseau, L., Fazzari, D., Attia, J., Gaildrat, P., Beauchaud, M. and Boeuf, G. (2003). Melatonin Modulates Secretion of Growth Hormone and Prolactin by Trout Pituitary Glands and Cells in Culture. *Endocrinology* **144**, 4648-4658.

Farooq, A. (2001). Solution structure of ERK2 binding domain of MAPK phosphatase MKP-3: Structural insights into MKP-3 activation by ERK2. *Mol. Cell* **7**, 387-399.

Farrell, A. and Olson, K. (1999). Cardiac natriuretic peptides: A physiological lineage of cardioprotective hormones? *Physiological and Biochemical Zoology* **73**, 1-11.

Feldman, A. L., Costouros, N. G., Wang, E., Qian, M., Marincola, F. M., Alexander, H. R. and Libutti, S. K. (2002). Advantages of mRNA amplification for microarray analysis. *Biotechniques* **33**, 906.

Ferl, R., Manak, M. and Reyes, M. (2002). The 14-3-3s. *Genome Biology* **3**, reviews 3010.1 - reviews 3010.7.

Feunteun, E., Acou, A., Lafaille, P. and Legault, A. (2000). The European Eel: prediction of spawner escapement from continental population parameters. . *Canadian Journal of Fisheries and Aquatic Sciences* **57**.

Fiol, D. E. and Kultz, D. (2005). Rapid hyperosmotic coinduction of two tilapia (Oreochromis mossambicus) transcription factors in gill cells. . *PNAS* **102**, 927-932.

Fontaine, M. (1936). Sur la maturation comple`te des organes ge´nitaux de l'anguille ma^le et l'e´mission spontane´e de ses produits sexuels. *C R Acad Sci Paris* **202**, 1312-1315.

Foster, D. L. and Nagatani, S. (1999). Physiological Perspectives on Leptin as a Regulator of Reproduction: Role in Timing Puberty. *Biol Reprod* **60**, 205-215.

Foster, R. G., Hankins, M., Lucas, R. J., Jenkins, A., Munoz, M., Thompson, S., Appleford, J. M. and Bellingham, J. (2003). Non-rod, non-cone photoreception in rodents and teleost fish. *Novartis Found Symp* **253**, 3-23; discussion 23-30, 52-5, 102-9.

Freed, E., Symons, M., Macdonald, S. G., McCormick, F. and Ruggieri, R. (1994). Binding of 14-3-3 proteins to the protein kinase Raf and effects on its activation. *Science* **265**, 1713-1716.

Fu, H., Subramanian, R. R. and Masters, S. C. (2000). 14-3-3 Proteins: Structure, Function, and Regulation. *Annual Review of Pharmacology and Toxicology* **40**, 617-647.

Fuglsang, A. T., Visconti, S., Drumm, K., Jahn, T., Stensballe, A., Mattei, B., Jensen, O. N., Aducci, P. and Palmgren, M. G. (1999). Binding of 14-3-3 protein to the plasma membrane H+-ATPase AHA2 involves the three C-terminal residues Tyr(946)-Thr-Val and requires phosphorylation of Thr(947). *J. Biol. Chem.* **274**, 36774–36780.

Gaildrat, P. and Falcon, J. (2000). Melatonin receptors in the pituitary of a teleost fish: mRNA expression, 2-[(125)I]iodomelatonin binding and cyclic AMP response. *Neuroendocrinology* **72**, 57-66.

Gaitskell, R. E. and Jones, I. C. (1971). Drinking and urine production in the European eel (*Anguilla anguilla* L.). *Gen Comp Endocrinol* **16**, 478-83.

Ganguly, S., Gastel, J. A., Weller, J. L., Schwartz, C., Jaffe, H., Namboodiri, M. A. A., Coon, S. L., Hickman, A. B., Rollag, M., Obsil, T. et al. (2001). Role of a pineal cAMP-

operated arylalkylamine N-acetyltransferase/14-3-3-binding switch in melatonin synthesis. *PNAS* **98**, 8083-8088.

Ganguly, S., Weller, J. L., Ho, A., Chemineau, P., Malpaux, B. and Klein, D. C. (2005). Melatonin synthesis: 14-3-3-dependent activation and inhibition of arylalkylamine N-acetyltransferase mediated by phosphoserine-205. *PNAS* **102**, 1222-1227.

Goss, G. G., Adamia, S., Galvez, F. (2001). Peanut lectin binds to a subpopulation of mitochonria-rich cellsin the rainbow trout gill epithelium. *American Journal of Physiology* **215**.

Gracey, A. Y., Troll, J. V. and Somero, G. N. (2001). Hypoxia-induced gene expression profiling in the euryoxic fish Gillichthys mirabilis. *Proceedings of the National Academy of Sciences of the United States of America* **98**, 1993-1998.

Green, N. M. (1975). Avidin. *Advances in Protein Chemistry* **29**, 85-133.

Gringhuis, S. I., Garcia-Vallejo, J. J., van Het Hof, B. and van Dijk, W. (2005). Convergent actions of I kappa B kinase beta and protein kinase C delta modulate mRNA stability through phosphorylation of 14-3-3 beta complexed with tristetraprolin. *Mol Cell Biol* **25**, 6454-63.

Grossel, M., Laliberte, S., Wood, S., Jensen, F. B. and Wood, C. M. (2001). Intestinal bicarbonate secretion in marine teleost fish: evidence for an apical, rather than basolateral Cl^- /HCO_3^+ exchanger. *Fish Physiology and Biochemistry* **24**, 81.

Gwag, B. J. (1998). A neuron-specific gene transfer by a recombinant defective Sindbis virus. *Mol. Brain Res.* **63**, 53-61.

Haas, M. and Forbush III, B. (2000). The Na-K-Cl cotransporter of secretory epithelia. *Annual Review of Physiology* **62**, 515-534.

Hahn, W. and Owens, G. (1988). The Molecular Biology of Neurological Disease. London: Butterworths.

Hain, J. H. W. (1975). The behaviour of migratory eels,Anguilla rostrata, in response to current, salinity and lunar period. *Helgoland Marine Research* **V27**, 211-233.

Halkin, D. and Rossby, T. (1985). The structure and transport of the Gulf Stream at 73 º west. *Journal of Physical Oceanography* **15**, 1439-1452.

Hall, D. (2006). Producing protein microarrays for drug discovery. *DrugPlus International.* Novmber.

Hall, S. H., Joseph, D. R., French, F. S. and Conti, M. (1988). Follicle-stimulating hormone induces transient expression of the protooncogene c-fos in primary Sertoli cell cultures. *Mol Endocrinol* **2**, 55-61.

Han, Y. S., Tzeng, W. N. and Yu, J. Y.-L. (2004). Cloning of the cDNA for thyroid stimulating hormone subunit and changes in activity of the pituitary–thyroid axis during silvering of the Japanese eel, Anguilla japonica. *Journal of Molecular Endocrinology* **32**, 179-194.

Han, Y. S., Yu, J. Y. L., Liao, I. C. and Tzeng, W. N. (2003). Salinity preference of silvering Japanese eel Anguilla japonica: evidence from pituitary prolactin mRNA levels and otolith Sr:Ca ratios. *Marine Ecology Progress Series* **259**, 253-261.

Hartley, J. A. S., R.L. and Berardini, M.D. (1993). Electrophoretic and chromatographic-separation methods used to reveal interstrand cross-linking of nucleic acids. *Journal of Chromatography - Biomedical Applications* **618**, 277-288.

Hawkings, G. S., Galvez, F. and Goss, G. G. (2004). Seawater acclimation causes independent alterations in Na^+/K^+- and H^+-ATPase activity in isolated mitochondria-rich cell subtypes of the rainbow trout gill. *J Exp Biol* **207**, 905-912.

Heinsbroek, L. T. N. (1991). A review of eel culture in Japan and Europe. *Aquaculture and Fisheries Management* **22**, 57-72.

Hentschel, H. and Elger, M. (1989). Morphology of glomerular and aglomerular kidneys. Basel: Karger.

Hernández-Rauda, R., Miguez, J. M., Ruibal, J. M. and Aldegunde, M. (2000). Effects of melatonin on dopamine metabolism in the hypothalamus and the pituitary of the rainbow trout, (*Oncorhynchus mykiss*). *Journal of Experimental Zoology* **287**, 440-444.

Higgs, D. R., Goodbourn, S. E., Lamb, J., Clegg, J. B., Weatherall, D. J. and Proudfoot, N. J. (1983). Alpha-thalassaemia caused by a polyadenylation signal mutation. *Nature* **306**, 398-400.

Hiller, Y., Gershoni, J. M., Bayer, E. A. and Wilchek, M. (1987). Biotin binding to avidin. Oligosaccharide side chain not required for ligand association. *Biochem J* **248**, 167-171.

Hirano, T. (1974). Some factors regulating water intake by the eel *Anguilla japonica*. *Journal of Experimental Biology* **61**, 737-747.

Hodge, C. (1998). Growth hormone stimulates phosphorylation and activation of elk-1 and expression of c-fos, egr-1, and junB through activation of extracellular signal-regulated kinases 1 and 2. *J. Biol. Chem.* **273**, 31327-31336.

Hubbard, T., Andrews, D., Caccamo, M., Cameron, G., Chen, Y., Clamp, M., Clarke, L., Coates, G., T. Cox, F.Cunningham et al. (2005). ENSEMBL. *Nucleic Acids Research* **33**, D447-D453.

Huising, M. O., Geven, E. J. W., Kruiswijk, C. P., Nabuurs, S. B., Stolte, E. H., Spanings, F. A. T., Verburg-van Kemenade, B. M. L. and Flik, G. (2006). Increased Leptin Expression in Common Carp (*Cyprinus carpio*) after Food Intake But Not after Fasting or Feeding to Satiation. *Endocrinology* **147**, 5786-5797.

Hutter, D., Chen, P., Barnes, J. and Liu, Y. (2000). Catalytic activation of mitogen-activated protein (MAP) kinase phosphatase-1 by binding to p38 MAP kinase: critical role of the p38 C-terminal domain in its negative regulation. *Biochem. J.* **352**, 155-163.

Ichimura, T., Ito, M., Itagaki, C., Takahashi, M., Horigome, T., Omata, S., Ohno, S. and Isobe, T. (1997). The 14-3-3 protein binds its target proteins with a common site located towards the C-terminus. *FEBS Letters* **413**, 273-276.

Isaia, J. (1984). Water and Nonelectrolyte Permeation. London: Academic Press.

Ishiguro, T., Saitoh, J., Yawata, H., Yamagishi, H., Iwasaki, S. and Mitoma, Y. (1995). Homogeneous Quantitative Assay of Hepatitis C Virus RNA by Polymerase Chain Reaction in the Presence of a Fluorescent Intercalater. *Analytical Biochemistry* **229**, 207-213.

Isobe, T., Hiyane, Y., Ichimura, T., Okuyama, T., Takahashi, N., Nakajo, S. and K., N. (1992). Activation of protein kinase C by the 14-3-3 proteins homologous with Exo1 protein that stimulates calcium-dependent exocytosis. *FEBS Lett* **308**, 121-4.

Jacobson, A. (1987). Purification and fractionation of Poly(A+) RNA. In *Guide to molecular cloning techniques*, vol. 152 eds. S. L. Berger and A. R. Kimmel), pp. 254-261. London: Academic Press.

James, B. D. and Higgins, S. J. (1985). Nucleic Acid Hybridization. Oxford: IRL Press Ltd.

Jirakulaporn, T. and Muslin, A. J. (2004). Cation Diffusion Facilitator Proteins Modulate Raf-1 Activity. *J. Biol. Chem.* **279**, 27807-27815.

Jones, M. D. and Foulkes, N. S. (1989). Reverse transcription of mRNA by Thermus aquaticus DNA polymerase. *Nucleic Acids Research* **17**, 8387-8388.

Joshi, B. and Mohinuddin, K. (2003). Red light accelerates and melatonin retards metamorphosis of frog tadpoles. *BMC Physiology* **3**, 9.

Kagawa, H., Tanaka, H., Ohta, H., Unuma, T. and Nomura, K. (2005). The first success of glass eel production in the world: basic biology on fish reproduction advances new applied technology in aquaculture. *Fish Physiology and Biochemistry* **31**, 193–199.

Kah, O., Dulka, J., Dubourg, P., Thibault, J. and Peter, R. E. (1987). Neuroanatomical substrate for the inhibition of gonadotrophin secretion in goldfish: Existence of a dopaminergic preoptico-hypophyseal pathway. . *Neuroendocrinology* **45**, 451-458.

Kah, O., Pontet, A., Danger, J. M., Dubourg, P., Pelletier, G., Vaudry, H. and Calas, A. (1989). Characterization, cerebral distribution and gonadotropin release activity of neuropeptide Y (NPY) in the goldfish. *Fish Physiology and Biochemistry* **V7**, 69-76.

Kaiya, H. and Takei, Y. (1996). Atrial and ventricular natriuretic peptide concentrations in plasma of freshwater- and seawater-adapted eels. *General and Comparative Endocrinology* **102**, 183-190.

Kaiya, H. and Takei, Y. (1996b). Changes in plasma atrial and ventricular natriuretic peptide concentration after transfer of eels from freshwater and sea water or vice versa. *General and Comparative Endocrinology* **104**, 337-345.

Kalujnaia, S., McWilliam, I. S., Feilen, A. L., Nicholson, J., Zaguinaiko, V. A., Hazon, N., Cutler, C. P., Balment, R. J., Cossins, A. R., Hughes, M. et al. (2007). Salinity adaptation and gene profiling analysis in the European eel (*Anguilla anguilla*) using microarray technology. *General and Comparative Endocrinology*.

Kalujnaia, S., McWilliam, I. S., Zaguinaiko, V. A., Feilen, A. L., Nicholson, J., Hazon, N., Cutler, C. P. and Cramb, G. (2007b). A transcriptomic approach to the study of osmoregulation in European eel *Anguilla anguilla*. *Physiol. Genomics*, 00059.2007.

Kang, T.-H. and Kim, K.-T. (2006). Negative regulation of ERK activity by VRK3-mediated activation of VHR phosphatase. *Nat Cell Biol* **8**, 863-869.

Karin, M. and Hunter, T. (1995). Transcriptional control by protein phosphorylation: signal transmission from the cell surface to the nucleus. *Curr Biol* **5**, 747-57.

Karnaky, J. J. K. (1998). Osmotic and ionic regulations. New York

CRC Press.

Karnaky, J. J. K., Kinter, W. B. and Stirling, C. E. (1976). Teleost chloride cell. II. Autoradiographic localization of gill Na+,K+-ATPase in killifiah (*Fundulus heteroclitus*) adapted to low and high salinity environments. *Journal of Cell Biology* **70**, 157-177, cited in Marshall, W.S., 1995.

Kelly, S. P. and Peter, R. E. (2006). Prolactin-releasing peptide, food intake, and hydromineral balance in goldfish. *Am J Physiol Regul Integr Comp Physiol* **291**, R1474-1481.

Kerr, M. K., Martin, M. and Churchill, G. A. (2000). Analysis of variance for gene expression microarray data. . *Journal of Computational Biology* **7**, 819-837.

Keyse, S. M. and Emslie, E. A. (1992). Oxidative stress and heat shock induce a human gene encoding a protein tyrosine phosphatase. *Nature* **359**, 644-647.

Kirsch, R., Guinier, D. and Meens, R. (1975). Water balance in the european eel (*Anguilla anguilla* L.). Role of the oesophagus in the utilisation of drinking water and a study of the osmotic permeability of the gills. *J Physiol (Paris)* **70**, 605-26.

Kjarland, E., Keen, T. J. and Kleppe, R. (2006). Does isoform diversity explain functional differences in the 14-3-3 protein family? *Curr Pharm Biotechnol* **7**, 217-23.

Klein, D. C., Ganguly, S., Coon, S. L., Shi, Q., Gaildrat, P., Morin, F., Weller, J. L., Obsil, T., Hickman, A. and Dyda, F. (2003). 14-3-3 Proteins in Pineal Photoneuroendocrine Transduction: How Many Roles? *Journal of Neuroendocrinology* **15**, 370-377.

Klychnikov, O. I., Li, K. W., Lill, H. and de Boer, A. H. (2006). The V-ATPase from etiolated barley (*Hordeum vulgare* L.) shoots is activated by blue light and interacts with 14-3-3 sproteins. *J. Exp. Bot.*, erl261.

Ko, M. (1990). An 'equalized cDNA library' by the reassociation of short double-stranded cDNAs. . *Nucleic Acid Research* **18**, 5705–5711.

Kohn, A., Chakravarty, D. and Kultz, D. (2003). Teleost Fh14-3-3a protein protects Xenopus oocytes from hyperosmolality. *J Exp Zoolog A Comp Exp Biol* **299**, 103-9.

Komourdjian, M. P., Saunders, R. L. and Fenwick., J. C. (1976). The effect of porcine somatotropin on growth and survival in seawater of Atlantic salmon (*Salmo salar*) parr. *Canadian Journal of Zoology* **54**, 531–535.

Korf, H. W., Schomerus, C., Maronde, E. and Stehle, J. H. (1996). Signal Transduction Molecules in the Rat Pineal Organ: Ca^{2+}, pCREB, and ICER. *Naturwissenschaften* **V83**, 535-543.

Koskinen, H., Krasnov, A., Rexroad, C., Gorodilov, Y., Afanasyev, S. and Molsa, H. (2004). The 14-3-3 proteins in the teleost fish rainbow trout (*Oncorhynchus mykiss*). *J Exp Biol* **207**, 3361-3368.

Kozak, M. (1983). Comparison of initiation of protein synthesis in procaryotes, eucaryotes, and organelles. *Microbiol Rev* **47**, 1-45.

Kultz, D., Chakravarty, D. and Adilakshmi, T. (2001). A novel 14-3-3 gene is osmoregulated in gill epithelium of the euryhaline teleost *Fundulus heteroclitus*. *J Exp Biol* **204**, 2975-2985.

Kurokawa, T., Uji, S. and Suzuki, T. (2005). Identification of cDNA coding for a homologue to mammalian leptin from pufferfish, *Takifugu rubripes*. *Peptides* **26**, 745-50.

Lander, E. S. (1999). Array of hope. *Nature Genetics* **21**, 3-4.

Lander, E. S. Linton, L. M. Birren, B. Nusbaum, C. Zody, M. C. Baldwin, J. Devon, K. Dewar, K. Doyle, M. FitzHugh, W. et al. (2001). Initial sequencing and analysis of the human genome. *Nature* **409**, 860-921.

Landy, A. (1989). Dynamic, Structural, and Regulatory Aspects of Lambda Site-specific Recombination. *Annu. Rev. Biochem.* **58**, 913-949.

Larsson, P., Hamrin, S. and Okla, L. (1990). Fat-content as a factor inducing migratory behaviour in the eel (*Anguilla anguilla* L) to the Sargasso Sea. *Naturwissenschaften* **77**, 488-490.

Lauder, G. V. and Liem, K. F. (1983). Patterns of diversity and evolution in ray-finned fishes. . Ann Arbor, MI: University of Michigan Press.

Le Meur, N., Lamirault, G., Bihouee, A., Steenman, M., Bedrine-Ferran, H., Teusan, R., Ramstein, G. and Leger, J. (2004). A dynamic, web-accessible resource to process raw microarray scan data into consolidated gene expression values: importance of replication. *Nucleic Acids Research* **32**, 5349-5358.

Lecomte-Finiger, R. (1992). Growth history and age at recruitment of European glass eel (*Anguilla anguilla*) as revealed by otolith microstructure. *Marine Biology* **114**, 205-210.

Lecomte-Finiger, R. (1994). The early life of the European eel. *Nature* **370**, 424.

Lewis, T. S., Shapiro, P. S. and Ahn, N. G. (1998). Signal transduction through MAP kinase cascades. *Adv Cancer Res* **74**, 49-139.

Li, L. Y., Liu, M. Y., Shih, H. M., Tsai, C. H. and Chen, J. Y. (2006). Human cellular protein VRK2 interacts specifically with Epstein-Barr virus BHRF1, a homologue of Bcl-2, and enhances cell survival. *J Gen Virol* **87**, 2869-78.

Lignot, J. H., Cutler, C. P., Hazon, N. and Cramb, G. (2002). Immunolocalisation of aquaporin 3 in the gill and the gastrointestinal tract of the European eel *Anguilla anguilla*. *Journal of Experimental Biology* **205**, 2656-2663.

Lin, H. and Randall, D. (1995). Proton pumps in fish gills. In *In Cellular and Molecular Approaches to Fish Ionic Regulation*, (ed. T. a. W. Shuttleworth, C.), pp. 229-255. San Diego: Academic Press.

Livak, J. and Schmittgen, T. (2001). Analysis of Relative Gene Expression Data Using Real-Time Quantitative PCR and the 22^{-DDCT} Method. *Methods* **25**, 402-408.

Loflin, P., Chen, C. A. and Shyu, A. (1999). Unravelling a cytoplasmic role for hnRNP D in the in vivo mRNA destabilization directed by the AU-rich element. *Genes Dev.* **13**, 1884-1897.

Loretz, C. and Takei, Y. (1997). Natriuretic peptide inhibition of intestinal salt absorption in the Japanese eel: physiological significance. *Fish Physiology and Biochemistry* **17**, 319-324.

Loretz, C. A. (1995). Electrophysiology of ion transport in the teleost intestinal cells. New York: Academic Press.

Mackintosh, C. (2004). Dynamic interactions between 14-3-3 proteins and phosphoproteins regulate diverse cellular processes. *Biochem J* **381**, 329-42.

Mancera, J. M. and McCormick, S. D. (1998). Evidence for Growth Hormone/Insulin-like Growth Factor I Axis Regulation of Seawater Acclimation in the Euryhaline Teleost *Fundulus heteroclitus*. *General and Comparative Endocrinology* **111**, 103-112.

Marchelidon, J., Schmitz, M., Houdebine, L. M., Vidal, B., Belle, N. L. and Dufour, S. (1996). Development of a Radioimmunoassay for European Eel Growth Hormone and Application to the Study of Silvering and Experimental Fasting. *General and Comparative Endocrinology* **102**, 360-369.

Marchetti, S. (2005). Extracellular signal-regulated kinases phosphorylate mitogen-activated protein kinase phosphatase 3/DUSP6 at serines 159 and 197, two sites critical for its proteasomal degradation. *Mol. Cell. Biol.* **25**, 854-864.

Marshall, W., Emberley, T., Singer, T., Bryson, S. and McCormick, S. (1999). Time course of salinity adaptation in a strongly euryhaline teleost, *Fundulus heteroclitus*: A muyltivariable approach. *Journal of Experimental Biology* **202**, 1535-1544.

Marshall, W. S. (1995). Transport processes in isolated teleost epithelia:opercular epithelium and urinary bladder. San Diego: Academic Press.

Marshall, W. S. and Grossel, M. (2006). The physiology of fishes. Boca Raton: CRC Press.

Marshall, W. S. and Singer, T. D. (2002). Cystic fibrosis transmembrane conductance regulator in teleost fish. *Biochimica et Biophysica Acta* **1566**, 16-27.

Marsigliante, S., Muscella, A., Barker, S. and Storelli, C. (2000). Angiotensin II modulates the activity of the Na+/K+ ATPase in eel kidney. *Journal of Endocrinology* **165**, 147-156.

Martinez, A.-S., Cutler, C. P., Wilson, G. D., Phillips, C., Hazon, N. and Cramb, G. (2005). Cloning and expression of three aquaporin homologues from the European eel (*Anguilla anguilla*): effects of seawater acclimation and cortisol treatment on renal expression. *Biology of the Cell* **97**, 615-627.

Masuda, K., Shima, H., Katagiri, C. and Kikuchi, K. (2003). Activation of ERK induces phosphorylation of MAPK phosphatase-7, a JNK specific phosphatase, at Ser-446. *J. Biol. Chem.* **278**, 32448-32456.

Matsuda, T. and Cepko, C. L. (2007). Controlled expression of transgenes introduced by in vivo electroporation. *PNAS* **104**, 1027-1032.

McCormick, S. D. (2001). Endocrine Control of Osmoregulation in Teleost Fish. *Amer. Zool.* **41**, 781-794.

McCormick, S. D., Moriyama, S. and Bjornsson, B. T. (2000). Low temperature limits photoperiod control of smolting in Atlantic salmon through endocrine mechanisms. *Am J Physiol Regul Integr Comp Physiol* **278**, R1352-1361.

McCormick, S. D. and Saunders, R. L. (1987). Preparatory physiological adaptations for marine life of salmonids: osmoregulation, growth, and metabolism. *Am. Fish Soc. Symposium* **1**, 211-229.

McNabb, F. (1992). Thyroid Hormones. In *Prentice Hall Endocrinology*, (ed. H. M.E.). New Jersey: Englewood Cliffs.

Minegishi, Y., Aoyama, J., Inoue, J. G., Miya, M., Nishida, M. and Tsukamoto, K. (2005). Molecular phylogeny and evolution of the freshwater eels genus Anguilla based on the whole mitochondrial genome sequences. *Mol Phylogenet Evol* **34**, 134-46.

Moore, B. W. and Perez, V. J. (1967). Specific acidic proteins of the nervous system. Woods Hole, MA: Prentice-Hall Inc.

Morgan, I. J., Potts, W.T.W. and Oates, K. (1994). Intracellular ion concentrations in branchial epithelial cells of brown trout (*Salmo trutta* L.) determined by x-ray microanalysis. *Journal of Experimental Biology* **194**, 139-151.

Morgan, I. J. and Potts, W. (1995). The effects of thiocynate on the intracellular ion concentrations of branchial epithelial cells of brown trout. *Journal of Experimental Biology* **198**, 1129-1232.

Moriarty, C. (1978). Eels, a natural and unnatural history.

Motais, R. and Isaia, J. (1972). Temperature-dependence of permeability to water and to sodium of the gill epithelium of the eel *Anguilla anguilla*. *Journal of Experimental Biology, (cited in Cutler, C. and Cramb, G., 2002, J. Exp. Biol. v205)* **56**, 587-600.

Murray, H. M. E. (2005). cDNA–GFP Fusion Libraries for Analyses of Protein Localization in Mouse Stem Cells. In *Biology*, vol. Master of Science in Biology. Waterloo, Canada: University of Waterloo.

Muslin, A. J., Tanner, J. W., Allen, P. M. and Shaw, A. S. (1996). Interaction of 14-3-3 with signaling proteins is mediated by the recognition of phosphoserine. *Cell* **84**, 889-97.

Nakanishi, K., Hashizume, S., Kato, M., Honjoh, T., Setoguchi, Y. and Yasumoto, K. (1997). Elevated expression levels of the 14-3-3 family of proteins in lung cancer tissues. *Hum Antibodies* **8**, 189-94.

Nguyen, H.-V., Stuart-Tilley, A., Alper, S. L. and Melvin, J. E. (2004). Cl-/HCO3- exchange is acetazolamide sensitive and activated by a muscarinic receptor-induced Ca^{2+} increase in salivary acinar cells. *Am J Physiol Gastrointest Liver Physiol* **286**, G312-320.

Nichols, R. J. and Traktman, P. (2004). Characterization of three paralogous members of the mammalian vaccinia related kinase family. *J. Biol. Chem.* **279**, 7934-7946.

Nichols, R. J., Wiebe, M. S. and Traktman, P. (2006). The vaccinia-related kinases phosphorylate the N' terminus of BAF, regulating its interaction with DNA and its retention in the nucleus. *Mol Biol Cell* **17**, 2451-64.

Ohara, O., Nagase, T., Ishikawa, K., Nakajima, D., Ohira, M., Seki, N. and Nomura, N. (1997). Construction and Characterization of Human Brain cDNA Libraries Suitable for Analysis of cDNA Clones Encoding Relatively Large Proteins. *DNA Research* **4**, 53-59.

Okamura, A., Yamada, Y., Tanaka, S., Horie, N., Utoh, T., Mikawa, N., Akazawa, A., and Oka, H. (2002). Atmospheric depression as the final trigger for the seaward migration of the Japanese eel *Anguilla japonica*. *Marine Ecology Progress Series* **234**, 281-288.

Oleksiak, M. F. and Crawford, D. L. (2006). Functional Genomics in Fishes: Insights into Physiological Complexity. Boca Raton, Fl: CRC Press.

Olsson, A. K. and Nanberg, E. (2001). A functional role for ERK in gene induction, but not in neurite outgrowth in differentiating neuroblastoma cells. *Exp. Cell Res.* **265**, 21-30.

Palstra, A. P., Cohen, E. G. H., Niemantsverdriet, P. R. W., van Ginneken, V. J. T. and van den Thillart, G. E. E. J. M. (2005). Artificial maturation and reproduction of European silver eel: development of oocytes during final maturation. *Aquaculture* **249**.

Palstra, A. P., van Ginneken, V. J. T., Murk, A. J. and van den Thillart, G. E. E. J. M. (2006). Are dioxin-like contaminants responsible for eel (*Anguilla anguilla*) drama? . *Naturwissenschaften* **93**, 145-148.

Pankhurst, N. W. (1982). Relation of visual changes to the onset of sexual maturation in the European eel *Anguilla anguilla* (L.). *J.Fish.Biol.* **21**, 127-140.

Park, Y.-J., Park, J.-G., Kim, S.-J., Lee, Y.-D., Rahman, S. and Takemura, A. (2006). Melatonin receptor of a reef fish with lunar-related rhythmicity: cloning and daily variations. *Journal of Pineal Research* **41**, 166-174.

Parrington, J. and Coward, K. (2002). Use of emerging genomic and proteomic technologies in fish phsiology. *Aquatic Living Resources* **15**, 193-196.

Patanjali, S., Parimoo, S. and Weissman, S. (1991). Construction of a uniform-abundance (normalized) cDNA library. *Proceedings of the National Academy of Sciences of the United States of America* **88**, 1943–1947.

Peirson, S. N., Butler, J. N. and Foster, R. G. (2003). Experimental validation of novel and conventional approaches to quantitative real-time PCR data analysis. *Nucleic Acids Research* **31**, e73.

Pelis, R. M. and McCormick, S. D. (2001). Effects of Growth Hormone and Cortisol on Na+-K+-2Cl- Cotransporter Localization and Abundance in the Gills of Atlantic Salmon. *General and Comparative Endocrinology* **124**, 134-143.

Perry, S. F., Beyers, M.L. and Johnson, D.A. (2000). Cloning and molecular characterisation of the trout (*Oncorhynchus mykiss*) vacuolar H+-ATPase B subunit. *Journal of Experimental Biology* **203**, 459-470.

Petr, P. (1968). The demonstration of chloride ions in the “chloride cells” of the gills of eels (Anguilla anguilla L.) adapted to sea water. *Cell and Tissue Research* **V92**, 422-427.

Peyon, P., Zanuy, S. and Carrillo, M. (2001). Action of Leptin on In Vitro Luteinizing Hormone Release in the European Sea Bass (Dicentrarchus labrax). *Biol Reprod* **65**, 1573-1578.

Pfaffl, M. W. (2001). A new mathematical model for relative quantitation. *Nucleic Acid Research* **29**, 2002-2007.

Pfaffl, M. W., Horgan, G. W. and Dempfle, L. (2002). Relative expression software tool (REST) for group-wise comparison and statistical analysis of relative expression resuls in real-time PCR. *Nucl. Acids Res.* **30**, e36.

Phillips, J. and Eberwine, J. H. (1996). Antisense RNA Amplification: A Linear Amplification Method for Analyzing the mRNA Population from Single Living Cells. *METHODS: A Companion to Methods in Enzymology* **10**, 283-288.

Philp, A. R., Bellingham, J., Garcia-Fernandez, J. and Foster, R. G. (2000). A novel rod-like opsin isolated from the extra-retinal photoreceptors of teleost fish. *FEBS Lett* **468**, 181-8.

Phimister, B. (1999). Going global. *Nature Genetics* **21**, 1.

Pierce, A. L., Dickey, J. T., Larsen, D. A., Fukada, H., Swanson, P. and Dickhoff, W. W. (2004). A quantitative real-time RT-PCR assay for salmon IGF-I mRNA, and its application in the study of GH regulation of IGF-I gene expression in primary culture of salmon hepatocytes. *Gen Comp Endocrinol* **135**, 401-11.

Pierce, A. L., Dickey, J. T., Larsen, D. A., Fukada, H., Swanson, P. and Dickhoff, W. W. (2004). A quantitative real-time RT-PCR assay for salmon IGF-I mRNA, and its application in the study of GH regulation of IGF-I gene expression in primary culture of salmon hepatocytes. *Gen. Comp. Endocrinol.* **135**, 401-411.

Poole, W. R. and Reynolds, J. D. (1998). Variability in growth rate in European eel *Anguilla anguilla* (L.) in a Western Irish catchment. . *Proc. R. Irish Acad.* **98B**, 141–145.

Pouyssegur, J., Volmat, V. and Lenormand, P. (2002). Fidelity and spatio-temporal control in MAP kinase (ERKs) signalling. *Biochem. Pharmacol.* **64**, 755-763.

Pozdeyev, N., Taylor, C., Haque, R., Chaurasia, S. S., Visser, A., Thazyeen, A., Du, Y., Fu, H., Weller, J., Klein, D. C. et al. (2006). Photic Regulation of Arylalkylamine N-Acetyltransferase Binding to 14-3-3 Proteins in Retinal Photoreceptor Cells. *J. Neurosci.* **26**, 9153-9161.

Prunet, P., Pisam, M., Claireaux, J. P., Boeuf, G. and Rambourg, A. (1994). Effects of growth hormone on gill chloride cells in juvenile Atlantic salmon (*Salmo salar*). *American Journal of Physiology* **266**, R850–R857.

Quackenbush, J. (2002). Microarray data normalization and transformation. *Nature Genetics* **32 Supplement**, 496-501.

Ramakers, C., Ruijter, J. M., Lekanne Deprez, R. H. and Moorman, A. F. M. (2003). Assumption-free analysis of quantitative real-time polymerase chain reaction (PCR) data. *Neuroscience Letters* **340**, 62-66.

Randall, D. J., Burggren, W. and French, K. (2002). Animal Physiology: Mechanisms and Adaptations. New York: W. H. Freeman.

Richards, J. G., Semple, J. W., Bystriansky, J. S. and Schulte, P. M. (2003). Na^+/K^+-ATPase α-isoform switching in gills of rainbow trout (Oncorhynchus mykiss) during salinity transfer. *J Exp Biol* **206**, 4475-4486.

Ririe, K., Rasmussen, R. and Wittwer, C. (1997). Product differentiation by analysis of DNA melting curves during the polymerase chain reaction. *Analytical Biochemistry* **245**, 154-160.

Robins, C. R., Cohen, D. M. and Robins, C. H. (1979). The eels *Anguilla* and *Histiobranchus*, photographed on the floor of the deep Atlantic in the Bahamas. *Bulletin of Marine Science* **29**, 401-405.

Romero, M. and Boron, W. (1999). Electrogenic Na+/HCO3- co-transporters: Cloning and physiology. *Annual Review of Physiology* **61**, 699-723.

Ross, J. (1995). mRNA Stability in Mammalian Cells. *Microbiological Reviews* **59**, 423-450.

Roth, D., Birkenfeld, J. and Betz, H. (1999). Dominant-negative alleles of 14-3-3 proteins cause defects in actin organization and vesicle targeting in the yeast Saccharomyces cerevisiae. . *FEBS Letters* **460**, 411-416.

Rousseau, K., Le Belle, N., Marchelidon, J., Schitz, M. and Dufour, S. (2002). Evidence for a negative feedback in the control of eel growth hormaone by thyroid hormones. *Journal of Endocrinology* **175**, 605-613.

Rowe, D., Thorpe, J. and Shanks, A. (1991). Role of fat stores in the maturation of male Atlantic salmon (*Salmo salar* L.) parr. *Canadian Journal of Fisheries and Aquatic Sciences* **48**, 405-413.

Russell, J. M. (2000). Sodium-Potassium-Chloride Cotransport. *Physiological Reviews* **80**, 211-276.

Saavedra, M. and Pousão-Ferreira, P. (2006). A preliminary study on the effect of lunar cycles on the spawning behaviour of the gilt-head sea bream, Sparus aurata. *Journal of the Marine Biological Association of the UK* **86**, 899-901.

Sabanayagam, C. R., Smith, C. L. and Cantor, C. R. (2000). Oligonucleotide immobilization on micropatterned streptavidin surfaces. *Nucl. Acids Res.* **28**, e33.

Sakamoto, T., McCormick, S. and Hirano, T. (1993). Osmoregulatory actions of growth hormone and its mode of action in salmonids: A review. *Fish Physiology and Biochemistry* **11**, 155-164.

Sakamoto, T., Shepherd, B. S., Madsen, S. S., Nishioka, R. S., Siharath, K., Richman, N. H., Bern, H. A. and Grau, E. G. (1997). Osmoregulatory Actions of Growth Hormone and Prolactin in an Advanced Teleost. *General and Comparative Endocrinology* **106**, 95-101.

Saunders, R. L., Fletcher, G. L. and Hew, C. L. (1998). Smolt development in growth hormone transgenic Atlantic salmon. *Aquaculture* **168**, 177-193.

Schena, M., D Shalon, Heller, R., A Chai, Brown, P. O. and Davis, R. W. (1989). Parallel human genome analysis: microarray-based expression monitoring of 1000 genes. *Proc Natl Acad Sci U S A* **93**, 10614–10619.

Schmidt, J. (1922). The breeding places of the eel. *Philosophical Transactions Royal Society* **211**, 179-208.

Schomerus, C. and Korf, H.-W. (2005). Mechanisms Regulating Melatonin Synthesis in the Mammalian Pineal Organ. *Ann NY Acad Sci* **1057**, 372-383.

Selvey, S., Thompson, E. W., Matthaei, K., Lea, R. A., Irving, M. G. and Griffiths, L. R. (2001). Beta-actin--an unsuitable internal control for RT-PCR. *Mol Cell Probes* **15**, 307-11.

Setoyama, C., Frunzio, R., Liau, G., Mudryj, M. and Crombrugghe, B. D. (1986). Transcriptional Activation Encoded by the v-fos Gene. *PNAS* **83**, 3213-3217.

Sevilla, A. (2004). c-Jun phosphorylation by the human vaccinia-related kinase 1 (VRK1) and its cooperation with the N-terminal kinase of c-Jun (JNK). *Oncogene* **23**, 8950-8958.

Sevilla, A., Santos, C. R., Vega, F. M. and Lazo, P. A. (2004). Human vaccinia-related kinase 1 (VRK1) activates the ATF2 transcriptional activity by novel phosphorylation on Thr-73 and Ser-62 and cooperates with JNK. *J. Biol. Chem.* **279**, 27458-27465.

Sgaier, S. K., Millet, S., Villanueva, M. P., Berenshteyn, F., Song, C. and Joyner, A. L. (2005). Morphogenetic and Cellular Movements that Shape the Mouse Cerebellum: Insights from Genetic Fate Mapping. *Neuron* **45**, 27-40.

Singh, H., Griffith, R. W., Takahashi, A., Kawauchi, H., Thomas, P. and Stegeman, J. J. (1988). Regulation of gonadal steroidogenesis in Fundulus heteroclitus by recombinant salmon growth hormone and purified salmon prolactin. *Gen Comp Endocrinol* **72**, 144-53.

Skadhauge, E. (1969). The mechanism of salt and water absorption in the intestine of the eel (*Anguilla anguilla*) adapted to waters of various salinities. *Journal of Physiology* **204**, 135-158.

Sloane, R. D. (1984). Preliminary observations of migrating adult freshwater eels (*Anguilla australis* Richardson) in Tasmania. *Australian Journal of Marine and Freshwater Research* **35**, 471–476.

Smith, H. W. (1931). The absorption and secretion of water and salts by the elasmobranch fishes. II. Marine elasmobranchs. *American Journal of Physiology* **98**, 296-310.

Smith, M., Burke, Z., Humphries, A., Wells, T., Klein, D., Carter, D. and Baler, R. (2001). Tissue-specific transgenic knockdown of Fos-related antigen 2 (Fra-2) expression mediated by dominant negative Fra-2. *Mol Cell Biol* **21**, 3704-13.

Snider, B. and Morrison-Bogorad, M. (1992). Brain non-adenylated mRNAs. *Brain Res Brain Res Rev.* **17**, 263-282.

Soares, M. B., Bonaldo, M. de F., Jelene, P., Su, L., Lawton, L., Efstratiadis, A. (1994). Construction and characterization of a normalized cDNA library. *Proceedings of the National Academy of Sciences USA* **91**, 9228-9232.

Soloaga, A., Thomson, S., Wiggin, G. R., Rampersaud, N., Dyson, M., Hazzalin, C., Mahadevan, L. and Arthur, J. S. C. (2003). MSK2 and MSK1 mediate the mitogen- and stress-induced phosphorylation of histone H3 and HMG-14. *EMBO J.* **22**, 2788-2797.

Southern, E. M. (1975). Detection of specific sequences among DNA fragments separated by gel electrophoresis. *Journal of Molecular Biology* **98**, 503-517.

Stone, R. (2003). Ecology. Freshwater eels are slip-sliding away. *Science* **302**, 221-2.

Sugiura, R. (2003). Feedback regulation of MAPK signalling by an RNA-binding protein. *Nature* **424**, 961-965.

Sullivan, G., Fryer, J. and Perry, S. (1996). Localisation of mRNA for proton pump (H^+ATPase) and Cl^-/HCO_3^- exchanger in rainbow trout gill. *Canadian Journal of Zoology* **74**, 2095-2103.

Sun, H., Charles, C. H., Lau, L. F. and Tonks, N. K. (1993). MKP-1 (3CH134), an immediate early gene product, is a dual specificity phosphatase that dephosphorylates MAP kinase in vivo. *Cell* **75**, 487-493.

Sundin, L. and Nilsson, G. E. (1998). Endothelin redistributes blood flow through the lamellae of rainbow trout gills. *Journal of Comparative Physiology B* **168**, 619-623.

Suzuki, K., Kawauchi, H. and Nagahama, Y. (1998). Isolation and characterisation of two distinct gonadotropins from chum salmon pituitary glands. *General and Comparative Endocrinology* **71**, 292-301.

Suzuki, R., Kaneko, T. and Hirano, T. (1991). Effects of osmotic pressure on prolactin and growth hormone secretion from organ-cultured eel pituitary. *Journal of Comparative Physiology B: Biochemical, Systemic, and Environmental Physiology* **161**, 147-153.

Suzuki, R., Kishida, M. and Hirano, T. (1990). Growth hormone secretion during longterm incubation of the pituitary of the Japanese eel, Anguilla japonica. *Fish Physiology and Biochemistry* **8**, 159-165.

Svedäng , H., Neuman, E. and Wickstrom, H. (1996). Maturation patterns in female European eel: Age and size at the silver eel stage. *Journal of Fish Biology* **48**, 342-351.

Svedäng , H., Wickstrom, H., Reizenstein, M., Holmgreen, K. and Florenius, P. (1998). Accuracy and precision in eel estimation, using otoliths of known and unknown age. *Journal of Fish Biology* **53**, 456-464.

Svedäng , H. and Wickstrom, H. (1997). Low fat contents in female silver eels: indications of insufficient energetic stores for migration and gonadal development. *Journal of Fish Biology* **50**, 475-486.

Takei, Y. and Balment, R. (1993). Natriuretic factors in nonmammalian vertebrates. Cambridge, UK: Cambridge University Press.

Takei, Y. and Hirose, S. (2002). The natriuretic system in eel, a key endocrine system for euryhalinity? *American Journal of Physiology* **282**, R940-R951.

Takei, Y. and Loretz, C. (2006). Endocrinology in The Physiology of Fishes. Boca Raton: CRC Press.

Takei, Y., Tsuchida, T. and Tanakadate, A. (1998). Evaluation of water intake in seawater adaptation in eels using a synchronized drop counter and pulse injector. . *Zool. Sci.* **15**, 677-682.

Takemura, A., Ueda, S., Hiyakawa, N. and Nikaido, Y. (2006). A direct influence of moonlight intensity on changes in melatonin production by cultured pineal glands of the golden rabbitfish, Siganus guttatus. *Journal of Pineal Research* **40**, 236-241.

Tanaka, H. (2003). Techniques for larval rearing. Melbourne: Blackwell.

Taylor, J. S., Braasch, I., Frickey, T., Meyer, A. and Van de Peer, Y. (2003). Genome Duplication, a Trait Shared by 22,000 Species of Ray-Finned Fish. *Genome Res.* **13**, 382-390.

Taylor, J. S., Van de Peer, Y., Braasch, I. and Meyer, A. (2001). Comparative genomics provides evidence for an ancient genome duplication event in fish. *Philos Trans R Soc Lond B Biol Sci* **356**, 1661-79.

Taylor, W. R. (1986). The Classification of Amino Acid Conservation. *J. Theor. Biol.* **119**, 205-218.

Tesch, F. W. (2003). The eel. Oxford, UK: Blackwell Science.

Tesch, F. W. and Greenwood, P. H. (1977). The Eel: Biology and Management of Anguillid Eels. London: Chapman and Hall.

Thompson, J. D., Gibson, T. J., Plewniak, F., Jeanmougin, F. and Higgins, D. G. (1997). The ClustalX windows interface: flexible strategies for multiple sequence alignment aided by quality analysis tools. *Nucleic Acids Research* **24**, 4876-4882.

Todd, J. L., Tanner, K. G. and Denu, J. M. (1999). Extracellular regulated kinases (ERK) 1 and ERK2 are authentic substrates for the dual-specificity protein-tyrosine phosphatase VHR. A novel role in down-regulating the ERK pathway. *J. Biol. Chem.* **274**, 13271-13280.

Trischitta, F., Denaro, M. G., Faggio, C. and Schettino, T. (1992). An attempt to determine the mechanisms of Cl^-exit across the basolateral membrane of eel intestine: Use of different Cl-transport pathway inhibitors. *Journal of Experimental Zoology* **265**, 11-18.

Tseng, G. C., Oh, M. K., Rohlin, L., Liao, J. C. and Wong, W. H. (2001). Issues in cDNA microarrays analysis : quality filtering, channel normalization, models of variations and assessment of gene effects. *Nucleic Acids Research* **29**, 2549-2557.

Tsuchida, T. and Takei, Y. (1998). Effects of homologous atrial natriuretic peptide on drinking and plasma ANG II levels in eels. *American Journal of Physiology-Regulatory Integrative and Comparative Physiology* **275**, R1605-R1610.

Tsukamoto, K., Izumi, N. and Tesch, W-.V. (1998). Do all freshwater eels migrate? *Nature* **396**, 635-636.

Tsukamoto, K. and Arai, T. (2001). Facultative catadromy of the eel *Anguilla japonica* between freshwater and seawater habitats. *Marine Ecology - Progress Series* **220**, 265-276.

Tucker, D. W. (1959). A New Solution to the Atlantic Eel Problem. *Nature* **183**, 495-501.

Tzeng, W. N., Wang, C.H., Wickstrom, H. and Reizenstein, M. (2000). Occurence of the semi-catadromous European eel *Anguilla anguilla* in the Baltic Sea. *Marine Biology* **137**, 93-98.

Underwood, H. (1990). The pineal and melatonin: regulators of circadian function in lower vertebrates. *Experientia* **46**, 120-128.

Usui, A. (1991). Eel culture. Oxford: Blackwell Scientific Publications Ltd.

Utida, S., Hirano, T., Oide, H., Ando, M., Johnson, D. W. and Bern, H. A. (1972). Hormonal control of the intestine and urinary bladder in teleost osmoregulation. *General and Comparative Endocrinology*, 317–327.

Van Der Hoeven, P. C., Van Der Wal, J. C., Ruurs, P., Van Dijk, M. C. and Van Blitterswijk, J. (2000). 14-3-3 isotypes facilitate coupling of protein kinase C-zeta to Raf-1: negative regulation by 14-3-3 phosphorylation. *Biochem J* **345 Pt 2**, 297-306.

van Ginneken, V., Haenen, O., Coldenhoff, K., Willemze, R., Antonissen, E., van Tulden, P., Dijkstra, S., Wagenaar, F. and van den Thillart, G. E. E. J. M. (2004). Presence of eel viruses in eel species from various geographic regions. *Bulletin of the European Association of Fish Pathologists* **24**, 268-271.

van Ginneken, V. J. T. (2006). Simulated Migration of European Eel (*Anguilla anguilla*, Linnaeus 1758). In *Biology*, vol. PhD. Wageningen: Wageningen University.

Van Utrecht, W. L. a. H., M.A. (1985). Notes on the eel larvae (*Anguilla anguilla* Linnaeus, 1758) from the central and eastern North Atlantic and on the glass eels from the European continental shelf. *Bijdragen tot de Dierkunde* **55**, 249-262.

Vangelder, R. N., Vonzastrow, M. E., Yool, A., Dement, W. C., Barchas, J. D. and Eberwine, J. H. (1990). Amplified RNA Synthesized from Limited Quantities of Heterogeneous cDNA. *Proceedings of the National Academy of Sciences of the United States of America* **87**, 1663-1667.

Vasioukhin, V., Degenstein, L., Wise, B. and Fuchs, E. (1999). The magical touch: Genome targeting in epidermal stem cells induced by tamoxifen application to mouse skin. *PNAS* **96**, 8551-8556.

Vaudry, D., Stork, P. J. S., Lazarovici, P. and Eiden, L. E. (2002). Signaling pathways for PC12 cell differentiation: making the right connections. *Science* **296**, 1648-1649.

Vega, F. M., Gonzalo, P., Gaspar, M. L. and Lazo, P. A. (2003). Expression of the VRK (vaccinia-related kinase) gene family of p53 regulators in murine hematopoietic development. *FEBS Lett.* **544**, 176-180.

Vega, F. M., Sevilla, A. and Lazo, P. A. (2004). p53 stabilization and accumulation induced by human vaccinia-related kinase 1. *Mol. Cell. Biol.* **24**, 10366-10380.

Vidal, B., Pasqualini, C., Le Belle, N., Holland, M. C., Sbaihi, M., Vernier, P., Zohar, Y. and Dufour, S. (2004). Dopamine inhibits luteinizing hormone synthesis and release in the juvenile European eel: a neuroendocrine lock for the onset of puberty. *Biol Reprod* **71**, 1491–1500.

Vøllestad, L. A. (1992). Geographic variation in age and length at metamorphosis of maturing European eel: environmental effects and phenotypic plasticity. *Journal of Animal Ecology* **61**, 41-48.

Vøllestad, L. A., Jonsson, B., Hvidsten, N. A., Næsje, T. F., Haraldstad, Ø. and J., R.-H. (1986). Environmental factors regulating the seaward migration of European silver eels (*Anguilla anguilla*). *Canadian Journal of Fisheries and Aquatic Sciences* **43**, 1909-1916, (Cited in Ellerby, D. et al, 2001).

Volmat, V., Camps, M., Arkinstall, S., Pouyssegur, J. and Lenormand, P. (2001). The nucleus, a site for signal termination by sequestration and inactivation of p42/p44 MAP kinases. *J. Cell Sci.* **114**, 3433-3443.

Wang, C. H. and Tzeng, W. N. (2000). The timing of metamorphosis and growth rates of American and European eel leptocephali: A mechanism of larval segregative migration. *Fisheries Research* **46**, 191-205.

Wang, E., Miller, L., Ohnmacht, G., Liu, E. and Marincola, F. (2000). High-fidelity mRNA amplification for gene profiling. *Nature Biotechnology* **18**, 457-459.

Wang, Y., Liu, C.L., Storey, J.D., Tibshirani, R.J., Herschlag, D. and Brown, P.O. (2002). Precision and functional specificity in mRNA decay. *Proceedings of the National Academy of Sciences USA* **99**, 5860-5865.

Watanabe, H. (2004). Essential role for phospholipase D2 activation downstream of ERK MAP kinase in nerve growth factor-stimulated neurite outgrowth from PC12 cells. *J. Biol. Chem.* **279**, 37870-37877.

Watson, J. D. and Crick, F. H. C. (1953). A Structure for Deoxyribose Nucleic Acid. *Nature* **3**, 737-738.

Weber, G. M., Powell, J. F., Park, M., Fischer, W. H., Craig, A. G., Rivier, J. E., Nanakorn, U., Parhar, I. S., Ngamvongchon, S., Grau, E. G. et al. (1997). Evidence that gonadotropin-

releasing hormone (GnRH) functions as a prolactin-releasing factor in a teleost fish (Oreochromis mossambicus) and primary structures for three native GnRH molecules. *J Endocrinol* **155**, 121-132.

Weissman, S. (1987). Molecular genetic techniques for mapping the human genome. *Mol Biol Med* **4**, 133–143.

Weltzien, F. A., Pasqualini, C., Le Belle, N., Vidal, B., Vernier, P. and Dufour, S. (2005). Brain expression of tyrosine hydroxylase and its regulation by steroid hormones in the European eel quantified by real-time PCR. In *Trends in Comparative Endocrinology and Neurobiology*, vol. 1040, pp. 518-520.

Weltzien, F. A., Pasqualini, C., Sebert, M. E., Vidal, B., Le Belle, N., Kah, O., Vernier, P. and Dufour, S. (2006). Androgen-dependent stimulation of brain dopaminergic systems in the female European eel (Anguilla anguilla). *Endocrinology* **147**, 2964-2973.

Weltzien, F. A., Pasqualini, C., Vernier, P. and Dufour, S. (2005). A quantitative real-time RT-PCR assay for European eel tyrosine hydroxylase. *General and Comparative Endocrinology* **142**, 134-142.

Wigham, T. and Ball, J. N. (1976). In vivo evidence for catecholaminergic inhibition of prolactin secretion in the teleostPoecilia latipinna. *Journal of Comparative Physiology B: Biochemical, Systemic, and Environmental Physiology* **V110**, 135-143.

Wilson, D. E. and Reeder, D. M. (1993). Mammal Species of the World. Washington D.C.: Smithsonian Institution Press.

Wilson, J., Laurent, P., Tufts, B., Benos, D., Donowitz, M., Vogl, A. and Randall, D. (2000). NaCl uptake by the branchial epithelium in freshwater teleost fish: an immunological approach to ion-transport protein localization. *Journal of Experimental Biology* **203**, 2279-2296.

Wilson, J., Randall, D., Donowitz, M., Vogl, A. and Ip, A. (2000b). Immunolocalization of ion-transport proteins to branchial epithelium mitochondria-rich cells in the mudskipper (*Periophthalmodon schlosseri*). *Journal of Experimental Biology* **203**, 2297-2310.

Wilson, R. W., Wilson, J. M. and Grossel, M. (2002). Intestinal bicarbonate secretion by marine teleost fish - why and how? *Biochimica et Biophysica Acta* **1566**, 182-193.

Wood, C. M., Gilmour, K. M. and Part, P. (1998). Passive and active transport properties of a gill model, the cultures branchial epithelium of the freshwater rainbow trout (*Oncorhynchus mykiss*). *Comparative Biochemistry and Physiology Part A* **119**, 87-96.

Xue, J., Tsang, C. W., Gai, W. P., Malladi, C. S., Trimble, W. S., Rostas, J. A. and Robinson, P. J. (2004). Septin 3 (G-septin) is a developmentally regulated phosphoprotein enriched in presynaptic nerve terminals. *J Neurochem* **91**, 579-90.

Yamamoto, K. and Yamauchi, K. (1974). Sexual maturation of Japanese eel and production of eel larvae in the aquarium. *Nature* **251**, 220-222.

Yang, X., Lee, W. H., Sobott, F., Papagrigoriou, E., Robinson, C. V., Grossmann, J. G., Sundstrom, M., Doyle, D. A. and Elkins, J. M. (2006). Structural basis for protein-protein interactions in the 14-3-3 protein family. *PNAS* **103**, 17237-17242.

Yang, Y. H., Dudoit, S., Luu, P., Lin, D. M., V., P., Ngai, J. and Speed, T. P. (2002). Normalization for cDNA microarray data: a robust composite method addressing single and multiple slide systematic variation. *Nucleic Acid Research* **30**.

Yaron, Z. and Sivan, B. (2005). Reproduction.

Yu, W. H., Kimura, M., Walczewska, A., Karanth, S. and McCann, S. M. (1997). Role of leptin in hypothalamic-pituitary function. *Proc Natl Acad Sci U S A* **94**, 1023-8.

Yuvaniyama, J., Denu, J. M., Dixon, J. E. and Saper, M. A. (1996). Crystal structure of the dual specificity protein phosphatase VHR. *Science* **272**, 1328-1331.

Zawilska, J. and Luvone, P. M. (1989). Catecholamine receptors regulating serotonin N-acetyltransferase activity and melatonin content of chicken retina and pineal gland: D2-dopamine receptors in retina and alpha-2 adrenergic receptors in pineal gland. *J Pharmacol Exp Ther* **250**, 86-92.

Zervas, M., Millet, S., Ahn, S. and Joyner, A. L. (2004). Cell Behaviors and Genetic Lineages of the Mesencephalon and Rhombomere 1. *Neuron* **43**, 345-357.

Zhang, Y., Proenca, R., Maffei, M., Barone, M., Leopold, L. and Friedman, J. M. (1994). Positional cloning of the mouse obese gene and its human homologue. *Nature* **372**, 425-32.

Zupan, L. A., Steffens, D. L., Berry, C. A., Landt, M. and Gross, R. W. (1992). Cloning and expression of a human 14-3-3 protein mediating phospholipolysis. Identification of an arachidonoyl-enzyme intermediate during catalysis. *J. Biol. Chem.* **267**, 8707-8710.